

Utah State University

DigitalCommons@USU

---

All Graduate Theses and Dissertations

Graduate Studies

---

5-2008

## Pathophysiology of Arboviral Encephalitides in Laboratory Rodents

Aaron L. Olsen  
*Utah State University*

Follow this and additional works at: <https://digitalcommons.usu.edu/etd>



Part of the [Immunopathology Commons](#), and the [Medicine and Health Sciences Commons](#)

---

### Recommended Citation

Olsen, Aaron L., "Pathophysiology of Arboviral Encephalitides in Laboratory Rodents" (2008). *All Graduate Theses and Dissertations*. 123.

<https://digitalcommons.usu.edu/etd/123>

This Dissertation is brought to you for free and open access by the Graduate Studies at DigitalCommons@USU. It has been accepted for inclusion in All Graduate Theses and Dissertations by an authorized administrator of DigitalCommons@USU. For more information, please contact [digitalcommons@usu.edu](mailto:digitalcommons@usu.edu).



PATHOPHYSIOLOGY OF ARBOVIRAL ENCEPHALITIDES  
IN LABORATORY RODENTS

by

Aaron L. Olsen

A dissertation submitted in partial fulfillment  
of the requirement for the degree

of

DOCTOR OF PHILOSOPHY

in

Bioveterinary Sciences

Approved:

---

John D. Morrey  
Major Professor

---

Jeffery O. Hall, D.V.M.  
Committee Member

---

Thomas J. Baldwin, D.V.M.  
Committee Member

---

Donal G. Sinex  
Committee Member

---

Timothy Gilbertson  
Committee Member

---

Thomas Bunch  
ADVS Department Head

---

Byron R. Burnham  
Dean of Graduate Studies

UTAH STATE UNIVERSITY  
Logan, Utah

2008

Copyright © Aaron L. Olsen 2008

All Rights Reserved

## ABSTRACT

Pathophysiology of Arboviral Encephalitides  
in Laboratory Rodents

by

Aaron L. Olsen, Doctor of Philosophy

Utah State University, 2008

Major Professor: Dr. John D. Morrey  
Department: Animal, Dairy, and Veterinary Sciences

Western equine encephalitis virus (WEEV) is an arboviral pathogen naturally found in North America. The primary disease phenotype associated with WEEV infection in susceptible hosts is a relatively long prodromal period followed by viral encephalitis. By contrast, in the current work, experimental inoculation of WEEV into the peritoneum of Syrian golden hamsters produced rapid death within approximately 96 h. It was determined that direct virus killing of lymphoid cells leads to death in WEEV-infected Syrian golden hamsters, and that inflammatory cytokines have the potential to enhance virus-induced lymphoid cell destruction. It was further concluded that WEEV retains its ability to cause encephalitis in Syrian golden hamsters, if hamsters survive the early stages of virus infection or if virus is introduced directly into the CNS.

Death in WEEV-infected hamsters is associated with lymphonecrotic lesions in the absence of pathological lesions in the central nervous system (CNS). Few clinical parameters were altered by WEEV infection, with the exception of circulating

lymphocyte numbers. Circulating lymphocyte numbers decreased dramatically during WEEV infection, and lymphopenia was identified as a consistent indicator of eventual death. Virus infection also increased serum concentrations of the cytokines interferon and tumor necrosis factor-alpha (TNF-alpha).

Hamster peritoneal macrophages exposed to WEEV expressed TNF-alpha in a dose-responsive manner. Macrophage expression of TNF-alpha could be significantly inhibited by treatment of cells with anti-inflammatory agents flunixin meglumine (FM) or dexamethasone (Dex). Anti-inflammatory treatment also protected macrophages from cytotoxicity associated with exposure to WEEV. Treatment of WEEV-infected hamsters with either FM or Dex significantly improved survival compared to placebo-treated controls. WEEV induced cytotoxicity in hamster splenocytes exposed to WEEV in a virus dose-responsive manner. Supernatant from WEEV-exposed macrophages significantly enhanced WEEV killing of splenocytes. Hamsters that survived the early stages of WEEV infection occasionally developed signs of neurological disease and died approximately 6 to 9 d after virus inoculation. These animals had histopathological lesions in the CNS consistent with alphavirus-induced encephalitis. Inoculation of WEEV directly into the CNS caused apparent encephalitic disease. Death following CNS inoculation of WEEV was rapid and concurrent with histopathological lesions in the CNS similar to lesions seen in encephalitic hamsters following peripheral inoculation.

(221 pages)

## ACKNOWLEDGMENTS

I thank my major professor, John D. Morrey, for his constant support and encouragement in my professional endeavors. He has been willing to consider uncommon ideas and give guidance on the best research paths to follow. He has been willing to work with me in the role of a nontraditional graduate student and has encouraged of me as I pursued my professional goals.

I would also like to recognize my committee, Jeff Hall, Tom Baldwin, Don Sinex, and Tim Gilbertson. Their input and insight has always been welcome. In particular, their willingness to support a dramatic shift in the direction of the research has allowed me to pursue the work that has eventually lead to the completion of my doctoral studies.

I appreciate the widespread support I have received from all members of the Institute for Antiviral Research at Utah State University. The technical support of people too numerous to mention has dramatically eased demands on my time and improved my ability to accomplish my goals. In particular I appreciate the members of the weekly “Leo Marvin” meetings for providing an excellent opportunity to share results and consider research ideas and plans.

I must also recognize the many faculty members at both Utah State University and Purdue University who eagerly shared their time, their knowledge, and their passions for science. In particular I mention Kevin M. Hannon in the Basic Medical Sciences Department at Purdue University for his willingness to engage me as a graduate student while also a veterinary student and for introducing me into the world of biomedical research. He showed me it was possible to be both veterinarian and researcher.

I must thank my dear wife, Cheryl, for her unflagging support. She has allowed me to pursue schooling first in the professional veterinary curriculum, and then as a graduate student at Utah State University. All the while she has done everything in her power to provide me with the time and means to accomplish my professional goals, at times at the sacrifice of family time, weekends, and evenings, and even family vacations. Truly, what has been accomplished could not have been done without her.

Finally, I am grateful to the faculty, staff, and students of the Animal, Dairy and Veterinary Science Department at Utah State University, and to the Office of the Vice President of Research also at Utah State University. They have provided both administrative support and personal encouragement to me in graduate student endeavors. They have indeed been a pleasure to work with. Thanks also go to the National Institutes of Health, since this work was partially supported by Contract NO1-AI-15435 from the Virology Branch, NIAID, NIH, and from Grant 1-U54-AI06357-01 from the Rocky Mountain Regional Centers of Excellence (JDM).

Aaron L. Olsen

## CONTENTS

	Page
ABSTRACT .....	iii
ACKNOWLEDGMENTS .....	v
LIST OF TABLES .....	ix
LIST OF FIGURES .....	x
INTRODUCTION .....	1
LITERATURE REVIEW .....	7
Arboviral Encephalitides .....	7
Atypical Disease Phenotypes Associated with Arboviral Infection .....	13
Experimental Alphavirus Infections in Syrian Golden Hamsters .....	17
Viral-Mediated Cell Killing Enhanced by Inflammatory Cytokines .....	21
Compounds .....	31
MATERIALS METHODS AND JUSTIFICATION.....	33
Compounds .....	33
Cell Lines.....	35
Cell Culture Procedures .....	35
Bioassay for Quantification of Tumor Necrosis Factor-Alpha Activity.....	36
Bioassay for Quantification of Interferon Activity.....	37
Viruses .....	38
Titration of Virus in Serum and Tissues.....	38
Macrophage Isolation and Testing.....	39
Splenocyte Isolation and Testing.....	41
Antiviral Efficacy.....	43
Animals.....	44
Blood-Brain Barrier Permeability Assay in Mice.....	44
Collection of Cerebrospinal Fluid and Measurement of Blood-Brain Barrier Permeability in Syrian Golden Hamsters .....	45
Measurement of Fluorescence .....	47
Time Course of Banzi Virus and Semliki Forest Virus Infection in Mice .....	48
Ampligen™ Efficacy Versus Banzi and Semliki Forest Viruses in Mice.....	49
Using Cerebrospinal Fluid to Measure Blood-Brain Barrier Permeability in WEEV-Infected Hamsters.....	49
Histopathology and Bacterial Isolation in Hamsters Inoculated with WEEV .....	50



Supportive, Antibacterial and Anti-Inflammatory Treatment of WEEV-Inoculated Hamsters .....	51
Evaluating the Relationship Between Circulating Lymphocyte Counts and Disease Outcome in WEEV-Inoculated Hamsters .....	52
Clinical Characterization and Time-Course of WEEV Infection in Hamsters .....	54
Evaluation of the Effect of Viral Dose and Dexamethasone Immunosuppression on Disease Phenotype and Outcome in Syrian Golden Hamsters .....	55
Correlation Between Early Expression of Serum Interferon and Disease Outcome in Hamsters Inoculated with WEEV .....	56
Intracranial Inoculation of WEEV in Hamsters .....	56
Statistical Evaluation .....	57
 RESULTS .....	 59
Virus Infection and Blood-Brain Barrier Permeability Changes in Mice.....	59
Blood-Brain Permeability Changes in Hamsters Inoculated with Western Equine Encephalitis Virus .....	70
Histopathology and Microbiology Associated with WEE Virus Infection in Hamsters .....	73
Supportive Care of WEE Virus Inoculated Hamsters.....	80
Characterization of Clinical and Cytokine Changes in Hamsters Inoculated with WEEV .....	95
The Effects of Viral Dose and Dexamethasone Immunosuppression on Disease Phenotype in WEEV-Inoculated Hamsters .....	113
Comparisons of Infection with Kern and California Strains of WEEV in the Syrian Golden Hamster .....	117
Identification of Potential Markers of Disease Outcome in WEEV- Inoculated Hamsters.....	124
<i>In vitro</i> Effects of WEEV on Hamster Macrophages and Splenocytes .....	139
Viral Encephalitis Disrupts the Function of the Blood-Brain Barrier .....	156
WEEV Infection in Syrian Golden Hamsters .....	162
Supportive Care and Dexamethasone Immunosuppression of WEEV Inoculated Hamsters.....	173
The Effects of Virus Dose and Virus Strain .....	176
Identification of Potential Markers of Outcome in Hamsters Inoculated with WEEV .....	179
<i>In vitro</i> Activity of WEEV in Hamster Splenocytes and Macrophages .....	182
Proposed Model of WEEV Infection in the Syrian Golden Hamster .....	187
Future Experiments.....	191
Conclusion and Summary .....	193
 REFERENCES .....	 198
 CURRICULUM VITAE.....	 222

## LIST OF TABLES

Table		Page
1	Time course of tissue viral titers in i.p. inoculated 7-8 wk old BABL/c mice.....	60
2	Effects of a single does of Ampligen™ administered at various times in relation to virus exposure on survival and brain virus titers in BLAB/c mice inoculated with Banzi virus or Semliki Forest virus.....	63
3	Description of rates of bacteria isolation and bacterial species isolated from WEEV- and sham-inoculated hamsters.....	78
4	Time course of tissue viral titers in WEEV inoculated hamsters.....	100
5	Clinical chemistry values in hamsters inoculated with WEEV.....	101
6	Hematological findings in hamsters inoculated with WEEV.....	103
7	Time course of tissue TNF-alpha concentrations in WEEV-inoculated hamsters.....	106
8	Time course of tissue interferon concentrations in WEEV-inoculated hamsters.....	107
9	Comparison of Mean Time to Death among hamsters inoculated with high and low doses of WEEV.....	114

## LIST OF FIGURES

Figure	Page
1 Time course of blood-brain barrier permeability in 7-8 wk old BALB/c mice inoculated i.p. with Banzi virus.....	61
2 Time course of blood-brain barrier permeability in 7-8 wk old BALB/c mice inoculated i.p. with Semliki.....	62
3 Average percentage weight change from initial body weight of Banzi virus-inoculated mice after a single i.p. dose of 1 mg/kg of Ampligen™ administered at various times in relation to virus exposure.....	65
4 Average percentage weight change from initial body weight of Semliki Forest virus-inoculated mice after a single i.p. dose of 1 mg/kg of Ampligen™ administered at various times in relation to virus exposure.....	68
5 Percentage of fluorescence detected in the brain vs. the serum (w/v) on 8 dpi of mice inoculated with Banzi virus and treated with a single i.p. dose of 1 mg/kg of Ampligen™ at various times in relation to virus exposure.....	69
6 Percentage of fluorescence detected in the brain vs. the serum (w/v) on 6 dpi of mice inoculated with SFV and treated with a single dose of 1 mg/kg of Ampligen™ at various times in relation to virus exposure.....	71
7 Time course of blood-brain barrier permeability in Syrian golden hamsters inoculated i.p. with WEEV.....	73
8 Comparison of fluorescence detected in the CSF vs. the serum (v/v) in Syrian golden hamsters that either survived or died following inoculation with WEEV via the i.p. route.....	74

9	Spleen from WEEV-infected hamsters at 48 hpi and 72 hpi .....	76
10	Brain from WEEV-infected hamsters at 132 and 144 hpi.....	79
11	Survival of Syrian golden hamsters following intracranial inoculation with WEEV or sham inoculation by the same route.....	81
12	Brains from hamsters following intracranial inoculation with WEEV.....	82
13	Effects of supportive care on the survival of WEEV-inoculated hamsters.....	84
14	Effects of supportive care on the weight change of WEEV-inoculated hamsters.....	84
15	Effects of high and low doses of enrofloxacin alone on the survival of Syrian golden hamsters inoculated with WEEV via the i.p. route.....	86
16	Effects of supportive with and without antibiotics on the survival of Syrian golden hamsters inoculated with WEEV via the i.p. route .....	86
17	Effects of supportive with and without antibiotics on the weight change of Syrian golden hamsters inoculated with WEEV via the i.p. route .....	87
18	Effects of anti-inflammatory treatment on the survival of Syrian golden hamsters inoculated with WEEV via the i.p. route .....	89
19	Effects of anti-inflammatory treatment on weight change of Syrian golden hamsters inoculated with WEEV via the i.p. route .....	90
20	Effects of anti-inflammatory treatment on the survival of Syrian golden hamsters inoculated with WEEV via the i.p. route .....	91
21	Effects of anti-inflammatory treatment on weight change of Syrian golden hamsters inoculated with WEEV via the i.p. route .....	92
22	Effects of anti-inflammatory treatment on the rectal body temperature of Syrian golden hamsters inoculated with WEEV via the i.p. route. ....	93

23	Composite representation of the effects of anti-inflammatory treatment on the survival of Syrian golden hamsters inoculated with WEEV via the i.p. route.....	94
24	Average percentage weight change from initial body weight of Syrian golden hamsters inoculated with WEEV or sham inoculated via the i.p. route .....	98
25	Average rectal body temperature of Syrian golden hamsters inoculated with WEEV or sham inoculated via the i.p .....	99
26	Numbers of circulating lymphocytes at various times post-virus inoculation in the whole blood of Syrian golden hamsters either sham inoculated or inoculated with WEEV via the i.p. route .....	105
27	Interferon concentrations at various times post-virus inoculation in the serum of Syrian golden hamsters inoculated with WEEV .....	108
28	TNF-alpha concentrations at various times post-virus inoculation in the serum of Syrian golden hamsters inoculated with WEEV .....	109
29	Survival of Syrian golden hamsters inoculated via the i.p. route with 2 different doses of WEEV .....	111
30	Changes in body weight of hamsters inoculated via the i.p. route with either a high (an LD <sub>90</sub> ) dose (10 <sup>3.5</sup> CCID <sub>50</sub> /animal) or a low (LD <sub>50</sub> ) dose (10 <sup>2.5</sup> CCID <sub>50</sub> /animal) of WEEV.....	113
31	Survival of WEEV-inoculated Syrian golden hamsters following either placebo or immunosuppressive treatment with dexamethasone .....	114
32	Rectal body temperatures of WEEV-inoculated Syrian golden hamsters following either placebo treatment or immunosuppressive treatment with dexamethasone .....	115
33	Serum virus titer in WEEV-inoculated Syrian golden hamsters following either placebo treatment or immunosuppressive treatment with dexamethasone .....	116
34	Survival of Syrian golden hamsters inoculated with 2 different strains of WEEV.....	118

35	Comparison of rectal body temperatures at 60 hpi in Syrian golden hamsters inoculated with 2 different strains of WEEV or strain inoculated at 60 hpi.....	119
36	Lymphocyte counts at 36 hpi in the whole blood of Syrian golden hamsters inoculated with 2 different strains of WEEV or strain inoculated.....	121
37	Serum virus titers at 36 hpi in hamsters inoculated via the i.p. route with 2 different strains of WEEV.....	122
38	Serum interferon concentrations at 36 and 48 hpi in hamsters inoculated with 2 different strains of WEEV.....	123
39	Comparison of circulating white blood cell counts at 72 and 84 hpi in whole blood from hamsters that either survived or succumbed to infection with WEEV.....	124
40	Comparison of circulating lymphocyte counts at 72 and 84 hpi in whole blood from hamsters that either survived or succumbed to infection with WEEV.....	127
41	Circulating white blood cell counts at 84 hpi in whole blood from hamsters that either survived or succumbed to infection with WEEV.....	128
42	Circulating lymphocyte counts at 84 hpi in whole blood from hamsters that either survived or succumbed to infection with WEEV.....	129
43	Survival of WEEV inoculated hamsters treated with flunixin meglumine or placebo treatments.....	131
44	Circulating white blood cell counts at 84 hpi in whole blood from hamsters inoculated with WEEV and treated with flunixin meglumine or placebo treatment.....	132
45	Circulating lymphocyte counts at 84 hpi in whole blood from hamsters inoculated with WEEV and treated with flunixin meglumine or placebo treatment.....	133
46	Survival of hamsters inoculated with WEEV.....	134

47	Concentration of interferon in the serum at 20 and 44 hpi from sham inoculated hamsters or hamsters that either survived or succumbed to WEEV infection.....	136
48	Concentration of TNF-alpha in serum at 44 hpi from sham inoculated hamsters or hamsters that either survived or succumbed to WEEV infection.....	137
49	Serum virus titers at 44 hpi from sham inoculated hamsters or hamsters that either survived or succumbed to WEEV infection.....	138
50	Rectal body temperature in sham inoculated hamsters or hamsters that either survived or succumbed to WEEV infection.....	140
51	TNF-alpha production by peritoneal macrophages after 18 h of exposure to various multiplicities of infection of WEEV.....	141
52	TNF-alpha production by peritoneal macrophages inoculated with various multiplicities of infection of WEEV at multiple times post-virus exposure.....	143
53	TNF-alpha production by peritoneal macrophages inoculated with WEEV at a MOI of 3 and treated with anti-inflammatory compounds.....	145
54	Cell viability of peritoneal macrophages following inoculation with WEEV at a MOI of 3, and treatment with anti-inflammatory compounds....	147
55	Cell viability of hamster splenocytes 3 d after inoculation with various multiplicities of infection of WEEV.....	149
56	Comparison of the ability of 2 different strains of WEEV to induce decreased cell viability in hamster lymphocytes <i>in vitro</i> after 3 d of incubation.....	150
57	Effects of treatment with the compound flunixin meglumine and dexamethasone on hamster splenocytes inoculated with WEEV.....	151
58	Effects of stimulated macrophage supernatant on the viability of hamster splenocytes exposed to WEEV.....	153

59	Cell viability of splenocytes cultured in the presence of supernatant from macrophages stimulated with WEEV and treated with anti-inflammatory compounds.....	155
60	Proposed disease model of WEEV infection in the Syrian golden hamster.....	188



## ABBREVIATIONS

µg	micrograms
Ab	antibody
AVOVA	analysis of variance
BaV	Banzi virus
BBB	blood-brain barrier
CCID <sub>50</sub>	50% cell culture infectious dose
CSF	cerebrospinal fluid
CSFV	classic swine Fever virus
CNS	central nervous system
COX	cyclooxygenase
CPE	cytopathic effect
dpi	days post-virus inoculation
DEX	dexamethasone
DMSO	dimethyl sulfoxide
Ds-RNA	double stranded RNA
EBSS	Earle's balanced salt solution
EDTA	ethylenediamine tetraacetic acid
EEEV	eastern equine encephalitis virus
EMCV	encephalomyocarditis virus
FBS	fetal bovine serum (FBS)
FM	flunixin meglumine

HIV	human immunodeficiency virus
hpi	hours post-virus inoculation
HBSS	Hanks' balanced salt solution
IL	interleukin
i.p.	intraperitoneal
MIP-2	macrophage inflammatory protein-2
mg	milligram
mL	milliliters
mM	millimolar
MEM	minimal essential medium
MDD	mean day to death
MTD	mean time to death
MW	molecular weight
NaFl	sodium fluorescein
NF-kappa-B	nuclear factor kappa-B
kg	kilogram
LD <sub>50</sub>	50% lethal dose
LD <sub>90</sub>	90% lethal dose
LRS	lactated Ringer's solution
MEM	minimal essential medium
MMP	matrix metalloproteinase
MOI	multiplicity of infection (CCID <sub>50</sub> of virus added per well on infection date/cells seeded per well initially)

ng	nanogram
RBC	red blood cell
RFV	Rift Valley Fever virus
RNA	ribonucleid acid
SARS	systemic acute respiratory syndrome
SFV	Semliki Forest virus
SIRS-MODS	severe inflammatory response syndrome- multiple organ dysfunction syndrome
s.c.	subcutaneous
s.d.	standard deviation
TGF-beta 1	transforming growth factor beta-1
TLR	toll-like receptor
TNF-alpha	tumor necrosis factor alpha
TRAIL	TNF related apoptosis inducing ligand
WBC	white blood cell
VEEV	Venezuelan equine encephalitis virus
WEEV	western equine encephalitis virus
WNV	West Nile virus

## INTRODUCTION

Arthropod borne viruses, or arboviruses, are commonly positive-stranded, membrane-bound, RNA viruses. Many arboviruses are recognized for their potential to cause viral encephalitis,<sup>94,224</sup> as well as their potential use as bioterror agents.<sup>215</sup> The continuing emergence and spread of new arboviral encephalitides highlights the importance of understanding the pathophysiological mechanisms associated with a viral infection of the brain.

However, it is recognized that in naturally occurring infections arborviral encephalitides undergo a peripheral nonneurological replication phase.<sup>94</sup> The pre-central nervous system phase of virus infection can present with a variety of disease symptoms and signs, such as fever, gastrointestinal complaints, pain, malaise, and lethargy.<sup>68,118,187</sup> In some instances histopathological lesions in peripheral organs may be identified following an infection with an arborviral encephalitide.<sup>63,64,186</sup> The presence of replicating virus in peripheral tissues presents the possibility for severe disease syndromes and possibly death prior to virus entry into the central nervous system or induction of viral induced pathology therein.

The purpose of this study was twofold: The first objective was to examine the ability of various arboviral encephalitides to alter the function of normal central nervous system physiology. It was originally hypothesized that breakdown of the blood-brain barrier (BBB), as shown by increased permeability of the BBB to fluorescent markers, is an integral component of the pathology associated with viral encephalitis. A supporting hypothesis was that that peripheral inoculation of animals with a viral encephalitide

would result in a central nervous system viral infection, which in turn would lower the ability of the blood-brain barrier to exclude fluorescent marker molecules, and that the degree of blood-brain barrier disruption as measured by fluorescent markers was correlated with the severity of disease.

The second purpose of this study was to determine the mechanisms of death in hamsters inoculated with western equine encephalitis virus (WEEV). The hypothesis was that animals that rapidly succumbed to virus infection were dying due to a peripheral systemic disease rather than a neurological virus infection. It was further hypothesized that as part of the nonneuronal disease processes inflammatory cytokines enhanced the ability of the virus to destroy cells. It was also hypothesized that WEEV retained its ability to cause encephalitis in hamsters. If a hamster survived the initial systemic disease phase, or the systemic phase was bypassed, the animal could develop a virus-induced central neurological disease. The specific aims of the project were as follows:

1. Evaluate the effect of infection with a viral encephalitides on the function of the blood-brain barrier in animals and correlate the blood-brain barrier function with disease outcomes. This was accomplished by injecting a fluorescent marker molecule into virus inoculated mice and hamsters, and measuring the amount of fluorescence in brain tissue or cerebrospinal fluid. Correlation with disease severity was evaluated by measuring the blood-brain barrier function in virus-inoculated mice treated with known effective antiviral compounds.

2. Characterize the non-neurological disease state noted in hamsters inoculated with the California strain of WEEV. This was done by measuring and examining multiple disease parameters in virus-infected hamsters including: serum biochemistry,

complete blood profiles, tissue histopathology, tissue and serum virus titers, and serum and tissue cytokine expression.

3. Determine the ability of WEEV to cause encephalitic disease in hamsters.

This was done by observing and performing post-mortem histopathological analysis on hamsters that survived the initial systemic phase of the disease but later succumbed. This was also accomplished by inoculating WEEV directly into the central nervous system of hamsters.

4. Explore the potential roles that inflammatory cytokines, including tumor necrosis factor-alpha and interferon, may play in the systemic disease phenotype of hamsters inoculated with WEEV. This was done by measuring the endogenous cytokine response to virus infection in WEEV-inoculated animals and attempting to correlate timing and degree of cytokine expression with the outcome, and by treating WEEV inoculated hamsters with various anti-inflammatory agents and monitoring disease outcome. Additional information was gained by evaluating the ability of WEEV to elicit a cytokine response in immune cells *in vitro*, and by measuring the ability of virus-induced cytokine expression to reduce the viability of primary immune cells *in vitro*.

To meet these specific aims the permeability of the BBB of mice inoculated with either Banzi or Semliki Forest viruses were evaluated. Follow-up experiments also examined BBB permeability in virus inoculated mice treated with the known antiviral compound Ampligen™.

Results garnered from BBB permeability studies in virus-inoculated mice indicated that changes to BBB permeability may be a pathophysiologic event common to multiple forms of viral encephalitis. To further examine the role of the BBB in other

animal models of virus infection with viral encephalitides the permeability of the BBB in hamsters inoculated with WEEV was examined. Experiments were unable to detect significant alterations to the permeability of the BBB to fluorescent markers in hamsters dying following inoculation with WEEV. It was observed over the course of multiple experiments that the majority of WEEV-inoculated hamsters that succumbed to virus infection died by approximately 96 h post-virus inoculation. From a combination of these 2 experiments it was hypothesized that hamsters were dying from some cause other than viral encephalitis, most likely a severe systemic viral disease. A series of experiments were conducted to characterize the clinical, hematological, and histopathological changes in hamsters inoculated with WEEV. Results from initial disease characterization experiments appeared to indicate a lack of neurologic disease but suggested the potential for a secondary bacterial septicemia. Therefore, experiments were conducted to isolate bacteria from WEEV-inoculated hamsters and to treat virus infected hamsters with antibiotics in an effort to eliminate the presumed septicemia.

As previously stated, the majority of WEEV-inoculated hamsters succumbed to virus infection by approximately 96 h post-virus inoculation, and that hamsters died without any observable histopathology in the central nervous system. However, it was observed that a small proportion of hamsters survived the initial disease phase only to die later, sometimes displaying signs of overt neurological disease. From these observations it was hypothesized that WEEV retained its ability to cause viral encephalitis in hamsters. To test this hypothesis virus inoculated hamsters dying late in the virus infection were assayed for histopathological changes to the central nervous system. A further test of the

hypothesis was performed by inoculated WEEV directly into the brain of hamsters and then observing disease outcome and histopathological changes in the brain.

Experiments showing moderate improvement in the disease outcome of WEEV-inoculated hamsters led to the hypothesis that animals were dying due to overwhelming systemic inflammation. Experiments designed to evaluate changes in serum biochemistry, to maximize anti-inflammatory therapy, and to block inflammation via immunosuppression were conducted to test this hypothesis.

It was also hypothesized that direct virus killing of target cells was the primary cause for pathology and mortality in hamsters, and that this disease phenotype is unique to the virus strain examined. Experiments evaluating the effect of virus dose on the severity of disease and comparing the disease phenotype in hamsters inoculated with one of 2 different virus strains were conducted to test these hypotheses.

Observations of note from disease characterizations included increases in serum concentration of the cytokines interferon and tumor necrosis factor-alpha (TNF-alpha), as well as a severe lymphopenia noted in the latter portions of the systemic disease. These parameters were examined further in attempts to identify antemortem markers of disease outcome and to further understand the pathogenesis of WEEV infection in hamsters.

Due to the observation that serum concentrations of the inflammatory cytokine TNF-alpha were increased in virus infected hamsters it was hypothesized WEEV could induce production of TNF-alpha from hamster macrophages *in vitro*. It was further hypothesized that common anti-inflammatory compounds could reduce the production of TNF-alpha from virus exposed macrophages. Studies examining the effect of WEEV on hamster peritoneal macrophages and the effect of concurrent treatment with anti-



inflammatory compounds were conducted to test this hypothesis. Due to the presence of lymphocytic necrosis in WEEV-infected hamsters it was hypothesized that WEEV could directly induce destruction of lymphoid cells. It was further hypothesized that inflammatory cytokines could enhance virus killing of lymphoid cells. To test this hypothesis a series of experiments examining the effect of WEEV, alone and in combination with the supernatant from WEEV stimulated macrophages, were conducted using hamster splenocytes.

## LITERATURE REVIEW

### **Arboviral Encephalitides**

Arboviruses are the most common cause of encephalitis worldwide.<sup>247</sup> Arboviral encephalitides are primarily small membrane-bound positive-stranded RNA viruses of the Flaviviridae family, and members of Togaviridae family particularly members of the Alphavirus genus.<sup>174,197</sup> These families of viruses have worldwide spread, present an ongoing widespread threat to human and animal health, and have been considered potential bioterror agents.<sup>215</sup> Encephalitic arboviruses of particular concern in North America include the flaviviruses West Nile and St. Louis encephalitis viruses, while alphaviruses of note include Venezuelan, eastern, and western equine encephalitis viruses.

In the current study 3 viruses were used: Banzi virus, a flavivirus, and Semliki Forest and western equine encephalitis viruses, both alphaviruses. While Banzi and Semliki Forest viruses are not naturally occurring threats to public health in North America, they were used in this study, as they have been in previous studies, as surrogates in place of related but more virulent virus species.<sup>9,58,112,184,216,217</sup>

Banzi virus was first isolated from the serum of a febrile boy in Johannesburg, South Africa in 1956.<sup>221</sup> The virus is serologically related to Uganda S and yellow fever viruses.<sup>36</sup> Little work has been done to examine the Banzi virus genome, but analysis of its *NS5* gene also shows a relationship to yellow fever virus.<sup>84</sup> Banzi virus has been isolated from mosquitoes, cattle, and rodents in South Africa, Mozambique, Zimbabwe and Kenya,<sup>159,160,163</sup> while neutralizing antibodies to Banzi virus have been found in

human sera from South Africa, Mozambique, Angola, Namibia and Botswana.<sup>138,221</sup>

Banzi virus is not a common human pathogen, but it has been associated with a case of febrile illness in Tanzania.<sup>248</sup> The natural transmission cycle of Banzi virus is poorly understood but the natural host is probably rodents. Experimental work with Banzi virus has been conducted almost exclusively in rodents, but Banzi virus infection can cause abortion in experimentally infected pregnant ewes.<sup>17</sup> In laboratory rodents inoculation with Banzi virus follows a typical biphasic pattern. Following peripheral inoculation the virus infects and replicates in multiple systemic tissues, particularly in lymphatic tissues,<sup>26</sup> and induces a febrile state.<sup>216</sup> Following the peripheral phase of infection the virus enters the brain, causing a lethal meningoencephalitis.<sup>112</sup> The primary cause of mortality in rodents associated with experimental infections appears to be due to viral induced pathology of the central nervous system, and is not associated with virus replication in peripheral tissues. Following virus inoculation mice found to be genetically resistant to mortality due to Banzi virus infection have similar levels of virus in peripheral non-neural tissues as that seen in susceptible mice, but they have significantly lower viral titers in the brain.<sup>26</sup> Additionally, both resistant and susceptible strains of mice have similar levels of virus replication, and similar degrees of mortality when the virus is inoculated intracranially.<sup>112</sup> The ability to survive virus infection in resistant strains of mice appears to be tied to the peripheral cell-mediated immune response as adoptive transfer of immune cells from resistant strains protects susceptible strains from virus-induced mortality,<sup>113</sup> while immunosuppression or T-cell depletion increases susceptibility regardless of mouse strain.<sup>25</sup> Most nucleoside analog antiviral drugs are poorly efficacious against Banzi virus infection in mice,<sup>218</sup> whereas, treatment

of animals with interferon,<sup>184</sup> or use of immunomodulatory and interferon inducing agents can be highly effective at limiting virus spread *in vivo* and at protecting animals from lethal infections.<sup>119,179,184,208,216</sup>

Semliki Forest virus is an Old World alphavirus and a prototypical member of the Semliki Forest complex of viruses. SFV was isolated from *Aedes abnormalis* mosquitoes collected in the Semliki Forest region of western Uganda in 1942.<sup>219</sup> Although infection with SFV has rarely been associated with human disease, experimental infection with SFV can cause encephalitis in horses, mice, rats, hamsters, rabbits, and guinea pigs.<sup>10,29,220,254</sup>

Two primary disease phenotypes occur in laboratory rodents following inoculation with SFV, with disease type, and severity being dependent upon, age and species of host, animal strain in the case of mice, and virus strain.<sup>231</sup> Inoculation of mice with viruses based upon the so-called avirulent strains of SFV (e.g. A7 strain) results in no apparent short-term disease, but produces a demyelinating pathology of the central nervous system if animals are allowed persist for adequate periods of time.<sup>16,70,130,189</sup> In comparison infections based upon the virulent strains (e.g. Original or L10 strains) will result in fatal encephalitis.<sup>16,189</sup> Following peripheral inoculation SFV animals develop viremia, and virus replication is detected in multiple body tissues, including spleen and muscle, before the virus invades the central nervous system.<sup>95,172</sup> The virus also infects brain endothelial cells, altering the function of the blood-brain barrier.<sup>74</sup> The primary target of SFV in the brain appears to be neurons.<sup>77,133</sup> Infection of neurons with either virulent or avirulent strains of SFV results in both apoptosis and necrosis,<sup>130,131,204</sup> with virulent strains causing more rapid and more widespread cell death.<sup>16</sup>

Similar to many other encephalitic arboviruses SFV is poorly sensitive to nucleoside analog antiviral agents such as ribavirin.<sup>38,217</sup> But SFV is sensitive to the antiviral effects of interferon and interferon inducers, but only if these agents are administered either previrus-exposure or very early in the virus infection.<sup>58,168,184,216,217</sup>

Western Equine Encephalitis virus, also known as Western Equine Encephalomyelitis virus, is a New World alphavirus, and the prototypical virus of the WEEV complex. Other members of the WEEV complex of viruses include the Highlands J, Fort Morgan, and Aura viruses. Phylogenetically, WEEV is mostly closely related to other New World alphaviruses: Eastern Equine Encephalitis virus and members of the Venezuelan Equine Encephalitis virus complex.<sup>37</sup> WEEV was originally isolated in 1930 from the brain of 2 horses in California during an outbreak of equine encephalitis.<sup>164</sup> Following isolation WEEV was shown to readily infect and cause disease in a wide variety of species, including monkeys, rats, mice, rabbits and guinea pigs. Mosquitoes are considered to be the primary transmission vector in naturally occurring infections. Mosquitoes of the *Aedes aegypti* species can be experimentally infected with WEEV and transmit it to new hosts.<sup>127</sup> Isolation of WEEV from *Culex tarsalis* mosquitoes in naturally occurring epizootic outbreaks identify this mosquito species as the principal natural arthropod vector.<sup>102</sup> WEEV is widely distributed in the western United States and Canada, and in South America.<sup>110,117,239</sup> In North America, WEEV is maintained in an endemic cycle involving birds (particularly finches and sparrows) and *Culex tarsalis* mosquitoes.<sup>35</sup>

Since WEEV was first isolated from the brain of a horse it was suspected of causing human disease.<sup>165</sup> The suspicion was confirmed in 1938 when WEEV was

isolated from the brain of a child with fatal encephalitis.<sup>109</sup> Since that time WEEV has been recognized as the cause of major epizootics in the years 1931, 1933-1935, 1937, 1938, 1941, 1944, 1947, 1950, and 1952.<sup>35</sup> Between the years of 1964 and 2005 a total of 639 confirmed cases of WEEV infections in humans have been reported.<sup>42</sup>

Disease in individuals infected with WEEV results in a typical biphasic disease pattern similar to that seen with other alphavirus encephalitides. There is a prodromal phase with symptoms of fever and headaches. This is similar to the disease signs noted in horses infected WEEV wherein signs of fever, anorexia, and mild depression are noted.<sup>227</sup> In many instances the disease does not progress beyond the initial febrile period. In those individuals in which the disease does progress symptoms may include restlessness, irritability, nuchal rigidity, photophobia, altered mental status, and paralysis.<sup>32,79,80</sup> Horses can present with parallel signs of ataxia, somnolence, a stiff neck, and head pressing. More severe signs may develop, including blindness, circling head tilt, nystagmus and seizures.<sup>68,88,227</sup> Pathological changes in the central nervous system of humans or horses infected with WEEV or New World alphavirus encephalitides are similar. Pathological lesions are most often seen in the brainstem, cerebellum, cerebrum and spinal cord. Lesions may include hemorrhage, lymphocytic infiltrate, perivascular cuffing, neuronal apoptosis and necrosis, and leptomeningitis.<sup>63,79,81,164,167,199</sup>

### **Blood-Brain Barrier in Viral Disease**

The blood-brain barrier (BBB) is a functional and structural component of the central nervous system (CNS) vasculature that serves important protective functions for the CNS. It is composed of highly specialized endothelial cells in the CNS vasculature.

The physical apposition of astrocyte foot-processes on the abluminal side of the endothelial cells, and the production of various trophic factors by astrocytes directly impacts the function of the BBB.<sup>104</sup> The specialized endothelium of the BBB is able to selectively transport molecules into the CNS (e.g. glucose, insulin) while limiting the entry of hydrophilic compounds and toxins as well as circulating leukocytes.

It has long been recognized that the ability of the BBB to exclude substances from the CNS is often compromised during infection and inflammation of the CNS. The exact mechanisms of BBB breakdown and its role in the disease progression of viral encephalitis are currently unknown. However, a number of inflammatory cytokines, whose expression levels can be increased in association with viral infection, have been demonstrated to increase permeability of the BBB. Levels of matrix metalloproteinases (MMPs) are increased in the cerebrospinal fluid of patients with human immunodeficiency virus (HIV) encephalitis, as is the permeability of the BBB.<sup>54</sup> Infection of mice with an avirulent strain of the Semliki Forest virus (SFV) significantly increased the expression of MMP-2 & 9, and increased the permeability of the BBB, while treatment with an inhibitor MMPs significantly improved the condition of the BBB.<sup>131</sup>

The exact role of the BBB in the pathophysiology of viral encephalitis is poorly understood. However, increased permeability of the BBB appears to be a vital component of viral encephalitic pathology. Mortality associated with infection of nonneuroinvasive strains of West Nile virus or Sindbis virus can be greatly enhanced by prior administration of lipopolysaccharide,<sup>151</sup> which is known to increase BBB permeability.<sup>151,250</sup> SFV can infect and damage endothelial cells of the BBB

endothelium.<sup>74</sup> Permeability of the BBB is also seen in encephalitis associated with HIV<sup>61</sup> and in murine models of lymphochoriomeningitis virus.<sup>5</sup>

A variety of methods have been used to evaluate the function of the BBB.

Leakage of systemic proteins, such as fibrinogen or albumin, into the CNS have been used to assess BBB permeability associated with HIV associated encephalitis,<sup>61</sup> simian immunodeficiency virus encephalitis<sup>148</sup> and a mouse model of experimental allergic encephalomyelitis induced by infection with an avirulent strain of SFV.<sup>74</sup> While these techniques have the benefit of using endogenous proteins they are highly dependent upon the skill of the evaluator, and are semiquantitative at best. Additional methods involve the injection of a radioactively labeled marker, as was used in a mouse model of lymphochoriomeningitis virus.<sup>5</sup> Use of radioactive markers can provide highly accurate and detailed information regarding the degree of BBB permeability, as well as giving the ability to spatially identify areas of variable BBB permeability within the CNS.

However, use of radioactive materials poses a potential risk to laboratory personnel and requires additional oversight and precautions for disposal of isotopes as well as animal remains. In contrast, fluorescent markers, such as sodium fluorescein (NaFl) provide a safe and relatively simple means to evaluate the function of the BBB. NaFl is a small molecular weight marker (MW 367) that has been widely used in a variety of model systems for evaluation of BBB permeability.<sup>65,75,97,108,140</sup>

### **Atypical Disease Phenotypes Associated with Arboviral Infection**

Broadly categorized arboviruses may be classified as being encephalitic or nonencephalitic depending upon the primary disease manifestation associated with viral



infection. However, atypical disease phenotypes can be observed. Nonencephalitic viruses can invade the central nervous system following a systemic disease phase. Also, primary encephalitides have the potential to cause severe disease in non-neuronal tissues. Finally, in experimental infections host-virus interactions appear to play a vital role in determining disease manifestations, as different species infected with the same virus can display widely divergent disease phenotypes.

Dengue virus is an arbovirus of the Flaviviridae family. The primary disease associated with dengue virus is dengue fever, a severe flu-like illness.<sup>178,226</sup> A less common but more severe form of dengue virus infection is dengue hemorrhagic fever, in which patients develop system-wide vascular leakage and hemorrhage, potentially leading to shock and death.<sup>202</sup> However, naturally occurring infections resulting in dengue virus encephalitis have been reported in both India,<sup>166</sup> Vietnam,<sup>225</sup> and Brazil<sup>223</sup> wherein patients exhibited a variety of neurological disease symptom including weakness, paralysis, confusion, headache, and alterations in the cerebrospinal fluid. Naturally occurring infections with the related flavivirus yellow fever virus have not been associated with cases of viral encephalitis. However, encephalitis has been reported in association with adverse reactions to commercial yellow fever vaccines, although these events are exceptionally rare.<sup>157</sup> Similarly monkeys inoculated with vaccine strain virus also have the potential to develop a viral encephalitis.<sup>155</sup>

The Rift Valley fever (RVF) virus of the family Bunyaviridae is a zoonotic disease primarily causing abortion, hepatitis, hemorrhage, and death among domestic ruminants.<sup>87</sup> It is transmitted to humans either via bites by infected mosquitoes or through contact with contaminated tissues. In humans infection with RVF is usually

associated with a self-limiting febrile illness,<sup>162</sup> and in more severe cases it can produce a potentially fatal hemorrhagic disease.<sup>86</sup> In rare instances, RVF can also proceed to infect the central nervous system and produce encephalitis, meningitis, and retinitis.<sup>2,4</sup> The Alkhumra virus, a bunyavirus related to RVF, is another arbovirus that primarily causes hepatitis and hemorrhagic manifestations, but it also the potential to cause viral encephalitis.<sup>153</sup>

Viral encephalitis is the primary human health concern associated with infection by many arboviruses of the Flavi- and Togaviridae families. However, there have been many reports of naturally occurring infections with arboviral encephalitides in which severe pathology occurs outside the CNS. Most arboviral encephalitides exhibit a biphasic disease pattern with an initial systemic phase of viral replication and dissemination in nonneuronal tissues, followed by a second phase of infection involving the central nervous system and encephalitis. The initial systemic phase of virus infection presents the possibility for tissue pathology, morbidity and mortality due to the peripheral virus infection in the absence of viral damage to the central nervous system. Avian species in particular appear to be sensitive to the non-neuronal aspects of arboviral infection. West Nile virus (WNV) infection in humans and horses follows the familiar biphasic disease pattern as seen with other viruses with that display initial signs of febrile disease followed by signs of encephalitis.<sup>34,50,101,118,187,211,222,250</sup> Furthermore, the histopathological lesions noted in naturally occurring infections in humans and horses are almost exclusively within the CNS.<sup>39,205,250</sup> Nonneuronal lesions associated with WNV infection are rarely identified in mammalian hosts. However, in avian hosts multiple species of birds infected with WNV develop splenomegaly and severe myocarditis in

addition to CNS lesions.<sup>228,233</sup> In contrast to the neuropathology seen in human infections of EEE,<sup>22</sup> a naturally occurring EEE infection in an egret resulted in severe hepatic necrosis and necrosis of sheathed arterioles in the absence of any detectable pathology in the CNS.<sup>92</sup> EEE infection of turkeys resulted in lymphocytic and pancreatic necrosis as well as high mortality.<sup>78</sup> Emus infected with EEEV experienced acute mortality and had necrosis in the liver and spleen<sup>240</sup> while in ostriches EEEV infection produced a hemorrhagic colitis.<sup>31</sup> Naturally occurring arboviral infections in mammals can also result in severe nonneuronal pathology. Horses diagnosed with an infection of EEEV were found to have necrotic lesions in the heart, intestine, urinary bladder and spleen in addition to CNS lesions.<sup>64</sup> Lethal human infections of VEEV cause necrosis in both spleen and lymph nodes in addition to central nervous system lesions.<sup>63</sup> A lethal disease phenotype of VEEV infection in humans occurs, which occurs primarily in children, is described as a fulminant infection, and is considered to be primarily due to the viral destruction of lymphocytes and lymphoid tissue and generally lacks pathological changes to the CNS.<sup>72</sup>

In experimentally infected animals the virus-host interaction appears to play a vital role in determining the propensity for an arbovirus to cause either encephalitis or pathological changes in nonneuronal tissues. As noted previously, West Nile virus is considered to be a primarily neurotropic pathogen and produces few histopathological lesions outside of the central nervous system. However, domestic chickens experimentally infected with WNV develop myocarditis and nephritis in addition to encephalitic lesions.<sup>213</sup> The Alphaviruses EEE, WEE, and VEE viruses are also considered primary encephalitides in humans and domestic mammals. However, as seen

with naturally occurring infections, experimental inoculations of domestic birds with Alphavirus encephalitides can often produce nonneuronal disease phenotypes. Chickens and turkeys inoculated with either EEEV or the Highlands J virus (from the WEEV complex of viruses) develop necrosis in multiple nonneuronal tissues, including heart, kidney, pancreas, and lymphoid tissues.<sup>99,100</sup> Infection of turkeys with WEEV results in lymphoid necrosis.<sup>55</sup> Guinea pigs or rabbits inoculated with a virulent strain of VEEV often develop lymphoid necrosis and die from an apparent shock-like death.<sup>93,236</sup> In contrast to the significant peripheral pathology noted in other species, mice inoculated with the EEEV, WEEV, VEEV or with West Nile virus develop a neurological disease with little peripheral signs of pathology.<sup>27,45,103,111,149,169,242</sup> Interestingly, mice also develop an encephalitic disease after inoculation with a vaccine strain of the hepatotropic yellow fever virus.<sup>30,43</sup> Although poorly understood, the host-virus relationship plays a vital role in determining the disease phenotype that will be observed.

### **Experimental Alphavirus Infections in Syrian Golden Hamsters**

Mice are by far the most commonly used animal model for studying alphavirus infections. However, hamsters are recognized as a potential animal model for the study of alphavirus pathogenesis and the testing of potential antiviral compounds.<sup>120</sup> Viruses that have been tested in hamsters include SFV, EEEV, WEEV, and VEEV. Hamsters infected with alphaviruses commonly develop viral encephalitic diseases, similar to those seen in mice and other laboratory animals as well as diseases seen in naturally occurring infections. However, other disease phenotypes with a predominantly peripheral pathology can occur in hamster models of alphavirus infections.

SFV is a strongly neurotropic virus that appears to efficiently infect neurons in the central nervous system. Adult hamsters exposed to aerosolized SFV express replicating virus in multiple organs, including lymphoid tissue, kidney, liver, and lungs.<sup>105</sup> The neurotropic nature of the virus is verified by the fact that nervous tissue develops the highest viral titers. Virus titers in the brain rise rapidly following virus exposure, reaching peak levels within 2 d. Shortly after SFV enters the brain hamsters develop a severe necrotic and hemorrhagic encephalitis.<sup>105</sup> SFV infection in neurons causes alterations and degeneration of cellular organelles leading to cell death.<sup>254</sup> Simultaneous with the neuronal infection by SFV, other CNS cell types respond via proliferation and hypertrophy, particularly in the case of astrocytes.<sup>253</sup> Histopathological lesions can be found throughout the brain and spinal cord by 4 d post-virus exposure, particularly within the olfactory bulb. Animals may also develop an acute hepatitis. Death usually ensues within 5 d following virus exposure.<sup>105</sup>

Previous reports on the study of WEEV virus infection in hamsters indicate the disease pathogenesis is similar to that described for SFV in hamsters. Following virus inoculation, animals develop both a febrile and central nervous system disease, and rapidly succumb to death within 6 d of virus exposure.<sup>255</sup> Hamsters inoculated with a virulent strain of WEEV show virus replication in multiple body tissues, including liver, lymphoid tissues and kidneys.<sup>120</sup> Hamsters also rapidly develop high virus titers in nervous tissue, followed by the appearance of CNS hemorrhage and necrotic histopathological lesions. Perivascular cuffing of lymphocytic cells and astrocyte hypertrophy accompanied the necrosis and hemorrhage.<sup>255</sup> As reported with other alphaviruses, WEEV infection in hamsters is sensitive to interferons and

immunomodulatory agents. Pretreatment of hamsters with either recombinant human interferon alpha/beta or an interferon inducer can protect up to 100% of animals inoculated with a lethal dose of WEEV, whereas placebo-treated animals rapidly succumb to virus infection by 5 d post-exposures.<sup>120</sup> Although not widely studied, EEEV infection in hamsters follows the pattern described for both SFV and WEEV, with widespread systemic replication of the virus followed by an invasion of the virus into the CNS and the production of very high virus titers in the brain.<sup>181</sup> EEEV in hamsters causes hepatic necrosis and lymphoid degeneration in the viscera. EEEV also readily infects neurons, causing necrosis and hemorrhage in the CNS accompanied by a primarily lymphocytic inflammation in the brain.<sup>71</sup> In addition to the CNS necrosis a severe vasculitis associated with nervous tissue has also been noted in the brain of EEEV inoculated hamsters.<sup>181</sup>

In contrast to the primarily CNS lesions noted in hamsters inoculated with SFV, EEEV, or WEEV, hamsters inoculated with virulent strains of VEEV develop histopathological lesions in peripheral organ tissues. Lesions in VEEV-infected hamsters include necrosis and degeneration in the pancreas affecting both islet and acinar cells<sup>90</sup> with subsequent glucose intolerance in surviving animals.<sup>192</sup> However, the most striking lesions are severe and rapid necrosis in thymus, spleen, lymph nodes and gut-associated lymphoid tissue and bone marrow.<sup>243</sup> Lesions can appear rapidly, with necrosis noted in the thymus occurring as soon as 2 d after subcutaneous inoculation with VEEV. Necrosis occurs in other lymphoid and hematopoietic tissues shortly thereafter until all of these tissue types examined display severe widespread necrosis.<sup>11,116</sup> In addition to the necrosis noted in the bone marrow, VEEV infection also

induces chromosomal changes in bone marrow tissue, resulting in aneuploidy, although the mechanisms for this effect is unknown.<sup>188</sup> Following infection animals die precipitously, with death occurring within 96 h post-virus inoculation.<sup>90,91</sup> Although live virus may be detected in the brains of hamsters inoculated with VEEV no animal has displayed histopathological lesions in the central nervous before the time of death.<sup>111</sup> The rapid death noted in VEEV infection in hamsters is apparently not due to viral induced damage of the CNS, but rather associated with an apparent septicemia and septic shock subsequent to destruction of gut-associated lymphoid tissues and bacterial translocation from the gastrointestinal tract into systemic circulation.<sup>91</sup> Gram-negative pleiomorphic rods identified as *Escherichia coli*, and *Proteus mirabilis* can be isolated from the blood of VEEV-infected hamsters. These organisms are consistent with normal gastrointestinal flora in hamsters. Furthermore, treatment of hamsters with antibiotics that have an activity spectrum against gram negative enterobacteria significantly prolong survival in VEEV-infected hamsters from less than 4 d to greater than eight. Although neurological involvement is apparently not the primary disease phenotype seen in VEEV-infected hamsters, the neurovirulence of the virus is confirmed by the observation that animals infected with virus strains of lesser virulence survive the initial period of lymphocytic necrosis, but die approximately eight to ten d post virus inoculation, showing severe necrosis and hemorrhage in the CNS.<sup>114,116</sup> Interestingly, the difference in pathogenicity between highly pathogenic and attenuated vaccine strains of VEEV appears to be related to the immune response of the individual animal. Hamsters infected with high doses of the TC-83 vaccine strain of VEEV show low mortality and delayed death. Furthermore, pre-inoculation of hamsters with a low dose of TC-83 protected animals from a

subsequent challenge with virulent VEE strains.<sup>53</sup> Similar protection can be gained by previous exposure to related alphavirus encephalitides such as WEEV virus.<sup>52</sup> However, splenectomized or immunosuppressed animals inoculated with the same TC-83 strain of VEEV display a disease phenotype very similar to that noted with virulent strains of VEEV, presenting with lymphoid necrosis and rapid death.<sup>114</sup>

Neurologic disease and neuropathology are the primary disease phenotype and the histopathological lesions seen in hamsters experimentally infected with alphaviruses. This disease pattern has been reported in hamsters inoculated with SFV, WEEV and EEEV viruses. However, hamsters inoculated with virulent strains of VEEV display a markedly different disease phenotype involving primarily lymphoid and hematopoietic necrosis, and animal mortality is at least in part associated with a secondary bacterial sepsis. This lymphocytic disease phenotype is distinct from the neurological disease phenotype observed in mice inoculated with VEEV<sup>45,111</sup> and appears to be consistent with the fulminant form of VEEV virus infection in some humans where death appears to be associated with peripheral lymphocytic necrosis rather than viral pathology in the CNS.<sup>72</sup>

### **Viral-Mediated Cell Killing Enhanced by Inflammatory Cytokines**

Cytokines perform vital functions in the immune response to viral infections. In many cases, cytokines confer antiviral properties on cells, and may provide cytoprotection. However, *in vitro* evidence indicates that cytokines may also interact with virus infected cells in a manner that potentiates mechanisms of cell death. The reasons that cytokines can enhance virus mediated cell killing are unclear. However, *in vivo* research results suggest that the cell death potentiation by cytokines may be involved



in negative outcomes due to virus infection, and that cytokine-virus interactions play significant roles in the morbidity and mortality associated with some human viral diseases.

As part of the cellular response to virus infection many cell types produce a wide range of cytokines. It is widely recognized that certain cytokines can have protective and antiviral effects in virus-infected cells. Human immunodeficiency virus-induced apoptosis of T lymphocytes can be reduced by treatment with interleukin (IL) -15.<sup>44</sup> The pro-inflammatory cytokine tumor necrosis factor-alpha (TNF-alpha) demonstrates antiviral activity against multiple viruses.<sup>7,249</sup> Treatment of mice with TNF-alpha can reduce expression of the hepatitis B virus genome in transgenic mice.<sup>89</sup> TNF-alpha inhibits murine cytomegalovirus replication, and this effect is synergistically enhanced when combined with interferon gamma.<sup>150</sup> TNF-alpha also inhibits replication of respiratory syncytial virus both *in vitro* and *in vivo*.<sup>176</sup> In particular, interferons have been widely studied for their ability to prevent virus-induced cytotoxicity. Interferon gamma acts to restrict virus replication in endothelial cells.<sup>96,124,212</sup> In animals and humans interferon and interferon inducers have proven to be effective against a wide array of viruses. Use of the interferon inducer Ampligen™ has been shown to prevent morbidity and mortality in animals experimentally infected with viruses such as BaV, SFV, WNV, Modoc virus, Punta Toro virus, WEEV, and VEEV.<sup>120,143,168,169,185,214</sup> The beneficial effects associated with Ampligen™ are primarily seen when treatment is performed in a prophylactic manner. The addition of virus-specific antiserum has been shown to extend the therapeutic window for the use of another interferon inducer, Poly IC:LC, to allow significant protection after animals displayed virus associated fever.<sup>216</sup>

Interferons alone have also proven effective. Use of recombinant alpha/beta interferons has protected animals from lethal infections due to WNV, WEEV, herpes simplex-2 virus, BaV and SFV.<sup>120,169,184</sup>

In contrast to the antiviral and cytoprotective cytokine effects noted previously, cytokines also have the potential to initiate or enhance cell killing in virus-infected cells. In some instances, there is a synergistic effect on virus induced cell death, and in many cases, the same cytokines that display antiviral and cytoprotective effects also participate in mechanisms of cell death. It is generally recognized that cell death associated with a virus infection can follow one of 2 basic pathways: necrosis and apoptosis. Necrosis involves the death of a cell as a result of physical damage or toxic agents. During necrosis, there is disruption of the mitochondria, swelling of the cell, disruption of organized structure, and lysis. Apoptosis is energy dependent and involves cell death in situations controlled by physiologic stimuli during development and hormonal signaling in response to DNA damage. During apoptosis, there is DNA condensation and fragmentation, cell shrinkage, and membrane blebbing. Cell death due to viral infection can result from either mechanism in that viruses may have toxic effects on the host cell, activate programmed cell death pathways, or both.

Treating cells with IL-8 can enhance the cytopathic effect of EMCV and vesicular stomatitis viruses.<sup>132</sup> Transforming growth factor-beta-1 (TGF-beta-1) synergistically enhances HIV induced apoptosis of T lymphocytes.<sup>245</sup> Apoptosis induced by an influenza virus and by equine influenza virus can be enhanced by TGF-beta-1.<sup>146,210</sup>

Interferons have the ability to potentiate virus-induced cell death. The ability of interferons to enhance virus induced cell death was first suggested by Cooper et. al., who

showed that treating mouse fibroblasts with interferon and Poly I:C, a double stranded-RNA (ds-RNA) molecule, produces a profound cytotoxic result.<sup>56</sup> Intracellular ds-RNA is absent during normal cellular function, but it is a common condition in many viral infections. Therefore, the cytotoxic effects of combined ds-RNA and interferon could presumably occur during a viral infection. Other studies suggest that the combination of ds-RNA and interferon can lead to either cellular apoptosis or necrosis depending upon other environmental conditions and the presence of various cytokines.<sup>122</sup> Additional studies have shown interferon's ability to enhance cell death in conjunction with virus infection. The presence of interferon alone does not induce apoptosis in murine embryonic fibroblasts, but the presence of virus and interferon together does, a result which can be mimicked by a combination of ds-RNA and interferon.<sup>235</sup> Treatment of fibroblasts with interferon-alpha sensitizes cells to virus induced apoptosis.<sup>15</sup> The exact mechanisms associated with interferon induced apoptosis are unclear, but interferon can activate the ds-RNA protein kinase,<sup>14,66</sup> or the RNase-L enzyme,<sup>40</sup> both of which can initiate apoptotic pathways.

The inflammatory cytokine TNF-alpha has long had a recognized ability to induce cell death, and in particular has been shown to synergistically enhance virus cell-killing. The *in vitro* cytopathic ability of Simian virus 5, a paramyxovirus, is positively correlated with increased concentrations of TNF-alpha in culture media, and the virus cytopathic effect is ameliorated by the use of TNF-alpha blocking antibodies<sup>147</sup> Tula virus, a hantavirus, synergistically interacts with TNF-alpha to speed and increase apoptosis in virus-infected cells *in vitro*.<sup>145</sup> Similarly, TNF -alpha speeds apoptosis in cells infected with vesicular stomatis virus<sup>139</sup> while viral proteins from the Epstein-Barr virus<sup>126</sup> or the

hepatitis B virus<sup>135</sup> significantly enhance the sensitivity of cells to apoptosis induced by TNF-alpha. TNF-alpha also plays an important role in inducing apoptosis in cells infected with a cytopathic strain of bovine viral diarrhea virus. Blockage of TNF-alpha activity significantly reduces the virus associated apoptosis.<sup>251</sup> Reovirus upregulates cellular receptors for the TNF-related apoptosis inducing ligand (TRAIL), which can enhance virus-induced apoptosis in both murine and human cell lines.<sup>51</sup> TRAIL also enhances viral-induced apoptosis in a hepatic cell line infected with dengue virus.<sup>158</sup>

The role of cytokines in enhancing cytotoxicity in virus infected cells is more difficult to demonstrate *in vivo*, and in many instances the relationship between inflammatory cytokines and increased cytotoxicity is only correlative. However, evidence reported in the literature appears to confirm the ability of some inflammatory cytokines to synergistically enhance virus cell-killing in the whole animal. Infection of rhesus macaques with pathogenic simian immunodeficiency virus results in elevated concentrations of IL-18 and enhanced T lymphocyte apoptosis when compared to infection with a non-pathogenic strain.<sup>121</sup> The cytokines IL-6, IL-10, and TNF-alpha are positively correlated with increased myocardial necrosis and increased mortality in mice inoculated with encephalomyocarditis virus (EMCV).<sup>246</sup> In pigs inoculated with classic swine fever virus serum concentrations of the cytokines TNF-alpha, IL-1a and IL-6 were increased and positively correlated with lymphoid depletion and lymphocyte apoptosis.<sup>206</sup> In chickens inoculated with the infectious bursa disease virus increased amounts of IL-6 and IL-18 correlate well with macrophage lysis and decreased numbers of macrophages.<sup>134,182</sup> Mice inoculated with an avirulent strain of SFV show decreased neuronal necrosis in animals that are lacking an active form of IL-4.<sup>129</sup>

Immunocompetent mice inoculated with a virulent strain of VEEV display severe splenic necrosis, whereas severe combined-immunodeficient mice infected with the same strain of VEEV do not show similar lymphoid necrosis, suggesting a role for the immune system in promoting necrosis.<sup>45</sup> A murine equivalent of human IL-8, macrophage inflammatory protein-2 (MIP-2) is increased in murine macrophages infected with EMCV, while the serum MIP-2 in mice inoculated with EMCV is similarly raised. Treatment of EMCV inoculated mice with anti-MIP-2 antibodies improves survival and lessens the degree of inflammation and necrosis in cardiac tissues.<sup>137</sup> Similar results are seen in animals infected with the cardiotropic Coxsackievirus, wherein treatment of Coxsackievirus infected mice with anti-MIP2 antibodies reduces mortality and reduces the severity of virus-associated histopathological lesions in cardiac tissue.<sup>136</sup> Liver biopsies from fatal human cases of yellow fever virus exhibit increased apoptosis, while also exhibiting increases in the concentrations of the cytokines TNF-alpha, interferon-gamma, and considerably higher concentrations of TGF-beta-1.<sup>190</sup> Indeed, this proposed interaction between yellow fever virus and inflammatory cytokines is hypothesized to be responsible for some of the characteristic histopathological lesions in the liver of virus infected individuals.<sup>191</sup>

### **Lymphopenia Associated with Arboviral Encephalitides**

Lymphopenia, a decrease in the number of circulating lymphocytes, is a nonspecific clinical laboratory finding observed in many disease states. It is commonly identified in association with infectious disease, and in particular in association with viral disease. Lymphopenia has often been noted in association with arboviral infections, both

in laboratory animals and in those occurring naturally. The degree of lymphopenia observed has often been found to have prognostic value in determining the outcome of a virus infection.

Broadly speaking, lymphopenia associated with viral disease is due to either sequestration of lymphocytes or lymphocyte destruction. Sequestration during a virus infection involves migration of lymphocytes from peripheral circulation into lymphatic organs, and minimization of recirculation, and is usually transient.<sup>69</sup> Increases in inflammatory cytokines appear to play important roles in directing the movement of lymphocytes out of the circulation. Increased concentrations of interferons in particular decrease recirculation of lymphocytes. Macaques inoculated with simian immunodeficiency virus expressed high amounts of interferon immediately preceding and during dramatic decreases in the numbers of circulating lymphocytes.<sup>201</sup> Mice inoculated with vesicular stomatitis virus display a substantial lymphopenia. This lymphopenia is absent in transgenic mice lacking the receptor for interferon alpha.<sup>123</sup> TNF-alpha can also affect the ability of lymphocytes to circulate in the blood. Injection of recombinant TNF-alpha into rats causes a transient lymphopenia.<sup>238</sup> Similarly, both mice and humans treated with endotoxin, a known inducer of TNF-alpha expression, also display a dramatic but transient decrease in circulating lymphocytes, suggesting a temporary redistribution of lymphocytes.<sup>57</sup> TGF-beta-1 also can alter circulating lymphocyte counts by moderating lymphocyte migration through tissues.<sup>76</sup>

In addition to viruses and cytokines altering the migration and recirculation of lymphocytes, lymphopenia in virus infection may be the result of virus and cytokine-mediated lymphocyte destruction. Interferons and TNF-alpha are 2 cytokines commonly

observed to be upregulated during a viral infection. Increased interferon concentrations can lead to lymphocyte apoptosis and death. Administration of the interferon inducer Poly IC to mice decreases the numbers of circulating lymphocytes and induces lymphocyte apoptosis by stimulating the expression and activation of the pro-apoptotic enzymes caspase-3 and caspase-8.<sup>13,161</sup> TNF-alpha alone can also induce apoptosis in lymphocytes.<sup>98</sup>

Virus infection alone may be able to induce apoptosis in lymphocytes. Lymphopenia occurs in humans, monkeys, ferrets, and mice infected with influenza viruses.<sup>18,49,125,252</sup> In mice inoculated the highly pathogenic H5N1 strain of influenza the decreased number of lymphocytes occurs simultaneously with decreasing concentrations of circulating interferon, indicating that the lymphopenia may be due to a direct viral destruction of lymphocytes.<sup>237</sup> Dogs infected with the paramyxoviral pathogen canine distemper virus displayed lymphopenia and increased apoptosis in correlation with increased viral antigen in their systems.<sup>209</sup> Swine infected with hog cholera virus show virus infection, necrosis of peripheral lymphoid tissues and severe lymphopenia.<sup>175</sup>

Although cytokines alone or virus alone may induce lymphocyte death, it is most likely that the lymphocytotoxic effects noted in virus-infected animals or people are due to an interaction between multiple effectors. This can be observed in multiple models of viral disease. Swine infected with the classic swine fever virus (CSFV) show viral-induced lymphocyte apoptosis,<sup>232</sup> and it appears that TNF-alpha plays an important role in lymphocyte destruction by enhancement of apoptosis in CSFV infected cells.<sup>206</sup> TNF-alpha also promotes lymphocytic apoptosis in cats infected with the coronavirus feline infectious peritonitis virus.<sup>234</sup> Additionally, lymphocytes in infants infected with

respiratory syncytial virus have upregulated tumor-necrosis factor receptors, making them more sensitive to apoptotic signals.<sup>200</sup>

Although lymphopenia is a nonspecific clinical laboratory finding in many viral infections, it has been evaluated for its prognostic value. Lymphopenia is detected in up to 97% of patients suffering from an infection with severe acute respiratory syndrome (SARS) virus.<sup>48</sup> Although lymphopenia does not show strong prognostic indicators of death associated with the SARS virus infection, it is strongly correlated with respiratory abnormalities detected in children via computed tomography.<sup>144</sup> The degree of lymphopenia in children infected with respiratory syncytial virus is strongly correlated with the severity of disease and the amount of therapeutic intervention necessary.<sup>177</sup> Lymphopenia is observed in bone marrow transplant recipients infected with cytomegalovirus, and death associated with cytomegalovirus infection is only observed in those patients in which the lymphopenia persists.<sup>73</sup> Lymphopenia is also a common finding in patients infected with West Nile virus, but severe lymphopenia has shown its prognostic value by being associated with either death or severe persistent neurological deficits in West Nile virus-infected individuals.<sup>59</sup> The relationship between viral disease and decreased numbers of circulating lymphocytes is not clear, but the presence and degree of lymphopenia has been shown to have prognostic value in naturally occurring infections, and may be used as a valuable tool in animal models of virus disease.

Although the exact mechanisms have not been investigated, lymphopenia is often noted as a clinical laboratory finding in both humans and animals infected with various arboviruses. Monkeys experimentally inoculated with flavivirus members of the tick-borne encephalitis group of viruses were observed to have severe lymphopenia before



death, in addition to the presence of lymphoid necrosis observed after death.<sup>128</sup>

Humans presenting with naturally occurring WNV infections often display profound lymphopenia, and the finding of lymphopenia in conjunction with other clinical signs of viral encephalitis is considered to be a diagnostic indicator of potential WNV infection.<sup>60</sup> Similarly, individuals infected with the Japanese encephalitis virus, a flavivirus related to WNV, consistently display severe lymphopenia, although it appears to be mediated by a predominant lack of T lymphocytes.<sup>46</sup> Experimental infections in guinea pigs with the pichinde virus, an Arenavirus, can also produce severe lymphopenia in conjunction with lymphatic and hepatic necrosis.<sup>115</sup> Alphavirus infections also have dramatic effects on the number of circulating lymphocytes. Humans infected with VEEV usually develop an absolute leukopenia, which is dominated by a dramatic lymphopenia.<sup>67</sup> In addition to viral encephalitis, ponies experimentally infected with a pathogenic strain of VEEV isolated in Chiapas, Mexico were found to have lymphopenia as well as necrosis and lymphocyte depletion in peripheral lymphoid organs.<sup>203</sup> Both guinea pigs and rhesus macaques experimentally infected with VEEV exhibit similar patterns of decreased numbers of circulating lymphocytes, with the onset of lymphopenia occurring within 2 d following virus exposure.<sup>241</sup> Indeed, the lymphopenia is still seen if animals are exposed to aerosolized VEEV<sup>196</sup> or even if animals are treated with a modified live vaccine of VEEV.<sup>195</sup> Similar, although not as severe, decreases in circulating lymphocytes are seen in rhesus macaques following exposure to aerosolized EEEV or WEEV.<sup>193,194</sup> Finally, although naturally occurring infections of encephalitic alphaviruses are rarely reported in species other than humans, equines, or birds, a case of EEEV infection in a young lamb

has been recently reported wherein the animal developed severe lymphopenia in addition to fever and neurological abnormalities preceding death.<sup>21</sup>

Decreased numbers of circulating lymphocytes is a common correlate of many viral infections. The exact mechanisms that result in lymphopenia are not always clear, but are likely the result of decreased lymphocyte recirculation in response to a variety of cytokines, or lymphocyte destruction as a result of virus infection, cytokine-mediated cell death, or very likely a combination of factors. Although mechanisms of lymphopenia are poorly understood, low lymphocyte counts often have prognostic value. The more severe or the greater the duration of lymphopenia, the poorer the disease outcomes. Finally, many arboviral infections, both naturally occurring and experimental, are associated with varying degrees of lymphopenia.

### **Compounds**

The interferon inducing agent Ampligen<sup>TM</sup> (poly I: poly C<sub>12</sub>U) is a known antiviral agent. Ampligen<sup>TM</sup> has proven to be effective against the viruses being tested here. The antiviral mechanisms of interferons and interferon inducers have previously been reviewed.<sup>62</sup> It is recognized that the primary mechanism of action of Ampligen<sup>TM</sup> is via activation of toll-like receptor-3 (TLR-3) on cells. This results in production of alpha/beta interferons. Interferons in turn induce an antiviral state within multiple cell types.

The compound flunixin meglumine (FM) (trade name Banamine<sup>TM</sup>) is a widely used anti-inflammatory compound approved for use in animals. Its primary mechanism of action is considered to be inhibition of cyclooxygenase (COX) enzymes. FM is a

broad spectrum COX inhibitor with significant inhibitory action against both COX-1 and COX-2.<sup>24</sup> In addition to its COX inhibitory actions FM inhibits the activity of nuclear factor kappa B (NF kappa B), an intracellular transcription factor involved in multiple inflammatory pathways.<sup>33</sup> FM has been widely used in treatment of pain and fever in animals, and reduces the endogenous response to endotoxin.<sup>152</sup>

Dexamethasone (DEX) is a synthetically derived glucocorticoid, with actions similar to endogenous cortisone. DEX and related glucocorticoids are widely used in both human and veterinary medicine to control inflammation and induce immunosuppression. The means by which DEX reduces inflammation are not fully understood. However, it can readily reduce the effects of multiple inflammatory stimuli including endotoxin and oxygen free radicals.<sup>82,85,244</sup>

## MATERIALS METHODS AND JUSTIFICATION

**Compounds**

Tumor necrosis factor-alpha, also known as cachectin, was provided as a lyophilized powder of its 17 kDa form (Sigma Aldrich, St. Louis, MO). It was dissolved in sterile phosphate buffered saline (PBS), aliquoted, and stored at -70 °C until used.

The interferon-inducing compound Ampligen™ (poly I: poly C<sub>12</sub>U) is a mismatched double-stranded (ds) RNA molecule with proven efficacy against both alphavirus- and flavivirus-associated encephalitis in experimental animal models.<sup>169,184</sup> The compound, (courtesy of David Strayer, Hemispherx Biopharma, Philadelphia, PA) was provided as a viscous 2.4 mg/mL solution (stored at -20 °C) and was diluted in diethylprocarbonate-treated sterile water to the appropriate concentrations.

The anti-inflammatory glucocorticoid dexamethasone was used in both animal-based and cell-based experiment. The compound used in animal studies was provided as a commercially available injectable form at a concentration of 2 mg/ml (Bimeda-MTC, Ontario, Canada). It was stored at 4 °C prior to use. For animals studies it was diluted as necessary in sterile saline prior to injection into animals. It was administered via i.p. injection at a dose of 0.6 or 2.2 mg/kg/d divided into twice daily doses. Dexamethasone used in cell-based assays was acquired as a powder (Sigma Aldrich, St. Louis, MO). It was dissolved in dimethyl sulfoxide (DMSO) to a stock concentration of 200 mM. The compound was subsequently diluted in cell culture media to the appropriate concentrations.

The anti-inflammatory compound flunixin meglumine was used in both animal-based and cell-based experiments. The compound used in animal studies was provided in a commercially available injectable form at a concentration of 50 mg/ml (Banamine™, Schering-Plough Animal Health, Omaha, NE). It was stored at room temperature prior use. For animal studies, it was diluted as necessary in sterile saline prior to injection into animals. It was administered via i.p. injection at a dose of 5 or 15 mg/kg/d divided into twice daily doses. Flunixin meglumine used in cell-based assays was acquired as a powder (Sigma Aldrich, St. Louis, MO). It was dissolved in dimethyl sulfoxide (DMSO) to a stock concentration of 200 mM. The compound was subsequently diluted in cell culture media to the appropriate concentrations.

The fluoroquinolone antibiotic enrofloxacin (Baytril®, Bayer Health Care, Shawnee Mission, KS) is an FDA approved drug for the treatment of susceptible bacterial infections in domestic animals, and has proven bactericidal activity against many gram negative and gram positive bacteria including most species of commensal enteric bacteria. Enrofloxacin was acquired as a commercially available injectable preparation at a concentration of 100 mg/ml. Enrofloxacin was stored at room temperature prior to use. It was diluted in sterile saline to the appropriate concentration prior to injection into animals. It was administered via i.p. injection at a dose of 10 or 100 mg/kg/d divided into twice daily doses.

The antimicrobial drug florfenicol is an FDA approved compound for the treatment of susceptible bacterial infections in domestic animals. It has a chemical structure and activity spectrum similar to chloramphenicol, and has proven efficacy against many anaerobic bacteria. It was acquired as a commercially available injectable

preparation at a concentration of 300 mg/ml (Nuflor™ Schering-Plough Animal Health, Omaha, NE). It was stored at room temperature prior to use. It was diluted in polyethylene glycol (Sigma-Aldrich, St. Louis, MO) to the appropriate concentrations immediately before use. Florfenicol was administered via i.p. injection at a dose of 80 mg/kg/d divided into twice daily doses.

### **Cell Lines**

All cell lines used were originally obtained from American Type Culture Collection (ATCC), (Rockville, MD). The NCTC clone 929 (L929) (ATCC; CCL-1) of strain L (connective tissue, mouse) was derived from a 100 d-old mouse in March of 1948. Strain L was one of the first cell lines to be established in continuous culture, and clone 929 was the first cloned strain developed. The parent line of BHK-21(C-13) (ATCC; CCL-10) was derived from the kidneys of 5 unsexed, 1-d-old hamsters in March, 1961, by I.A. Macpherson and M.G.P. Stoker. Following 84 d of continuous cultivation, interrupted only by an 8-d preservation by freezing, clone 13 was initiated by single-cell isolation. The Vero 76 cell line was initiated from the kidney of a normal adult African green monkey on March 27, 1962, by Y. Yasumura and Y. Kawakita at the Chiba University in Chiba, Japan.

### **Cell Culture Procedures**

All cells were cultured with minimum essential medium with Earle's balanced salts (MEM/EBSS) and nonessential amino acids (Hyclone Laboratories, Inc., Logan, UT). Medium was supplemented with 10% (v/v) fetal bovine serum (FBS) (Hyclone), as well as with penicillin-streptomycin at 100 I.U/ml and 100 µg/ml, respectively. Cells

were cultured at 37 °C in a humidified 5% CO<sub>2</sub>-95% air environment. All cells were first plated in either 75 cm<sup>2</sup> or 175 cm<sup>2</sup>, canted-neck, culture flasks. Cells were passaged as needed by aspirating the culture media and dissociating the cells with 0.25% solution of porcine trypsin in Hank's Balanced Salt Solution (HBSS) with ethylenediamine tetraacetic acid (EDTA), without calcium and magnesium (Sigma Aldrich, St. Louis, MO).

### **Bioassay for Quantification of Tumor Necrosis Factor-Alpha Activity**

Quantitation of TNF-alpha in biological samples was accomplished via the use of the L929 mouse fibroblasts cell line, known to be sensitive to the cell-death signals of TNF-alpha when cultured in the presence of actinomycin D. The procedure for quantitation was similar to that as previously described by Hogan et al.<sup>107</sup> Briefly, 4x10<sup>4</sup> L929 cells per well were plated in 96-well cell culture microplates (Corning Costar®), and allowed to culture overnight. Samples of animal serum, tissue homogenate, or culture supernatant were diluted as needed in MEM containing 10% FBS. These samples were in turn diluted through 8 serial dilutions (e.g. 1:2, 1:2, 1:4, 1:8, 1:16, 1:32, 1:64, 1:128, and 1:256). Diluted samples were added to confluent cell monolayers in triplicate. An equal volume of MEM containing actinomycin D at a concentration of 8 µg/ml was immediately added to each well, resulting in a final concentration of 5% FBS and 4 µg/ml of actinomycin D in each well. Samples were allowed to incubate at 37 °C in a humidified 5% CO<sub>2</sub>-95% air environment. After incubation for 18-20 h L929 cell viability was determined by means of the Cell-Titer Blue™ cell viability assay system (Promega, Madison, WI) according to the manufacturers instructions. Samples were

analyzed on an fmax 96-well plate fluorometer (Molecular Devices, Sunnyvale, CA) using an excitation wavelength of 544 nm, and fluorescence measured at 590 nm. Assay functionality was verified by simultaneously assaying the ability of recombinant murine TNF-alpha (Sigma-Aldrich, St. Louis, MO) to reduce cell viability. One unit (U) of TNF-alpha activity was defined as the concentration of sample needed to decrease cell viability by 50% when compared with untreated control cells. Results were reported as the number of units per milliliter of serum or media, or gram of tissue assayed.

### **Bioassay for Quantification of Interferon Activity**

The concentration of interferon in samples, either serum or tissue homogenate, was determined by seeding 96-well, flat-bottomed plates with  $4 \times 10^4$  BHK-21 cells per well then incubating for 1 d. The confluent monolayers were then treated with the sample to be assayed. Samples were initially diluted at a ratio of 1:10 in cell culture media, followed by an additional 7 serial dilutions (e.g. dilutions of 1:10, 1:20, 1:40, 1:80, 1:160, 1:320, 1:640, and 1:1280). Cells were immediately infected with the encephalomyocarditis virus (EMCV). The concentration of virus used was previously determined by placing  $\log_{10}$  dilutions of virus stock on confluent monolayers of BHK-21 cells and determining the minimum concentration of virus that would produce a >90% decrease in cell viability after 3 d when compared with non-infected control wells. After cultures were incubated for 3 d in the presence of the virus and sample, cells viability was determined by means of the Cell-Titer Blue™ cell viability assay system (Promega, Madison, WI) according to the manufacturers' instructions. Samples were analyzed on an fmax 96-well plate fluorometer (Molecular Devices, Sunnyvale, CA) using an



excitation wavelength of 544 nm, and fluorescence measured at 590 nm. Interferon activity was identified by the ability of samples to prevent virus-induced cell death.

One unit (U) of interferon activity was defined as the concentration of sample needed to decrease virus-induced cell death by 50% when compared non-infected control wells. Results were reported as the number of units per milliliter of serum or gram of tissue assayed.

## **Viruses**

Unless otherwise noted all viruses used were originally obtained from the American Type Culture Collection (ATCC, Manassas, VA). Banzi virus (BaV), H336 strain ATCC VR-414, was passaged 3 times in Vero 76 cells. Semliki Forest virus (SFV), original strain ATCC VR-1247 was passaged in 2 times in Vero 76 cells. Two strains of western equine encephalitis Virus (WEEV) were used. The ATCC VR-70 strain, referred to as the California strain, was passaged 3 times in Vero 76 cells. The Kern strain, obtained from Dr. Kenneth Olson at Colorado State University (Fort Collins, CO), was passaged 3 times in Vero 76 cells. Unless otherwise stated all experiments involving WEEV used the California strain of the virus.

## **Titration of Virus in Serum and Tissues**

The virus titers in tissues or serum were assayed using the virus-yield assay<sup>171</sup> wherein a specific volume of tissue homogenate or heparinized serum was added to the first tube of a series of dilution tubes. Serial log<sub>10</sub> dilutions were made and added to Vero 76 cells in 96-well microplates. Three d later for SFV and WEEV, and 7 d later in the case of BaV, visual identification of cytopathic effect (CPE) was used to identify the end-

point of infection. Four replicates were used to calculate the infectious doses per gram of tissue. Results were reported as  $\log_{10}$  cell culture infectious dose units (CCID<sub>50</sub>)/gram of tissue or milliliter of serum.

### **Macrophage Isolation and Testing**

Activated hamster peritoneal macrophages were used to assess the ability of WEEV to stimulate TNF-alpha production *in vitro*. Hamsters received 5 ml intraperitoneal injections of sterile 4% brewer's thioglycollate (Sigma Aldrich, St. Louis MO). Thioglycollate solution was sterilized via autoclave, and then stored in the dark at room temperature for approximately one month prior to use. Macrophages were harvested 3 d after thioglycollate injection. Hamsters were euthanized via carbon dioxide inhalation. Immediately following euthanasia animals were injected intraperitoneally with approximately 50 ml of MEM supplemented with 10% FBS. Media was collected and centrifuged at 800 x g for 10 min on an Omnifuge RT model centrifuge. Following centrifugation the supernatant was discarded and the remaining cells were re-suspended in additional MEM with 10% FBS. Before cell suspension was added to cell culture plates, nucleated-cell numbers were quantified via manual counting on a hemocytometer. Tests were performed in 2 different cell plate configurations, with  $2 \times 10^5$  cells per well in 96-well flat-bottom culture plates or  $10 \times 10^6$  cells per flask in 25 cm<sup>2</sup> cell culture flasks. Cell preparations were cultured 2 h at 37°C before being washed 2 times with ice-cold media to select for macrophages and remove non-adherent cells.

The ability of a virus to stimulate macrophages to produce TNF-alpha was initially determined by adding various log dilutions of virus stock to adherent

macrophages in multi-well plates. Cell culture supernatant was collected at various times post-virus inoculation and stored at  $-70^{\circ}\text{C}$  until assayed. Data from initial macrophage stimulation experiments were used to determine optimal virus concentration and optimal time of culture supernatant collection. The ability of various compounds to suppress TNF- $\alpha$  expression in virus-stimulated macrophages were assayed by treating triplicate wells of macrophages seeded in 96-well plates with various half-log dilutions of compounds (e.g. 1000, 320, 100, and 32  $\mu\text{M}$ ). Cells were immediately treated with the virus at a multiplicity of infection (MOI) of 3. Each concentration of the compound was also incubated in duplicate on macrophages in the absence of virus to determine the degree of drug-induced cytotoxicity. Each plate had 4 wells that received no compound treatment, but were cultured in the presence of a nonvirus cell lysate at a dilution identical to that used for diluting virus stocks. These wells acted as nonvirus normal cell controls. Cell lysate was prepared by using nonvirus exposed Vero 76 cells prepared in a manner identical to that used in preparing the virus stocks. An additional 4 wells per plate received the virus only and no drug to determine the degree of virus-induced cytotoxicity. Cultures were incubated at  $37^{\circ}\text{C}$  with 5%  $\text{CO}_2$  in MEM with 10% FBS and 25  $\mu\text{g}/\text{mL}$  of gentamicin for 18 h before supernatant was collected and stored at  $-70^{\circ}\text{C}$  until being assayed. Following supernatant collection, fresh media was added to macrophage containing wells, and macrophage cell viability was assayed by means of the Cell-Titer Blue™ cell viability assay as previously described. Cell viability was reported as a percentage compared to cell control wells. Corrected cell viability on virus-inoculated wells was calculated by adding the difference in cell viability between control wells and drug toxicity wells to the cell viability value in virus inoculated wells. TNF-

alpha concentration was determined by means of the L929 TNF-alpha bioassay as previously described. Relative increases in TNF-alpha were determined by measuring the TNF-alpha concentration in the supernatant from wells containing macrophages that received virus only, or virus and compound in combination and comparing that with the TNF-alpha concentration in supernatant from wells containing non-virus treated macrophages. Each compound was tested on at least 3 separate preparations of peritoneal macrophages.

Flasks containing  $10^7$  macrophages were inoculated with WEEV at a MOI of one or inoculated with a similar dilution of non-virus cell lysate. Cells were incubated for 18 h as previously described, after which the cell culture supernatant was collected. Flasks containing an equal amount of virus but without macrophages were incubated concurrently with the macrophage-containing flasks, and the contents were also collected at 18 hpi. Various compounds intended to reduce TNF-alpha expression were added to flasks containing an equal amount of the virus, both with and without macrophages, and incubated concurrently with other cell culture flasks. Samples were assayed for virus concentrations and TNF-alpha concentrations as described elsewhere. The collected supernatants were then stored at  $-70\text{ }^{\circ}\text{C}$  until used in splenocyte testing.

### **Splenocyte Isolation and Testing**

Hamster splenocytes were used to evaluate the ability of WEEV to directly cause destruction of hamster lymphoid cells. Hamsters were euthanized by carbon dioxide inhalation, after which spleens were collected using an aseptic technique. Spleens were cut into smaller pieces and placed in a dounce homogenizer with 5-7 ml of MEM

supplemented with 5% FBS and were homogenized by moving the plunger up and down 10 times. Spleen homogenate was centrifuged at 800 x g for 10 min in an Omnifuge RT model centrifuge. Supernatant was discarded and the cells were resuspended in red cell lysis buffer (Sigma Aldrich, St. Louis, MO) for 5 to 10 min with periodic mixing. An equal volume of MEM with 5% FBS was added to the cell suspension in the lysis buffer, and the cells were centrifuged at 800 x g for 10 min. The supernatant was discarded and the cells were resuspended in 5 to 10 ml MEM with 5% FBS. Histopaque® (Sigma Aldrich, St. Louis MO) high density gradient solution was layered underneath the cell suspension and the cells were centrifuged at 1500 x g for 15 min. The viable cells at the media-Histopaque® interface were aspirated, mixed with 15 ml media, and centrifuged at 800 x g for 10 min. Following centrifugation the supernatant was discarded and the cells were resuspended in MEM with 10% FBS. Cell numbers were quantified by counting on a hemocytometer. Cells were added to 96-well cell culture plates at a concentration of  $3 \times 10^5$  cells per well in a volume of 100  $\mu$ L. To assay the ability of the virus to directly initiate lymphocytic cell death various log dilutions of WEEV stocks were added to cell-containing wells and cell viability was determined 3 d later by the Cell-Titer Blue™ cell viability assay as previously described. Cell viability was reported as a percentage when virus inoculated cells were compared to untreated control cells.

To assay the ability of virus-stimulated cytokines produced from peritoneal macrophages to enhance virus-mediated cell killing, 96-well plates of splenocytes were prepared as described above. An equal volume of cell culture supernatant collected from flasks as described above was then added to splenocyte-containing wells in triplicate.

Additional WEE virus, approximately 1 log in excess of the virus measured in macrophage culture supernatant, was added to similarly treated triplicate wells. Six wells per plate contained splenocytes with neither virus nor macrophage supernatant. An additional 6 wells per plate received additional virus only but no supernatant. Splenocyte culture plates were incubated as previously described for 3 d, after which cell viability was assayed. Cell viability was reported as the percentage of cell viability compared to non-treated control wells. Tests for virus-induced cell killing and macrophage supernatant enhancement of viral cell killing was tested on at least 3 separate preparations of splenocytes.

### **Antiviral Efficacy**

The antiviral efficacy of drugs was determined by seeding triplicate wells of 96-well, flat-bottomed plates with  $4 \times 10^4$  Vero 76 cells per well then incubating for 1 d. The confluent monolayers were then treated with 8 serial half-log dilutions of the drug or control (e.g. 1000, 320, 100, 32, 10, 3.2, 1.0, 0.32  $\mu\text{g}/\text{mL}$ ). Cells were immediately infected with 5 CCID<sub>50</sub> of virus. Each concentration of drug was also incubated in duplicate on cells in the absence of virus to determine the degree of drug induced cytotoxicity. Each plate had 6 wells that received neither virus nor drug to act as normal cell controls, 6 wells that received virus only and no drug to determine the degree of virus induced CPE, and quadruplicate wells receiving sterile water to determine the amount of background fluorescence when cell viability was measured. Plates were incubated at 37°C with 5% CO<sub>2</sub> in MEM with 1% FBS and 25  $\mu\text{g}/\text{mL}$  of gentamicin for 3 d in the case of SFV or WEEV, and for 6 d in the case of BaV. The antiviral effect was determined by

visually scanning individual wells and estimating the percentage of cytotoxicity present. Following visual assessment cell viability was measured via the Cell-Titer Blue™ cell viability assay as previously described.

The 50% effective concentration ( $EC_{50}$ ) was defined as the concentration of the drug required to reduce virus-induced CPE by 50%. The 50% inhibitory concentration ( $IC_{50}$ ) was defined as the concentration of the drug that resulted in a 50% decrease in cell viability when compared to cell controls. The selectivity index (SI) was defined as the ratio of the  $IC_{50}$  to the  $EC_{50}$ . Interferon alfacon-1 was used as a positive control in all Vero 76 cell-based antiviral assays.

## **Animals**

Female BALB/c mice (*Mus musculus*) 7-8 wk old (18-20 g) were obtained from Charles River Laboratories (Wilmington, MA). Female Syrian golden hamsters (*Mesocricetus auratus*) were also obtained from Charles River Laboratories. All animals were quarantined at the animal housing facilities at Utah State University for 1 wk prior to the beginning of the experiment. All animals were fed standard rodent chow and tap water *ad libitum*. All experiments were conducted in an AAALAC-accredited facility.

## **Blood-Brain Barrier Permeability Assay in Mice**

For evaluation of BBB permeability to small molecular weight compounds, mice were injected with 10 mg of NaFl (Sigma Aldrich, St. Louis MO) in a volume of 0.1 ml of sterile saline, administered i.p. To obtain the serum, animals were anesthetized with ketamine HCl (100-200 mg/kg) i.p. 45 min after the NaFl injection. Blood was collected

into serum separator tubes (Sarstedt, Newton, NC) by retro-orbital bleeding. Blood samples were stored for at 4 °C for approximately 30 min to allow for clotting, after which they were centrifuged at 7,000 rpm for 7 min. The serum was removed and stored at -70 °C until processing. Animals were sacrificed immediately following blood collection. Transcardial perfusion to remove blood from the vasculature was performed by making an incision in the right atrium of the heart, and gently injecting sterile phosphate-buffered saline (PBS) through the left ventricle until the expelled blood ran clear. The brain was removed, weighed, homogenized in 1 ml of sterile PBS and stored at -70 °C until processing.

#### **Collection of Cerebrospinal Fluid and Measurement of Blood-Brain Barrier Permeability in Syrian Golden Hamsters**

Cerebrospinal fluid (CSF) was collected from anesthetized hamsters in a technique slightly modified from that described for the collection of CSF from rats.<sup>83</sup> A CSF-collecting device was made by extracting a 30-ga needle from its plastic hub and placing the nonsharp end into an approximately 30 cm length of Tygon© (Saint-Gobain Performance Plastic, Akron, Ohio) tubing (0.25 mm inner diameter). The needle was then placed into the cannula-holding arm of the stereotaxic device (David Kopf Instruments, Tujunga, California) parallel to the ground. A second 30-gauge needle attached to a 1-ml syringe was inserted into the opposite end of the tubing. Hamsters were anesthetized with i.p. ketamine and xylazine at doses of 100 mg/kg and 5 mg/kg, respectively, and the fur at the caudal base of the skull was shaved. Animals were then placed into the stereotaxic device (Model 902, David Kopf Instruments) with the



animal's snout oriented horizontally or slightly downward and the body of the animal rolled underneath the snout such that the neck was in a flexed position allowing access to the cisterna magna. Anesthesia was maintained as needed with isoflurane anesthetic gas delivered via a nosepiece in a nonrebreathing manner. A 5-mm skin incision was made at the base of the skull on the midline. The needle in the stereotaxic arm was advanced into the incision and into the perispinal musculature. The needle was further advanced with mild suction placed upon the attached syringe until clear CSF from the cisterna magna was visualized entering the tubing and into the syringe. In general, the ideal location for collection of CSF was on the midline and 4 mm caudal from the top of the skull. If resistance was encountered during advancement of the needle it was removed, slight modifications were made to the location of the needle, either left or right, up or down. The needle was then reinserted until CSF was collected. If visible blood or contamination was noted in the tubing the needle was removed and the tubing was flushed with sterile saline followed by air before making another attempt to collect CSF. CSF samples were diluted at a rate of 1:100 and total numbers of cells in each sample were counted manually using a hemocytometer.

For evaluation of BBB permeability to small molecular weight compounds hamsters were injected with 100 mg of NaFl (Sigma Aldrich, St. Louis, MO) in a volume of 0.1 ml of sterile saline, administered i.p. To obtain CSF, animals were anesthetized via i.p. injection of ketamine and xylazine as previously described. Anesthesia was initiated 45 min after the NaFl injection, and CSF was collected as described. Immediately following CSF collection blood was collected into serum-separator tubes (Sarstedt, Newton, NC) by retro-orbital bleeding. Blood samples were stored for at 4 °C for

approximately 30 min to allow for clotting, after which they were centrifuged at 7,000 rpm for 7 min, and the serum was removed. The serum and CSF were stored at -70°C until processing.

### **Measurement of Fluorescence**

Protein was precipitated from samples with trichloroacetic acid (TCA) to remove potential background fluorescence. Cerebrospinal fluid and serum samples were diluted 1:10 in 20% TCA, while brain samples were homogenized in PBS then centrifuged at 3,000 rpm for 5 min, after which the resulting supernatant was diluted 1:10 in 20% TCA. All samples were incubated in TCA at 4°C for 24 h. Samples were centrifuged at 10,000 rpm for 15 min to remove precipitated protein. The supernatant was removed and diluted with equal volumes of sodium borate buffer (0.05 M, pH 10), resulting in a final concentration of 10% TCA and 0.025 M sodium borate buffer. Samples were analyzed on an fmax 96-well plate fluorometer (Molecular Devices, Sunnyvale, CA) using an excitation wavelength of 480 nm, and fluorescence was measured at 538 nm. A standard curve for the quantitation of NaFl in the samples was generated by simultaneously analyzing samples of a known NaFl concentration in 10% TCA and 0.025 M borate buffer. The degree of BBB permeability was measured as the percentage (w/v) of NaFl in a gram of brain tissue per the amount of NaFl in a milliliter of serum. For assays using CSF instead of brain tissue the degree of fluorescence per red blood cell (RBC) in the circulating blood was calculated for each individual animal using the observed fluorescence and assuming  $7.5 \times 10^6$  RBC per  $\mu\text{L}$  of whole blood. The amount of fluorescence detected in CSF samples attributable to RBC contamination was calculated

by multiplying the number of RBCs observed in individual samples by the fluorescence per RBC and this amount was subtracted from the observed fluorescence value for CSF samples. This corrected CSF fluorescence value was used to determine BBB permeability and was measured as the percentage of NaFl in a milliliter of CSF per the amount of NaFl in a milliliter of serum.

### **Time Course of Banzi Virus and Semliki Forest Virus Infection in Mice**

For viral infection studies in mice, animals were inoculated with either LD<sub>50</sub> or LD<sub>90</sub> doses of Banzi or Semliki Forest viruses diluted in minimum essential medium (MEM). These viral doses correlated to 10 or 100 50%-cell culture infectious doses (CCID<sub>50</sub>) per animal, respectively for BaV and 10<sup>4</sup> or 10<sup>5</sup> CCID<sub>50</sub> per animal, respectively for SFV. All virus inoculations were performed via the intraperitoneal (i.p.) route. In initial experiments, to determine the time course of virus dissemination in mice, animals were inoculated with LD<sub>50</sub> doses of either BaV or SFV. Starting 1 d post-virus inoculation (dpi) and continuing daily until 10 dpi, with one additional set of tissues harvested on 14 dpi, groups of 4 virus-inoculated animals and one sham-inoculated animal were sacrificed, and tissue samples were collected. Tissue samples collected from each mouse included serum, liver, kidney, spleen, and brain. Samples were homogenized in MEM by manual stomaching, and then stored at -70°C until assayed for virus titer.

Experiments to determine the time course of BBB permeability alterations associated with virus infection were conducted using an LD<sub>50</sub> dose of virus. Beginning on 1 dpi, 3 virus-inoculated animals and 2 sham-inoculated animals were assayed for BBB permeability to (NaFl) each d until 10 dpi.

### **Ampligen™ Efficacy Versus Banzi and Semliki Forest Viruses in Mice**

Mice were inoculated with LD<sub>90</sub> doses of virus for all experiments wherein mice were treated with Ampligen™. Groups of 25 virus-infected mice (35 for placebo-treated animals) and 6 sham-infected mice were treated i.p. with 1 mg/kg of Ampligen™ or vehicle. Ten virus-infected and 3 sham-infected mice were assayed for BBB permeability to NaFl on either 6 dpi (SFV) or 8 dpi (BaV). On the same day, 5 animals from each group were assayed for brain virus titers. The remaining animals were monitored for weight change and survival until 21 dpi. Ampligen™ was administered as a single treatment at 24 h before, 4-6 h before or 24 h after virus inoculation.

### **Using Cerebrospinal Fluid to Measure Blood-Brain Barrier Permeability in WEEV-Infected Hamsters**

Hamsters were inoculated intraperitoneally with an LD<sub>90</sub> dose of WEEV. This viral dose correlates to 10<sup>3.5</sup> CCID<sub>50</sub> per animal. Beginning 24 h post-virus inoculation (hpi) and continuing every 24 h until concluding at 96 hpi 3 randomly selected virus inoculated animals were assayed for BBB permeability by injection with NaFl and collection of CSF, as previously described.

Following the identification of the time point at which the peak permeability appeared to occur, a second experiment was conducted in which animals were inoculated with an approximately LD<sub>50</sub> dose of WEEV, a viral dose correlating to 10<sup>2.5</sup> CCID<sub>50</sub> per animal. At 72 hpi all virus- and sham-inoculated animals were assayed for BBB

permeability using injection of NaFl and collection of serum and CSF. Animals were allowed to recover from anesthesia and were monitored for survival until 204 hpi.

### **Histopathology and Bacterial Isolation in Hamsters Inoculated with WEEV**

To identify potential histopathological lesions associated with the virus infection, hamsters were inoculated with a 10x LD<sub>90</sub> dose of WEEV. At various time points post-virus inoculation, animals were subjected to transcardial perfusion, as a means for tissue fixation in preparation for histopathological analysis. Animals were deeply anesthetized with ketamine and xylazine at doses of 200 mg/kg and 10 mg/kg, respectively, administered via the i.p. route. When the animal no longer showed signs of response to a toe pinch the thoracic cavity was opened, and the right atrium of the heart was incised. A needle attached to a large syringe or peristaltic pump was inserted into the left ventricle, and cold phosphate-buffered saline (PBS) was introduced into the left ventricle until the discharge from the incision of the right atrium ran clear. The PBS was followed by a similar volume of 4% paraformaldehyde to fix tissues. Finally, the abdominal cavity was opened, and the entire animal was placed in a container of 4% paraformaldehyde. The whole animal was then delivered to the Utah Veterinary Diagnostic Laboratory (UVDL) for complete necropsy and preparation of histopathological samples. All tissue slides were reviewed by a Diplomate of the American College of Veterinary Pathology.

Tissues of WEEV-inoculated animals were assayed separate at various times post-virus inoculation for the presence of bacteria. For collection of tissue and blood samples for isolation of bacteria, animals were euthanized via an intraperitoneal injection of sodium pentobarbital. Immediately following euthanasia the ventral thoracic and

abdominal areas were shaved, and a surgical scrub of povidone-iodine was applied liberally. Then, using sterilized instruments and aseptic technique, the abdominal and thoracic cavities were opened. Blood was collected directly from the heart using a 22-gauge needle attached to a 3-ml syringe. Small samples of the right cranial lung lobe, spleen, liver, and kidney were also collected. All samples were immediately placed into 10 ml of thioglycollate broth supplemented with hemin and vitamin K (Hardy Diagnostics, Santa Maria, CA). Samples were submitted to the UVDL for isolation and characterization of bacterial isolates. Digital photomicrographs of histopathological lesions were taken and provided by the UVDL.

#### **Supportive, Antibacterial and Anti-Inflammatory Treatment of WEEV-Inoculated Hamsters**

Treatments were instituted to treat potential septic shock in WEEV-inoculated hamsters. Animals were inoculated intraperitoneally with an LD<sub>90</sub> dose of WEEV. Supportive treatments were begun 12 h prior to virus inoculation and were continued every 12 h throughout the course of the experiment. These treatments consisted of lactated ringers solution (LRS) with 5% dextrose. LRS was warmed to 37 °C in a water bath prior to administration, and delivered subcutaneously at quantities that would replace weight loss from the previous weight measurement assuming 1 ml of the LRS was equivalent to 1 gram of body weight, up to a maximum of 10 ml/animal at each treatment point. Fluids could be administered up to twice daily as indicated by weight loss. Additional supportive treatments included administration of the antibiotics florfenicol or enrofloxacin and the anti-inflammatory agents flunixin meglumine, or

dexamethasone, using doses and schedules as previously described. The various supportive treatments were given singly and in various combinations depending upon specific experimental requirements.

### **Evaluating the Relationship Between Circulating Lymphocyte Counts and Disease Outcome in WEEV-Inoculated Hamsters**

Experiments were conducted to investigate the correlation between decreases in circulating lymphocyte numbers and poor disease outcome in hamsters inoculated with WEEV. Estimation of both nucleated and nonnucleated cells in whole blood were conducted with the use of a Coulter Counter model ZBI electronic particle counter (Beckman Coulter, Fullerton, CA). To collect whole blood hamsters were anesthetized with ketamine and xylazine administered via the i.p. route at a dose of 100 mg/kg and 5 mg/kg, respectively. Blood from the periorbital sinus of anesthetized hamsters was collected into tubes containing the anticoagulant sodium citrate (40 mg/mL). Sufficient blood was collected to result in an approximate final sodium citrate concentration of 4 mg/mL. Device calibration and automated counts of both red blood cells and nucleated cells using the particle counter were conducted following the manufacturer's instructions. For red blood cell (RBC) counts anticoagulated blood samples were first diluted at a ratio of 1:500 in hematology diluent (Clinical Diagnostic Solutions, Plantation, FL), followed by a second dilution in hematology diluent of 1:100, resulting in a final dilution of 1:50,000. Samples were then analyzed on the device. To calculate nucleated cell numbers samples of anticoagulated whole blood was diluted 1:500 in the hematology lysing agent CDS 3DP/C (Clinical Diagnostic Solutions, Plantation, FL), prior to being

analyzed on the counting device. Each sample was analyzed on the machine 3 times in a randomized order. The final concentration of RBC in the samples (RBCs/ $\mu$ L whole blood) was determined by multiplying the average result for a given sample by 100. The concentration of nucleated cells in a sample (nucleated cells/ $\mu$ L whole blood) was considered to be the average of the analysis results for the given sample.

To determine the numbers of individual leukocyte types a manual differential count was performed. Approximately 15-20  $\mu$ L of anticoagulated blood was placed on one end of a glass microscope slide. A second glass slide was used to spread the blood sample into a thin film on the glass slide. The blood film was allowed to air dry before being fixed and stained in eosin and Wright-Giemsa stains (Dip Quick staining kit, Jorgensen Laboratories, Loveland, CO). A manual differential was performed by reviewing each stained blood sample under a microscope and classifying the first 100 nucleated cells observed as lymphocyte, monocyte/macrophage, neutrophil, basophil or eosinophil. The percentage of each cell type as determined by this manual count was multiplied by the total number of nucleated cells previously determined to calculate the quantity of the various leukocyte populations in the sample.

To determine the relationship between circulating lymphocyte counts and disease outcome hamsters were inoculated intraperitoneally with an approximate LD<sub>50</sub> dose of WEEV or were sham-inoculated. Blood samples were collected at various time points post-virus inoculation and total nucleated cell numbers and differential leukocyte population numbers were calculated as described. Animals were then monitored for mortality associated with WEEV infection.



In a subsequent experiment, hamsters were inoculated with an LD<sub>90</sub> dose of WEEV and received treatment with either flunixin meglumine or placebo as previously described. Blood samples were collected at various time points post-virus inoculation and total nucleated cell numbers and differential leukocyte population numbers were calculated as described. Animals were then monitored for mortality associated with WEEV infection.

### **Clinical Characterization and Time-Course of WEEV Infection in Hamsters**

An experiment was conducted to measure multiple clinical and inflammatory parameters in hamsters infected with WEEV. Animals were inoculated intraperitoneally with either an LD<sub>90</sub> dose of WEEV or were sham inoculated. Beginning at the time of the infection and every 12 h thereafter until the end of the experiment at 84 hpi all animals were individually weighed and rectal body temperatures were measured. Beginning at 12 hpi and continuing until the conclusion of the experiment 3 virus-inoculated animals were humanely euthanized and the following samples were taken: whole blood, serum, liver, kidney, spleen, and brain. At the conclusion of the experiment all sham-inoculated animals were euthanized and processed in a similar manner. Serum and whole blood were collected and prepared as previously described. Tissue samples were individually weighed and placed in 9 volumes (w/v) of MEM with 2% FBS for homogenization, resulting in a tissue homogenate with a 1:10 dilution. Whole blood was used for measurement of RBC counts, nucleated cell counts, and differential leukocyte counts as previously described. Immediately following collection, serum clinical biochemistry values were measured by the use of the Vetscan automated serum chemistry

analyzer (Abaxis, Union City, CA) using the comprehensive diagnostic profile.

Parameters measured included: albumin, alkaline phosphatase, alanine aminotransferase, amylase, blood urea nitrogen, calcium, creatinine, globulin, glucose, potassium, sodium, phosphorous, and total protein. Remaining serum and tissue homogenates were stored at -70°C until processing. Virus titers and concentrations of TNF-alpha and interferon activity were measured in all serum and tissue homogenate samples as previously described.

#### **Evaluation of the Effect of Viral Dose and Dexamethasone Immunosuppression on Disease Phenotype and Outcome in Syrian Golden Hamsters**

Hamsters were inoculated intraperitoneally with either an LD<sub>50</sub> or an LD<sub>90</sub> dose of WEEV. Twice daily following inoculation animals were weighed and observed for death.

Animals were separately inoculated intraperitoneally with an LD<sub>90</sub> dose of the California strain of WEEV. Additional animals were inoculated with a CCID<sub>50</sub> equivalent dose of the Kern strain of WEEV. A third group received a sham inoculation. Twice daily following inoculation animals were weighed, rectal body temperature was measured, and animals were observed for death. Serum was collected from animals at 36 and 48 h post-virus inoculations and assayed for the presence of interferon via the interferon bioassay. In a subsequent experiment animals were inoculated with either an LD<sub>50</sub> dose of the California strain of WEEV, a CCID<sub>50</sub> equivalent dose of the Kern strain of WEEV, or were sham-inoculated. Beginning 5 d prior to virus inoculation, and continuing through the duration of the experiment, animals were received either

intraperitoneal injections of dexamethasone at a dose of 4.4 mg/kg/d divided into twice daily doses, or with a drug vehicle. Twice daily following inoculation animals were weighed, rectal body temperature was measured, and animals were observed for death.

### **Correlation Between Early Expression of Serum Interferon and Disease Outcome in Hamsters Inoculated with WEEV**

Hamsters were inoculated intraperitoneally with a LD<sub>50</sub> dose of WEEV. Twice daily following inoculation animals were weighed, rectal body temperature was measured, and animals were observed for death. Serum was collected from animals at 20 and 44 h post-virus inoculations and assayed for the presence of interferon via the interferon bioassay as previously described.

### **Intracranial Inoculation of WEEV in Hamsters**

Hamsters were anesthetized with an intraperitoneal injection of a combination of ketamine and xylazine at a dose of 100 mg/kg and 5 mg/kg, respectively. Anesthesia was maintained via the use of isoflurane administered at a rate of 2% of inspired air. The head and cranial neck of the hamsters was shaved and a solution of povidone iodine was applied to the skin followed by an application of 70% ethanol. Animals were restrained within a stereotaxic device. A midline incision was made over the dorsal portion of the skull. Underlying connective tissue was dissected away bluntly. A 0.3-mm diameter hole, located 1 mm to the right of midline and 1 mm rostral to suture joining the parietal and occipital skull bones was drilled through the skull. A 30-gauge needle attached to a low volume syringe (Hamilton Company, Reno, NV) was inserted to a depth of 3 mm

below the surface of the skull. A total of 10 CCID<sub>50</sub> of WEEV was injected into the right cerebral hemisphere in a total volume of 10 µL of unsupplemented MEM. To prevent backflow or leakage of the virus-containing media the needle was allowed to remain in place for approximately 1 min following injection of the virus. Following removal of the needle the drill hole in the skull was observed to ensure that no significant hemorrhage had occurred as a result of the injection. After needle removal the skin was closed with a series of wound clips (Stoelting, Wood Dale, IL). Post-surgery animals were observed until they had recovered from anesthesia sufficiently to hold themselves upright and move about the cage. Sham-inoculated animals underwent the same procedure, but they received an injection of MEM without any virus present.

All animals received a once daily dose of interferon alfacon (infergen), at a dose of 5 µg/kg/d. The first dose was administered approximately 4 h before virus inoculation, and treatment was continued through the duration of the experiment. Twice daily following inoculation, animals were weighed, rectal body temperature was measured, and animals were observed for death. At the time of death, or at 204 hpi in the case of survivors, animals were transcardially perfused with saline and 4% paraformaldehyde as previously described, and submitted to the UVDL for necropsy and histopathological analysis.

### **Statistical Evaluation**

Differences in survival of different populations of animals were evaluated via the Kaplan Meier survival analysis. Differences in tissue virus titer, mean day to death (MDD) or mean h to death (MHD), nucleated cell counts, serum cytokine concentrations,

and changes in whole body weight were analyzed by an unpaired, two-tailed *t* test.

Analysis of variance (ANOVA) was not used for the preceding statistical analysis due to the possibilities of different sample sizes for different treatment groups. ANOVA with the Bonferroni correction was used for statistical analysis of macrophage and splenocyte based assays, including TNF-alpha concentrations post-virus exposure, and cell viability in either splenocytes or macrophages post-virus exposure. ANOVA was also used for analysis of changes in BBB permeability. Comparison of splenocyte viability following exposure to supernatant from WEEV-stimulated macrophages was analyzed by use of the unpaired two-tailed *t* test.

## RESULTS

### **Virus Infection and Blood-Brain Barrier Permeability Changes in Mice**

Mice were inoculated with either SFV or BaV and a variety of parameters were assayed to determine the effects of virus infection on the blood-brain barrier in mice. The infectious viral titers in the plasma, spleen, kidney, liver and brain were determined over a course of time in mice inoculated i.p with either BaV or SFV (Table 1). Peak viral brain titers in BaV-infected mice was  $8.3 \pm 0.8 \log_{10}$  CCID<sub>50</sub>/gram of brain tissue on 8 dpi, while peak viral brain titers for SFV infected mice was  $7.5 \pm 0.5 \log_{10}$  CCID<sub>50</sub>/g of tissue on 6 dpi. Similarly, the time course of BBB permeability to NaFl was determined in mice inoculated with either BaV or SFV. The permeability of the BBB in BaV-infected mice began increasing at 4 dpi, with peak penetration of fluorescent dye occurring on 9 dpi (Figure 1). Brain fluorescence reached 12.4% of that in serum (w/v) on 9 dpi, which is greater than a 4-fold increase in comparison to the 2-3% noted in sham-infected animals. In SFV-infected mice BBB permeability began to increase on 5 dpi, with peak permeability occurring on 7 dpi (Figure 2). Peak brain fluorescence reached 8.1% of serum fluorescence (w/v), which was approximately 3-fold higher than the 2-3% fluorescence seen in sham-infected animals. Interestingly, in both virus infection models peak fluorescence was reached 1 d after expected peak virus titers in the brain. The data were used to identify the time of virus entry into the brain as well as peak brain titers and peak fluorescence for subsequent experiments.

Treatment with Ampligen™ significantly improved the outcome for mice inoculated with BaV, but only if it was administered prior to virus inoculation (Table 2).

TABLE 1: Time course of tissue viral titers in i.p.-inoculated 7-8 wk old BALB/c mice.

		Days post-viral injection – viral titers (log <sub>10</sub> infectious doses/g tissue or mL plasma)													
Virus	Tissue	1	2	3	4	5	6	7	8	9	10	14	14		
BaV	Serum	(1/4) <sup>a</sup>	(1/4)	(1/4)	(3/4)	(1/4)	(0/4)	(2/4)	(4/4)	(1/4)	(1/4)	(1/4)	(1/4)		
		NC <sup>b</sup>	NC	NC	3.3 ± 0.8	NC	NC	3.7 ± 3.9	7.6 ± 0.8	NC	NC	NC	NC		
BaV	Spleen	(1/4)	(1/4)	(1/4)	(3/3)	(3/4)	(2/4)	(1/4)	(2/4)	(3/4)	(4/4)	(0/4)	(0/4)		
		NC	NC	NC	3.6 ± 0.5	4.9 ± 0.6	4.3 ± 0.6	NC	3.5 ± 1.2	3.5 ± 1.2	4.0 ± 0.7	NC	NC		
BaV	Kidney	(0/4)	(0/4)	(0/4)	(3/4)	(1/4)	(0/4)	(2/4)	(2/4)	(2/4)	(3/4)	(0/4)	(0/4)		
		NC	NC	NC	3.4 ± 0.5	NC	NC	2.8 ± 0.2	6.6 ± 4.1	4.0 ± 1.0	3.9 ± 0.8	NC	NC		
BaV	Liver	(0/4)	(1/4)	(1/4)	(2/4)	(2/4)	(0/4)	(0/4)	(2/4)	(2/4)	(3/4)	(0/4)	(0/4)		
		NC	NC	NC	2.6 ± 0.0	3.2 ± 0.2	NC	NC	4.4 ± 2.0	3.8 ± 1.4	4.6 ± 2.2	NC	NC		
BaV	Brain	(0/4)	(0/4)	(0/4)	(1/4)	(2/4)	(2/4)	(1/4)	(4/4)	(4/4)	(4/4)	(1/4)	(1/4)		
		NC	NC	NC	NC	3.6 ± 0.1	3.6 ± 1.4	NC	8.3 ± 0.8	6.7 ± 0.8	7.3 ± 2.0	NC	NC		
SFV	Serum	(4/4)	(4/4)	(3/4)	(0/4)	(0/4)	(0/4)	(0/4)	(0/4)	(0/4)	-	(0/4)	(0/4)		
		4.2 ± 0.2	4.7 ± 0.5	2.4 ± 0.8	NC	NC	NC	NC	NC	NC	-	NC	NC		
SFV	Spleen	(4/4)	(4/4)	(4/4)	(4/4)	(2/4)	(1/4)	(0/4)	(0/4)	(0/4)	-	(0/4)	(0/4)		
		3.6 ± 1.8	4.8 ± 0.9	4.6 ± 0.5	3.9 ± 0.7	2.5 ± 0.2	NC	NC	NC	NC	-	NC	NC		
SFV	Kidney	(4/4)	(4/4)	(4/4)	(2/4)	(1/4)	(1/4)	(0/4)	(0/4)	(0/4)	-	(0/4)	(0/4)		
		3.7 ± 2.1	4.1 ± 1.0	2.7 ± 0.3	2.4 ± 0.2	NC	NC	NC	NC	NC	-	NC	NC		
SFV	Liver	(4/4)	(4/4)	(4/4)	(1/4)	(0/4)	(1/4)	(0/4)	(0/4)	(0/4)	-	(0/4)	(0/4)		
		3.3 ± 2.0	4.6 ± 0.8	3.4 ± 0.3	NC	NC	NC	NC	NC	NC	-	NC	NC		
SFV	Brain	(0/4)	(3/4)	(4/4)	(4/4)	(4/4)	(4/4)	(4/4)	(4/4)	(4/4)	-	(0/4)	(0/4)		
		NC	1.7 ± 1.2	5.2 ± 0.3	6.4 ± 0.9	6.9 ± 1.1	7.5 ± 0.5	6.9 ± 1.4	7.3 ± 0.6	5.8 ± 1.0	-	NC	NC		

<sup>a</sup>Number of samples with detectable virus/total animals assayed.<sup>b</sup>NC- Not Calculated. Means were not calculated when most samples were below the limits of detection.

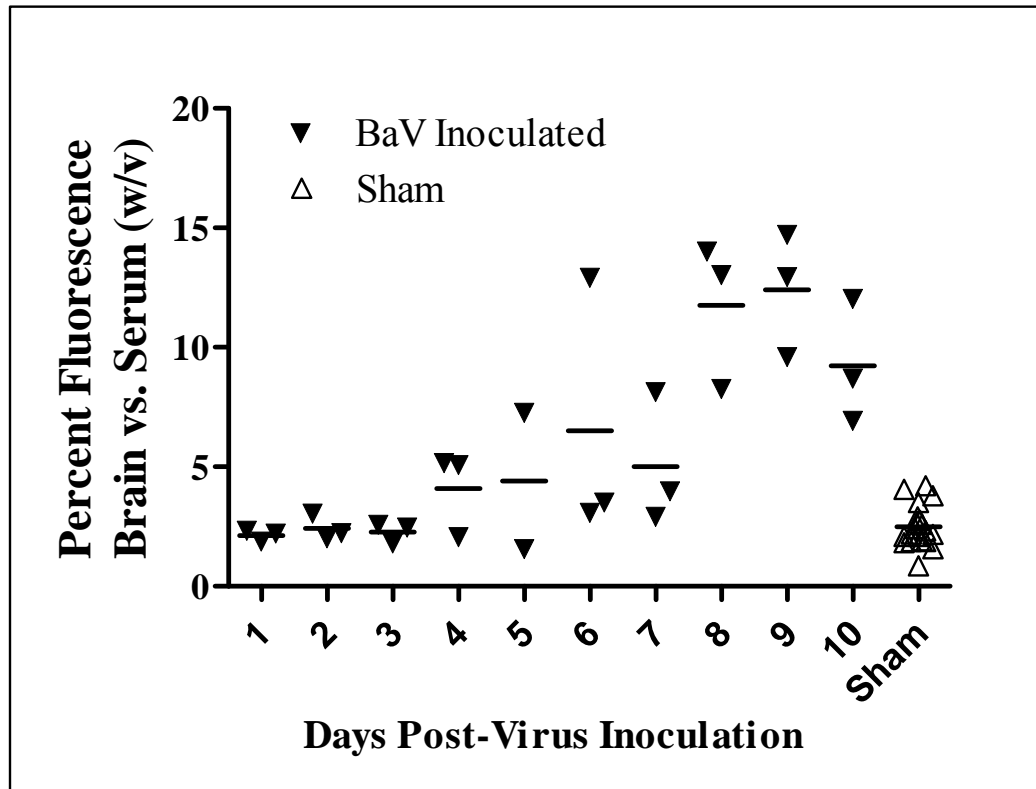


Figure 1: Time course of blood-brain barrier permeability in 7-8 wk old BALB/c mice inoculated i.p. with Banzi virus. Percentage of fluorescence measured in 1 g of brain tissue vs. the amount of fluorescence measured in 1 ml of serum 45 min after i.p. injection of sodium fluorescein dye.



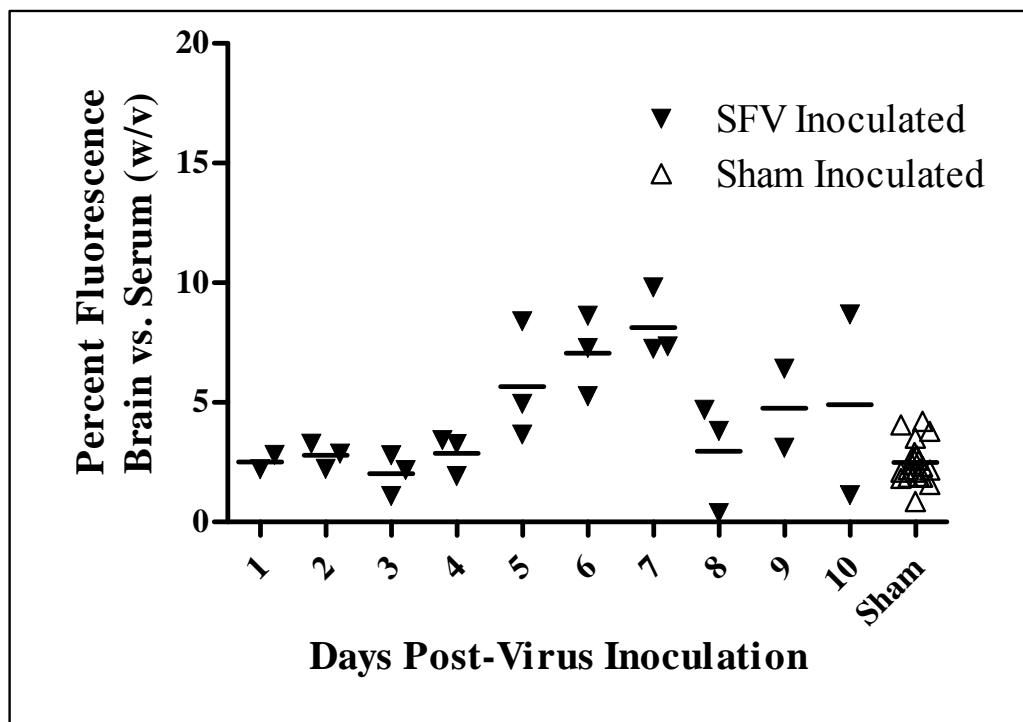


Figure 2: Time course of blood-brain barrier permeability in 7-8 wk old BALB/c mice inoculated i.p. with Semliki virus. Percentage of fluorescence measured in 1 g of brain tissue vs. the amount of fluorescence measured in 1 ml of serum 45 min after i.p. injection of sodium fluorescein dye.

Table 2: Effects of a single dose of Ampligen administered at various times in relation to virus exposure on survival and brain virus titers in BALB/c mice inoculated with Banzai virus or Semliki Forest virus.

Compound	Virus	Dose (mg/kg/day)	Uninfected toxicity control		Infected, treated		
			Surv/Totals	Surv/Totals	Surv/Totals	MDD <sup>a</sup> ± SD	Brain Virus Titer
Ampligen (24 h pre)	Banzi	1	3/3 (100%)	9/10 (90%)****	14.0 ± 0.0	2.3 ± 0.1***	
Ampligen (4-6 h pre)	Banzi	1	3/3 (100%)	7/10 (70%)****	12.3 ± 1.5	3.8 ± 1.0***	
Ampligen (24 h post)	Banzi	1	3/3 (100%)	0/10 (0%)	12.8 ± 3.1*	7.0 ± 2.1	
Placebo (24 h pre)	Banzi	-	3/3 (100%)	0/20 (0%)	10.4 ± 1.8	9.1 ± 0.1	
Normal Control		-	3/3 (100%)	-	-	-	
Ampligen (24 h pre)	Semliki Forest	1	3/3 (100%)	4/10 (30%)	9.0 ± 1.1*	6.2 ± 1.9	
Ampligen (4-6 h pre)	Semliki Forest	1	3/3 (100%)	7/10 (70%)****	7.7 ± 1.5	5.5 ± 1.5	
Ampligen (24 h post)	Semliki Forest	1	3/3 (100%)	3/10 (30%)	7.4 ± 1.8	7.9 ± 1.1	
Placebo (24 h pre)	Semliki Forest	-	3/3 (100%)	2/20 (10%)	7.6 ± 1.3	7.4 ± 1.2	
Normal Control		-	3/3 (100%)	-	-	-	

<sup>a</sup>Mean day to death of mice dying before day 21

\*p<0.05, \*\*\*p<0.001 compared to placebo treated controls

Placebo-treated animals had 0% survival following BaV inoculation, with a MDD of  $10.4 \pm 1.8$ , whereas, mice receiving a single 1 mg/kg dose of Ampligen™ 24 h prior to virus inoculation had 90% survival ( $p < 0.001$ ) with a single mouse dying on 14 dpi, while BaV inoculated mice treated with Ampligen™ 4-6 h before virus exposure had 70% survival ( $p < 0.001$ ), with a MDD of  $12.3 \pm 1.5$ . Delaying treatment to 24 h post-virus inoculation resulted in 0% survival, although the MDD of  $12.8 \pm 3.1$  was significantly ( $t = 2.732$ ,  $p < 0.05$ ) later than that seen in placebo-treated animals.

Ampligen™ treatment prior to virus exposure resulted in significantly reduced viral titers in the brains of BaV-inoculated mice, as measured at 8 dpi. Placebo-treated mice had viral brain titers of  $9.1 \pm 0.1 \log_{10}$  CCID<sub>50</sub>/g of brain tissue. At 8 dpi mice treated with Ampligen™ 24 h prior to virus inoculation had titers of  $2.3 \pm 0.1 \log_{10}$  CCID<sub>50</sub>/g ( $t = 20.19$ ,  $p < 0.001$ ), and those treated 4-6 h before virus injection had titers of  $3.8 \pm 1.0 \log_{10}$  CCID<sub>50</sub>/g ( $t = 10.40$ ,  $p < 0.001$ ). When treatment was delayed until 24 h after virus inoculation, titers rose to  $7.0 \pm 2.1 \log_{10}$  CCID<sub>50</sub>/g, which was not significantly different than placebo-treated animals. However, delaying treatment to 24 h after virus inoculation did cause titers to be significantly higher than with animals receiving Ampligen™ 24 h ( $t = 5.045$ ,  $p < 0.01$ ), and 4-6 h before virus exposure ( $t = 3.022$ ,  $p < 0.05$ ).

The beneficial effects of Ampligen™ treatment on survival and brain virus titer of mice challenged with BaV were mirrored in its ability to significantly improve weight change in virus-inoculated mice (Figure 3). Placebo-treated animals had an average weight change of  $-13.1\% \pm 8.8\%$  on 8 dpi. In contrast, on the same day post-virus exposure animals receiving 1 mg/kg of Ampligen™ 24 h prior to virus inoculation

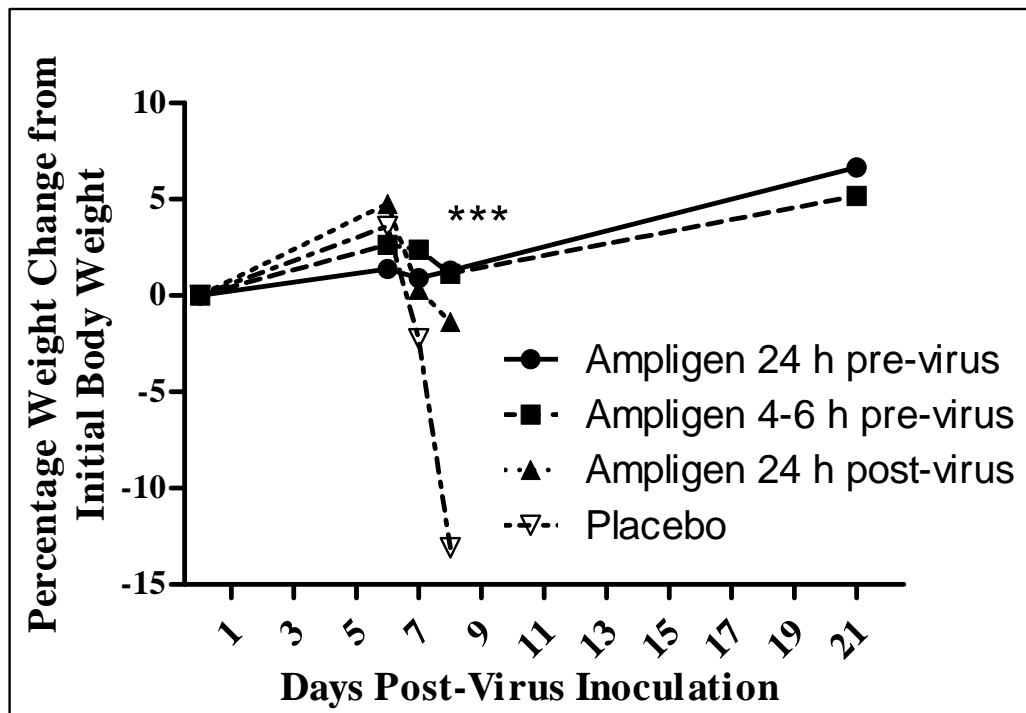


Figure 3: Average percentage weight change from initial body weight of Banzi virus-inoculated mice after a single i.p. dose of 1 mg/kg of Ampligen™ administered at various times in relation to virus exposure. \*\*\* $p < 0.001$  compared to placebo-treated animals.

had an average weight change of  $+1.3\% \pm 4.4\%$  ( $t= 6.712$ ,  $p<0.001$ ), while animals treated with Ampligen™ 4-6 h prior to virus exposure had weight change of  $+1.1\% \pm 7.2\%$  ( $t=5.909$ ,  $p<0.001$ ). Mice treated with Ampligen™ 24 h after virus exposure had an average weight change of  $-1.4\% \pm 5.2\%$  on 8 dpi, which was also significantly different than with placebo-treated animals ( $t=5.916$ ,  $p<0.001$ ).

Treatment with a single 1 mg/kg dose of Ampligen™ was able to significantly improve the outcome for mice inoculated with SFV (Table 2). Placebo-treated animals displayed 10% survival, with a MDD of  $7.6 \pm 1.3$ . Animals that received 1 mg/kg of Ampligen™ 24 h prior to virus exposure had 40% survival, which was not significantly higher than with placebo-treated animals. However, treatment of SFV inoculated mice with Ampligen™ 24 h before virus exposure extended the MDD to  $9.0 \pm 1.1$ , which was significantly longer ( $t=2.294$ ,  $p<0.05$ ) than with placebo-treated animals. When compared to placebo-treated animals those mice treated with Ampligen™ 4-6 h prior to virus inoculation had a significantly higher survival rate, with 70% of the animals surviving ( $p<0.001$ ), while animals treated with Ampligen™ 24 h after virus inoculation had 30% survival which was not significantly higher than with placebo-treated animals.

Treatment with Ampligen™ did not significantly reduce brain viral titers on 6 dpi as compared to placebo treatment in SFV inoculated mice (Table 2). However, it is interesting to note that mice treated with Ampligen™ 4-6 h before virus exposure had a brain viral titer of  $5.4 \pm 1.5 \log_{10} \text{CCID}_{50}/\text{g}$ , which was significantly ( $t=2.987$ ,  $p<0.05$ ) lower than the brain viral titer observed in mice that received Ampligen™ 24 h after virus exposure, which was  $7.8 \pm 1.1 \log_{10} \text{CCID}_{50}/\text{g}$ .

Ampligen™ treatment also significantly improved weight change in SFV-inoculated mice (Figure 4). Placebo-treated animals had an average weight change of  $-22.3\% \pm 9.7\%$  on 7 dpi. In contrast, animals receiving 1 mg/kg of Ampligen™ 24 h prior to virus inoculation had an average weight change of  $-9.6\% \pm 8.8\%$  ( $t=3.169$ ,  $p<0.01$ ), while animals treated with Ampligen™ 4-6 h prior to virus exposure had a weight change of  $-4.7\% \pm 9.7\%$  ( $t=4.166$ ,  $p<0.001$ ). Mice treated with Ampligen™ 24 h after virus exposure had an average weight change of  $-20.1\% \pm 9.6\%$  on 7 dpi, which was not significantly different than with placebo-treated animals.

Blood-brain barrier permeability was assayed in SFV-inoculated mice on 6 dpi, and in BaV-inoculated mice on 8 dpi using i.p. injections of NaFl. In both SFV- and BaV-inoculated mice BBB permeability was assayed 1 d prior to expected peak permeability to avoid the death loss of a substantial number of placebo-treated mice. A time of 45 minutes between administration of NaFl and collection of serum and brain samples for assay was based on previously published reports using a similar technique.<sup>97</sup> Treatment with Ampligen™ prior to virus exposure was able to significantly decrease BBB permeability associated with BaV-induced encephalitis (Figure 5). The brains of placebo-treated animals had  $9.4\% \pm 3.7\%$  (w/v) of the fluorescence found in their serum. Mice receiving Ampligen™ 24 h before virus exposure had a measurement of brain fluorescence of  $2.8\% \pm 1.0\%$  ( $t=6.096$ ,  $p<0.001$ ), and mice receiving Ampligen™ 4-6 h before virus exposure had a measurement of brain fluorescence of  $4.0\% \pm 2.7\%$  ( $t=3.564$ ,  $p<0.01$ ). In those animals treated with Ampligen™ 24 h after virus inoculation the brain fluorescence was  $5.8\% \pm 2.3\%$  of serum fluorescence, which was not significantly lower

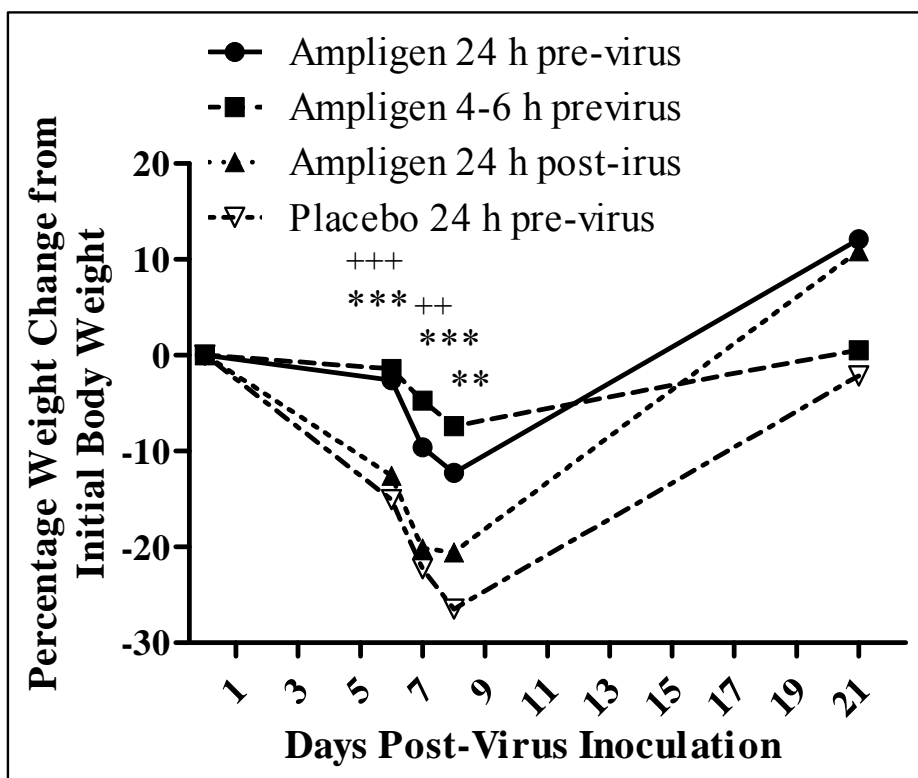


Figure 4: Average percentage weight change from initial body weight of Semliki Forest virus-inoculated mice after a single i.p. dose of 1 mg/kg of Ampligen™ administered at various times in relation to virus exposure. \* $p < 0.05$ , \*\* $p < 0.01$ , \*\*\* $p < 0.001$  compared to placebo-treated animals. + $p < 0.05$ , ++ $p < 0.01$ , +++ $p < 0.001$  compared to mice receiving Ampligen™ 24 h post-virus exposure

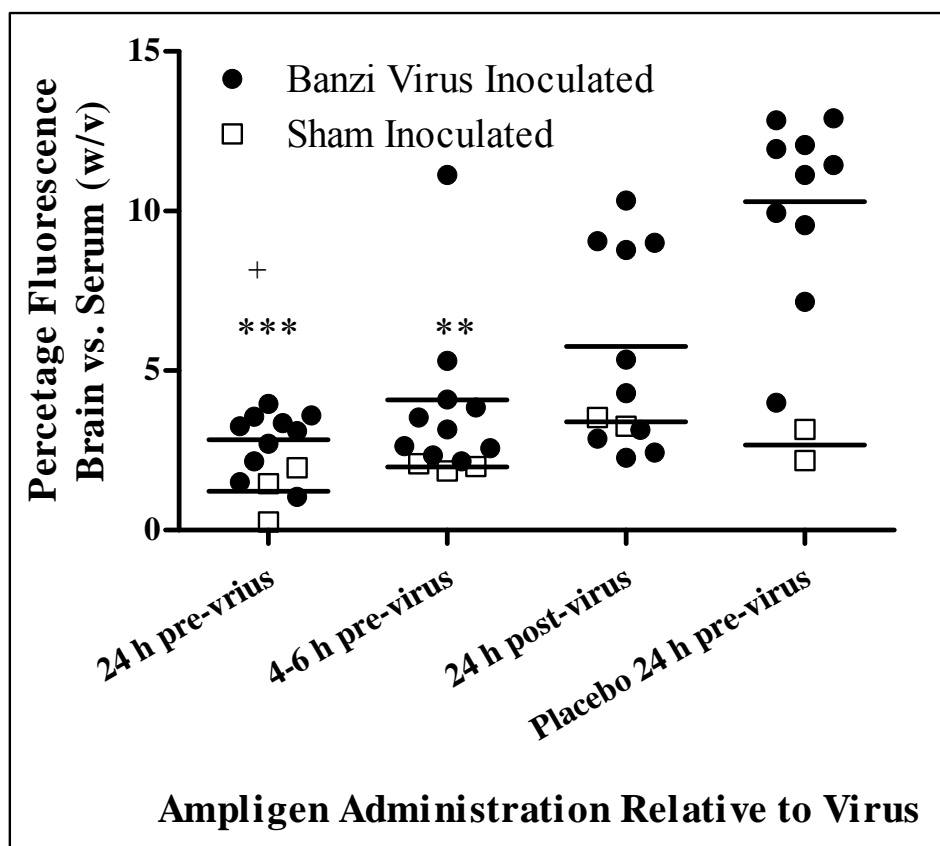


Figure 5: Percentage of fluorescence detected in the brain vs. the serum (w/v) on 8 dpi of mice inoculated with Banzi virus and treated with a single i.p. dose of 1 mg/kg of Ampligen™ at various times in relation to virus exposure. \*\*p<0.01, \*\*\*p<0.001 compared to placebo. +p<0.05 compare to Ampligen™ administration at 24 h post-virus inoculation.



than placebo-treated animals, but was significantly higher than animals treated with Ampligen™ 24 h prior to virus inoculation ( $t=3.039$ ,  $p<0.05$ ).

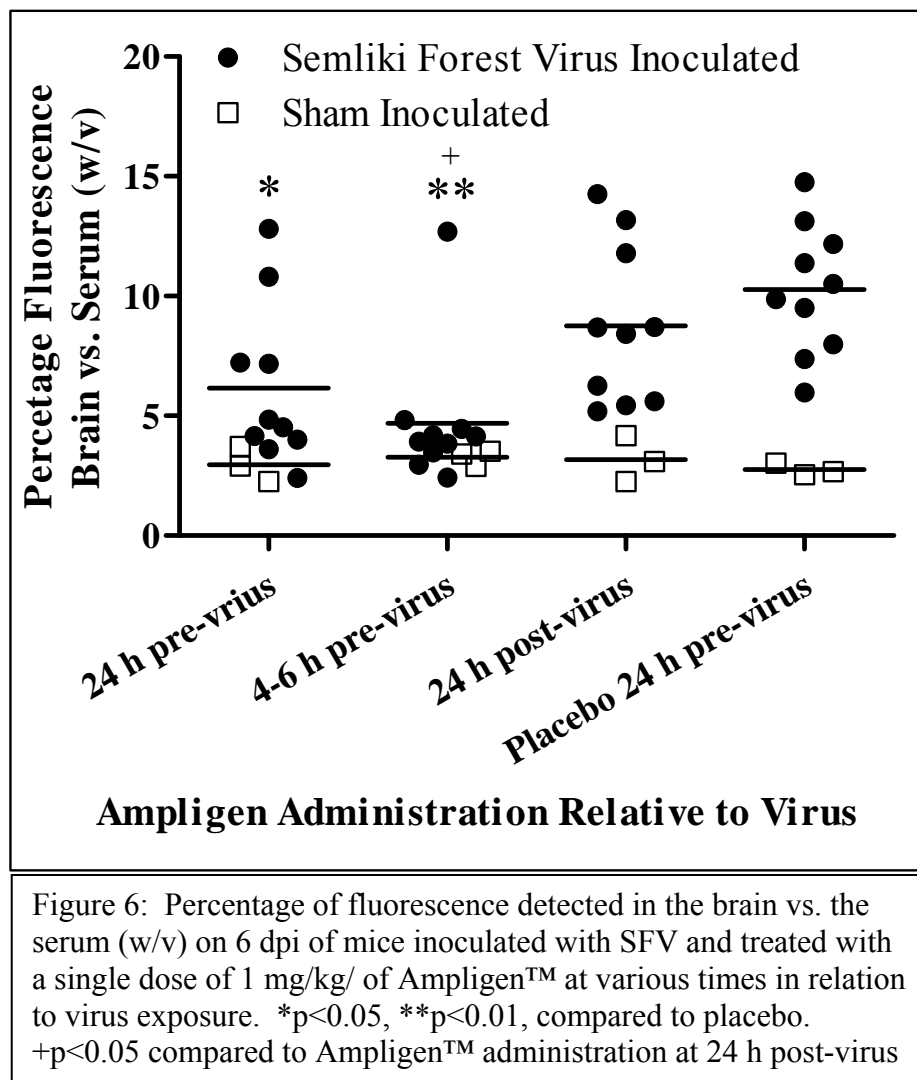
Treatment of mice with Ampligen™ prior to virus exposure resulted in significantly decreased BBB permeability associated with SFV induced encephalitis when compared to placebo-treated SFV-inoculated mice (Figure 6). The brains of placebo-treated animals had  $11.3\% \pm 2.3\%$  (w/v) of the fluorescence found in their serum.

Administration of Ampligen™ to mice 24 h before virus exposure resulted in brain fluorescence of  $6.2\% \pm 3.4\%$  ( $t=2.991$ ,  $p<0.05$ ), and animals treated with Ampligen™ 4-6 h before virus exposure displayed a measurement of brain fluorescence of  $4.7\% \pm 2.9\%$  ( $t=4.086$ ,  $p<0.01$ ). In those animals treated with Ampligen™ 24 h after virus inoculation the brain fluorescence was  $8.8\% \pm 3.3\%$  of serum fluorescence, which was not significantly lower than placebo-treated animals, but was significantly higher than animals treated with Ampligen™ 4-6 h prior to virus inoculation ( $t=2.947$ ,  $p<0.05$ ).

No significant differences in weight change or BBB permeability were detected between groups of sham-inoculated mice, regardless of treatment regimen.

### **Blood-Brain Permeability Changes in Hamsters Inoculated with Western Equine Encephalitis Virus**

Due to the apparent relationship between increased BBB and viral encephalitis observed in mice inoculated with either BaV or SFV it was decided to explore the potential for similar relationships in hamsters inoculated with WEEV, a virus related to SFV. The ability to collect CSF from hamsters in a non-lethal manner provided a new technique for evaluating the relationship between the BBB and viral encephalitis.



Hamsters were inoculated intraperitoneally with an approximately LD<sub>50</sub> dose of WEEV and BBB permeability was assayed in 3 animals every 24 h following virus exposure, by comparing fluorescence measured in the cerebrospinal fluid to that measured in the serum. At 72 h post-virus inoculation (hpi) virus-inoculated animals had an average ratio of  $1.79\% \pm 0.29$  when the CSF fluorescence was compared to that of serum, representing an approximate 1.8-fold increase in comparison to the ratio of  $1.01\% \pm 0.76\%$  measured in uninfected controls (Figure 7). A similarly increased permeability ratio of  $1.79\% \pm 1.42\%$  in the CSF versus the serum was again measured at 96 hpi, immediately preceding death. Subsequently, in an attempt to correlate changes in BBB permeability with death associated with WEEV infection, animals were again inoculated with an LD<sub>50</sub> dose of virus. The BBB permeability as measured by the ratio of fluorescence in the CSF versus the serum was then measured at 72 hpi, and animals were monitored for death. The average ratio of fluorescence in the CSF of animals that survived virus infection (n=12) was  $0.68\% \pm 0.52\%$ , nonsurviving animals (n=9) had an average fluorescence ratio of  $1.12\% \pm 0.78\%$ , while sham-inoculated animals (n=3) had a ratio of  $0.60\% \pm 0.16\%$  (Figure 8). Although the nonsurviving animals had a 1.7-fold increase in BBB permeability when compared to surviving animals and an almost 1.9-fold increase when compared to sham-inoculated animals there was no statistically significant difference. There also was not any apparent correlation between the degree of BBB permeability and time of death (data not shown).

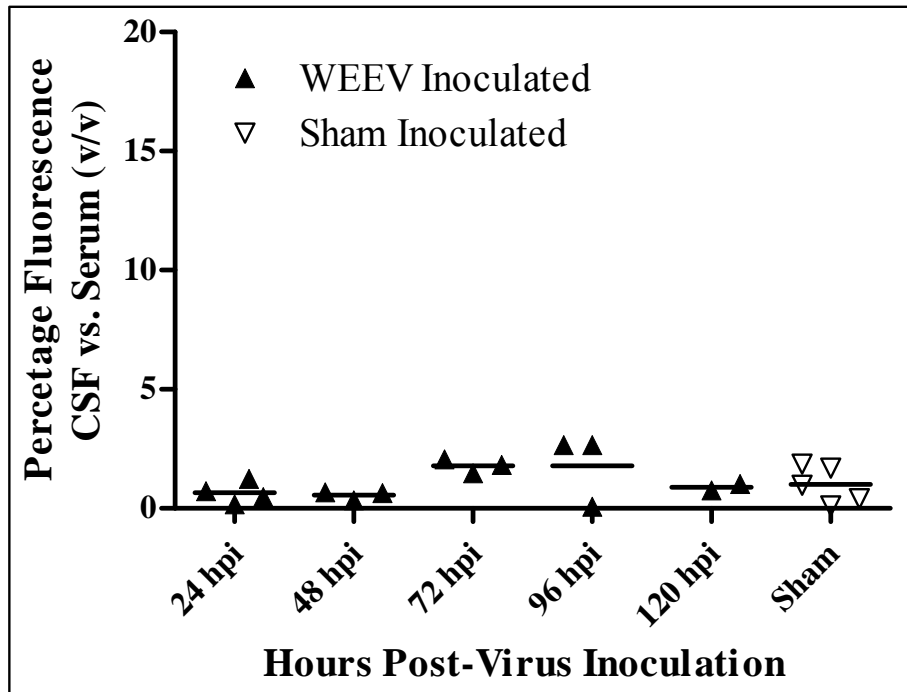


Figure 7: Time course of blood-brain barrier permeability in Syrian golden hamsters inoculated i.p. with WEEV. Percentage of fluorescence measured in 1 ml of CSF vs. the amount of fluorescence measured in 1 ml of serum 45 min after i.p. injection of sodium fluorescein dye.

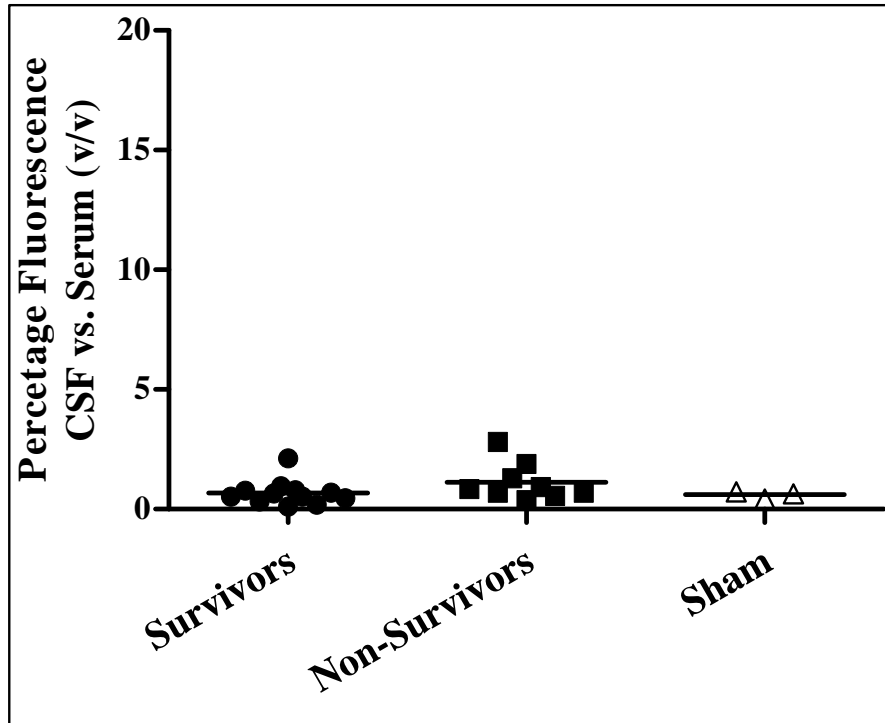


Figure 8: Comparison of fluorescence detected in the CSF vs. the serum (v/v) in Syrian golden hamsters that either survived or died following inoculation with WEEV via the i.p. route. Fluorescence measured at 72 hpi.

### **Histopathology and Microbiology Associated with WEE Virus Infection in Hamsters**

Due to the lack of a detectable correlation between BBB permeability and death in hamsters inoculated with WEEV studies were conducted with the intent of identifying sites of virus associated pathology within the animal. Due to initial histopathological results additional studies were conducted to investigate a potential role for secondary bacterial infections.

Hamsters were inoculated intraperitoneally with a 10x LD<sub>90</sub> dose of WEE virus. Beginning at 24 hpi 3 virus-inoculated animals were sacrificed and various tissues, including spleen, thymus, kidney, brain, and spinal cord were collected for histopathological evaluation. An additional 3 animals were similarly sacrificed and tissues collected every 24 h thereafter until all animals had succumbed to virus infection. At 24 and 48 hpi no lesions were observed in any tissue evaluated. However, by 72 hpi lymphocytosis and severe necrotic lesions were seen in the spleen (Figure 9). Lymphocytic necrosis in various lymph nodes was also occasionally noted. Histopathological lesions in other tissues were rarely seen. By 96 hpi all virus-inoculated animals had died.

Initial histopathological results of splenic necrosis were consistent with conditions of septicemia and indicated the potential for a secondary bacterial involvement. To test the hypothesis of death due to bacterial infections secondary to WEEV infection a separate experiment was conducted in which animals were again intraperitoneally inoculated with a 10x LD<sub>90</sub> dose of WEE virus or sham-inoculated. At 72 and 84 hpi both virus and sham-inoculated animals were sacrificed, and samples of the lung, kidney,

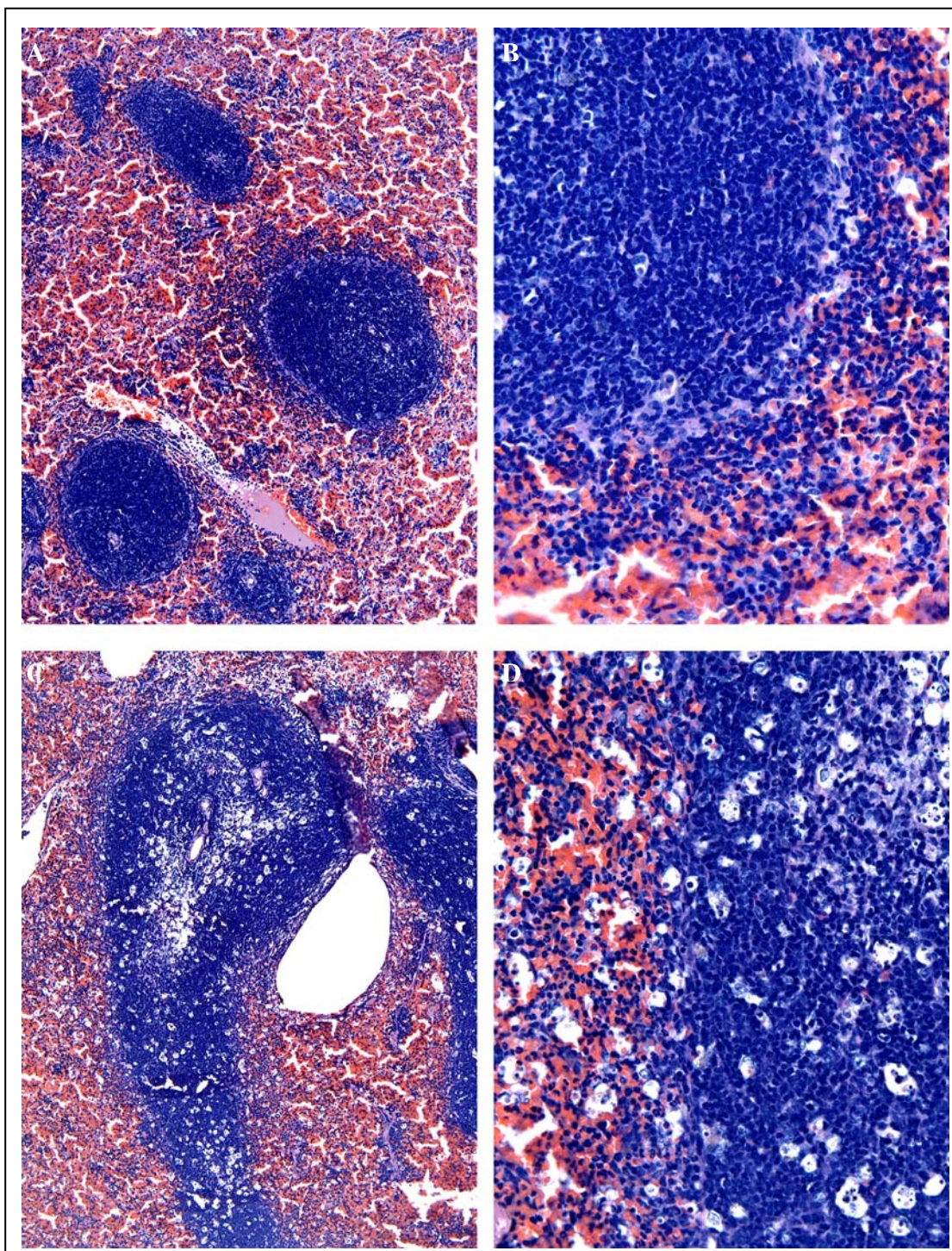


Figure 9: Spleen from WEEV-infected hamsters at 48 hpi (A 100x & B 400x magnification) and 72 hpi (C 100x & D 400x). No evidence of necrosis is seen at 48 hpi. By 72 hpi lymphocytosis and necrosis are evident throughout areas of the spleen.

liver, spleen, and blood were aseptically collected and cultured for the isolation and identification of bacteria. At 72 hpi bacterial species isolated include: *Aerococcus viridans*, *Corynebacterium sp.*, *Streptococcus sp.*, and *Kryptococcus sp.* A similar *Corynebacterium sp.* was identified from samples collected at 84 hpi, as well a *Staphylococcus sp.*. Bacteria isolated from samples taken from sham-inoculated animals include: *Corynebacterium sp.*, *Aerococcus sp.*, and *Pastuerlla sp.* Bacteria were isolated from 10 out of the 40 samples that were submitted. This represents isolation of bacteria from 10/30 samples collected from virus-inoculated animals (4/6 animals sampled), and 5/10 samples from sham-inoculated animals (2/2 animals) (Table 3).

As described later in experiments evaluating the effects of anti-inflammatory treatment on WEEV inoculated animals it was noted that some hamsters would survive beyond the initial disease period in which the majority of animals die by approximately 96 hpi . A proportion of the surviving animals would then die at between 144-204 hpi (6-9 dpi), occasionally displaying signs of overt neurological disease such as head-tilt, circling, tremors, or paralysis. To evaluate the possibility of viral induced neuropathology animals that survived the initial disease phase but succumbed at the later time points were submitted for necropsy and histopathological analysis. In these animals there was evidence of previous necrotic lesions in the spleen that appeared to be resolving. Other lesions included meningitis, cerebral hemorrhage, and perivascular cuffing with lymphocytic infiltrate into nervous tissue (Figure 10).

The ability of WEEV to induce viral encephalitis was further investigated by inoculating hamsters intracranially into the right cerebral hemisphere with 100 CCID<sub>50</sub> of WEEV (n=5) or sham inoculating hamsters (n=4) as a negative control. The



Table 3: Description of rates of bacteria isolation and bacterial species isolated from WEEV- and sham-inoculated hamsters.

Bacteria isolated from 6/8 hamsters WEEV: 4/6 Sham: 2/2		Bacteria isolated from 10/40 samples WEEV: 5/30 Sham: 5/10	
Time of Sample Collection	72 hpi	84 hpi	Sham
Bacterial species isolated	<i>Corynebacterium</i> <i>Aerococcus viridans</i> <i>Streptococcus sp.</i> <i>Kryptococcus sp.</i>	<i>Corynebacterium</i> <i>Staphylococcus sp.</i>	<i>Corynebacterium</i> <i>Aerococcus sp.</i> <i>Pasteurella</i>

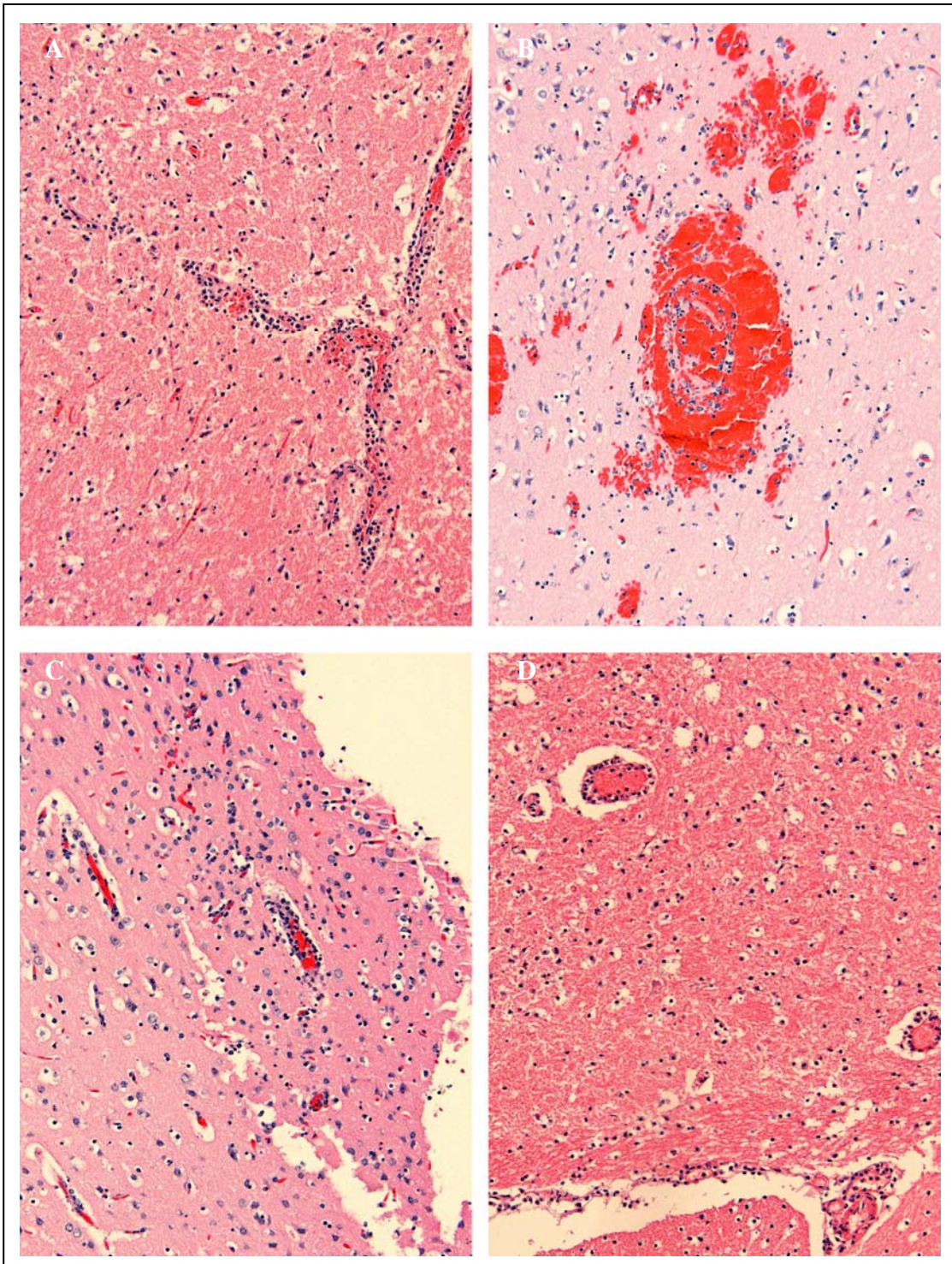


Figure 10: Brain from WEEV-infected hamsters at 132 (A & B) and 144 (C & D) hpi. Brains show evidence of hemorrhage, lymphocytic perivascular cuffing, and inflammatory infiltrate.

intracranially inoculated hamsters were monitored for morbidity and mortality. Animals that were moribund were euthanized with both euthanized and dead animals being submitted for necropsy and histopathological assessment. Beginning at 36 hpi virus-inoculated animals began to show observable signs of disease. Epistaxis was a common sign among virus-inoculated animals. Signs of neurological involvement included paralysis, tremors, apparent hyperesthesia, circling, ataxia, increased agitation, and head tilt. All virus-inoculated animals but 1 was dead by 72 hpi while no sham-inoculated animals showed any signs of disease (Figure 11). All sham-inoculated animals were subsequently sacrificed and submitted for necropsy. Lesions in virus-inoculated animals were similar to, albeit more severe than, those observed in animals that survived the initial stages of peripheral disease, but later succumbed to apparent viral encephalitis. Lesions noted include hemorrhage, necrosis, meningitis and lymphocytic infiltration of the nervous tissue (Figure 12). No lesions were seen in nonneuronal tissue. No histopathological lesions were noted in any sham-inoculated animal.

### **Supportive Care of WEE Virus Inoculated Hamsters**

As previously stated, initial results of histopathological changes in hamsters dying due to inoculation with were consistent with lesions noted in animals suffering from septicemia and/or bacteremia. To test the hypothesis that WEEV inoculated hamsters were dying due to a bacteremia secondary to virus infection or due to inflammatory reactions to either virus or secondary bacteria a series of experiments were conducted to evaluate the effects of various combinations of supportive care on hamsters inoculated with WEE virus. As previously described, supportive care consisted of treatment either

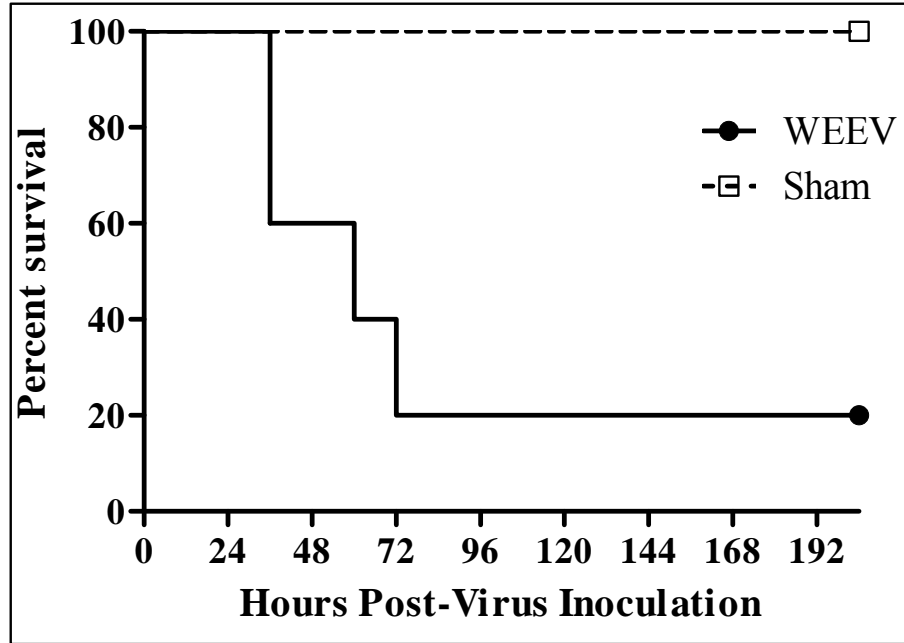


Figure 11: Survival of Syrian golden hamsters following intracranial inoculation with WEEV or sham inoculation by the same route.

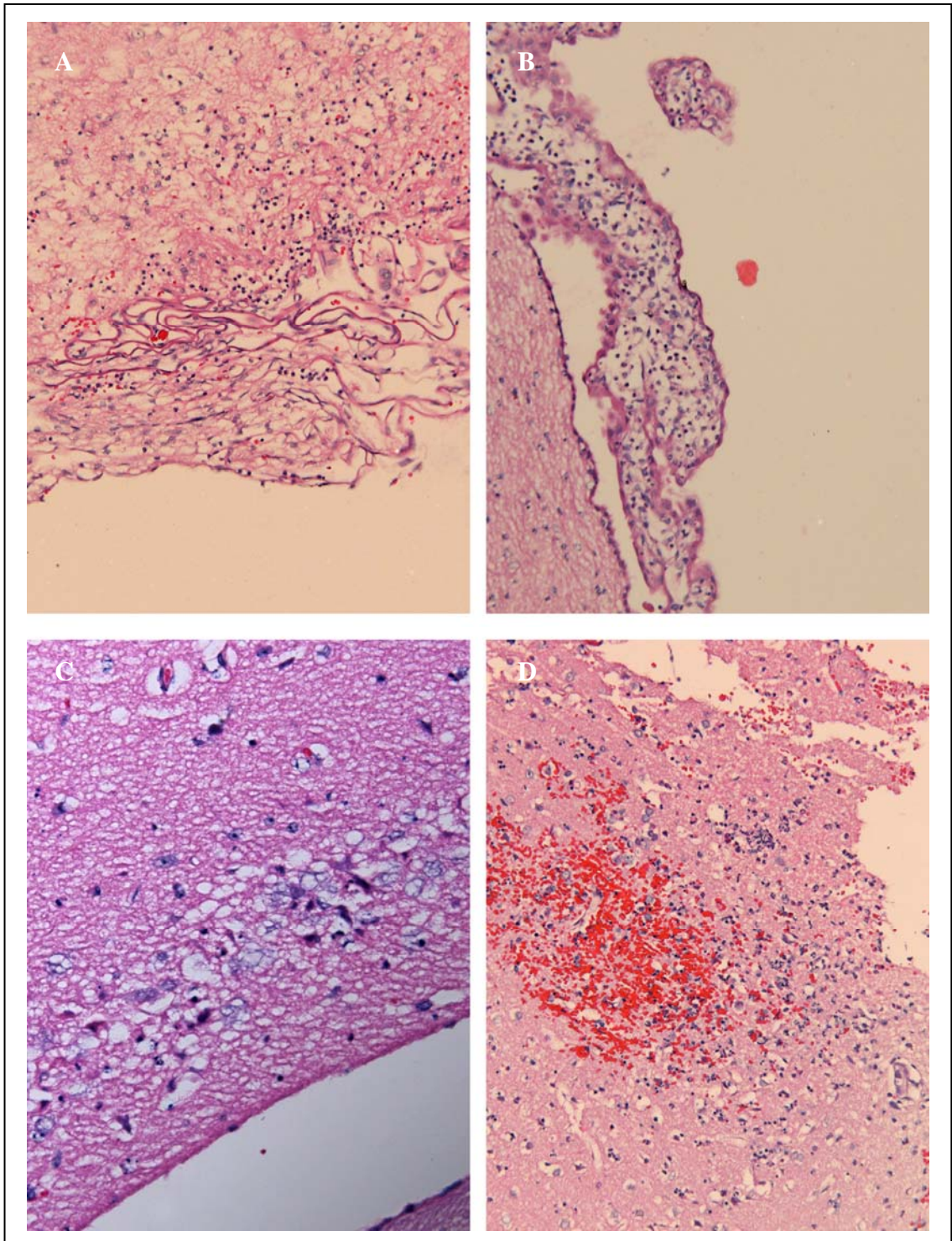


Figure 12: Brains from hamsters following intracranial inoculation of WEEV. Animals were submitted for necropsy following death at 36 (A & B) and 48 (C & D) hpi. Brains show evidence of hemorrhage, lymphocytic perivascular cuffing, and inflammatory infiltrate.

singly or in combination with anti-inflammatory agents, antibiotics, and/or subcutaneous fluids. In all experiments hamsters were inoculated intraperitoneally with a 10x LD<sub>90</sub> dose of WEEV. In the initial experiment animals received either a placebo treatment with drug vehicles (n=10) or supportive care in the form of an intraperitoneal treatment with the antibiotic enrofloxacin at a dose of 20 mg/kg/d, the anti-inflammatory agent flunixin meglumine (FM) at a dose of 5 mg/kg/d, and subcutaneous fluids as needed (n=10). Animals were monitored for weight change and mortality. Placebo-treated hamsters had 0% survival with all animals being dead by 108 hpi, while treated animals had 10% survival at 204 hpi. However, treated animals had significantly improved survival as evaluated by Kaplan-Meier survival analysis ( $p < 0.05$ ) (Figure 13). Animals receiving supportive care also had a weight change of  $0.4 \pm 3.4\%$  and  $3.4 \pm 1.5\%$  at 72 and 96 hpi, respectively. These values were significantly improved compared to a weight change of  $-4.6 \pm 1.7\%$  ( $t=3.964$ ,  $p < 0.01$ ) and  $-16.5 \pm 12.7\%$  ( $t=4.947$ ,  $p < 0.01$ ) measured in placebo-treated animals at 72 and 96 hpi, respectively (Figure 14). To better understand the role of antibiotic therapy in the improved survival noted in hamsters receiving supportive care a follow-up experiment was conducted in which WEE virus-inoculated hamsters were treated with a placebo (n=14) a high dose (200 mg/kg/d) of enrofloxacin (n=13) and a low dose (20 mg/kg/d) of enrofloxacin (n=13) without any additional supportive treatment. All virus inoculated animals were dead by 132 hpi, and there was no significant difference in survival detected regardless of treatment (Figure 15).

To test the hypothesis that bacteria resistant to the initial antibiotic of choice, enrofloxacin, were participating in the disease conditions observed, and to better

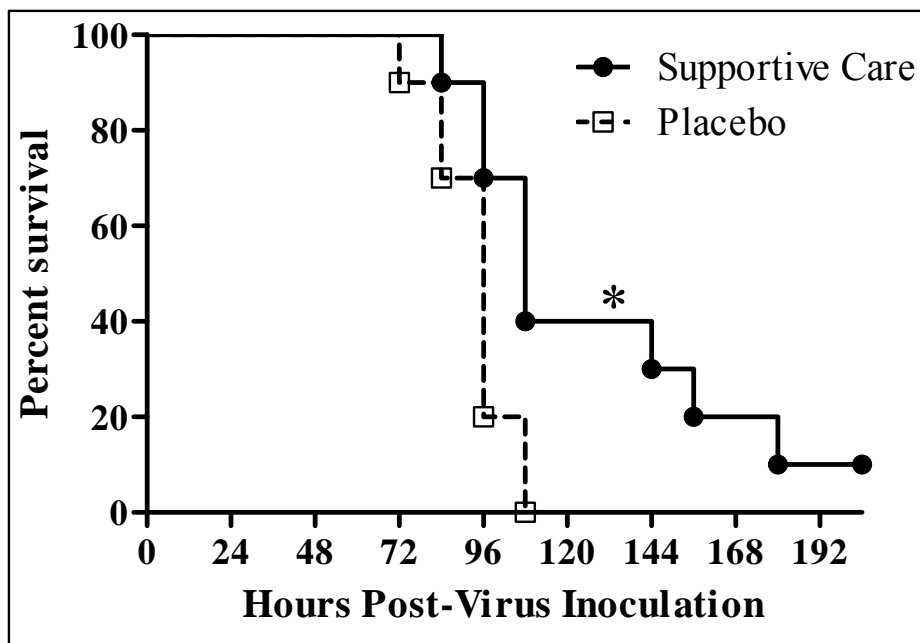


Figure 13: Effects of supportive care on the survival of WEEV inoculated hamsters. \* $p < 0.05$  compared to placebo-treated animals.

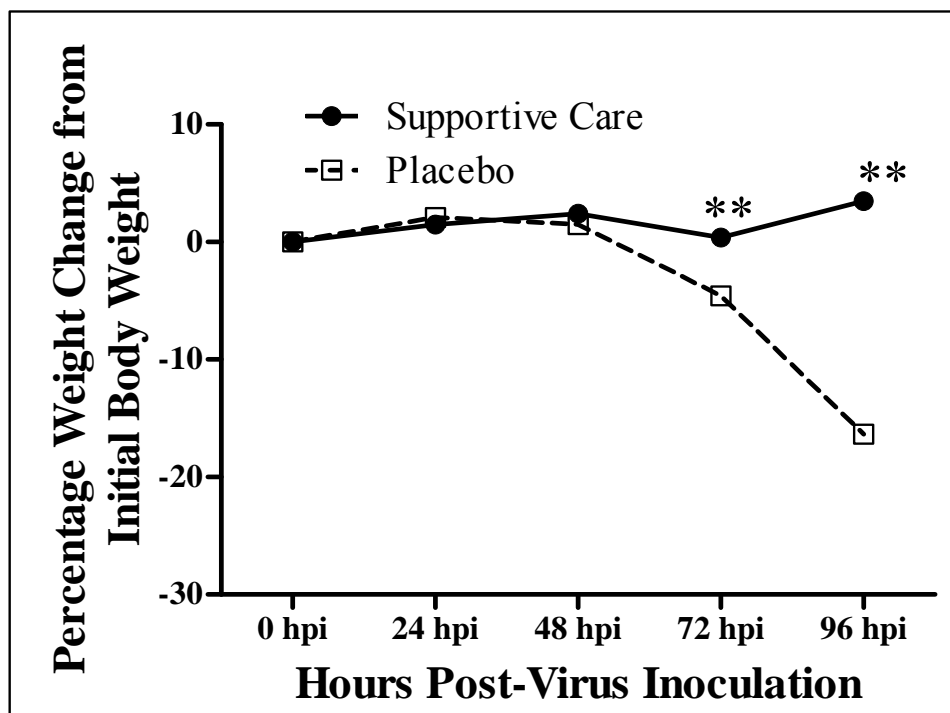


Figure 14: Effects of supportive care on the weight change of WEEV-inoculated hamsters. \*\* $p < 0.01$  compared to placebo-treated animals

elucidate the role of supportive and anti-inflammatory treatment in the improved responses observed in WEEV infected hamsters a subsequent experiment was conducted in which animals received placebo treatment, supportive care of fluids and anti-inflammatory agents, or supportive care in combination with the antibiotics enrofloxacin or florfenicol. Florfenicol treatment was toxic in hamsters as evidenced by the weight loss and mortality seen in sham-inoculated animals receiving treatment (data not shown). Among virus-inoculated hamsters those animals receiving florfenicol treatment (n=13) or florfenicol in combination with enrofloxacin (n=13) had a 0% survival rate, while placebo-treated animals (n=20) had 10% survival at 204 hpi. Although not statistically significantly different, those animals that received enrofloxacin treatment with supportive care (n=13), or supportive care alone (n=13) both had 30% survival at 204 hpi (Figure 16). Furthermore, at 84 hpi placebo-treated animals had an average weight change of  $-1.7 \pm 4.1\%$  (Figure 17). Animals receiving supportive care alone or supportive care with enrofloxacin had a significantly improved weight change. Those receiving supportive care alone had an average weight change of  $+4.2 \pm 2.8\%$  ( $t=4.239$ ,  $p<0.001$ ), and those animals that received enrofloxacin in addition to supportive care had an average weight change of  $3.9\% \pm 3.2\%$  at 84 hpi ( $t=3.666$ ,  $p<0.01$ ).

Results from previous experiments appeared to indicate that anti-inflammatory treatment was the primary effector of improved survival in WEEV inoculated hamsters. To test the hypothesis that inflammation plays a substantial role in the pathogenesis of WEEV infection in hamsters an experiment was conducted wherein hamsters were inoculated intraperitoneally with a  $10\times$  LD<sub>90</sub> dose of WEEV and then received a placebo treatment (n=20), or a treatment with FM at doses of either 5 mg/kg/d (n=15), or 15



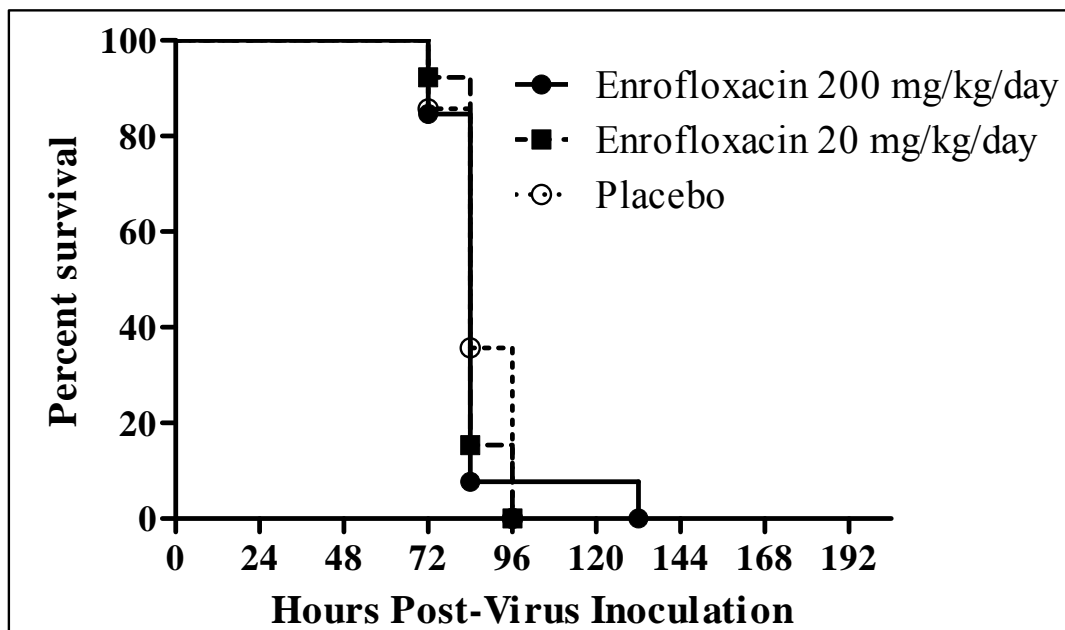


Figure 15: Effects of high and low doses of enrofloxacin alone on the survival of Syrian golden hamsters inoculated with WEEV via the i.p. route.

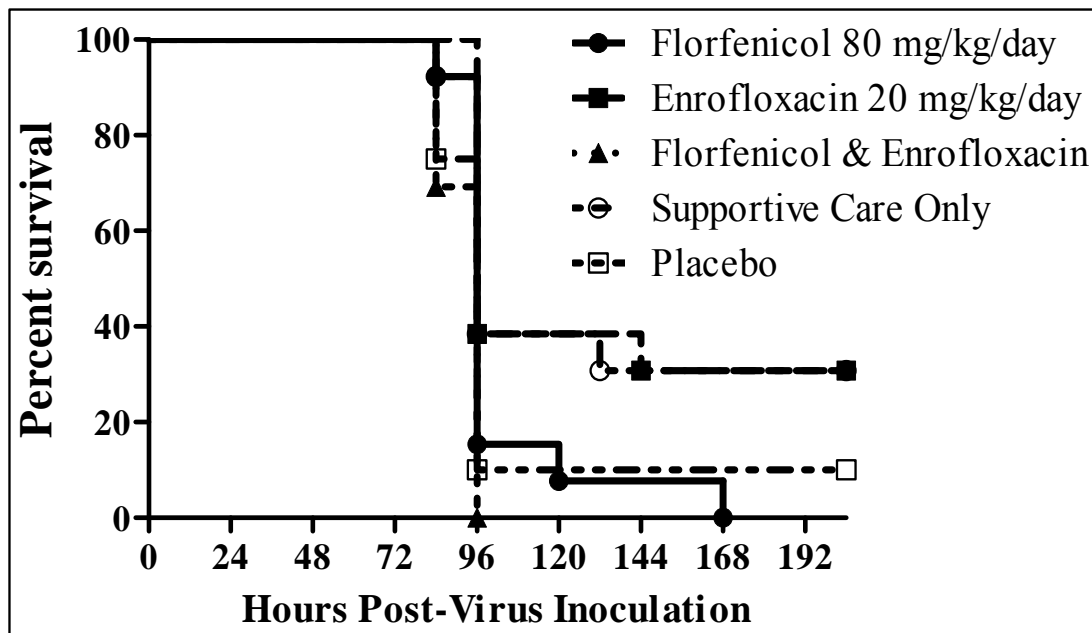


Figure 16: Effects of supportive treatment with and without antibiotics on the survival of Syrian golden hamsters inoculated with WEEV via the i.p. route.

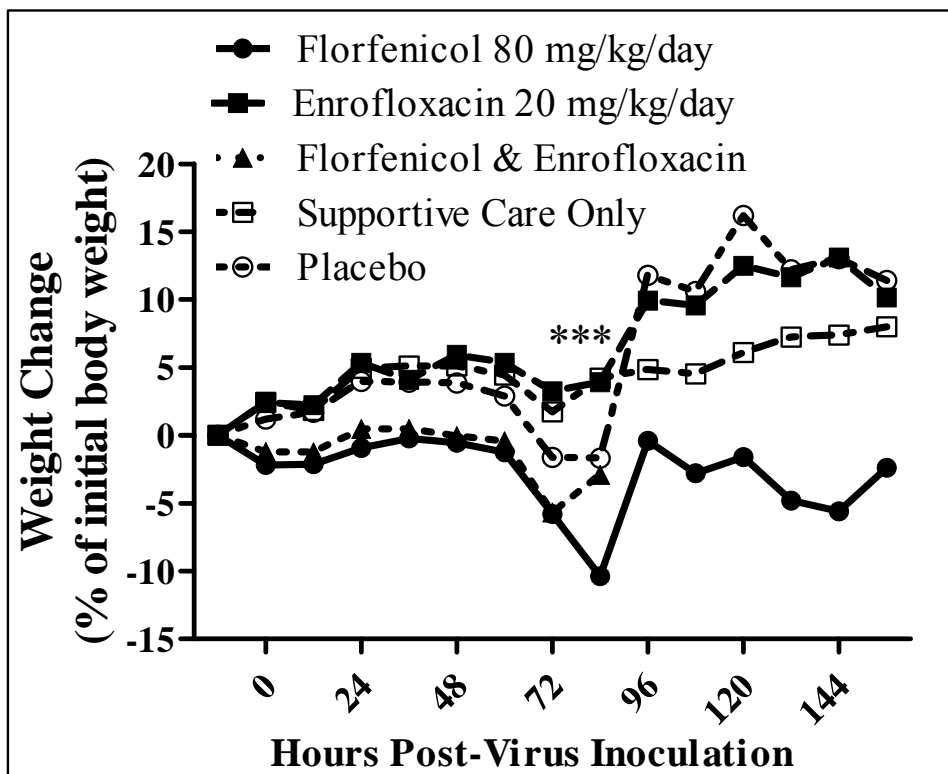


Figure 17: Effects of supportive with and without antibiotics on the weight change of Syrian golden hamsters inoculated with WEEV via the i.p. route. \*\*\*p<0.001 compared to placebo-treated animals.

mg/kg/d (n=15). Animals were monitored for weight change and death. Hamsters receiving the placebo treatment had 0% survival with all animals being dead by 96 hpi (Figure 18). Animals receiving flunixin meglumine at either dose had 20% survival at 204 hpi, which was significantly better than in placebo-treated animals ( $p < 0.05$ ).

Additionally, animals receiving FM at 15 mg/kg/d had an average weight change of  $-0.5\% \pm 4.2\%$ , which was significantly better than the weight change of  $-4.9\% \pm 4.2\%$  seen in placebo-treated animals ( $t = 2.745$ ,  $p < 0.05$ ) (Figure 19). In a separate experiment, hamsters were inoculated intraperitoneally with  $10 \times LD_{90}$  dose of WEEV. Animals were then treated with either placebo (n=10), or dexamethasone at 0.6 mg/kg/d (n=10) administered intraperitoneally. Animals were monitored for changes in body temperature, weight change, and death. Placebo-treated animals had 10% of animals surviving to 204 hpi, with all mortalities occurring by 84 hpi (Figure 20). Animals receiving anti-inflammatory treatment with dexamethasone had 60% survival at 204 hpi, which was statistically significantly higher than that seen in placebo-treated animals ( $p < 0.01$ ). The dexamethasone treatment did not significantly alter weight change in virus-inoculated animals (Figure 21); however, it did significantly inhibit the febrile response at 60 and 72 hpi. Placebo-treated animals had average rectal body temperatures of  $39.6 \pm 0.7$  °C and  $39.2 \pm 0.8$  °C at 60 and 72 hpi, respectively. Hamsters treated with DEX had average body temperatures of  $38.3 \pm 1.1$  °C ( $t = 3.475$ ,  $p < 0.01$ ) and  $38.3 \pm 0.8$  °C ( $t = 3.045$ ,  $p < 0.01$ ) (Figure 22).

A composite of the effects of anti-inflammatory and antimicrobial treatment in hamsters inoculated with WEEV was constructed using data from multiple experiments (Figure 23). Animals in the composite were categorized by treatment modality.

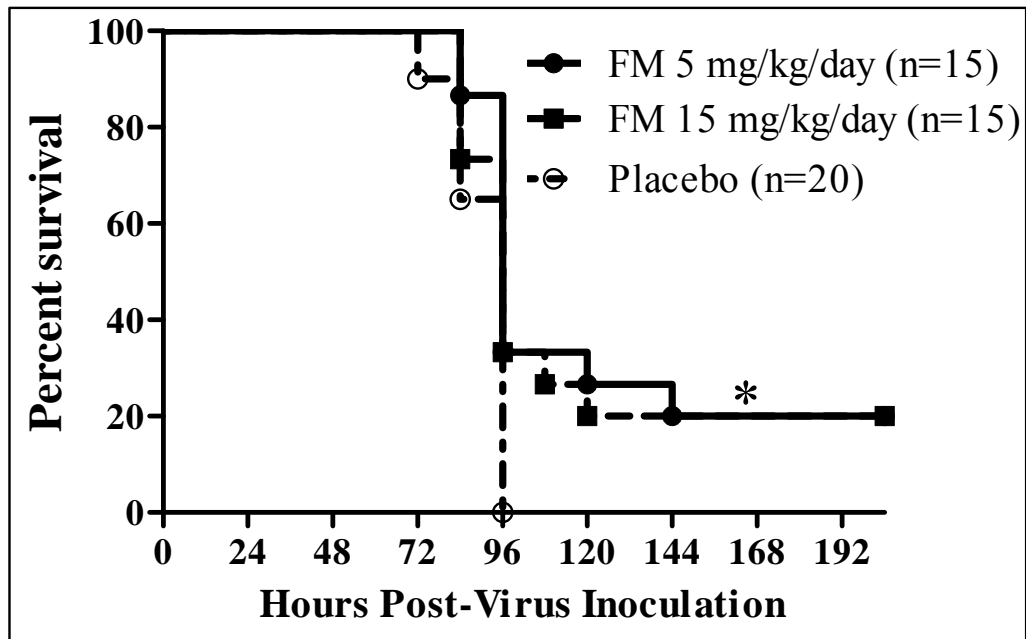


Figure 18: Effects of anti-inflammatory treatment on the survival of Syrian golden hamsters inoculated with WEEV via the i.p. route. \* $p < 0.05$  compared to placebo-treated animals. FM=Flunixin meglumine

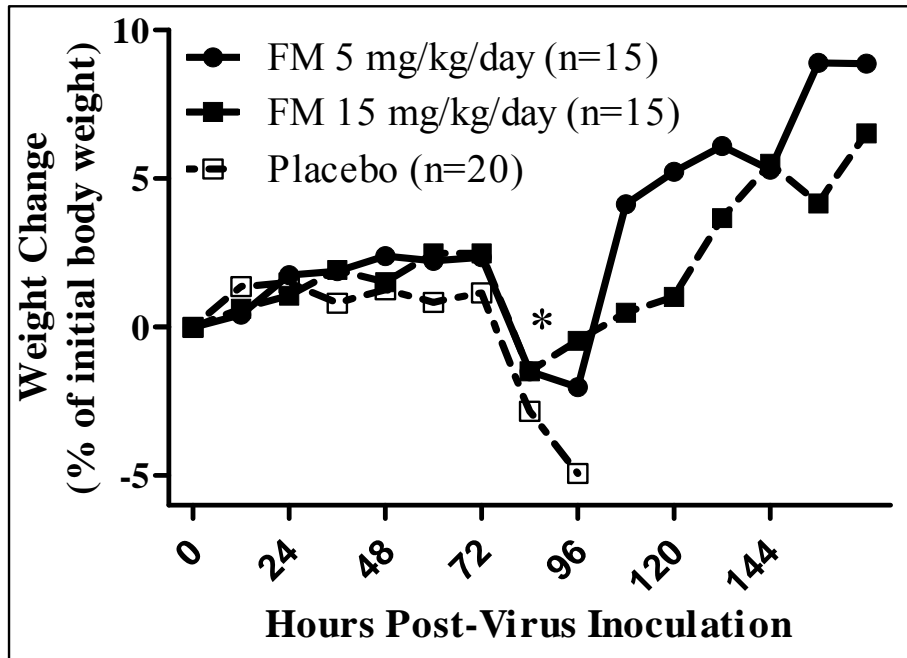


Figure 19: Effects of anti-inflammatory treatment on weight change of Syrian golden hamsters inoculated with WEEV via the i.p. route. \* $p < 0.05$  compared to placebo-treated animals. FM=Flunixin meglumine

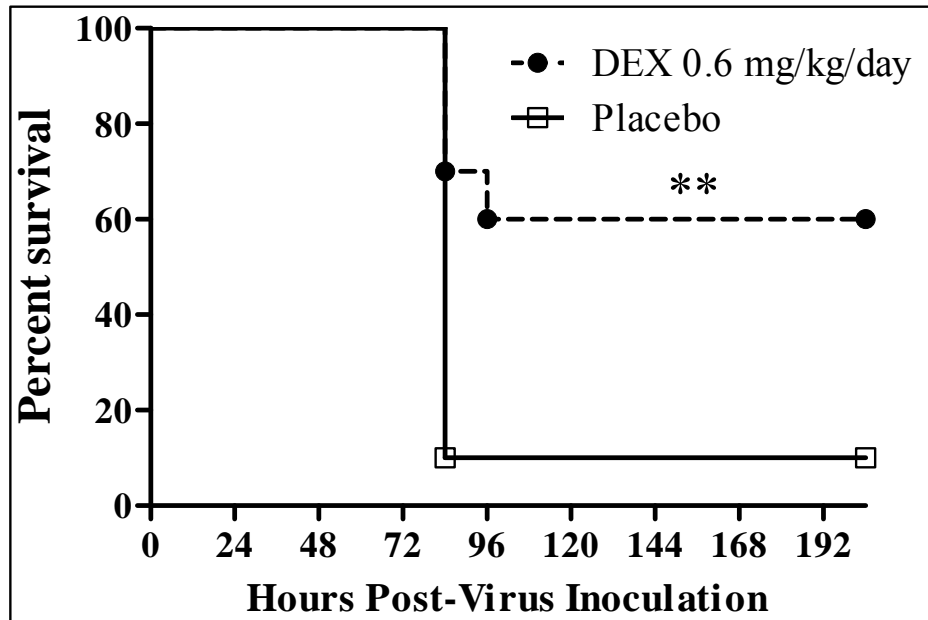


Figure 20: Effects of anti-inflammatory treatment on the survival of Syrian golden hamsters inoculated with WEEV via the i.p. route.

\*\* $p < 0.01$  compared to placebo-treated animals.

DEX=Dexamethasone

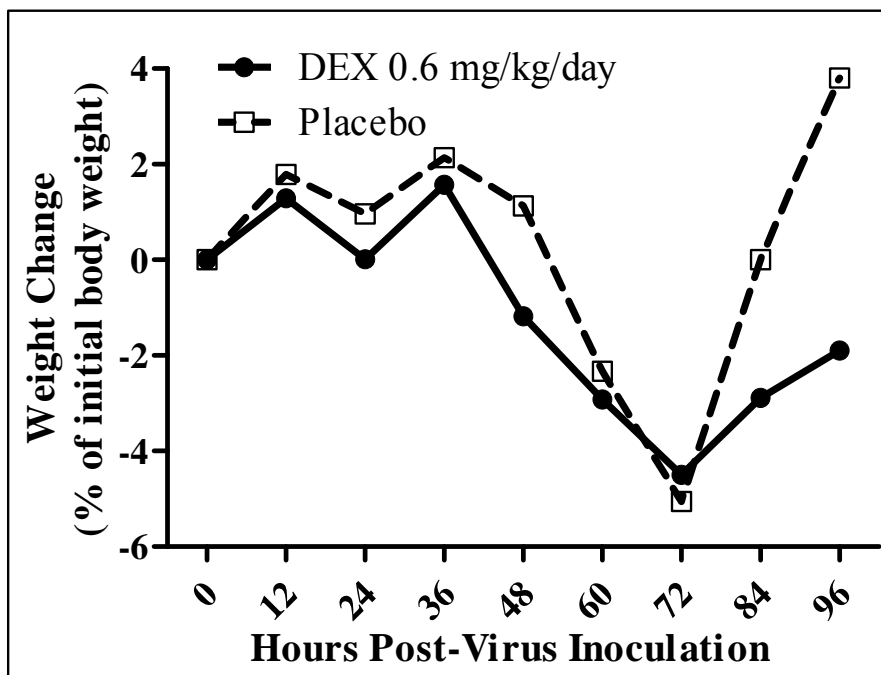


Figure 21: Effects of anti-inflammatory treatment on weight change of Syrian golden hamsters inoculated with WEEV via the i.p. route. DEX=Dexamethasone

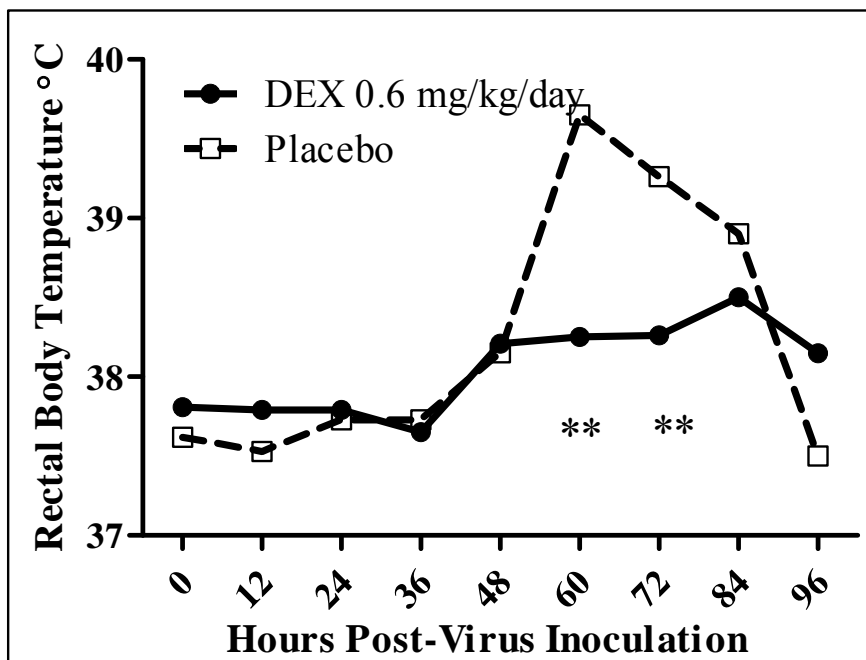


Figure 22: Effects of anti-inflammatory treatment on the rectal body temperature of Syrian golden hamsters inoculated with WEEV via the i.p. route. \*\*p<0.01 compared to placebo-treated animals. DEX=Dexamethasone



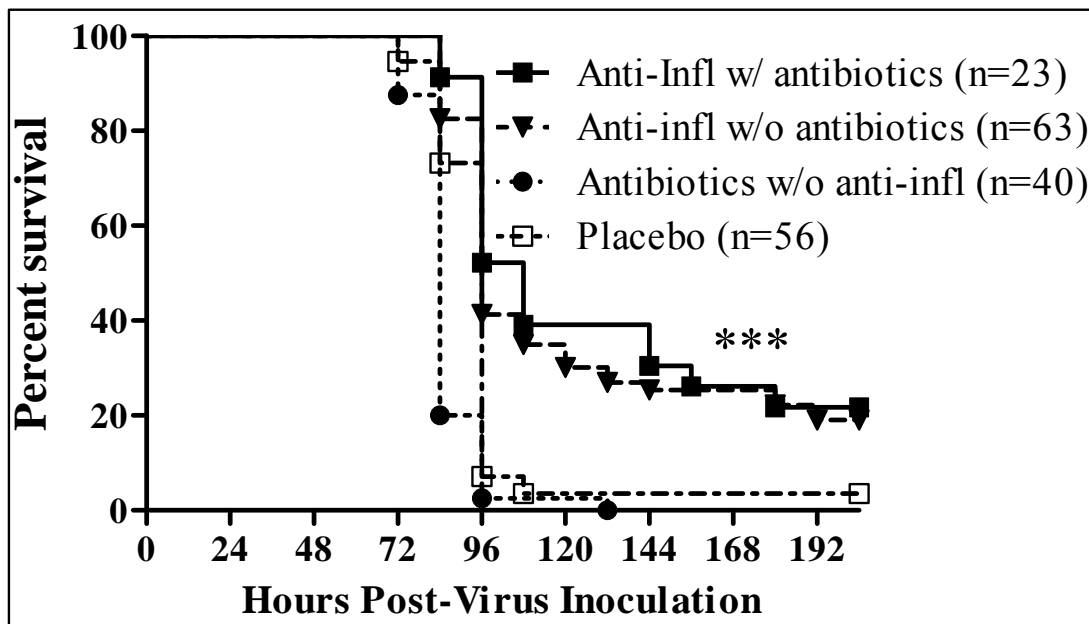


Figure 23: Composite representation of the effects of anti-inflammatory treatment on the survival of Syrian golden hamsters inoculated with WEEV via the i.p. route. Results represent data collected from four separate experiments using anti-inflammatory treatment with or without antibiotic treatment, antibiotic treatment without anti-inflammatory treatment, and placebo treatment. \*\*\* $p < 0.001$  compared to placebo and antibiotic only treated animals.

Treatment groups included the following: anti-inflammatory treatment with antibiotics (n=23), anti-inflammatory treatment without antibiotics (n=63), antibiotic treatment without anti-inflammatory treatment (n=40), and placebo-treated animals receiving neither antibiotic nor anti-inflammatory treatment (n=56). This composite excluded animals receiving drugs with apparent toxicity, such as florfenicol. There was no significant difference between groups receiving either placebo or antibiotic treatment without anti-inflammatory treatment. Indeed, the results for these two groups are almost identical with animals receiving antibiotic treatment alone having 2.5% survival at 108 hpi and 0% survival at 204 hpi. Placebo-treated animals had 3.6% at both 108 and 204 hpi. There was no significant difference between the survival of animals receiving anti-inflammatory agents in combination with antibiotics or anti-inflammatory agents alone.

However, both groups receiving anti-inflammatory treatment had significantly improved survival rates compared to placebo-treated animals, and those receiving antibiotics alone ( $p < 0.001$ ). At 108 hpi animals receiving antibiotics in addition anti-inflammatory treatment had 39.1% survival while those receiving anti-inflammatory treatment alone had 34.9% survival. By 204 hpi the survival rate had dipped to 21.7% and 19.0%, respectively.

### **Characterization of Clinical and Cytokine Changes in Hamsters Inoculated with WEEV**

Results from previous experiments evaluating the effects of anti-inflammatory agents on the disease outcome in WEEV inoculated hamsters indicated that the inflammatory response was at least partially responsible for the morbidity and mortality

observed. It was hypothesized that infection with WEEV could induce an overwhelming inflammatory response producing a clinical syndrome similar to SIRS-MODS as described in humans. Therefore, to test this hypothesis and to gain a fuller understanding of the clinical characteristics of WEEV infection in hamsters an experiment was conducted wherein hamsters were inoculated intraperitoneally with a 10x LD<sub>90</sub> dose of WEEV and multiple clinical parameters were measured over time. Body weight and body temperature were measured in all animals every 12 h, and all animals were observed for morbidity and mortality. Also, every 12 h after virus exposure, and continuing until all animals were dead, 3 randomly selected virus-inoculated animals were sacrificed, and samples were collected for analysis. Parameters measured included, complete blood counts, serum biochemistry panels, virus titers, and interferon concentrations, as well as TNF-alpha concentrations in serum, liver, spleen, kidney, and brain. The intent of this experiment was to identify parameters and trends for future analysis. No statistical analysis of data was conducted.

Virus-inoculated animals appeared to be normal and healthy until approximately 60 hpi, at which time they began to assume a hunched appearance and display decreased activity. As diseased animals progressed towards death they became increasingly lethargic and unresponsive until becoming moribund immediately preceding death. Occasionally, blood was noted on the external nares and muzzle indicating probable epistaxis. Death occurred at approximately 96-108 hpi. No obvious neurological disease signs were observed prior to death.

There was no apparent difference in the daily weight change between sham-inoculated and virus-inoculated animals until 60 hpi, when virus-inoculated animals had

an average weight change of  $-0.8\% \pm 4.0\%$ , compared to an average weight change of  $5.1\% \pm 2.3\%$  seen in sham-inoculated animals (Figure 24). After 60 hpi, virus-inoculated animals lost weight precipitously until the time of death. Similarly, alterations in normal body temperature in virus-inoculated animals were not noted until 60 hpi. At that time sham-inoculated animals had an average rectal body of  $37.5\text{ }^{\circ}\text{C}$  compared to the abnormally elevated temperature of  $39\text{ }^{\circ}\text{C}$  seen in WEEV-inoculated animals (Figure 25).

The infectious viral titers in the plasma, spleen, kidney, liver and brain were determined over a course of time in hamsters inoculated with WEEV (Table 4). Serum virus titers peaked at 36 hpi with  $3.1 \pm 1.3 \log_{10}$  CCID<sub>50</sub>/ml serum simultaneously with the spleen virus titers measured at  $4.8 \pm 0.7 \log_{10}$  CCID<sub>50</sub>/gram of tissue. Brain virus titers peaked approximately 24 h before death at 72 hpi, with  $8.25 \pm 0.0 \log_{10}$  CCID<sub>50</sub>/gram of tissue.

Serum biochemistry parameters were also measured in animals over the course of the infection with WEEV via the use of the VetScan automated serum chemistry device (Abaxis, Union City, CA) (Table 5). Virus-inoculated animals had notable increases in alanine aminotransferase, glucose, phosphorus, and potassium at various time points post-virus inoculation, when compared with sham inoculated animals. Virus-inoculated animals had average alanine aminotransferase (ALT) concentrations of  $209 \pm 107$ ,  $192 \pm 117$ , and  $173 \pm 10$  U/L at 12, 72 and 84 hpi, respectively. This represents an approximately 4-fold increase over the average ALT of  $49 \pm 5$  U/L measured in sham-inoculated animals. Sham inoculated animals had an average serum glucose concentration of  $161 \pm 41$  mg/dL. In contrast, virus-inoculated animals had increased serum glucose concentrations ranging from  $255 \pm 81$  mg/dL at 36 hpi to  $387 \pm 88$

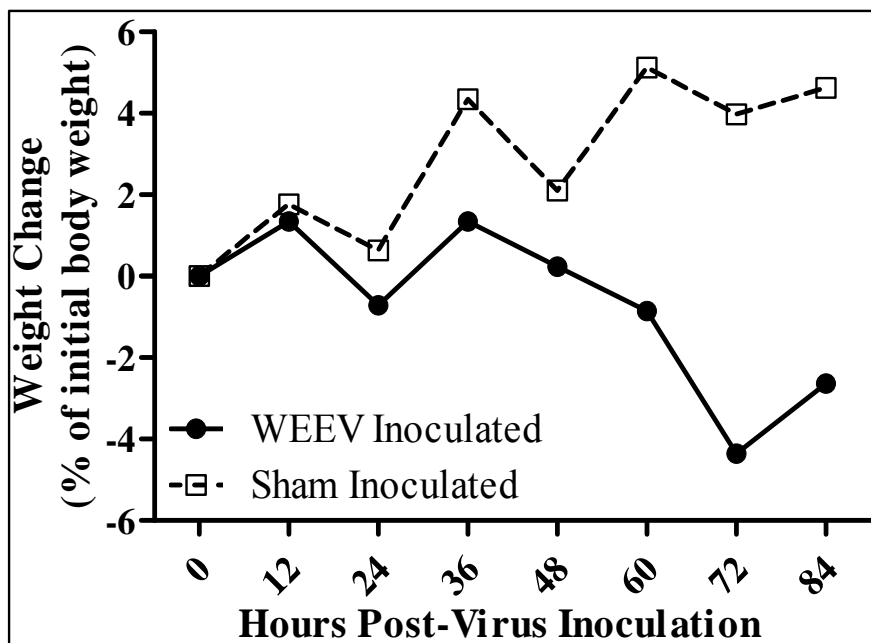


Figure 24: Average percentage weight change from initial body weight of Syrian golden hamsters inoculated with WEEV or sham-inoculated via the i.p. route.

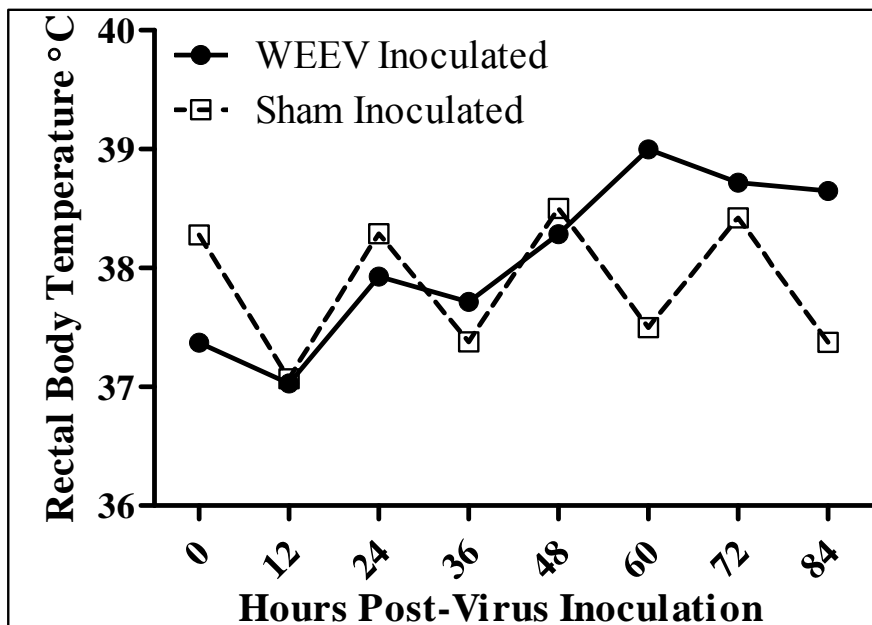


Figure 25: Average rectal body temperature of Syrian golden hamsters inoculated with WEEV- or sham-inoculated via the i.p. route.

TABLE 4: Time course of tissue viral titers in WEEV-inoculated hamsters.

		Hours post-viral injection – viral titers (log <sub>10</sub> infectious doses/g tissue or mL plasma)						
Virus	Tissue	12	24	36	48	60	72	84
WEEV	Serum	(0/3) <sup>a</sup>	(1/3)	(3/3)	(3/3)	(1/3)	(3/3)	(1/2)
		NC <sup>b</sup>	NC	3.8 ± 0.3	3.1 ± 1.3	NC	2.8 ± 1.6	NC
WEEV	Spleen	(0/3)	(1/3)	(3/3)	(3/3)	(3/3)	(3/3)	(2/2)
		NC	NC	4.8 ± 0.7	3.9 ± 0.4	3.0 ± 1.6	4.2 ± 0.9	2.1 ± 0.9
WEEV	Kidney	(0/3)	(0/3)	(1/3)	(0/3)	(2/3)	(2/3)	(2/2)
		NC	NC	NC	NC	2.75 ± 0.0	3.6 ± 0.5	3.8 ± 1.1
WEEV	Liver	(0/3)	(1/3)	(3/3)	(1/3)	(2/3)	(3/3)	(1/2)
		NC	NC	3.5 ± 0.7	NC	4.4 ± 1.2	5.2 ± 0.4	NC
WEEV	Brain	(0/3)	(1/3)	(3/3)	(3/3)	(3/3)	(3/3)	(2/2)
		NC	NC	4.0 ± 1.8	5.8 ± 1.1	6.2 ± 3.4	8.3 ± 0.0	6.5 ± 3.2

<sup>a</sup>Number of samples with detectable virus/total animals assayed.

<sup>b</sup>NC- Not Calculated. Means were not calculated when most samples were below the limits of detection.

Table 5: Clinical chemistry values in hamsters inoculated with WEEV.

Clinical Chemistry	Hours post-virus inoculation								
	Sham	12	24	36	48	60	72	84	
Test	Units								
ALP	U/L	112 ± 17	135 ± 4	195 ± 72	137 ± 15	151 ± 28	151 ± 25	136 ± 17	197 ± 17
ALT	U/L	49 ± 5	209 ± 107	72 ± 13	60 ± 17	69 ± 38	72 ± 28	192 ± 117	173 ± 10
Amylase	U/L	1770 ± 268	1712 ± 608	1550 ± 346	787 ± 142	990 ± 215	1610 ± 240	2008 ± 1841	± 494
T-bilirubin	mg/dL	0.3 ± 0.0	0.3 ± 0.07	0.2 ± 0.06	0.2 ± 0.06	0.2 ± 0.06	0.2 ± 0.06	0.2 ± 0.0	0.2 ± 0.0
BUN	mg/dL	24 ± 2.8	23 ± 1.4	23 ± 1.0	18 ± 1.5	22 ± 0.6	18 ± 5.2	18 ± 0.6	19 ± 7.0
Creatinine	mg/dL	0.3 ± 0.07	0.2 ± 0.0	0.3 ± 0.06	0.3 ± 0.06	0.3 ± 0.06	0.2 ± 0.0	0.2 ± 0.06	0.2 ± 0.0
Glucose	mg/dL	161 ± 41	319 ± 83	307 ± 85	255 ± 81	345 ± 152	387 ± 88	281 ± 122	342 ± 41
Calcium	mg/dL	11.8 ± 0.4	13.6 ± 0.7	11.2 ± 0.7	11.5 ± 0.3	12.7 ± 1.2	11.3 ± 1.2	10.1 ± 0.1	10.0 ± 0.6
Phosphorus	mg/dL	6.6 ± 0.6	9.8 ± 0.6	7.7 ± 1.6	7.5 ± 0.3	10.3 ± 1.5	8.2 ± 2.2	9.6 ± 1.8	8.7 ± 1.5
Sodium	mg/dL	144 ± 4.3	145 ± 4.2	140 ± 4.9	141 ± 3.0	143 ± 4.2	146 ± 4.2	140 ± 1.5	141 ± 0.7
Potassium	mg/dL	5.7 ± 0.5	7.8 ± 0.0	5.0 ± 0.0	5.9 ± 0.5	7.8 ± 1.0	6.7 ± 1.5	7.0 ± 0.1	7.9 ± 0.4
T-Protein	grams/dL	6.3 ± 0.7	5.9 ± 0.1	5.6 ± 0.3	5.6 ± 0.7	5.5 ± 0.3	5.5 ± 0.6	5.4 ± 0.3	5.1 ± 0.3
Albumin	grams/dL	4.4 ± 0.5	4.2 ± 0.1	3.5 ± 0.4	3.7 ± 0.4	3.3 ± 0.3	3.6 ± 0.5	3.5 ± 0.1	3.4 ± 0.4
Globulin	grams/dL	1.9 ± 0.4	1.8 ± 0.1	2.1 ± 0.2	1.8 ± 0.3	2.2 ± 0.1	1.9 ± 0.2	1.9 ± 0.3	1.7 ± 0.1

ALP = alkaline phosphatase; ALT = alanine aminotransferase; T-bilirubin = total bilirubin;

BUN = blood urea nitrogen; T protein = total protein



mg/dL at 60 hpi. This represents up to an approximately 2.4-fold increase in the serum glucose of virus-inoculated animals when compared to sham inoculated animals. In examination of serum electrolytes sham-inoculated animals had serum concentrations for phosphorus  $6.6 \pm 0.6$  mg/dL. In comparison, virus-inoculated animals had increased serum phosphorus concentrations ranging from a low of  $7.5 \pm 0.3$  mg/dL at 48 hpi to a high of  $10.3 \pm 1.5$  mg/dL at 48 hpi. Serum potassium in virus-inoculated animals was intermittently increased compared to  $5.7 \pm 0.5$  mg/dL observed in sham-inoculated animals. Virus-inoculated animals had elevated serum potassium concentrations on  $7.8 \pm 0.0$ ,  $7.8 \pm 1.0$ ,  $7.0 \pm 0.1$ , and  $7.9 \pm 0.4$  mg/dL at 12, 48, 72, and 84 hpi, respectively. In the case of glucose and phosphorus there was no obvious temporal pattern associated with the increased serum concentrations noted in virus inoculated animals. However, the elevated potassium concentrations appeared to be more likely to occur late in the disease process.

Hematological parameters were monitored in WEEV-infected hamsters over time (Table 6). No notable changes were detected in either the hematocrit or total red blood cells counted over the course of the virus infection. Total white blood cell (WBC) counts in virus-inoculated animals were relatively unchanged over the course of the infection except at 48 when hamsters had a moderately decreased WBC count of  $3484 \pm 1577$  cells/ $\mu$ L, and at 84 hpi when hamsters had a moderately increased WBC count of  $11857 \pm 5843$  cells/ $\mu$ L. In comparison sham-inoculated animals had an average WBC count of  $6899 \pm 852$  cells/ $\mu$ L. The primary cause for the decrease in WBC seen at 48 hpi appears to be associated with decreased circulating lymphocytes, as circulating neutrophil

Table 6: Hematological findings in hamsters inoculated with WEEV.

Hematology		Hours post-virus inoculation							
		Sham	12	24	36	48	60	72	84
WBC	cells/ $\mu$ L	6898 $\pm$ 852	6983 $\pm$ 1586	5269 $\pm$ 1641	7220 $\pm$ 2849	3484 $\pm$ 1577	8620 $\pm$ 2324	8450 $\pm$ 2172	11857 $\pm$ 5843
RBC	M/ $\mu$ L	6.6 $\pm$ 0.3	6.7 $\pm$ 0.5	6.6 $\pm$ 0.4	7.6 $\pm$ 0.1	7.3 $\pm$ 0.6	6.0 $\pm$ 0.4	7.2 $\pm$ 1.0	7.9 $\pm$ 1.6
Hct	%	49.2 $\pm$ 1.3	49.0 $\pm$ 0.0	50.7 $\pm$ 1.2	51.7 $\pm$ 1.2	47.7 $\pm$ 2.1	47.7 $\pm$ 1.5	55.0 $\pm$ 3.6	52.0 $\pm$ 5.7
NE	cells/ $\mu$ L	2287 $\pm$ 323	2261 $\pm$ 1042	2552 $\pm$ 913	4884 $\pm$ 2526	2369 $\pm$ 1020	5421 $\pm$ 1610	5428 $\pm$ 1670	5303 $\pm$ 38
LY	cells/ $\mu$ L	4338 $\pm$ 818	4425 $\pm$ 620	2540 $\pm$ 778	2075 $\pm$ 372	1000 $\pm$ 484	2888 $\pm$ 1912	2649 $\pm$ 789	7467 $\pm$ 3459
MO	cells/ $\mu$ L	273 $\pm$ 149	297 $\pm$ 77	178 $\pm$ 42	160 $\pm$ 53	115 $\pm$ 83	310 $\pm$ 70	302 $\pm$ 171	516 $\pm$ 401

WBC = white blood cells; RBC = red blood cells; Hct = hematocrit; NE = neutrophils; LY = Lymphocytes; MO = monocytes

and monocyte numbers remained relatively unchanged over the time course measured. Sham-inoculated animals had an average lymphocyte count of  $4338 \pm 817$  cells/ $\mu$ L. Virus-inoculated animals initially had very similar numbers of lymphocytes, but the average number of circulating lymphocytes began noticeably decreasing at 24 hpi and reached a nadir of  $1000 \pm 484$  cells/ $\mu$ L at 48 hpi before rebounding somewhat at 60 and 72 hpi (Figure 26).

Concentrations of the cytokines TNF-alpha (Table 7) and IFN (Table 8) were measured over time in the serum and tissues of WEEV-inoculated animals. Interferon was undetectable in the serum of virus-inoculated animals at 12 and 24 hpi. At 36 hpi, serum interferon concentrations increased rapidly, with animals having an average serum interferon level of  $357 \pm 34$  U/ml (Figure 27). The interferon concentrations decreased to an average of  $144 \pm 118$  U/ml at 48 hpi, and appeared to be detected only sporadically after that time. In other tissues interferon concentrations were detected sporadically, with no apparent pattern. However, at 72 hpi all 3 animals sampled had detectable interferon in the liver, kidney and spleen with interferon concentrations of  $644 \pm 860$ ,  $43 \pm 17$ , and  $812 \pm 805$  U/gram of tissue, respectively. No sham-inoculated animal had detectable concentrations of interferon in any tissue sampled. TNF-alpha was detected in the serum of virus-inoculated animals beginning at 12 hpi and continuing for the duration of the experiment. TNF-alpha concentrations began noticeably increasing at 36 hpi and peaked at 60 hpi with concentrations of  $58 \pm 26$  U/ml of serum (Figure 28). No TNF-alpha was detected at any time point in the liver, kidney or brain of WEEV-inoculated animals. In the spleen of virus-inoculated animals elevated TNF-alpha concentrations of  $134 \pm 67$  U/g were measured at 12 hpi. Thereafter, TNF-alpha was detected only sporadically

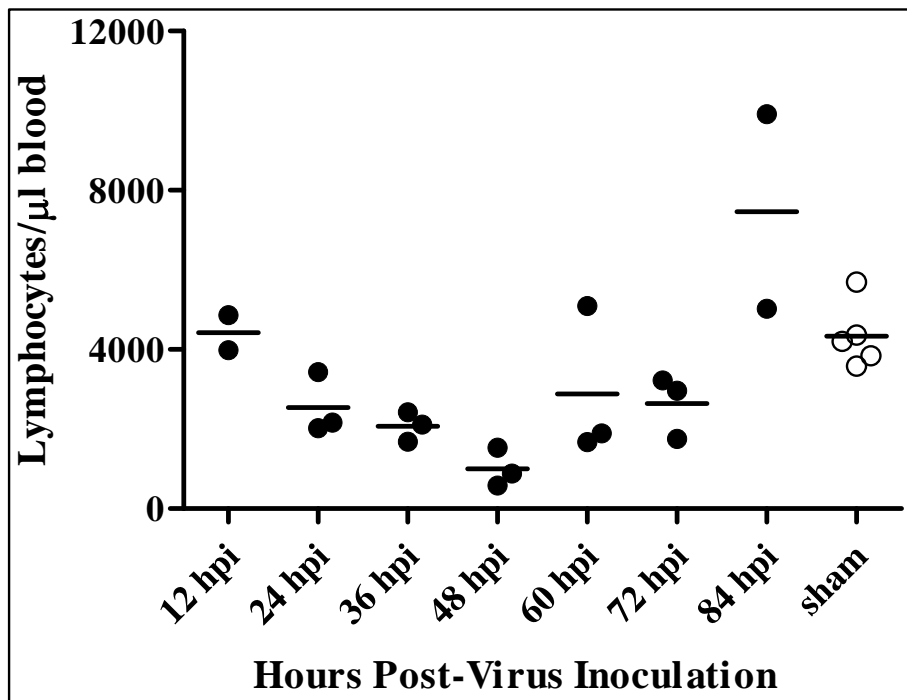


Figure 26: Numbers of circulating lymphocytes at various times post-virus inoculation in the whole blood of Syrian golden hamsters either sham-inoculated or inoculated with WEEV via the i.p. route.

TABLE 7: Time course of tissue TNF-alpha concentrations in WEEV-inoculated hamsters.  
 Hours post-viral injection – cytokine concentrations  
 (Units of activity/g tissue or mL plasma)

Cytokine	Tissue	Sham	12	24	36	48	60	72	84
Tumor Necrosis Factor-alpha		(0/5)	(3/3)	(3/3)	(2/3)	(3/3)	(3/3)	(3/3)	(1/2)
	Serum	NC	15 ± 4	16 ± 7	19 ± 11	31 ± 20	58 ± 26	28 ± 24	NC
		(0/5)	(3/3)	(1/3)	(2/3)	(1/3)	(2/3)	(1/3)	(1/3)
	Spleen	NC	134 ± 67	NC	54 ± 51	NC	26 ± 11	NC	NC
		(0/5)	(0/3)	(0/3)	(0/3)	(0/3)	(0/3)	(0/3)	(0/3)
	Kidney	NC	NC	NC	NC	NC	NC	NC	NC
	(0/5)	(0/3)	(0/3)	(0/3)	(0/3)	(0/3)	(0/3)	(0/3)	
Liver	NC	NC	NC	NC	NC	NC	NC	NC	
	(0/5)	(0/3)	(0/3)	(0/3)	(0/3)	(0/3)	(0/3)	(0/3)	
Brain	NC	NC	NC	NC	NC	NC	NC	NC	

<sup>a</sup>Number of samples with detectable cytokine/total animals assayed.

<sup>b</sup>NC- Not Calculated. Means were not calculated when most samples were below the limits of detection.

TABLE 8: Time course of tissue interferon concentrations in WEEV-inoculated hamsters.  
 Hours post-viral injection – cytokine concentrations  
 (Units of activity/g tissue or mL plasma)

Cytokine	Tissue	Sham	12	24	36	48	60	72	84
Interferon		(0/5) <sup>a</sup>	(0/3)	(0/3)	(3/3)	(2/3)	(1/3)	(1/3)	(0/2)
	Serum	NC <sup>b</sup>	NC	NC	357 ± 38	114 ± 118	NC	NC	NC
		(0/5)	(0/3)	(0/3)	(1/3)	(1/3)	(1/3)	(2/3)	(1/2)
	Spleen	NC	NC	NC	NC	NC	NC	1208 ± 598	NC
		(0/5)	(1/3)	(2/3)	(3/3)	(3/3)	(3/3)	(3/3)	(2/2)
	Kidney	NC	NC	60 ± 46	191 ± 208	209 ± 231	76 ± 76	42 ± 17	99 ± 101
		(0/5)	(0/3)	(0/3)	(3/3)	(0/3)	(1/3)	(3/3)	(2/2)
Liver	NC	NC	NC	33 ± 16	NC	NC	644 ± 860	59 ± 42	
	(0/5)	(0/3)	(0/3)	(0/3)	(1/3)	(0/3)	(0/3)	(1/3)	
Brain	NC	NC	NC	NC	NC	NC	NC	NC	

<sup>a</sup>Number of samples with detectable cytokine/total animals assayed.

<sup>b</sup>NC- Not Calculated. Means were not calculated when most samples were below the limits of detection.

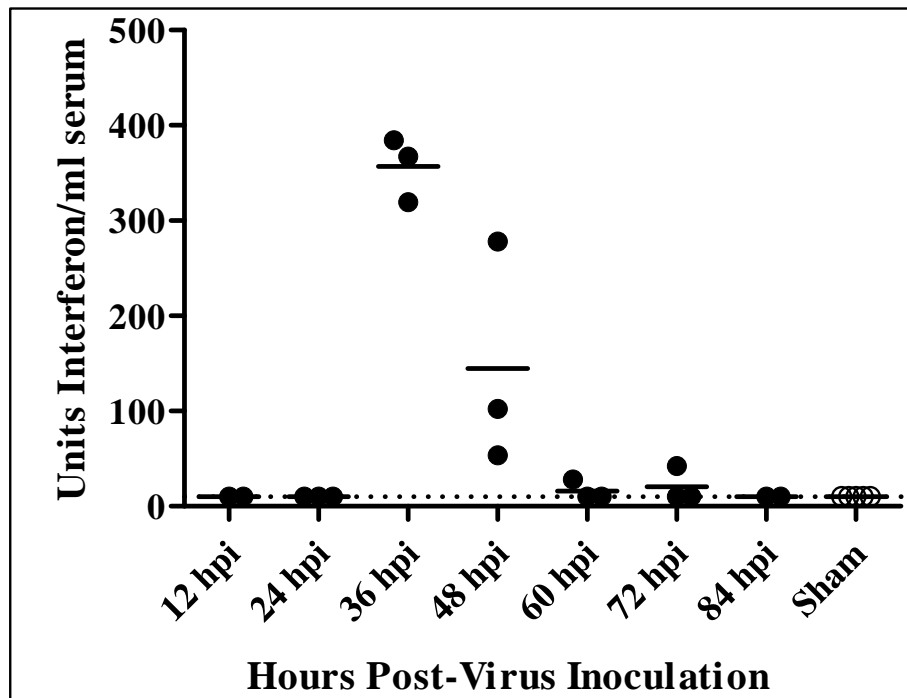


Figure 27: Interferon concentrations at various times post-virus inoculation in the serum of Syrian golden hamsters inoculated with WEEV. Dashed line indicates limit of detection.

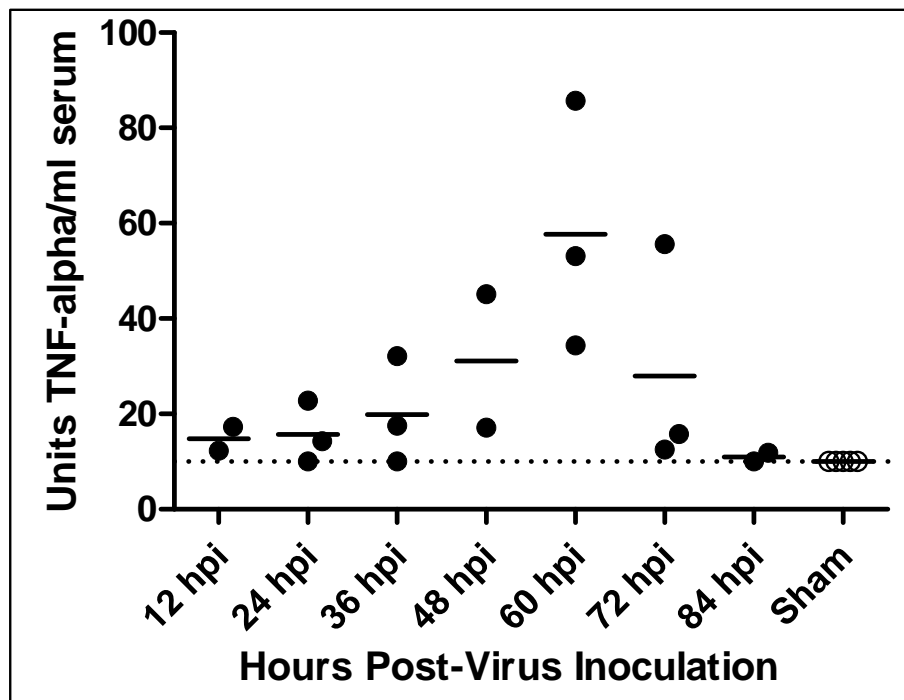


Figure 28: TNF-alpha concentrations at various times post-virus inoculation in the serum of Syrian golden hamsters inoculated with WEEV. Dashed line indicates limit of detection.



in the spleen. No TNF-alpha was detected in any sample assayed from sham-inoculated animals.

An additional clinical observation made over the course of multiple experiments was that a small proportion of animals occasionally survived the initial disease phase and appeared healthy and normal. These animals had weight gain comparable to that of noninfected controls and no overt signs of disease. However, beginning at approximately 144 hpi some of the surviving animals would begin to die. Signs of neurological involvement such as head-tilt, circling, tremors, and paralysis were occasionally noted. However, the most commonly noted clinical sign was acute death. The exact proportion of animals that survived the initial disease period as well as the proportion of animals that would later succumb to disease was highly dependent upon viral dose and the use of any exogenous therapy.

#### **The Effects of Viral Dose and Dexamethasone Immunosuppression on Disease Phenotype in WEEV-Inoculated Hamsters**

Additional experiments were conducted with the intent of better characterizing the relationship between virus dose, the immune and inflammatory response, and disease phenotype and outcome. To compare the effects of different viral doses 20 hamsters each were inoculated intraperitoneally with either a LD<sub>50</sub> or a 10x LD<sub>90</sub> dose of WEEV. Animals were monitored for mortality. Animals inoculated with the higher viral dose had 0% survival, while those inoculated with the lower dose had 20% survival ( $p < 0.05$ ) (Figure 29). Additionally, among those animals from either group that died, those that received the higher viral dose had a significantly greater degree of weight loss

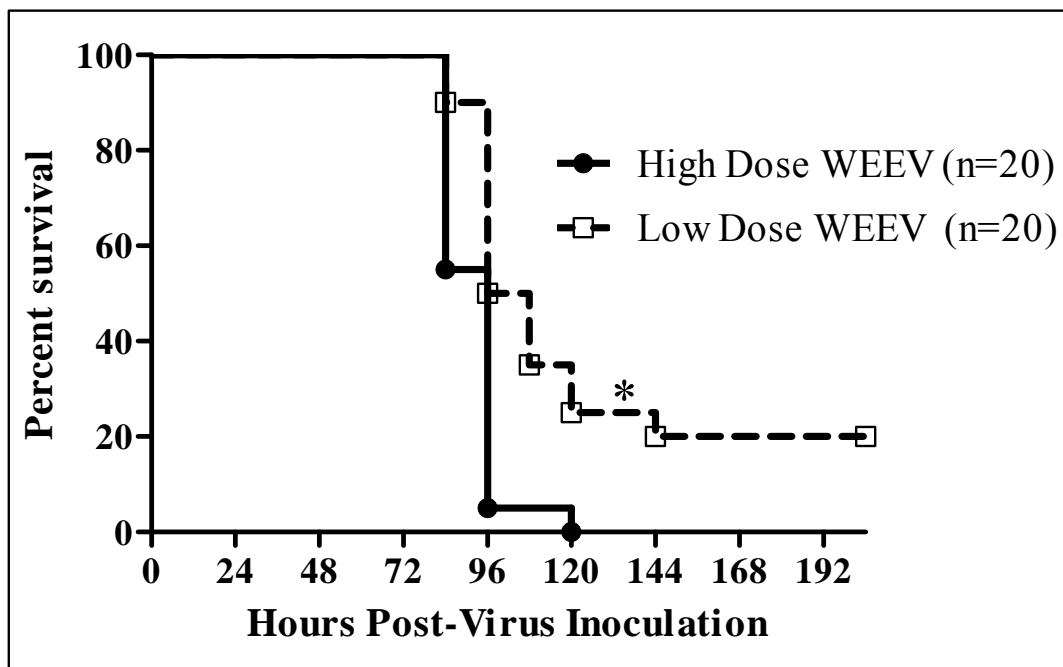


Figure 29: Survival of Syrian golden hamsters inoculated via the i.p. route with either a high (an LD<sub>90</sub>) dose ( $10^{3.5}$  CCID<sub>50</sub>/animal) or a low (LD<sub>50</sub>) dose ( $10^{2.5}$  CCID<sub>50</sub>/animal) of WEEV. \*p<0.05 compared to low dose WEEV.

(Figure 30). At 72 hpi, hamsters that received the high viral dose had weight changes of  $-5.4\% \pm 3.4\%$ , which was significantly more severe than the weight change of  $-3.0\% \pm 3.4\%$  ( $t=2.040$ ,  $p<0.05$ ) seen among nonsurvivors inoculated with the lower viral dose. Furthermore, among those animals from either group that died, the mean time to death (MTD) in animals receiving the higher viral dose was  $91.2 \pm 9.0$  h, which was statistically significantly shorter than the MTD of  $102.8 \pm 15.1$  h seen among those receiving the lower viral dose ( $t=2.839$ ,  $p<0.01$ ) (Table 9).

Hamsters were treated with an immunosuppressive dose of dexamethasone ( $n=5$ ) or treated with drug vehicle ( $n=5$ ) beginning 5 d prior to inoculation with an  $LD_{50}$  dose of WEEV. Dexamethasone-treated animals had 0% survival, with all animals dying at 84 hpi (Figure 31). This was not significantly different than the 20% survival observed in vehicle-treated animals. At 60 hpi vehicle-treated animals had an average body temperature of  $39.3 \pm 0.2$  °C, which was significantly higher than the  $38.4 \pm 0.2$  °C measured in sham-inoculated animals ( $t=5.419$ ,  $p<0.01$ ) (Figure 32). Dexamethasone treatment was able to suppress the febrile response somewhat, as drug-treated animals had an average body temperature of  $38.7 \pm 0.8$  °C at the same time point, which was not significantly different than in the sham-inoculated animals. Simultaneous with its suppression of the febrile response, dexamethasone treatment altered viral titers in virus-inoculated animals. At 60 hpi 3 out of 5 vehicle-treated animals had detectable virus in their serum, with an average virus titer of  $2.0 \pm 0.5$   $\log_{10}$  CCID<sub>50</sub>/mL. In contrast, virus was detected in all 5 samples tested from dexamethasone treated animals, which also had a significantly higher average serum virus titer of  $5.3 \pm 0.5$   $\log_{10}$  CCID<sub>50</sub>/mL ( $t=10.66$ ,  $p<0.001$ ) (Figure 33).

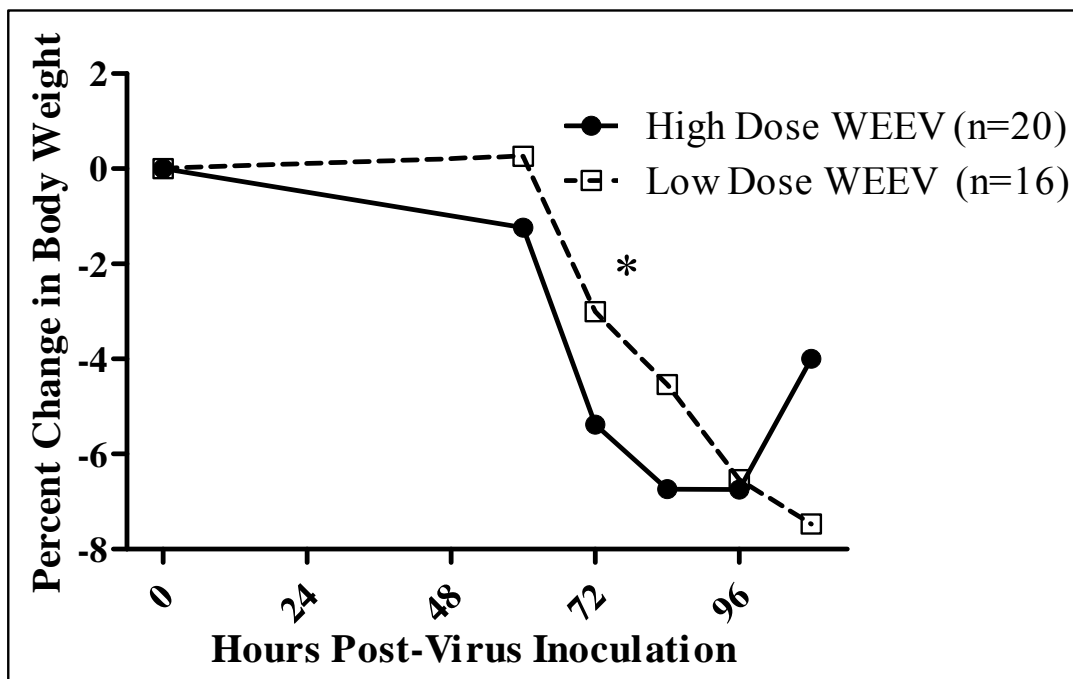


Figure 30: Changes in body weight of hamsters inoculated via the i.p. route with either a high (an LD<sub>90</sub>) dose ( $10^{3.5}$  CCID<sub>50</sub>/animal) or a low (LD<sub>50</sub>) dose ( $10^{2.5}$  CCID<sub>50</sub>/animal) of WEEV. \*p<0.05 compared to low dose WEEV.

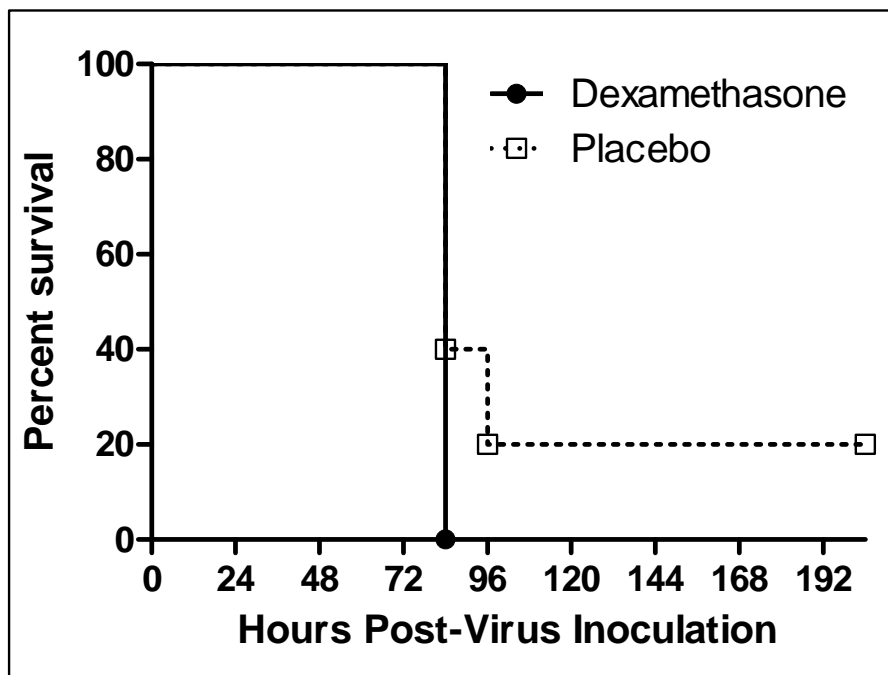


Figure 31: Survival of WEEV-inoculated Syrian golden hamsters following either placebo or immunosuppressive treatment with dexamethasone.

Table 9: Comparison of Mean Time to Death among Syrian golden hamsters inoculated with either a high (an LD<sub>90</sub>) dose ( $10^{3.5}$  CCID<sub>50</sub>/animal) or a low (LD<sub>50</sub>) dose ( $10^{2.5}$  CCID<sub>50</sub>/animal) of WEEV.

Treatment Group	Mean Time to Death (hours)
High Dose WEEV	91.8 ± 8.9**
Low Dose WEEV	102.8 ± 15.1

\*\*p<0.01 Compared to Low Dose WEEV

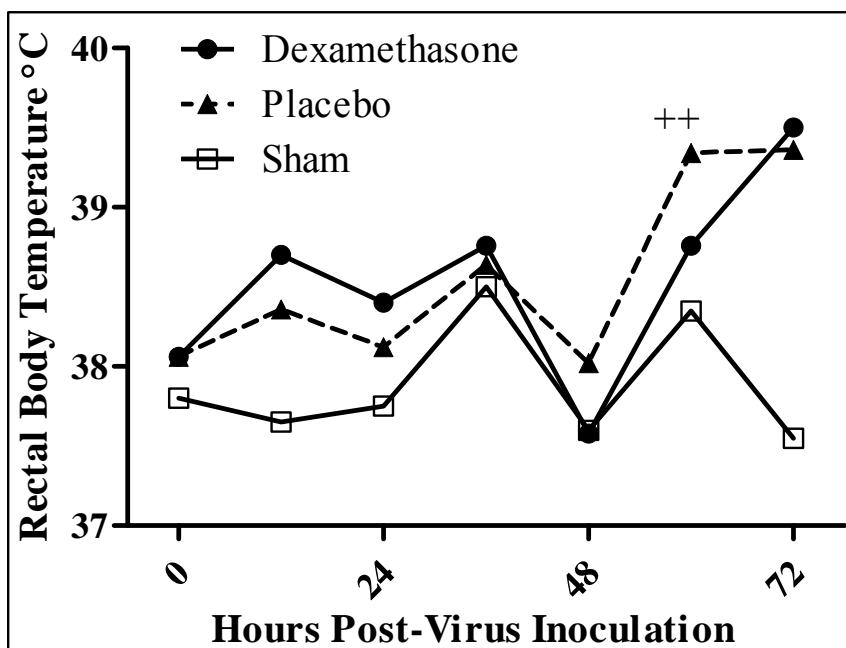


Figure 32: Rectal body temperatures of WEEV-inoculated Syrian golden hamsters following either placebo treatment or immunosuppressive treatment with dexamethasone. ++ $p < 0.01$  Compared to sham-inoculated animals

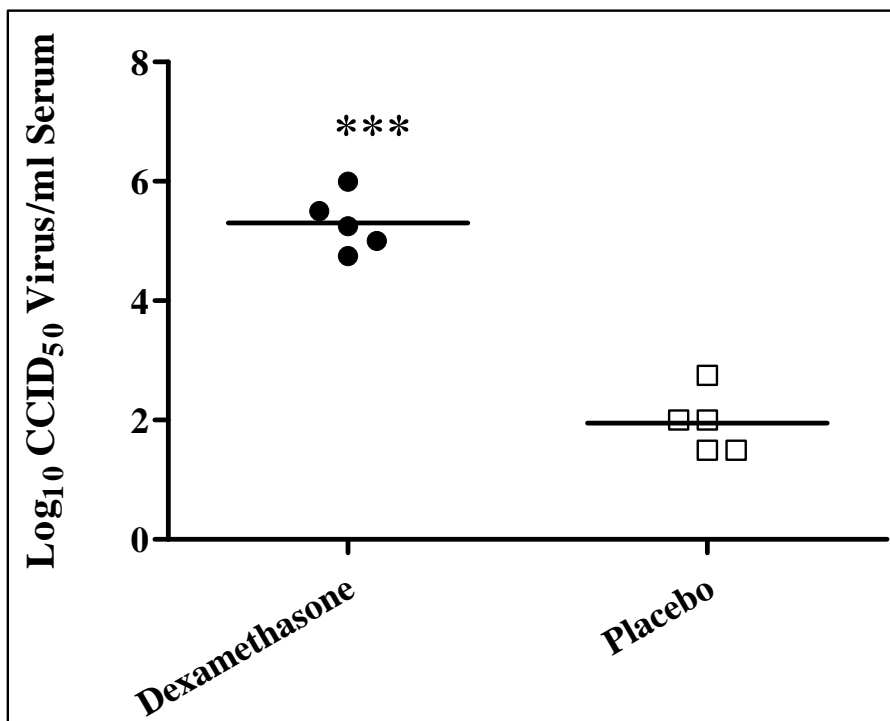


Figure 33: Serum virus titer in WEEV-inoculated Syrian golden hamsters following either placebo treatment or immunosuppressive treatment with dexamethasone. \*\*\*p<0.001 compared to placebo-treated animals.

### **Comparisons of Infection with Kern and California Strains of WEEV in the Syrian Golden Hamster**

It was hypothesized that the disease phenotype of rapid death associated with lymphocytic necrosis as previously described was a condition unique not only to hamsters, but to the specific virus strain used. Therefore experiments were conducted to compare certain disease phenotype characteristics in hamsters inoculated with the previously used California strain of WEEV and a separate distinct virus strain, the Kern strain. Hamsters were inoculated intraperitoneally with  $10^{3.5}$  CCID<sub>50</sub> per animal of the California (CA) strain of WEEV (n=10), equivalent to a LD<sub>90</sub> dose as previously determined in viral titration experiments. Simultaneously, additional groups of hamsters were inoculated with  $10^{3.5}$  CCID<sub>50</sub> per animal of the Kern strain of WEEV (n=5), or were sham-inoculated (n=5). Animals were monitored for disease and death. Animals inoculated with the CA strain followed similar disease patterns as described previously, displaying lymphopenia, fever, and rapid death. Animals inoculated with the CA strain had 20% survival, with all mortalities occurring by 96 hpi (Figure 34). The survival in Kern inoculated animals was significantly different than that observed in CA inoculated animals as determined by Kaplan-Meier analysis (p<0.01). Kern inoculated hamsters had 40% survival with fatalities occurring between 288 and 312 hpi. At 60 hpi the rectal body temperature of animals inoculated with the CA strain was  $39.0 \text{ }^\circ\text{C} \pm 0.8 \text{ }^\circ\text{C}$ , which was significantly higher than the average rectal body temperature of  $37.5 \text{ }^\circ\text{C} \pm 0.6 \text{ }^\circ\text{C}$  (t=3.796, p<0.01) seen in Kern-inoculated animals or the  $37.5 \text{ }^\circ\text{C} \pm 0.4 \text{ }^\circ\text{C}$  measured in sham-inoculated animals (t=3.798, p<0.01) (Figure 35).



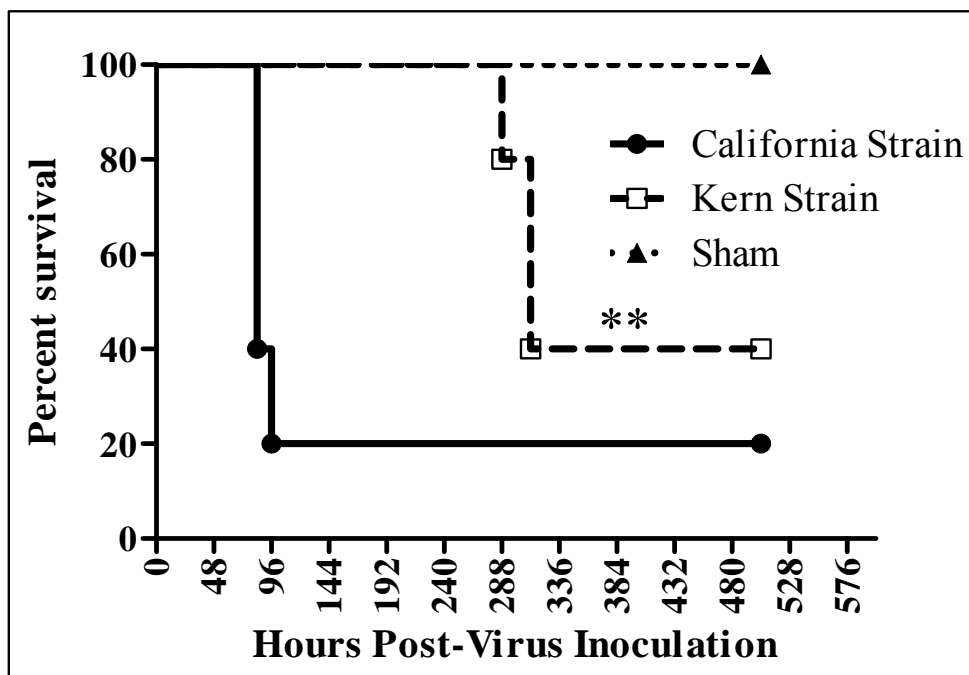


Figure 34: Survival of Syrian golden hamsters inoculated with two different strains of WEEV. \*\* $p < 0.01$  compared to hamsters inoculated with the California strain of WEEV.

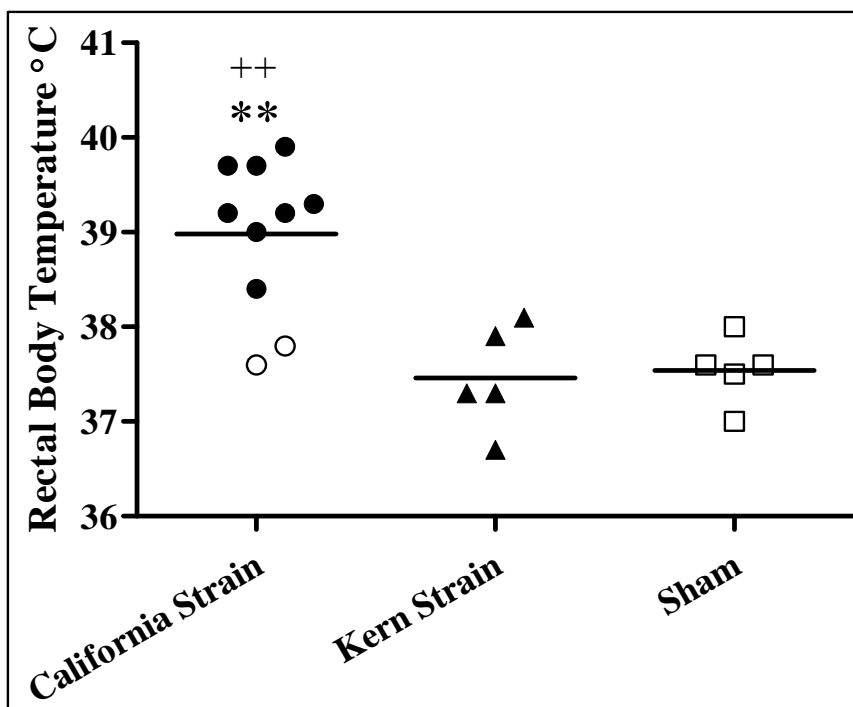


Figure 35: Comparison of rectal body temperatures at 60 hpi in Syrian golden hamsters inoculated with two different strains of WEEV or strain inoculated at 60 hpi. \*\* $p < 0.01$  compared to sham inoculated animals, ++ $p < 0.01$  compared to animals inoculated with the Kern strain of WEEV. Open circles indicate animals that survived infection with the California strain of WEEV.

Blood samples were collected from all animals at 36 hpi and assayed for serum interferon, serum virus titers, and circulating lymphocyte counts. Blood was also collected at 48 hpi and assayed for serum interferon concentrations. At 36 hpi CA-inoculated hamsters had an average circulating lymphocyte count of  $3605 \pm 3290$  cell/ $\mu$ L of whole blood (Figure 36). While this was not significantly different than the  $5708 \pm 2033$  cell/ $\mu$ L seen in sham-inoculated animals it was significantly lower than the  $7943 \pm 2244$  cell/ $\mu$ L measured in Kern-inoculated animals ( $t=2.634$ ,  $p<0.05$ ). The virus was detected in the serum of all CA-inoculated animals at 36 hpi, with a mean serum virus titer of  $4.9 \pm 1.5 \log_{10}$  CCID<sub>50</sub>/mL of serum (Figure 37). This was significantly higher than the mean titer of  $2.7 \pm 1.5 \log_{10}$  CCID<sub>50</sub>/mL measured in Kern-inoculated animals wherein only 3 of the 5 animals had detectable virus titer ( $t=2.772$ ,  $p<0.05$ ). At 36 hpi 1 sham-inoculated animal had a detectable interferon concentration in the serum, and sham animals had a mean interferon concentration of  $24.0 \pm 31.3$  U/mL. Hamsters inoculated with the CA strain also had only 1 animal with detectable concentrations of interferon in the serum and had an average serum concentration of  $36.7 \pm 31.3$  U/mL. In contrast, all but 1 Kern-inoculated animal had detectable amounts of serum interferon and had a mean concentration of  $361.4 \pm 206.3$  U/mL, which was statistically significantly higher than the concentrations measured in CA-inoculated animals ( $t=4.415$ ,  $p<0.001$ ) (Figure 38). By 48 hpi serum concentrations had altered, with no detectable interferon measured in sham-inoculated animals. Among CA strain-inoculated animals interferon concentrations were increased, wherein 9 out of 10 animals had detectable amounts of interferon in their serum and a mean concentration of  $125.0 \pm 128.7$  U/mL. The interferon concentrations in Kern animals had decreased, with only 1 out of 5 animals having serum

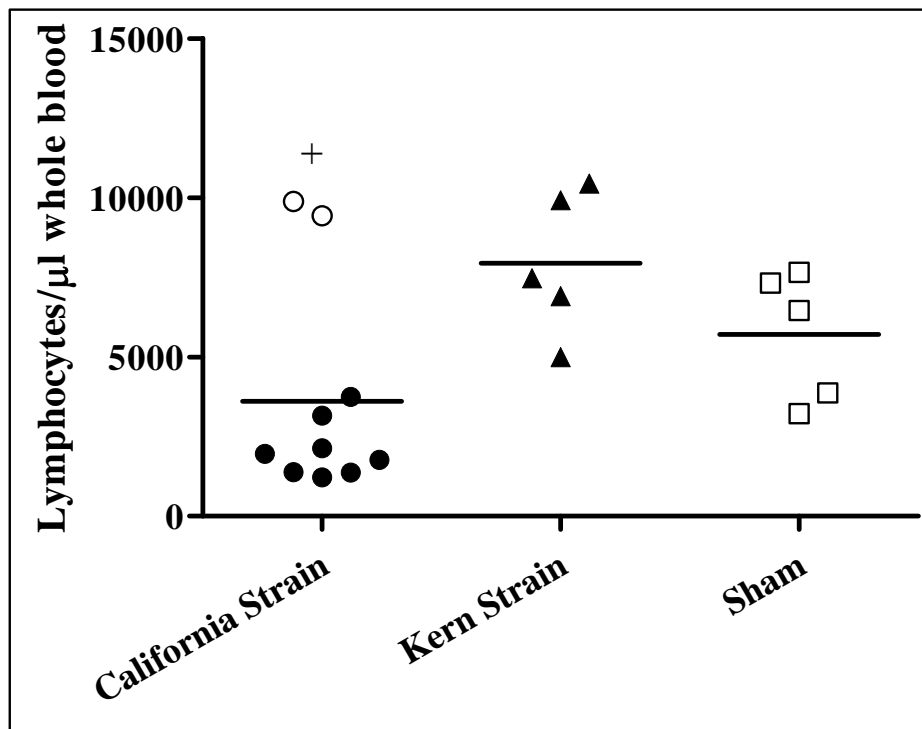


Figure 36: Lymphocyte counts at 36 hpi in the whole blood of Syrian golden hamsters inoculated with two different strains of WEEV or strain inoculated. + $p < 0.05$  compared to animals inoculated with the Kern strain of WEEV. Open circles indicate animals that survived infection with the California strain of WEEV.

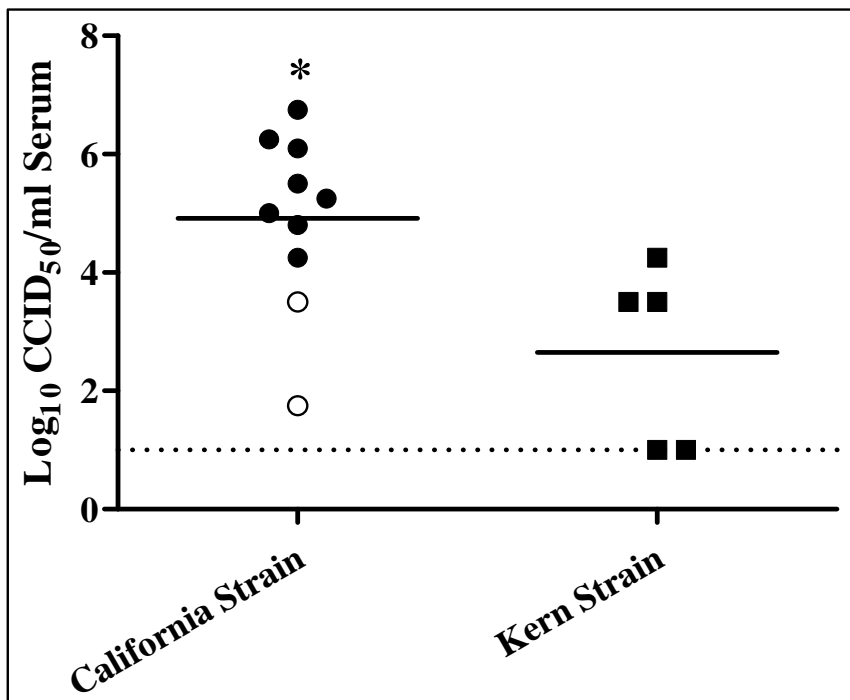


Figure 37: Serum virus titers at 36 hpi in hamsters inoculated via the i.p. route with two different strains of WEEV. \* $p < 0.05$  compared to animals inoculated with the Kern strain of WEEV. Open circles indicate animals that survived infection with the California strain of WEEV.

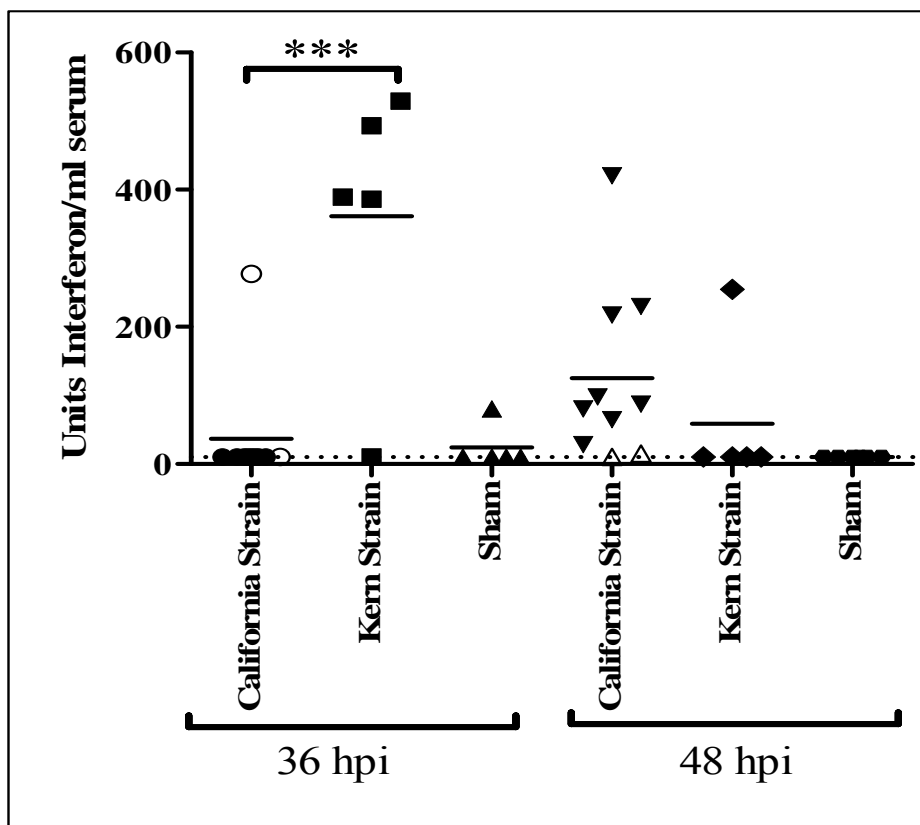


Figure 38: Serum interferon concentrations at 36 and 48 hpi in hamsters inoculated with two different strains of WEEV. \*\*\* $p < 0.001$  California strain-inoculated animals compared to Kern strain-inoculated animals. Open circles and open triangles indicate animals that survived infection with the California strain of WEEV.

interferon concentrations above the limits of detection and having a mean interferon concentration of  $59.0 \pm 109.5$  U/mL, which was not significantly different than that seen in CA-inoculated animals.

### **Identification of Potential Markers of Disease Outcome in WEEV-Inoculated Hamsters**

It had been previously noted that hamsters develop severe lymphopenia associated with WEEV infection, but that lymphocyte counts in animals subsequently surviving WEEV infection were higher (Figure 36). It was also noted that hamsters inoculated with the Kern strain of virus displayed significantly different serum interferon concentrations at early time-points in virus infection (Figure 38). Therefore, experiments were conducted to evaluate lymphocyte counts and serum cytokine concentrations as indicators of disease outcome. Hamsters were either inoculated intraperitoneally with an LD<sub>50</sub> dose of WEEV or sham-inoculated, and monitored for death. At various time points both before and/or after virus inoculation blood samples were collected and analyzed for numbers of circulating WBC and circulating lymphocytes. For the current experiments animals alive after 108 hpi were considered survivors. At 72 hpi sham-inoculated animals (n=5) had an average WBC count of  $4220 \pm 1746$  cells/ $\mu$ L of whole blood (Figure 39). In comparison animals that subsequently survived the WEEV infection (n=4) had an average WBC count of  $2663 \pm 782$  cells/ $\mu$ L and nonsurvivors (n=6) had  $1871 \pm 461$  cells/ $\mu$ L, which was significantly lower than in sham-inoculated animals ( $t=3.197$ ,  $p<0.05$ ). A separate group of animals was assayed at 84 hpi. At that time point sham-inoculated animals (n=5) had an average WBC count of  $7040 \pm$

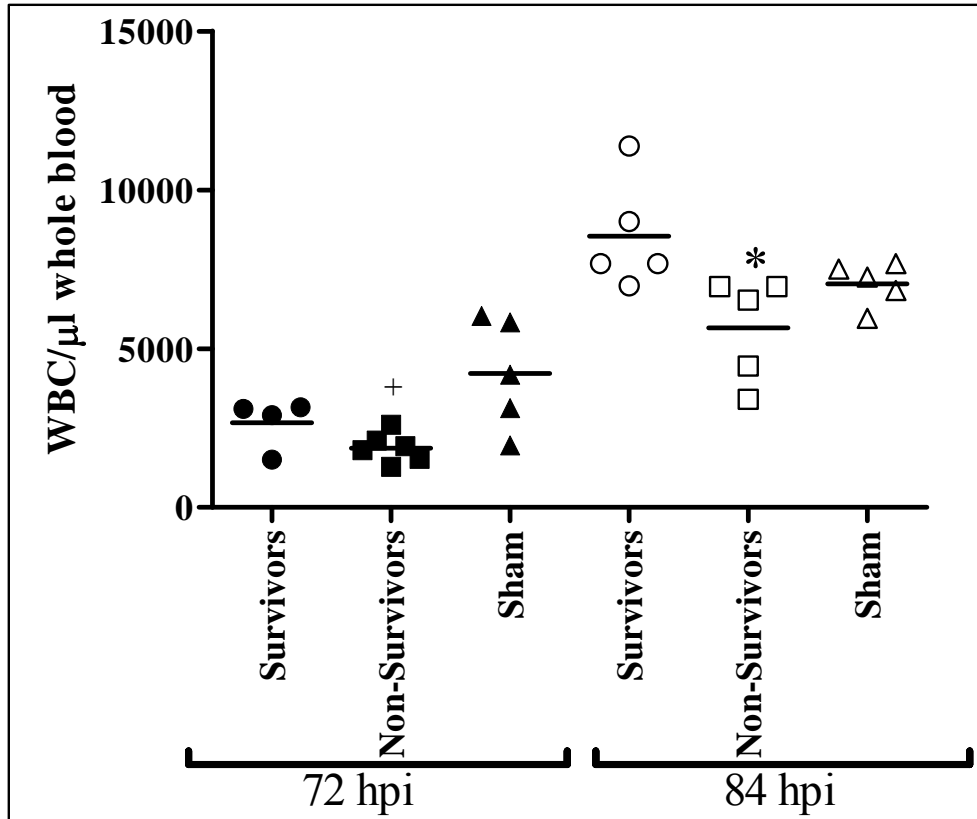


Figure 39: Comparison of circulating white blood cell counts at 72 and 84 hpi in whole blood from hamsters that either survived or succumbed to infection with WEEV. \* $p < 0.05$  WEEV nonsurvivors compared to sham inoculated animals, + $p < 0.05$  WEEV nonsurvivors compared to WEEV survivors.



688 cells/ $\mu$ L. WEEV survivors (n=5) had  $8540 \pm 1746$  cells/ $\mu$ L and nonsurvivors (n=5) had  $5655 \pm 1632$  cells/ $\mu$ L, which was significantly lower than survivors ( $t=2.700$ ,  $p<0.05$ ), but not significantly different than in sham-inoculated animals. Highly statistically significant differences between survivors and nonsurvivors were noted when lymphocyte counts in the same groups of animals were assayed (Figure 40). At 72 hpi, sham-inoculated animals had an average of  $2665 \pm 597$  cells/ $\mu$ L compared to  $945 \pm 378$  cells/ $\mu$ L in survivors (not statistically significant), and  $216 \pm 184$  cells/ $\mu$ L in nonsurvivors ( $t=4.120$ ,  $p<0.01$  vs. survivors,  $t=9.593$ ,  $p<0.001$  vs. sham). At 84 hpi sham-inoculated animals had average lymphocyte counts of  $4762 \pm 740$  cells/ $\mu$ L compared to  $3528 \pm 943$  cells/ $\mu$ L in survivors, and  $467 \pm 221$  cells/ $\mu$ L in nonsurvivors ( $t=7.063$ ,  $p<0.001$  vs. survivors,  $t=12.42$ ,  $p<0.001$  vs. sham).

In a separate experiment animals were again inoculated intraperitoneally with an  $LD_{50}$  of WEEV or were sham-inoculated. Previous to virus inoculation blood samples were collected from all animals and analyzed for WBC and lymphocyte counts, and animals were then randomly assigned to virus or sham-inoculation groups. No significant differences in either WBC or lymphocyte counts were detected between groups previous to virus inoculation (data not shown). Blood samples were collected and analyzed at 84 hpi, and animals were monitored for disease outcome. At 84 hpi sham inoculated animals (n=5) had average WBC counts of  $7834 \pm 1565$  cells/ $\mu$ L compared to  $5382 \pm 2037$  cells/ $\mu$ L in survivors (n=5) and  $6514 \pm 2279$  cells/ $\mu$ L in nonsurvivors (n=15) (Figure 41). Lymphocyte counts in the same animals were  $3752 \pm 1232$  cells/ $\mu$ L in sham-inoculated animals,  $2703 \pm 1375$  cells/ $\mu$ L in survivors, and  $1498 \pm 637$  cells/ $\mu$ L in nonsurvivors ( $t=2.369$ ,  $p<0.05$  vs. survivors,  $t=4.759$   $p<0.001$  vs. sham) (Figure 42).

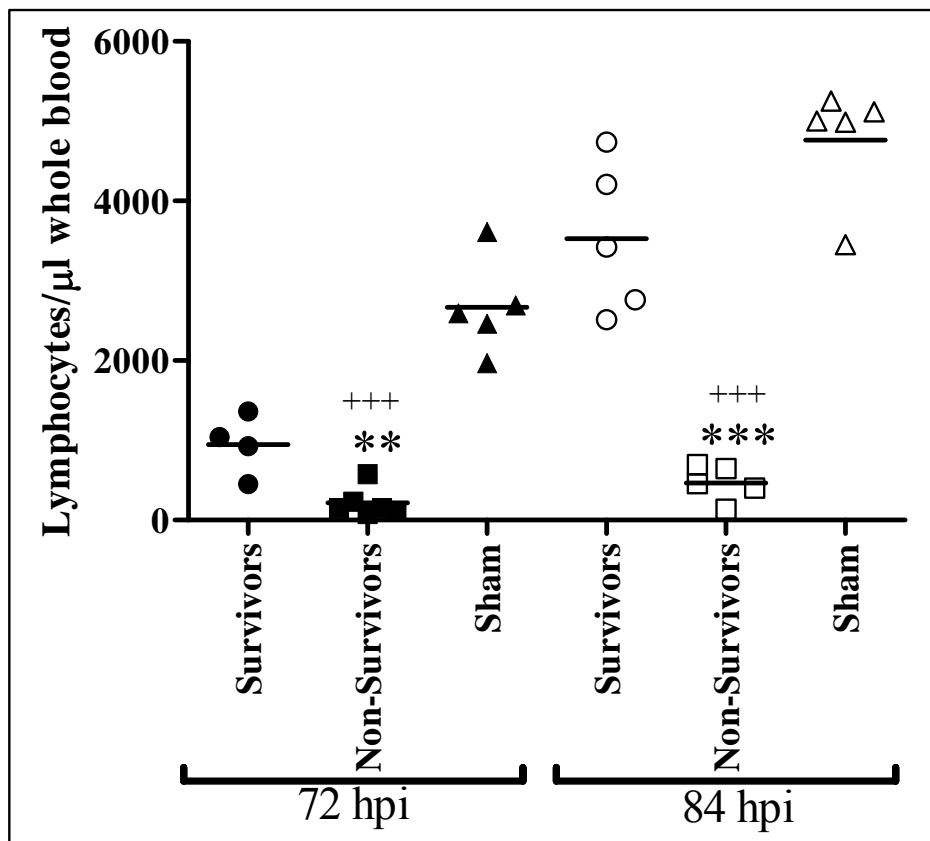


Figure 40: Comparison of circulating lymphocyte counts at 72 and 84 hpi in whole blood from hamsters that either survived or succumbed to infection with WEEV. \*\* $p < 0.01$ , \*\*\* $p < 0.001$  WEEV nonsurvivors compared to sham-inoculated animals, +++ $p < 0.001$  WEEV nonsurvivors compared to WEEV survivors.

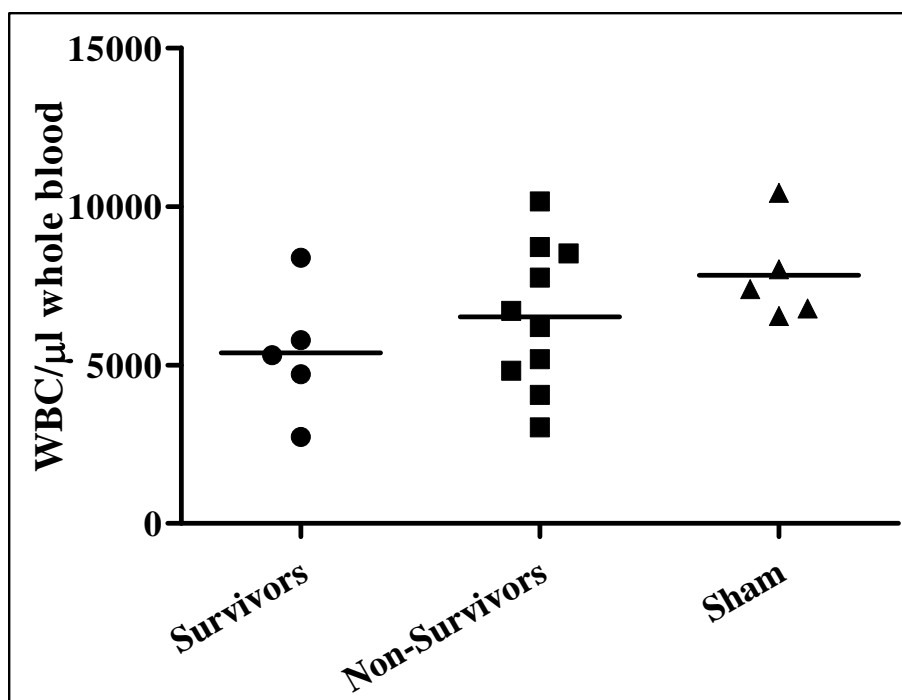


Figure 41: Circulating white blood cell counts at 84 hpi in whole blood from hamsters that either survived or succumbed to infection with WEEV.

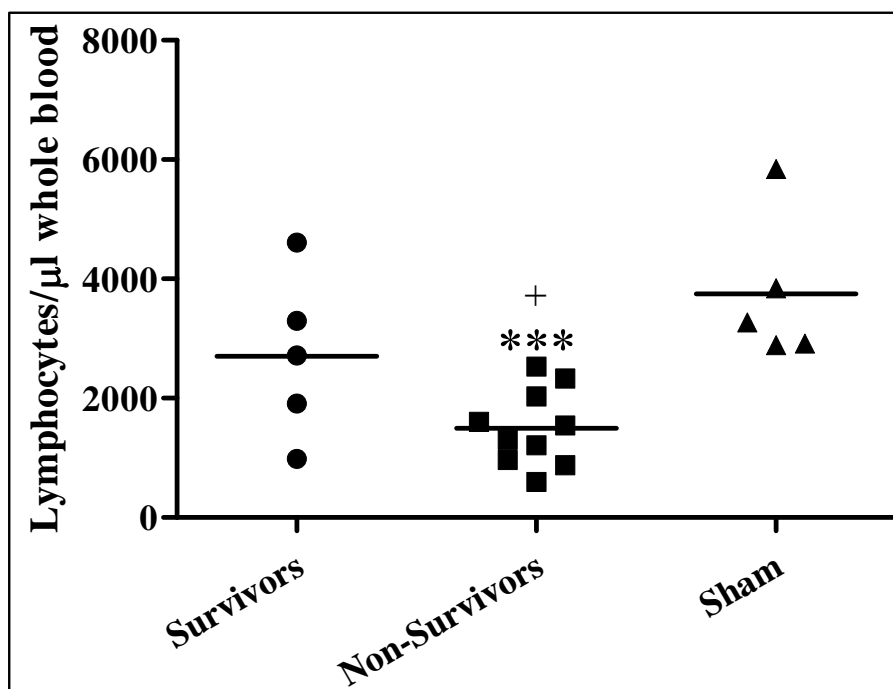


Figure 42: Circulating lymphocyte counts at 84 hpi in whole blood from hamsters that either survived or succumbed to infection with WEEV. \*\*\* $p < 0.001$  WEEV nonsurvivors compared to sham-inoculated animals, + $p < 0.05$  WEEV nonsurvivors compared to WEEV survivors.

In a third related experiment animal blood samples were collected from animals for WBC and lymphocyte counts, followed by random assignment of animals to different treatment groups. Hamsters were inoculated with a 10x LD<sub>90</sub> dose of WEEV or were sham-inoculated. Hamsters then received treatment with flunixin meglumine (5 mg/kg/d) as previously described or received placebo treatment. Blood was collected at 84 hpi and analyzed for WBC and lymphocyte counts. Animals were monitored for disease outcome. No significant differences in either WBC or lymphocyte counts were noted between any groups prior to virus inoculation (data not shown). By 108 hpi all placebo-treated animals were dead; while FM-treated animals had 40% survival at 108 hpi (Figure 43). At 84 hpi sham-inoculated animals treated with FM (n=4) had an average WBC count of  $8188 \pm 2103$  cells/ $\mu$ L, placebo-treated animals (n=3) had an average of  $8175 \pm 2575$  cells/ $\mu$ L, FM-treated animals that subsequently survived beyond 108 hpi (n=4) had  $4720 \pm 802$  cells/ $\mu$ L, while nonsurvivors (n=6) had a mean of  $6285 \pm 855$  cells/ $\mu$ L (Figure 44). Lymphocyte counts in the same animals were  $4065 \pm 2055$  cells/ $\mu$ L in sham-inoculated animals,  $1408 \pm 271$  cells/ $\mu$ L in placebo-treated animals,  $2375 \pm 963$  cells/ $\mu$ L in survivors, and  $1292 \pm 434$  cells/ $\mu$ L in nonsurvivors ( $t=2.952$ ,  $p<0.05$  vs. sham) (Figure 45).

Hamsters were inoculated intraperitoneally with an LD<sub>50</sub> dose of WEEV and monitored for disease outcome. Serum was collected at various times post-virus inoculation and assayed for cytokine concentration. Animals with cytokine concentrations below the limits of detection were considered to have a concentration at the lower limits of the assay (10 U/mL). Virus inoculated animals had a 40% survival rate, with all mortalities occurring by 108 hpi (Figure 46). Serum was collected at 20 and

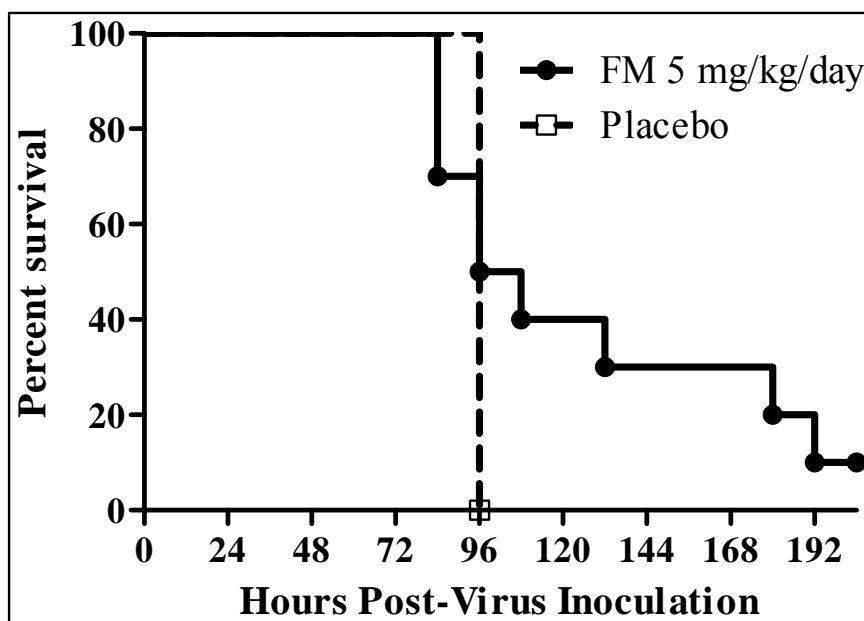


Figure 43: Survival of WEEV inoculated hamsters treated with flunixin meglumine or placebo treatments.

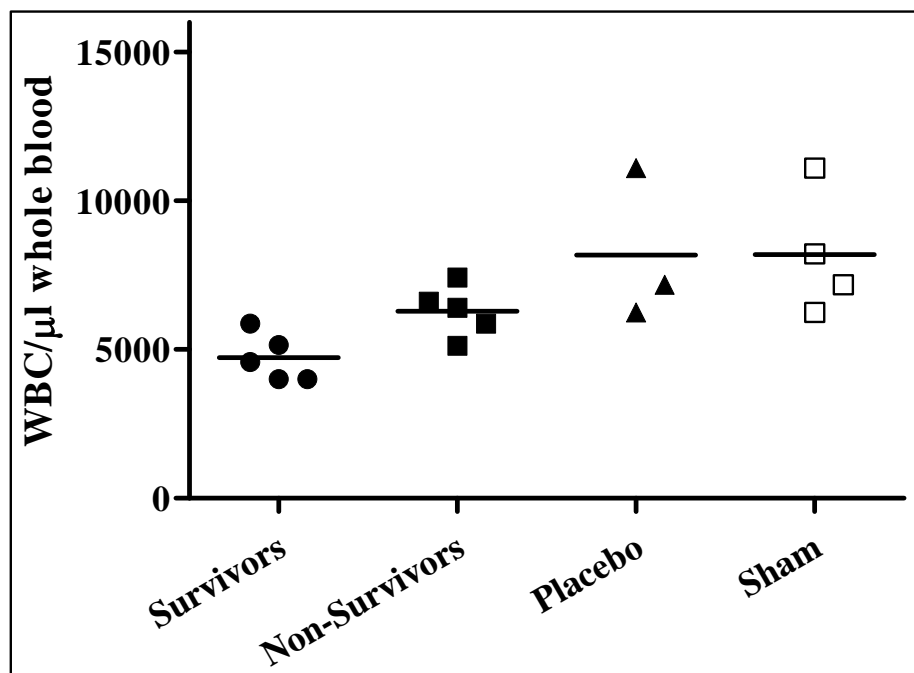


Figure 44: Circulating white blood cell counts at 84 hpi in whole blood from hamsters inoculated with WEEV and treated with flunixin meglumine or placebo treatment. Survivors=animals persisting beyond 108 hpi.

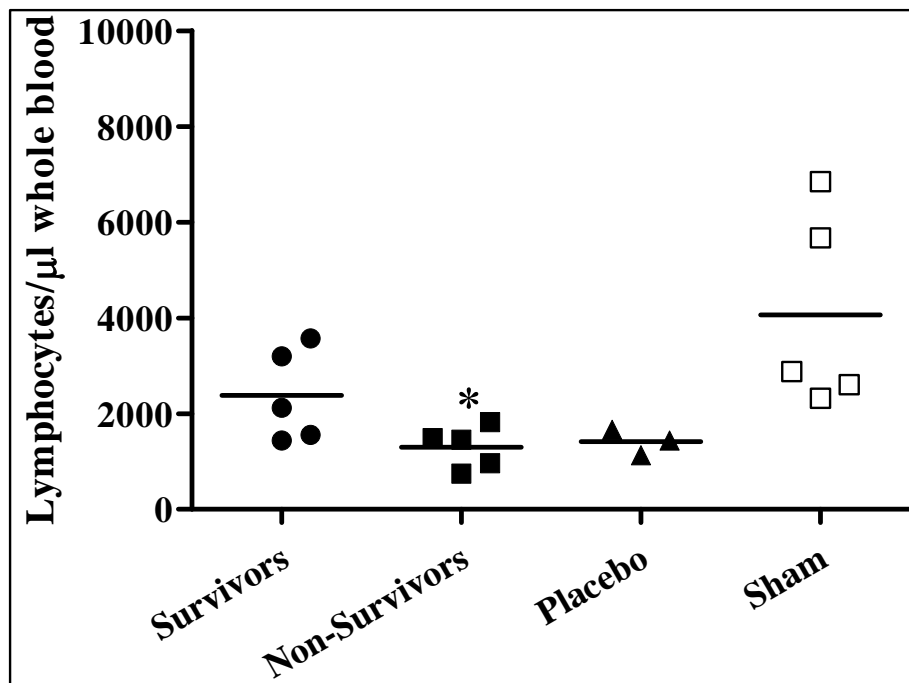


Figure 45: Circulating lymphocyte counts at 84 hpi in whole blood from hamsters inoculated with WEEV and treated with flunixin meglumine or placebo treatment. Survivors=animals persisting beyond 108 hpi. \* $p < 0.05$  Nonsurvivors compared to sham-inoculated animals.



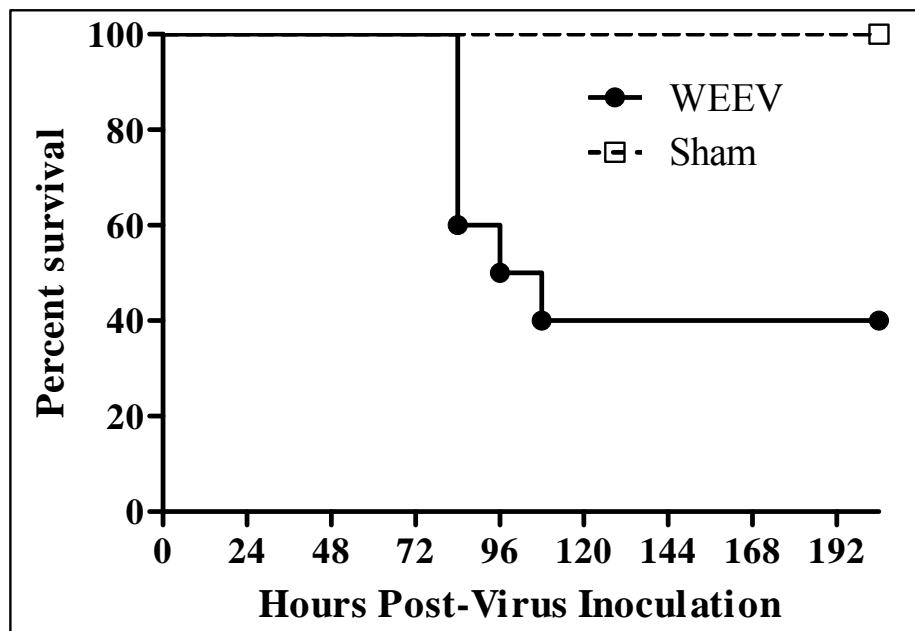


Figure 46: Survival of hamsters inoculated with WEEV. Serum samples were collected to measure cytokine concentrations in WEEV survivors and nonsurvivors.

44 hpi and assayed for interferon concentrations (Figure 47). At 20 hpi sham-inoculated animals (n=3) had no samples with interferon above the lower limits of detection. Of the animals that survived virus infection (n=4) had detectable interferon at 20 hpi, with a serum interferon concentration of  $20 \pm 20$  U/mL, whereas 3 of the nonsurviving animals (n=6) had detectable interferon with an average of  $117 \pm 163$  U/mL. At 44 hpi the same groups of animals had  $\leq 10$  U/mL in sham-inoculated animals, 3 out of 4 survivors had detectable interferon with an average of  $114 \pm 147$  U/mL, and 3 of 6 nonsurvivors had detectable interferon with an average of  $182 \pm 204$  U/mL. No statistically significant differences were detected between survivors and nonsurvivors at either time point. Serum TNF-alpha concentrations were also measured in the same animals at 44 hpi (Figure 48). Serum concentrations of TNF-alpha in sham-inoculated animals were  $\leq 10$  U/mL. Surviving animals had an average of  $32 \pm 44$  U/mL, and non-surviving animals had an average concentration of  $270 \pm 199$  U/mL ( $t=2.311$ ,  $p<0.05$  vs. survivors). Virus titer assays were also conducted on the serum samples collected at 44 hpi. No virus was detected from sham-inoculated animals. At 44 hpi surviving animals had an average virus titer of  $1.6 \pm 0.1 \log_{10}$  CCID<sub>50</sub>/mL of serum, and only 1 of the 4 animals had a serum virus concentration above the limit of detection (Figure 49). Meanwhile, virus was detected in the serum of all non-surviving animals, with a mean serum virus concentration of  $5.4 \pm 1.2 \log_{10}$  CCID<sub>50</sub>/mL, which was significantly higher than that seen in surviving animals ( $t=6.217$ ,  $p<0.001$ ).

Finally, body temperature was also measured in animals every 12 h during the course of the disease, and correlated with disease outcomes. Similar to that described previously, rectal body temperatures were seen to increase in virus-inoculated animals,

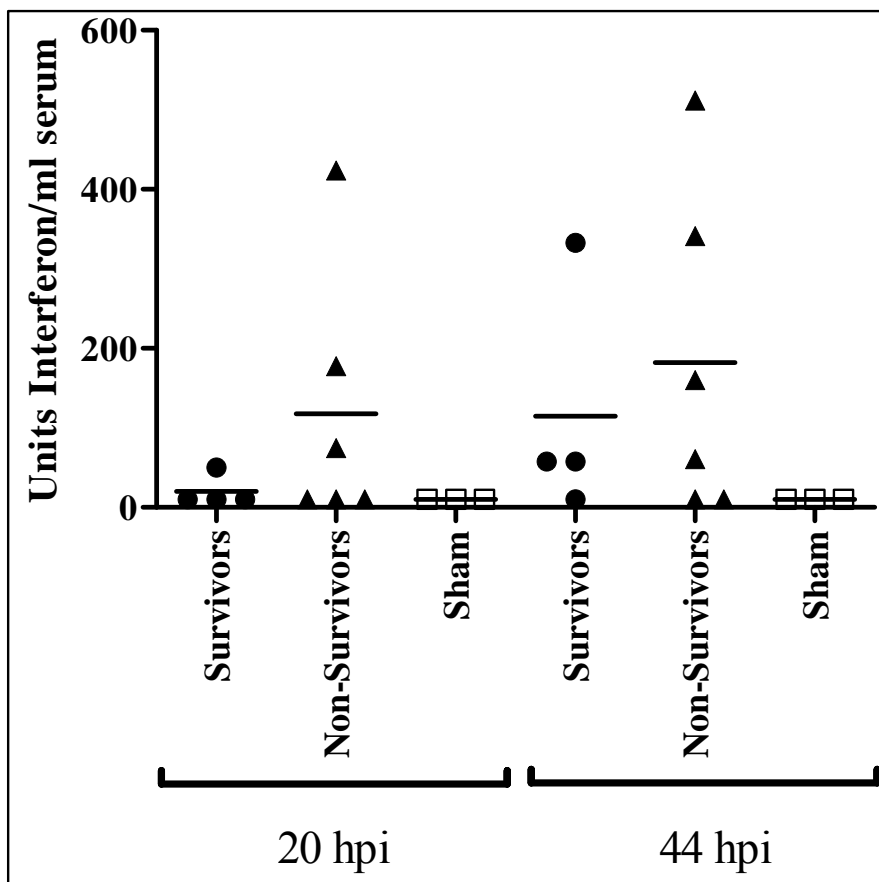


Figure 47: Concentration of interferon in the serum at 20 and 44 hpi from sham-inoculated hamsters or hamsters that either survived or succumbed to WEEV infection.

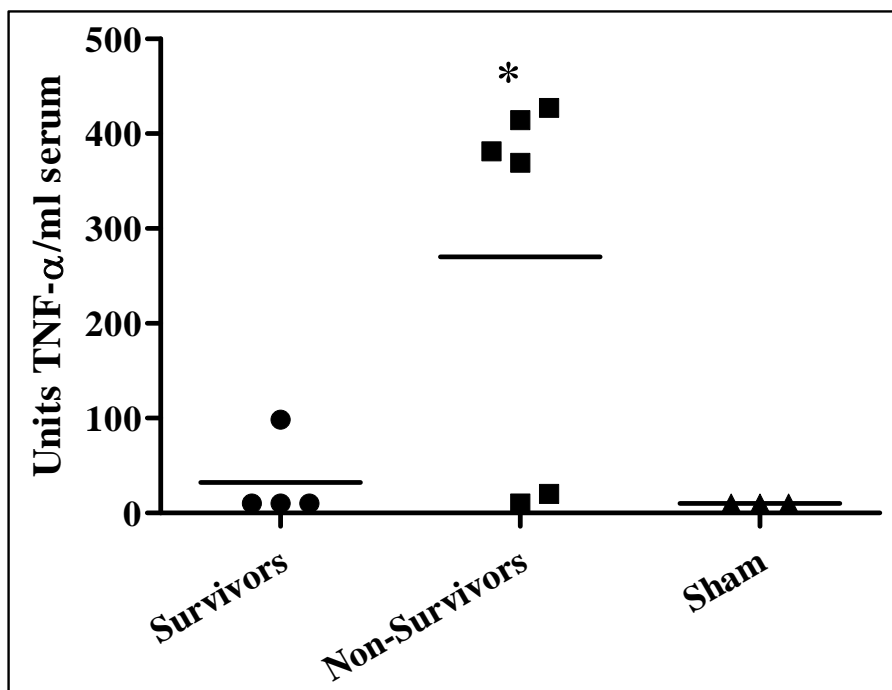


Figure 48: Concentration of TNF- $\alpha$  in serum at 44 hpi from sham-inoculated hamsters or hamsters that either survived or succumbed to WEEV infection. \* $p < 0.05$  Nonsurvivors compared to survivors.

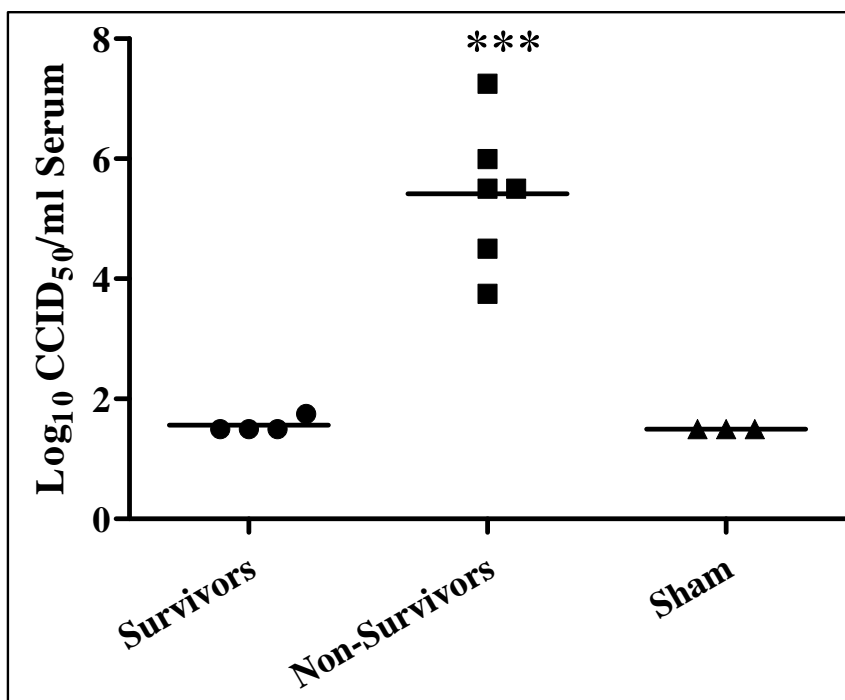


Figure 49: Serum virus titers at 44 hpi from sham-inoculated hamsters or hamsters that either survived or succumbed to WEEV infection. \*\*\* $p < 0.001$  Nonsurvivors compared to survivors.

and particularly in nonsurvivors, beginning approximately 60 hpi, peaking at 72 hpi, and then rapidly declining before death. At 72 hpi the mean rectal temperature of sham-inoculated animals was  $37.9\text{ }^{\circ}\text{C} \pm 0.4\text{ }^{\circ}\text{C}$  compared to an average temperature of  $37.9\text{ }^{\circ}\text{C} \pm 0.2\text{ }^{\circ}\text{C}$  in survivors. Nonsurviving animals had an average rectal body temperature of  $39.9\text{ }^{\circ}\text{C} \pm 0.3\text{ }^{\circ}\text{C}$ , which was statistically significantly higher than either sham-inoculated animals ( $t=7.051$ ,  $p<0.001$ ) or WEEV survivors ( $t=7.428$ ,  $p<0.001$ )(Figure 50).

### ***In vitro* Effects of WEEV on Hamster Macrophages and Splenocytes**

Previous *in vivo* experiments indicated a potential role for inflammatory cytokines in the pathogenesis of WEEV in hamsters. Therefore, experiments were conducted to examine the ability of WEEV to induce production of TNF-alpha in macrophages *in vitro*, and to evaluate the ability of previously used anti-inflammatory agents to mitigate the TNF-alpha response in macrophages. Hamster peritoneal macrophages were inoculated with various multiplicities of infections (MOIs) of WEEV. After incubation supernatant was collected and assayed for TNF-alpha concentrations. In an initial experiment supernatant was collected at 18 hpi. Macrophage release of TNF-alpha in response to virus appeared to occur in a dose-responsive manner (Figure 51). When compared with cells in control wells that were not exposed to virus macrophages inoculated with a MOI of 5 expressed an average of a  $63.5 \pm 3.7$ -fold increase, those exposed to an MOI of 0.5 had an average of a  $9.0 \pm 1.0$ -fold increase, and those exposed to an MOI of 0.05 had a  $1.3 \pm 0.1$ -fold increase in TNF-alpha expression. Macrophages exposed to lower MOIs did not have detectable TNF-alpha in excess of that seen in control cells.

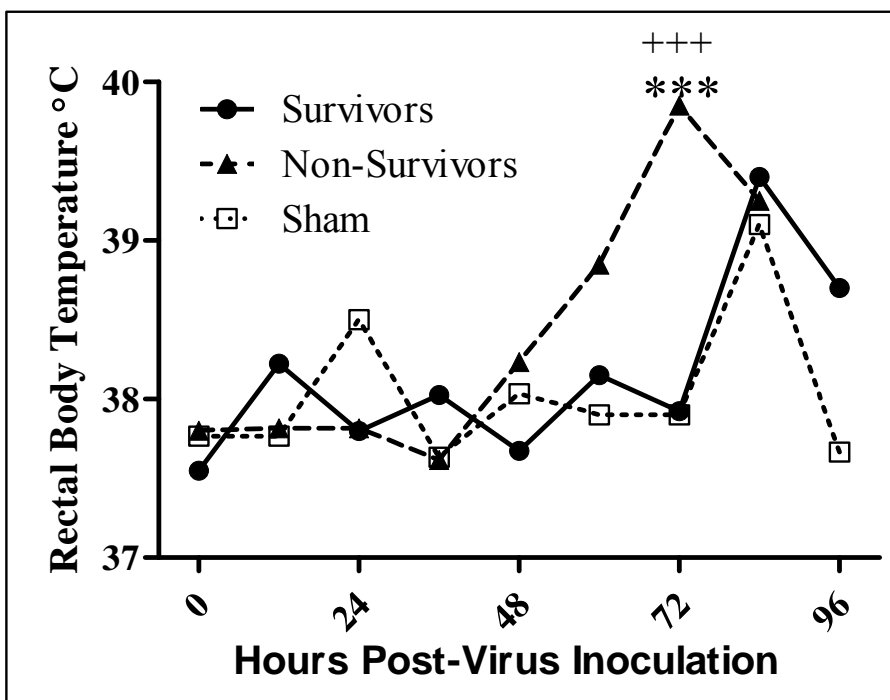


Figure 50: Rectal body temperature in sham-inoculated hamsters or hamsters that either survived or succumbed to WEEV infection. \*\*\* $p < 0.001$  Nonsurvivors compared to survivors, +++ $p < 0.001$  Nonsurvivors compared to sham-inoculated animals.

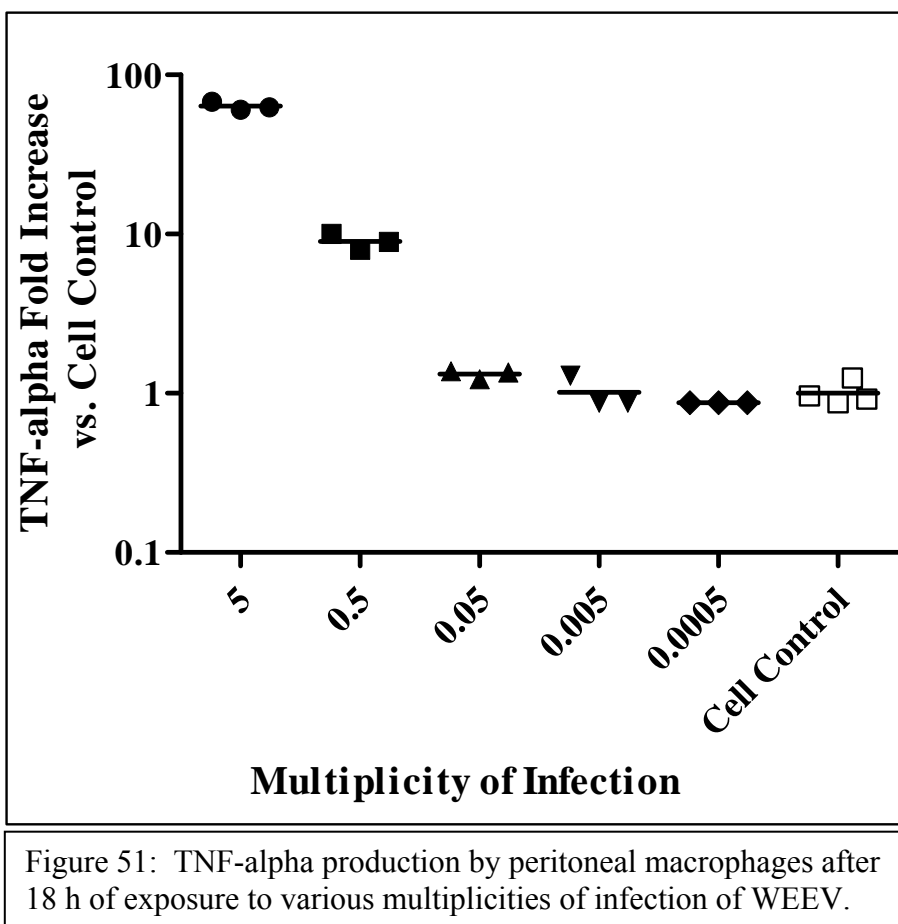


Figure 51: TNF-alpha production by peritoneal macrophages after 18 h of exposure to various multiplicities of infection of WEEV.



To determine the time post-virus exposure when the highest expression of TNF-alpha could be measured macrophages were inoculated with WEEV at MOIs of 0.05, 0.5, and 5, and supernatants were collected at 12, 18, 24, and 36 hpi, and assayed for TNF-alpha concentrations. Macrophages continued to show an apparent virus dose response in regards to the concentration TNF-alpha measured (Figure 52). The time point of 18 hpi produced the highest concentrations of TNF-alpha. Those macrophages inoculated with an MOI of 5 had an average of  $99.9 \pm 17.3$ -fold increase over non-virus inoculated control macrophages. In comparison supernatants from other macrophages inoculated with an MOI of 5 and collected at 12, 24 and 36 hpi had average fold increases with an MOI of 5 had an average of  $99.9 \pm 17.3$ -fold increase over non-virus inoculated control macrophages. In comparison supernatants from other macrophages with an MOI of 5 had an average of  $99.9 \pm 17.3$ -fold increase over non-virus inoculated control macrophages. In comparison supernatants from other macrophages inoculated with an MOI of 5 and collected at 12, 24 and 36 hpi had average fold increases of  $35.1 \pm 10.3$ ,  $13.4 \pm 2.0$ , and  $74.6 \pm 17.4$ , respectively. All subsequent experiments with peritoneal macrophages used a collection time of 18 hpi when assaying for TNF-alpha and for assaying for cell viability. Peritoneal macrophages were seeded into 96-well plates, and either inoculated with WEEV at an MOI of 3, or sham-inoculated with nonvirus cell lysate at a similar dilution. Macrophage containing wells, both virus and sham inoculated, were simultaneously treated with various concentrations of the test compounds dexamethasone and flunixin meglumine, or were left untreated. At 18 hpi cell culture supernatant was collected and assayed for concentrations of TNF-alpha. Virus control wells that received no addition of test compound had an average of a

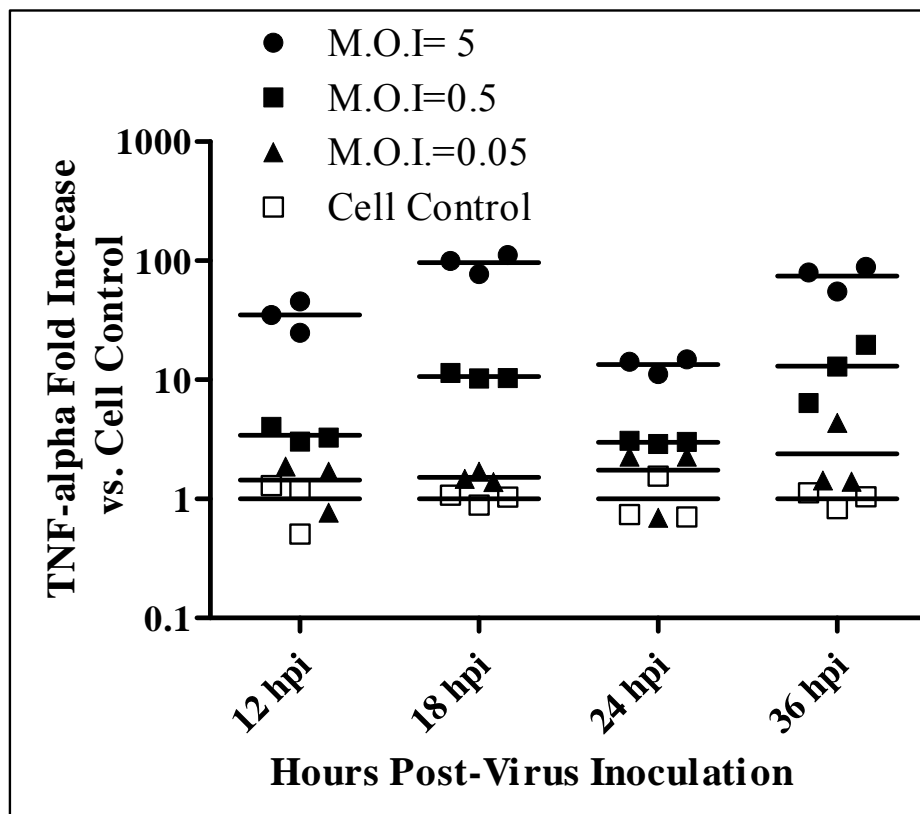


Figure 52: TNF-alpha production by peritoneal macrophages inoculated with various multiplicities of infection of WEEV at multiple times post-virus exposure.

42.9 ± 25.8-fold increase in TNF-alpha concentrations compared to untreated cell control wells (Figure 53). Virus exposed macrophages treated with dexamethasone at concentrations of 1000 µM, 320 µM, 100 µM, and 32 µM had fold-increases in TNF-alpha concentrations of 3.5 ± 2.8, 13.8 ± 11.4, 17.6 ± 14.8, and 12.9 ± 10.0, respectively. Of the dexamethasone concentrations tested only those virus exposed macrophages treated with 1000 µM of dexamethasone displayed statistically significantly lower concentrations of TNF-alpha than virus controls ( $t=5.718$ ,  $p<0.01$ ). In comparison, wells similarly treated with flunixin meglumine at concentrations of 1000 µM, 320 µM, 100 µM, and 32 µM had fold increases of TNF-alpha of 1.7 ± 1.2, 13.5 ± 11.5, 17.1 ± 17.8, and 20.7 ± 23.5, respectively, when compared to control wells. Similar to the results measured with dexamethasone, only treatment with a concentration of 1000 µM of flunixin meglumine significantly reduced TNF-alpha concentrations ( $t=5.988$ ,  $p<0.01$ ). There were no significant differences in the increase of TNF-alpha between dexamethasone and flunixin meglumine-treated cells receiving similar micromolar concentrations. Treatment of macrophages with either dexamethasone or flunixin meglumine in the absence of virus did not produce detectable concentrations of TNF-alpha (data not shown).

Macrophage cell viability was also measured at 18 hpi. Virus control wells had an average cell viability of 60.9 ± 12.7%, when compared to cell control wells. Wells treated with dexamethasone at concentrations of 1000 µM, 320 µM, 100 µM, and 32 µM had mean cell viability values of 55.9 ± 13.9, 72.2 ± 12.8%, 67.2 ± 13.8%, and 67.8 ± 15.6%, respectively, none of which were significantly different than the virus controls. However, dexamethasone treated toxicity wells had an average decrease in cell

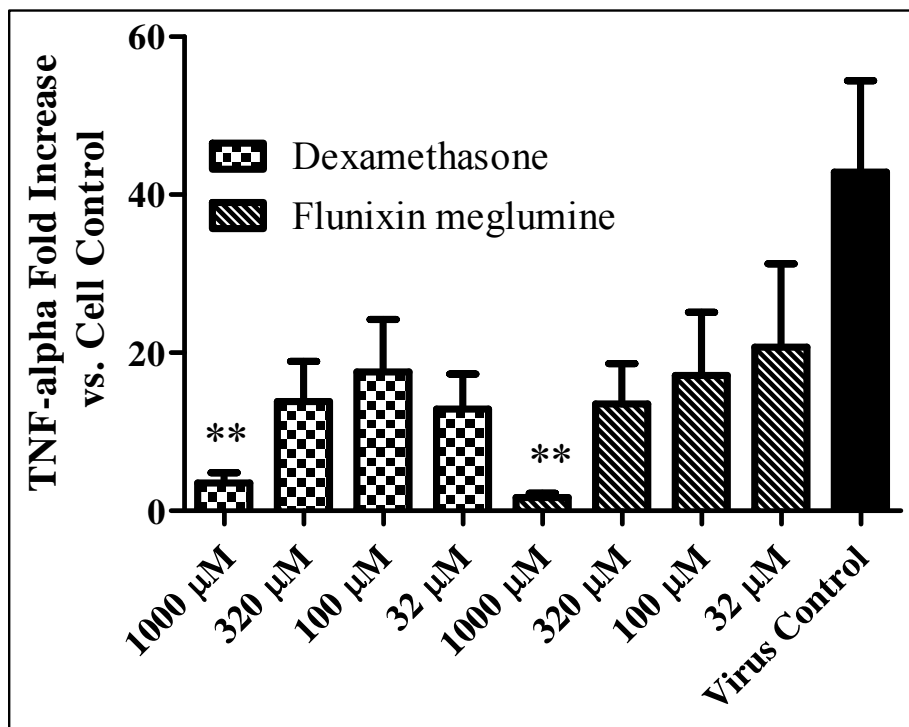


Figure 53: TNF-alpha production by peritoneal macrophages inoculated with WEEV at a MOI of 3 and treated with anti-inflammatory compounds. \*\*p<0.01 compared to virus control macrophages.

viability of  $28.3 \pm 7.3\%$  compared to cell controls. Therefore, when the cell viability in wells treated with both virus and dexamethasone was corrected for toxicity, wells treated with  $1000 \mu\text{M}$  of dexamethasone had average cell viability of  $83.3 \pm 7.3\%$ , which was statistically significantly higher than virus inoculated wells ( $t=4.186$ ,  $p<0.01$ ) (Figure 54). Cells treated with flunixin meglumine showed minimal toxicity at all concentrations tested, and no correction of cell viability was necessary. Virus-inoculated wells treated with flunixin meglumine at concentrations of  $1000 \mu\text{M}$ ,  $320 \mu\text{M}$ ,  $100 \mu\text{M}$ , and  $32 \mu\text{M}$  had mean cell viability values of  $94.5 \pm 6.2\%$ ,  $78.9 \pm 13.5\%$ ,  $69.5 \pm 10.9\%$ , and  $73.8 \pm 12.3\%$ , respectively. Flunixin meglumine significantly improved cell viability in virus-inoculated macrophages at concentrations of  $1000 \mu\text{M}$  ( $t=6.280$ ,  $p<0.001$ ) and  $320 \mu\text{M}$  ( $t=3.366$ ,  $p<0.05$ ), when compared to virus controls. Cell viability in flunixin meglumine-treated wells was not significantly different than that measured in dexamethasone-treated wells of similar micromolar concentrations after cell viability was corrected for toxicity.

Previous *in vivo* experiments indicated a relationship between WEEV infection in hamsters and the spleen and other lymphoid tissues. Therefore, experiments were conducted to examine the ability of WEEV to alter cell viability of primarily lymphoid cells derived from the spleen. Additional experiments were conducted to determine if WEEV induced cytokines from peritoneal macrophages could further modulate the effect of WEEV on splenocytes. To that end, splenocytes were exposed to various MOIs of WEEV and later tested for cell viability. WEEV was able to reduce cell viability in primary hamster splenocytes in an apparent dose-responsive manner (Figure 55), wherein it was observed that cells inoculated with WEEV at MOI rates of 1.0, 0.1, and 0.01

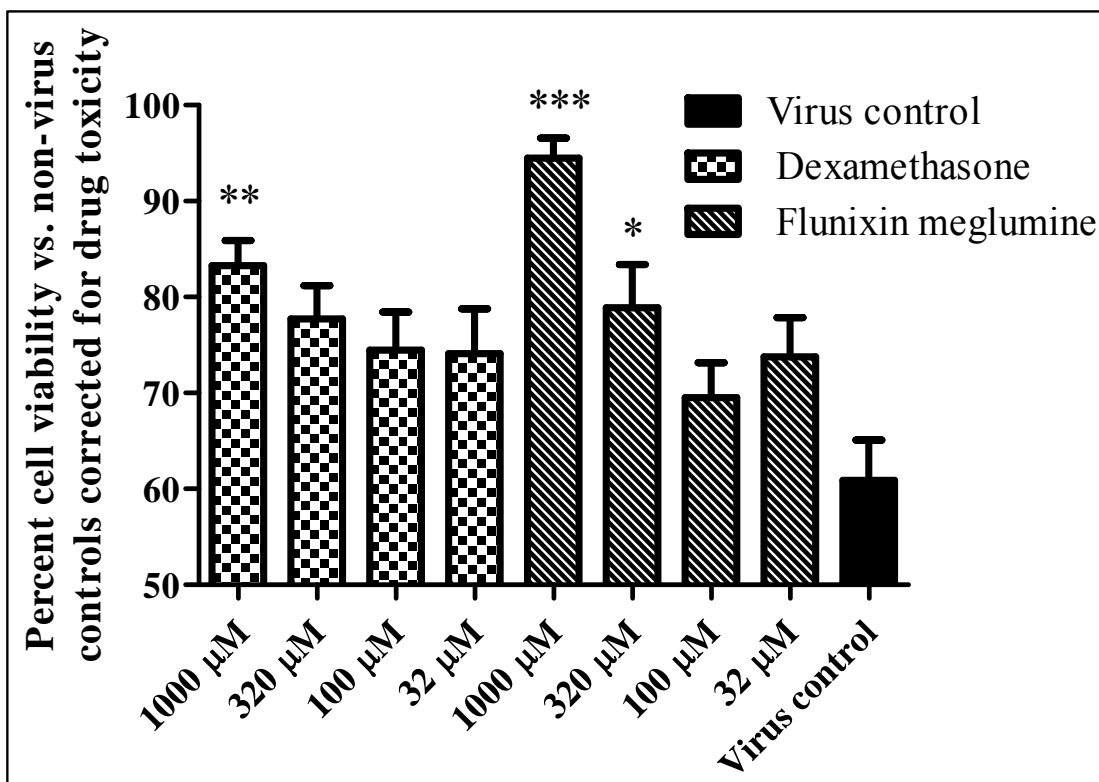


Figure 54: Cell viability of peritoneal macrophages following inoculation with WEEV at an MOI of 3, and treatment with anti-inflammatory compounds. Cell viability corrected for drug toxicity measured in nonvirus, compound-treated macrophages. \* $p < 0.05$ , \*\* $p < 0.01$ , \*\*\* $p < 0.001$  compared to virus control macrophages.

had cell viability rates of  $29.8 \pm 3.1\%$ ,  $66.0 \pm 3.9\%$ , and  $83.5 \pm 3.9\%$ , respectively, when compared to non-infected cell controls. Assays to measure the TNF-alpha in the supernatant from WEEV-inoculated splenocytes were conducted similar to those used following exposure of macrophages to virus. However, no TNF-alpha could be detected via the cell-based assay used.

When a comparison was made between the ability of the CA and Kern strains of WEEV to affect splenocytes directly it was found that the CA strain of WEEV reduced splenocyte viability significantly more so than the Kern strain (Figure 56). Kern strain inoculated onto primary hamster splenocytes at MOIs of 0.1 and 0.01 produced cell viability of  $87.0 \pm 6.7\%$  and  $96.0 \pm 2.1\%$ , respectively. These in turn were significantly higher than the  $66.0 \pm 3.9\%$  ( $t=6.584$ ,  $p<0.001$ ), and  $83.5 \pm 3.9\%$  ( $t=3.912$ ,  $p<0.05$ ) cell viability previously described in splenocytes inoculated with similar amounts of virus using the CA strain.

In a similar manner to that used in macrophages, the compounds flunixin meglumine and dexamethasone were evaluated for their ability to modulate the effects of WEEV on splenocytes (Figure 57). There was no apparent effect in cells treated with the compounds. The presence of substantial cytotoxicity associated with each compound used limited the ability to test for drug effect.

Splenocytes were exposed to a culture supernatant that had been treated in 1 of 3 ways for 18 h: peritoneal macrophages incubated in the absence of any known stimulus, peritoneal macrophages incubated in the presence of WEEV at an MOI of 1, or culture media incubated in a similar manner lacking macrophages but containing equivalent amounts of virus. Samples of supernatants were assayed for infectious virus titers

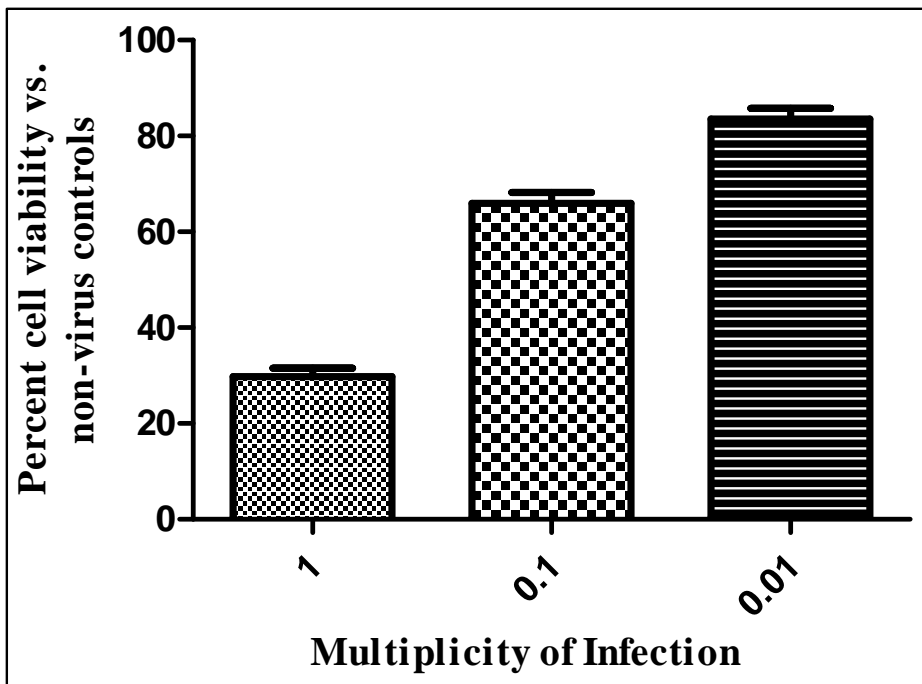


Figure 55: Cell viability of hamster splenocytes 3 d after inoculation with various multiplicities of infection of WEEV.



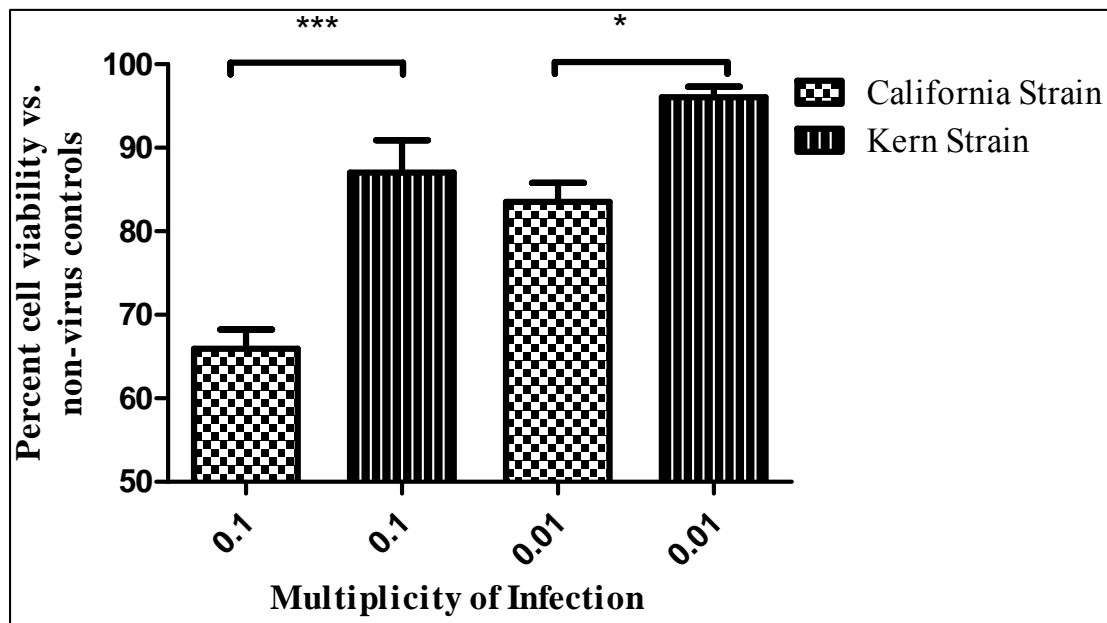
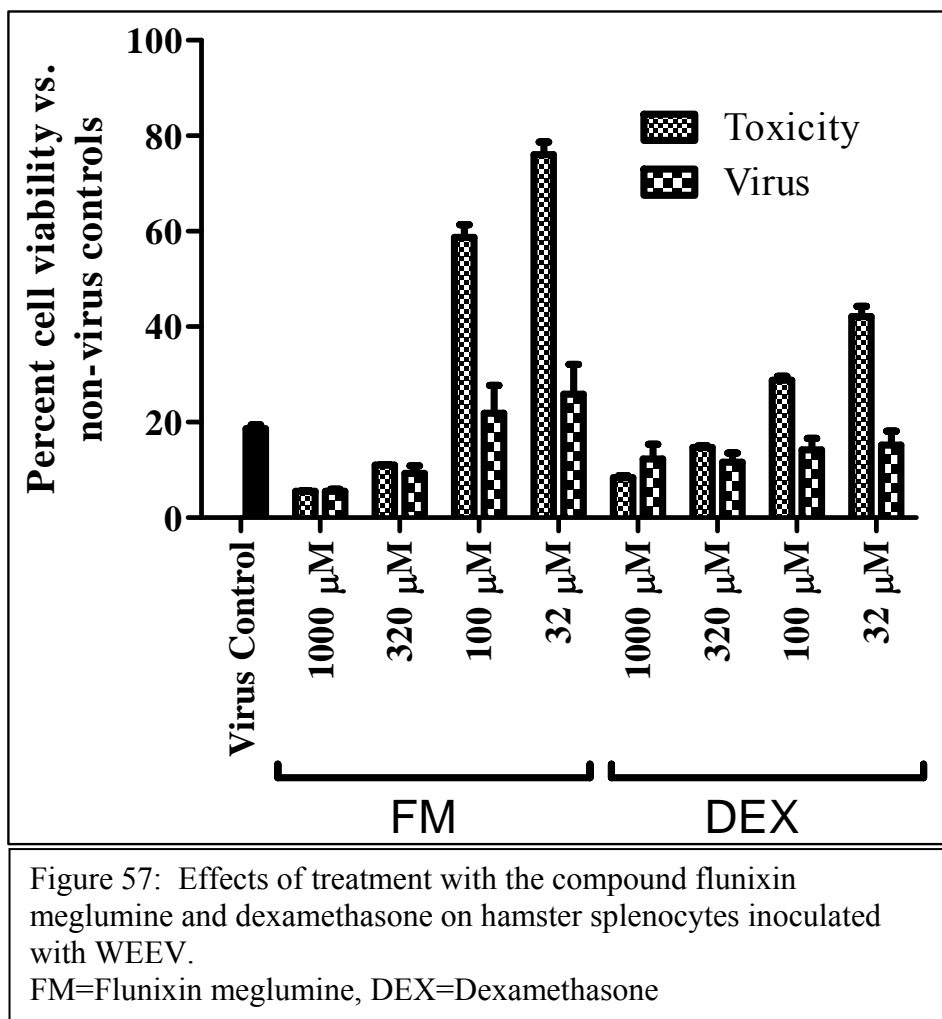


Figure 56: Comparison of the ability of two different strains of WEEV to induce decreased cell viability in hamster lymphocytes in vitro after 3 d of incubation. \* $p < 0.05$ , \*\*\* $p < 0.001$  Kern strain compared to California strain of WEEV.



prior to exposure of splenocytes. No significant differences in virus titer were detected between treatment types whether virus was incubated in the presence or absence of macrophages. No virus was detected in supernatant from macrophages incubated in the absence of virus. An additional amount of virus stock, approximately 1 log in excess of that detected in culture supernatants, was added to each splenocyte culture exposed to culture supernatant, resulting in a MOI of approximately 1.0. This was done to ensure that even minor or undetectable differences in virus titers of cell culture supernatant did not significantly affect the response of splenocytes.

Splenocytes inoculated with virus only and no culture supernatant had a cell viability rate compared to cell controls of  $45.5 \pm 9.1\%$  (Figure 58). The addition of macrophage supernatant-lacking virus stimulation resulted in a cell viability rate of  $54.6 \pm 8.1\%$ , while the addition of supernatant containing WEEV incubated in the absence of macrophages produced cell viability of  $45.6 \pm 8.49\%$ . When culture supernatant from macrophages exposed to WEEV was added to the splenocyte culture, it resulted in a cell viability rate of  $26.2 \pm 3.9\%$ , which was significantly lower than in the virus control ( $t=5.961$ ,  $p<0.001$ ), non-stimulated macrophages, ( $t=8.715$ ,  $p<0.001$ ) or WEEV incubated in the absence of macrophages ( $t=5.961$ ,  $p<0.001$ ). No other combination of WEEV and/or macrophages produced significant differences in splenocyte viability.

In subsequent tests, splenocytes were similarly exposed to supernatant from macrophage cultures. In this instance, supernatant came from macrophages exposed to WEEV, or WEEV incubated in the absence of macrophages as previously described. Additional supernatants came from similarly prepared culture conditions with the

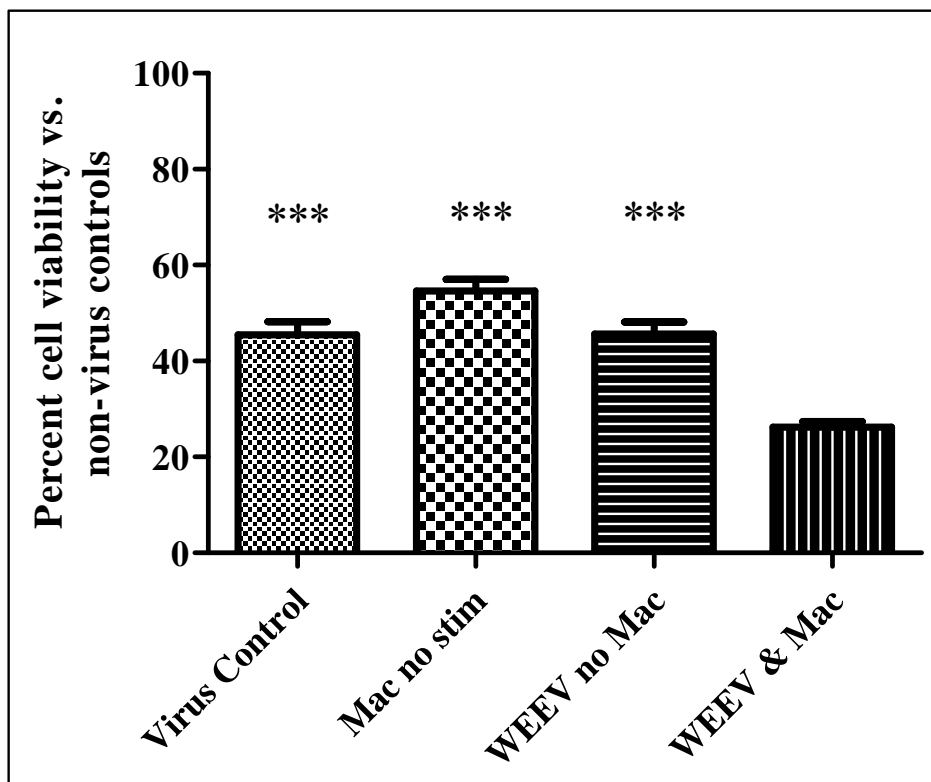


Figure 58: Effects of stimulated macrophage supernatant on the viability of hamster splenocytes exposed to WEEV. Mac no stim=Supernatant from nonstimulated macrophages; WEEV no Mac=Culture media containing WEEV incubated in the absence of macrophages; WEEV & Mac=Culture supernatant from macrophages stimulated with WEEV. \*\*\* $p < 0.001$  compared to splenocytes exposed to supernatant from WEEV-stimulated macrophages.

addition of flunixin meglumine or dexamethasone added at concentrations of 1000 and 320  $\mu\text{M}$ , respectively, added prior to the incubation of virus in the presence or absence of macrophages (Figure 59). The exposure of virus to either flunixin meglumine or dexamethasone did not significantly alter detectable virus titers (data not shown). Treatment of splenocytes with virus only resulted in cell viability of  $52.4 \pm 3.9\%$ , while the addition of supernatant containing WEEV incubated in the absence of macrophages resulted in cell viability of  $46.9 \pm 6.1\%$ . The use of supernatant from macrophages exposed to WEEV resulted in cell viability of  $29.1 \pm 1.4\%$ , which was statistically significantly lower than in either virus controls ( $t=15.29$ ,  $p<0.001$ ) or virus incubated without macrophages ( $t=12.22$ ,  $p<0.001$ ), confirming the earlier noted effects of supernatant from WEEV-stimulated macrophages. The addition of dexamethasone to macrophage cultures exposed to WEEV resulted in splenocyte viability of  $23.8 \pm 1.4\%$  compared to the  $25.1 \pm 3.3\%$  viability of splenocytes exposed to culture media containing virus and dexamethasone without macrophages. Cells exposed to culture supernatant containing virus and flunixin meglumine in the absence and presence of macrophages had cell viability rates of  $10.3 \pm 1.6\%$  and  $10.5 \pm 1.6\%$ , respectively. There was no detectable benefit to splenocyte viability associated with treating macrophages with anti-inflammatory agents prior to collection of supernatant for use in splenocytes. However, the apparent cytotoxicity associated with residual drug in the supernatant treated with dexamethasone or flunixin meglumine limit effective analysis of the drug's effects on the agents produced by macrophages which in turn, enhance splenocyte destruction in culture.

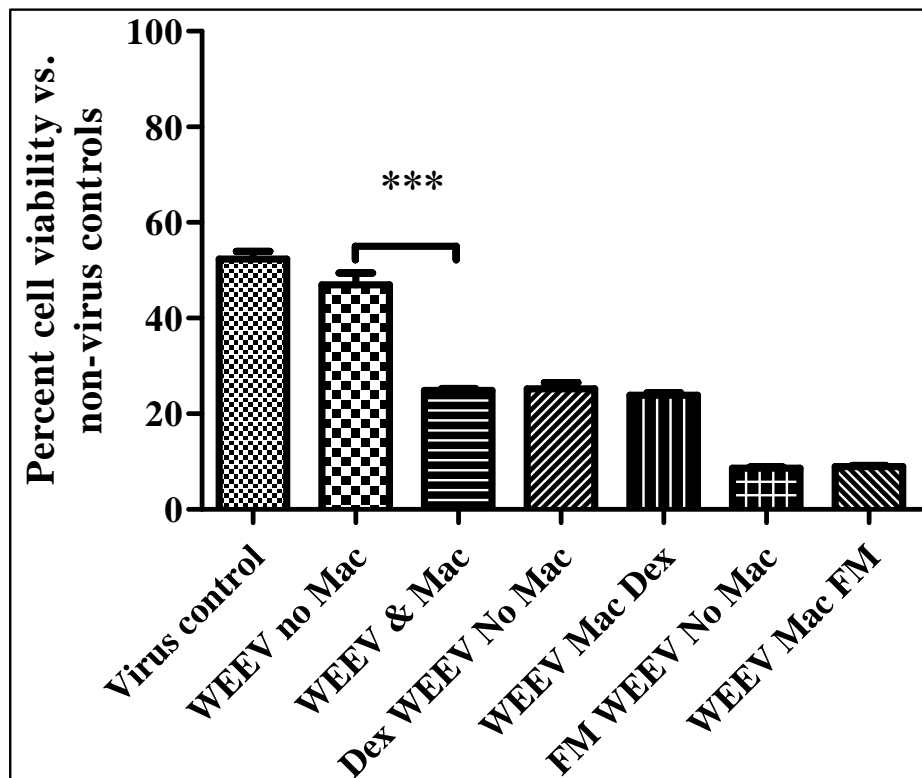


Figure 59: Cell viability of splenocytes cultured in the presence of supernatant from macrophages stimulated with WEEV and treated with anti-inflammatory compounds. \*\*\* $p < 0.001$  Comparison between use of supernatant from WEEV-stimulated macrophages or WEEV incubated without macrophages.

**WEEV no Mac**=WEEV incubated in culture media without macrophages

**WEEV & Mac**=Supernatant from WEEV-stimulated macrophages

**Dex WEEV No Mac**=WEEV incubated in culture media with Dexamethasone (320  $\mu\text{M}$ ) without macrophages

**WEEV Mac Dex**=Supernatant from macrophages stimulated with WEEV and treated with dexamethasone (320  $\mu\text{M}$ )

**FM WEEV No Mac**=WEEV incubated in culture media with flunixin meglumine (1000  $\mu\text{M}$ ) without macrophages

**WEEV Mac FM**=Supernatant from macrophages stimulated with WEEV and treated with flunixin meglumine (1000  $\mu\text{M}$ ).

## DISCUSSION

Arboviral infections are a worldwide threat to both human and animal health. Disease caused by arboviruses varies widely depending upon the virus, the host species, and a multitude of virus-host interactions. This is true even for viruses primarily considered to be encephalitides. Having a proper understanding of viral pathophysiological mechanisms is vital to the goals of proper diagnosis and treatment of arboviral disease.

### **Viral Encephalitis Disrupts the Function of the Blood-Brain Barrier**

It was initially hypothesized that the permeability of the blood-brain barrier of mice to the small molecular weight marker sodium fluorescein would increase during the course of disease following inoculation with a viral encephalite. This hypothesis was confirmed by measuring up to 4-fold increases in BBB permeability in virus-inoculated animals when compared to sham inoculated animals. An additional hypothesis was that BBB permeability would correlate with disease outcome following treatment with the interferon inducer Ampligen™, an antiviral agent previously shown to be effective against the viruses tested. This hypothesis was confirmed by measurement of significantly decreased permeability of the BBB and significantly improved weight change and survival of mice that received treatment with the immunomodulatory agent Ampligen™ prior to virus exposure.

Treatment of viral encephalitis presents a clinical challenge, with few effective therapies. Improved understanding of the role of the BBB in both health and disease is

vital to understanding the challenges associated with treating viral encephalitis, and will also aid in developing new strategies for treatment of viral encephalitis. The results presented here highlight several aspects of the role of the BBB in viral encephalitis including the following: that increases in permeability of the BBB is a pathophysiologic event common to many forms of viral encephalitis, such as arboviruses, that the degree of BBB permeability correlates directly with disease severity; and that increased permeability of the BBB may play an important role in the pathophysiology of viral encephalitis. Showing the ability of two disparate viral species to produce similar changes in the permeability of the BBB to NaFl reinforces the probability that breakdown of the BBB is a pathophysiological event common to many forms of viral encephalitis. This suggests that similar changes may occur in humans infected with encephalitic viruses from the *Flavivirus* or *Togavirus* families of viruses, such as West Nile or Venezuelan equine encephalitis viruses.

In addition to quantifying the degree of increased BBB permeability, the data show a positive correlation between increased degrees of BBB permeability and increased disease severity. This was shown in studies in which Ampligen™ treatment significantly decreased the degree of BBB permeability while simultaneously decreasing mortality and weight loss associated with virus inoculations. Ampligen™ has been proven to be effective against many viruses in a wide range of animal models.<sup>143,168,169,185,214</sup> Ampligen™ is a double-stranded RNA molecule, and its antiviral activity is recognized to be due to its ability to induce the expression of alpha/beta interferons via stimulation of the toll-like receptor 3 which responds to the presence of double-stranded RNA.<sup>180</sup> The exact means by which Ampligen™ treatment of virus-



inoculated animals resulted in a lessening of the degree of BBB permeability is not known, although it is likely that the decreased BBB permeability measured in virus-inoculated animals associated with Ampligen™ treatment is due to the systemic antiviral effects of the drug, and not due to any direct effect of either Ampligen™ or interferon on the BBB itself. Reducing systemic as well as nervous tissue titers of virus would most likely result in a blunting of the inflammatory response, which in turn would minimize associated pathological changes throughout the animal. This view is supported by the result that administration of Ampligen™ 24 h after virus challenge did not improve outcome, regardless of the absence of detectable virus in central nervous system tissues or detectable changes in BBB permeability at the time of Ampligen™ administration.

It should also be noted that BBB permeability in virus inoculated mice began increasing only after virus was detectable in the brain (Table 1, Figure 1, and Figure 2). This is particularly true in the case SFV inoculated mice wherein relatively high virus titers could be measured in brain tissue as soon as 2 dpi, but increases in BBB permeability were not apparent until at least 5 dpi. Therefore, these results do not suggest that increases in the BBB permeability, as measured by NaFl, lead to virus invasion of the central nervous system. Indeed, it is most likely an opposite effect, wherein virus infection of the CNS and subsequent immune and inflammatory reactions within the CNS promote the increased BBB permeability observed here.

The correlation between high degrees of BBB permeability and poor disease outcomes appears to be clear. The data suggest that measuring BBB permeability provides a CNS-specific and quantifiable marker of disease in animal models of viral encephalitis. Identification of appropriate disease markers is necessary to better

characterize viral encephalitis in animal models, and is vital for evaluating the efficacy of antiviral compounds and therapies. A variety of assays for assessing the condition of animals inoculated with encephalitic viruses have been used. But, with the exception of histopathology, sensitive markers of disease that are specific for involvement of the CNS have been difficult to identify in animal models of viral encephalitis. Common human symptoms of CNS infection with an encephalitic virus include headache, nuchal rigidity, and altered mental status.<sup>8,183</sup> It is difficult, if not impossible, to evaluate and characterize similar disease syndromes in laboratory animals. Virus titers in the target tissue are a common measurement tool in virological studies. However, as seen here with SFV-inoculated animals (Table 2), a high viral load in the CNS does not always correlate to a poor disease outcome for experimental animals. Standard serum biochemical analyses are unable to detect abnormalities in the CNS. Changes in body weight can be easily measured and, as seen here, weight loss may correlate with the progression of disease while amelioration of weight loss can indicate efficacy of an antiviral agent. However, weight change is a nonspecific marker of general health which can be affected by environmental conditions, reproductive status, and administration of drugs or experimental therapeutic compounds, and does not provide any information specific to the CNS. Measurement of CNS function via neurological exams and evaluation of motor functions have been previously used in animal models of viral encephalitis.<sup>170</sup> While these techniques can provide valuable information, they are subjective and their value may depend upon the skill of the observer. Histopathological evaluation of CNS tissues is an ideal technique, for animal model development, for disease characterization and drug efficacy studies. However, this requires the services or

training of an experienced pathologist, and its use may be limited by availability of pathological services or cost concerns. Similarly, specialized imaging techniques such as computerized tomography or magnetic resonance imaging may be useful for examining changes in the CNS of infected animals, but they are not widely available because of cost, and biocontainment concerns.

As with all assays, the measurement of BBB permeability to NaFl or a similar-sized marker has certain limitations, and hence should not be considered as a replacement for other established assays. However, it did provide a quantifiable means for evaluating the function of the BBB. We observed that BBB permeability gradually increased over the course of the disease and appeared to peak shortly before the majority of animals began to die from virus infection. Degree of permeability in virus-inoculated animals at the apparent peak of disease severity was up to 4-fold higher than the consistently low BBB permeability measured in sham-inoculated animals.

Permeability measurements in virus-inoculated animals appeared to be a sensitive indicator of the antiviral efficacy of Ampligen™. Mice treated with Ampligen™ 24 h after inoculation with Banzi virus had no improvements in survival (Table 2), but had reduced post-virus weight loss that was highly significantly different, and presumably better, than placebo-treated animals (Figure 3). Meanwhile, no statistically significant difference was detected between the BBB permeability measurements of the same Ampligen™-treated animals and placebo-treated animals. (Figure 5). Similarly, in the case of mice inoculated with Semliki Forest virus animals receiving Ampligen™ 4-6 h before virus had highly significantly improved survival compared to placebo-treated animals, but also had brain virus titers nearly identical to those detected in placebo-

treated animals (Table 2). However, when BBB permeability was measured in the same group of SFV-inoculated mice, Ampligen™-treated animals had significantly lower permeability than measured in placebo-treated animals. In both animal models the BBB permeability assay showed some benefits over currently available assays by identifying a false positive result of ameliorated weight loss in the BaV model and a false negative result of high brain viral titers in the SFV model. The use of a BBB permeability assay in no way replaces the use of established assay techniques. Indeed, the results described here highlight the importance of using multiple assay methods to fully characterize animal models of viral disease and antiviral effects of potential therapeutics

One of the functions of the BBB is to limit entry of foreign molecules into the CNS. It does so by severely limiting the penetration of hydrophilic or charged molecules that lack a specific transport system, such as that for glucose. The result of this barrier function is generally poor distribution to CNS tissue of most pharmacological compounds, including the majority of currently available antiviral agents. It has been suggested that investigating means to increase permeability of the BBB to enhance entry of antiviral agents into the CNS may provide a therapeutic strategy for the treatment of viral encephalitis. Such a strategy has proven effective in an animal model of herpes virus infections in the brain in which Acyclovir treatment was administered in conjunction with the use of a synthetic bradykinin analog used to temporarily permeabilize the BBB.<sup>28</sup> The exact relationship between increased BBB permeability in viral encephalitis and disease outcomes is unknown. However, the results presented here showing a correlation between increased BBB permeability and increased disease severity strongly suggest that any technique intended to increase BBB permeability

would be contraindicated in animal models of either BaV or SFV infection, or in humans infected with related members of the *Flavivirus* or *Togavirus* families of viruses. Such a conclusion is consistent with other published reports evaluating the connection between BBB permeability and viral encephalitis.<sup>23,151</sup> A possible explanation for the correlation of BBB break-down, as well as a reason for avoiding any technique that would increase BBB permeability in clinical cases of viral encephalitis may be that, as previously stated, the increases in BBB permeability associated with viral encephalitis are due to inflammation in the CNS. Breakdown of the BBB eliminates the immunoprivileged status of the CNS, allowing entry of signaling molecules that act as mediators of both inflammation and cell death, as well as the entry of inflammatory cells. The subsequent CNS damage from the entry of such inflammatory mediators and cells may be more severe than that induced by the virus alone. Further study will be necessary to fully understand the relationship between the increased permeability of the BBB and disease severity in viral encephalitis.

### **WEEV Infection in Syrian Golden Hamsters**

The changes in BBB permeability noted in mice inoculated with viral encephalitides encouraged a similar approach in hamsters inoculated with WEEV. Hamsters are highly susceptible to death due to WEEV infection when inoculated intraperitoneally with WEEV.<sup>120</sup> It was presumed that the animals were dying due to viral encephalitis. The ability to collect cerebrospinal fluid in a minimally invasive, non-terminal manner provided the potential to measure BBB permeability to NaFl by measuring NaFl concentrations in CSF rather than in brain tissue. This provided a means

to use BBB permeability in a longitudinal fashion not practical in mouse models of viral encephalitis, and provided the ability to assess increased BBB permeability as an antemortem marker of disease outcome. It was hypothesized that BBB permeability in hamsters inoculated with WEEV, as measured using the CSF, would increase as virus disease severity progressed, in a manner similar to that observed in mice inoculated with viral encephalitides. This hypothesis proved to be false. Although there was a moderate increase in the ratio of fluorescence measured in CSF vs. serum noted in virus inoculated animals when compared to sham inoculated animals (Figure 7) there was no correlation between the degree of fluorescence measured in CSF and disease outcome (Figure 8). Furthermore, the ratios of fluorescence measured in the CSF WEEV of hamsters were minor compared to those seen previously in mice inoculated with either Banzi or Semliki Forest viruses.<sup>179</sup>

The lack of apparent changes in the BBB preceding death in WEEV-infected hamsters led to an investigation of the cause of death in WEEV-inoculated hamsters. A review of previously published reports regarding the disease processes of Venezuelan equine encephalitis virus infections in Syrian golden hamsters indicates the presence of severe lymphocytic necrosis induced by viral infection followed by systemic septicemia and rapid death, all with the absence of central nervous system pathology.<sup>91,243</sup> Therefore, it was hypothesized that a similar disease state was occurring in hamsters inoculated with WEEV via the i.p. route. Specifically, it was hypothesized that WEEV-inoculated hamsters develop a systemic lymphonecrotic disease in the absence of lesions within the central nervous system. A secondary hypothesis was that systemic lymphonecrosis was followed by a secondary septicemia due to bacterial translocation from the

gastrointestinal tract, and that hamsters then rapidly die from septic shock in a syndrome similar to that described as systemic inflammatory response syndrome and the subsequent multiple organ dysfunction syndrome (SIRS-MODS). To test these hypotheses, and to more fully characterize WEEV infection in Syrian golden hamsters, experiments were conducted to assay multiple components of disease progression, including virus titers, histopathology, cytokine response, serum biochemistry analysis, clinical hematology, and bacteriology, over the time course of virus infection. An additional experiment was conducted to evaluate the response of animals to virus injected directly into the brain.

The hypothesis that WEEV inoculation into hamsters causes systemic lymphonecrosis in the absence of observable central nervous system pathology was proven correct. The virus titers in serum and tissues followed closely those previously reported for WEEV infection in hamsters (Table 4),<sup>120</sup> although the shorter sampling interval in the current study may allow for a more precise description of viral kinetics and the identification of the time of peak viral titers. Histopathological lesions were consistently seen in the spleen, occurring at or after 72 hpi in virus inoculated-animals (Figure 19). Splenic lesions occurred approximately 36-48 h after peak spleen virus titers, with an average peak of 4.8 log<sub>10</sub> CCID<sub>50</sub>/g of tissue. Other lesions noted in animals that died late during the systemic portion of the disease (between 72 and 108 hpi), including pathological changes in the liver and adrenal glands, were considered incidental as they are commonly seen associated with hypoxia occurring during the end terminal stages of many disease processes. Also of particular note is the absence of detectable histopathological changes to the central nervous system at the time of death in

animals dying from the systemic phase of disease. The lymphonecrotic lesions seen in the spleen are consistent with those reported for hamsters and guinea pigs experimentally infected with VEEV<sup>11,93,111</sup> and are consistent with lesions seen in animal models of septic shock.<sup>106</sup> Furthermore, the splenic necrosis seen in hamsters infected with WEEV was consistent with lesions seen in naturally occurring human cases of VEEV.<sup>63</sup>

Concentrations of TNF-alpha and interferon were measured in the serum and tissues of WEEV-inoculated hamsters over time. Serum interferon concentrations were initially undetectable before rapidly peaking at 36 hpi, after which serum interferon quickly returned to concentrations below the limits of detection (Figure 12). Interestingly, peak serum interferon concentration coincided temporally with peak serum and spleen virus titers indicating that the presence of virus in serum or other tissues is probably inducing the expression of interferon. Serum TNF-alpha concentrations were also low or undetectable during the earliest stages of virus infection. However, a noticeable rise in serum TNF-alpha was noted at 48 hpi, before serum concentrations peaked at 60 hpi and then subsided (Figure 13). The exact trigger of the increased serum TNF-alpha is uncertain as the peripheral virus titers were waning at the time that TNF-alpha concentrations were increasing. However, the increased concentrations of TNF-alpha overlap the time frame of lymphopenia (Figure 11), and the peak TNF-alpha concentration at 60 hpi coincides with the peak febrile response measured in WEEV-inoculated hamsters (Figure 10). This suggests that TNF-alpha is possibly contributing to both of these observed events in a manner similar to that which has been described for TNF-alpha with other clinical disease states.<sup>57,238</sup> In contrast to the serum from WEEV-



infected animals, and somewhat surprisingly, detectable amounts of either interferon or TNF-alpha in virus-infected tissues were only sporadic, with no apparent pattern to their expression. The significance of the lack of consistently detectable cytokines in the tissues assayed is uncertain.

It was hypothesized that WEEV infection provided an endogenous environment that allowed a secondary bacterial septicemia which may have been ultimately responsible for the demise of WEEV-infected hamsters via an inflammatory syndrome similar to SIRS-MODS in humans. This hypothesis was in due course shown to be false. To test this hypothesis an attempt was made to isolate bacteria from virus inoculated animals, and animals were treated animals with the antibiotics enrofloxacin and florfenicol. Various bacterial species were successfully isolated form WEEV-inoculated animals at stages late in the systemic disease phase. However, similar microbial species were simultaneously isolated from sham-inoculated animals (Table 3). Additionally, the species isolated are common environmental bacteria, such as Staphylococcal or Streptococcal species, or bacteria commonly considered to be commensal organisms in hamsters, such as the Corynebacterial species. This led to the conclusion that all bacteria isolated were possibly contaminants, in spite of efforts to collect samples under aseptic conditions. Further evidence suggesting that bacteria isolated from WEEV-inoculated hamsters were contaminants, and further disproving the hypothesis that secondary septicemia contributed to the death of hamsters infected with WEEV came from studies testing the ability of antibiotics to improve survival in virus-infected animals. When hamsters were treated with enrofloxacin alone and without any anti-inflammatory agent, animals did not show any improvement compared to placebo-treated animals (Figure 25).

A lack of improvement with antibiotics is in direct contrast to earlier reported studies of VEEV infection in hamsters wherein antibiotics blocked early death in virus-infected animals. Enrofloxacin is a broad spectrum antibiotic with activity against what would be considered the most common species of bacteria that would cause septicemia, such as *Escheria coli*, and *Staphylococcus spp.* The inability of enrofloxacin to improve disease outcome would most likely indicate bacteria outside its spectrum of activity, or a non-bacterial cause of death. Enrofloxacin is poorly effective against anaerobic bacteria, and the microbial isolation techniques employed did not attempt to isolate anaerobes. Therefore, an experiment was conducted that included the antibiotic florfenicol, an agent with recognized activity against most anaerobic bacteria. Use of florfenicol alone, or in combination with enrofloxacin was again unable to improve the outcome for WEEV-inoculated hamsters, in spite of the addition of anti-inflammatory treatment (Figure 26). Florfenicol did cause some apparent toxicity in sham-inoculated animals (data not shown). Hamsters have a well recognized sensitivity to the ability of various antibiotics to disrupt normal intestinal flora. This may explain the toxicity noted with the use of florfenicol. However, the toxicity did not manifest itself until several d after all virus inoculated animals had died, and it cannot account for the death in those virus infected hamsters.

In a further attempt to identify a SIRS-MODS like clinical syndrome, and to better characterize WEEV infection in hamsters serum from WEEV-inoculated animals was assayed for common clinical biochemistry values and monitored over the course of disease. Surprisingly, few alterations were seen in the serum biochemistry values of virus-inoculated animals compared to sham-inoculated animals (Table 5). The only

serum parameter to be altered sufficiently to note was alanine aminotransferase (ALT), which was elevated approximately 4-fold compared to sham-inoculated animals at 12 hpi, immediately post-virus inoculation. ALT was again elevated in the late systemic phase of the disease at 72 and 84 hpi to approximately 4 times that noted in sham inoculated animals. While it is worth noting such an increase, the biological significance of a relatively minor increase is questionable. Increased ALT levels may be associated with the suspected hypoxic damage to livers noted in livers in end-terminal diseased animals. The quantities of serum glucose, potassium and phosphorus were also noted to be elevated in virus inoculated hamsters compared to sham inoculated animals. The reason for the increases noted is unclear. Possible explanations for increased serum glucose include the choice of anesthetics, a combination of ketamine and xylazine, which are known to increase serum glucose. Release of endogenous cortisol in response to stress, whether to the virus infection or to handling of animals, can induce a transient hyperglycemia. Increased serum potassium can be seen in cases of anuric or oliguric renal failure, or with massive tissue necrosis. Both possibilities may occur in hamsters which die due to system WEEV infection, but it would be expected that such changes would be noted only during the latter portions of the systemic disease, which was not the case observed here. Hyperphosphatemia may also be noted in renal failure, or may be increased, along with other electrolytes, in dehydrated animals. The lack of any apparent temporal pattern (i.e. levels increasing or decreasing over time) associated with the quantities of serum glucose, potassium, and phosphorus indicate that the differences observed between virus inoculated animals and sham inoculated animals are probably not associated with viral pathology. The most likely causes for the elevated concentrations

for these 3 parameters are either hemolysis or prolonged contact of serum with RBC after blood collection. RBCs contain high concentrations of glucose, potassium, and phosphorous, which may be released into serum if a blood sample is not properly and promptly processed after collection. Any future studies involving serum biochemistry in WEEV inoculated hamsters must make every effort to appropriately collect and handle blood samples to eliminate such potentially confounding results as noted here.

Perhaps what is more significant in the serum biochemistry is what is absent. Specifically, it had been hypothesized that animals were dying due to bacterial septicemia and a subsequent inflammatory syndrome similar to the SIRS-MODS complex noted in humans with septicemia. Such a disease syndrome is characterized by severe dysfunction of multiple organ systems and is in part diagnosed clinically via alterations in serum biochemistry values.<sup>19,20</sup> Increased values of BUN and creatinine would indicate kidney dysfunction, or increased ALP, ALT, or bilirubin would indicate liver damage or dysfunction. Except as previously noted, hamsters infected with WEEV displayed little or no alteration to serum biochemistry values, even at the latter stages of disease immediately preceding death. The absence of expected changes in serum biochemistry that would indicate organ dysfunction further contradicts the hypothesis that a secondary bacterial infection is contributing to death in WEEV-infected hamsters.

Hematological values were measured over time in WEEV-inoculated animals (Table 6). The hematocrits of virus-infected animals were elevated to an average of 55.0% and 52.0% at 72 and 84 hpi, respectively, compared to a mean hematocrit of 49% in sham-inoculated animals. The degree of increase should be considered moderate, and it is most likely due to the dehydration associated with anorexia and malaise in febrile animals.

Otherwise, the erythron of virus-infected animals was unremarkable. In contrast, the leukogram and, in particular, the circulating lymphocyte count displayed marked changes in WEEV-inoculated hamsters. At 48 hpi a temporary mild decrease in the total white blood cell count was detected, coinciding with a more severe lymphopenia (Figure 11). The circulating WBC count returned to approximately normal at all time points afterwards. However, lymphocyte counts remained low in most animals measured until 84 hpi when lymphocyte numbers appeared to rise somewhat.

It has been observed in multiple experiments that a subset of WEEV-infected hamsters would survive the early systemic phase of the disease without any obvious negative side-effects. A very small subset of the surviving animals would then begin to die between approximately 144 and 216 hpi (6-9 dpi) (Figures 23, 26, 28, and 33). Among those animals dying at these later time points some would display disease signs characteristic of nervous system damage, such as circling, tremors, and limb paralysis. The observed phenomenon only occurred if animals were inoculated with a virus dose that was sufficiently high to cause death in a majority of animals. Animals inoculated with lower viral doses would survive infection without any apparent negative sequelae. Interestingly, these events began to occur 48 h after peak viral titers were measured in brain tissue, a time interval similar to that observed between peak viral titers in the spleen at 36 hpi, and severe splenic necrosis beginning to occur at 72 hpi. This observation regarding the time interval between viral invasion of an organ and manifestation of pathological lesions may explain the absence of nervous system pathology at the time of animal death at approximately 96 hpi in spite of very high viral titers in nervous tissue. Simply put, the virus has not had adequate time in the CNS to cause visible pathologic

damage. The observation that some hamsters would eventually develop CNS disease following WEEV inoculation led to the hypothesis that WEEV retained its ability to cause viral encephalitis in hamsters. This hypothesis was shown to be correct. To test the hypothesis that WEEV can induce CNS disease, WEEV-infected hamsters that survived the initial systemic disease but succumbed after 144 hpi were submitted for necropsy and histopathological analysis. These animals often displayed resolving necrotic lesions in the spleen. They also had lesions of encephalitis and meningitis in the CNS (Figure 20). These lesions included extravasation of lymphocytic cells into the perivascular space, lymphocytic infiltration of nervous tissue, and hemorrhage in the brain. These histopathological lesions in the central nervous system are consistent with those seen in other infections with related alphaviruses, such as VEEV infections in humans<sup>63</sup> and horses;<sup>199</sup> WEEV infections in humans<sup>6</sup> and in monkeys;<sup>194</sup> and EEEV infections in humans<sup>22</sup> and horses.<sup>64</sup> To confirm that the lesions observed in the CNS of hamsters dying late in the disease process were due to WEEV, and to definitively show the ability of WEEV to induce encephalitis in hamsters, animals were inoculated with virus directly into the right cerebral hemisphere. Incidentally, the virus dose inoculated into the brain was sufficiently low that it would have been unlikely to induce death if inoculated via the peripheral route. Intracranially inoculated animals began to die within 36 hpi, and all but 1 virus inoculated-animal were dead by 72 hpi. These animals displayed overt signs of central nervous system involvement including circling, paralysis, apparent hyperesthesia and head tilt. Histopathological lesions in the CNS of hamsters inoculated intracranially were similar to, albeit more severe than, those observed in hamsters dying late in the disease following peripheral inoculation (Figure 21).

Furthermore, hamsters inoculated intracranially did not show evidence of pathological changes in nonneuronal tissues. It is worth noting that the interval between virus introduction into the brain and the onset of morbidity and mortality is similar to the time interval between peak virus titer in the brain and apparent encephalitis observed in animals following peripheral virus inoculation. No sham-inoculated animals showed any observable signs of disease during the same time period. Histological observations of the brain of sham inoculated animals were lacking in any lesions of significance, except minor traces associated with the introduction of a needle into nervous tissue. These results lead to the conclusion that death in hamsters inoculated via the i.p. route is likely not caused by bacteremia or a syndrome similar to SIRS-MODS. It is also concluded that WEEV retains its ability to cause lethal encephalitis in hamsters whether inoculated peripherally or directly into the CNS. It is further concluded that the primary cause of death in WEEV-infected hamsters following peripheral inoculation is not encephalitis, but rather sequelae associated with lymphocytic necrosis. The presence of virus in the brain at the time of death means that viral damage to neurons can not be precluded as a contributor to the death of WEEV-infected hamsters. It is recognized that as much as 12 h or more may pass between the time a cell ceases to function and dies, and the time when histopathological changes may be observed via a light microscope. It is possible that because of the vital role the CNS plays in sustaining life, that sufficient damage to the CNS may occur such that an animal dies but no detectable lesions in the CNS are present. However, the severe histopathological changes noted in the brains of hamsters inoculated with WEEV intracerebrally suggests that an animal dying from viral encephalitis due to WEEV with an absence of histopathological lesions within the central

nervous system is unlikely. Finally, it is concluded that severe lymphopenia is a reliable antemortem marker of death, and the mechanisms associated with lymphopenia may contribute to animal death. A corollary to these conclusions is the observation that pathology and substantial cell death will occur approximately 48-72 h after the establishment of a virus infection in susceptible tissues

### **Supportive Care and Dexamethasone Immunosuppression of WEEV- Inoculated Hamsters**

Data gained from experiments evaluating histopathological changes in hamsters inoculated with WEEV showing lymphocytic necrosis (Figure 19) were consistent with previously published reports of hamsters inoculated with VEEV.<sup>243</sup> Results from previous studies involving VEEV in hamsters indicated that animals were dying due to bacterial translocation from the intestines allowed by viral destruction of intestinal lymphatic tissue. Therefore, it was hypothesized that WEEV-inoculated hamsters were dying due to an endotoxemia/septicemia secondary to viral destruction of lymphatic tissue in the gastrointestinal tract. Standard clinical therapy for individuals suffering from endotoxemia is broad spectrum antibiotics in combination with anti-inflammatory therapy and cardiovascular support in the form of fluids. Therefore, the initial experiment testing this hypothesis centered on the administration of the antibiotic enrofloxacin in combination with supportive fluids and anti-inflammatory treatment with flunixin meglumine. Later experiments also used dexamethasone as an anti-inflammatory. Interestingly, fluoroquinolone compounds, such as the antibiotic enrofloxacin, have been evaluated for the antiviral properties,<sup>198</sup> while, there are no



published reports indicating that either flunixin meglumine or dexamethasone have any direct antiviral properties. Flunixin meglumine is a widely used veterinary anti-inflammatory agent whose primary mechanism of action is considered to be broad inhibition of cyclooxygenase enzymes.<sup>24</sup> FM has also been shown to inhibit nuclear factor kappa-B,<sup>33</sup> a ubiquitous transcription factor involved in many components of inflammation and the immune response to viruses.<sup>12,33,207</sup> Dexamethasone is a steroid hormone with wide ranging systemic effects *in vivo*, not the least of which is potent inhibition of inflammation.<sup>173,244</sup>

Experimental results initially appeared to confirm the hypothesis that animals died due to septicemia as animals receiving supportive care had a moderate but statistically significant improvement in survival compared to placebo-treated animals (Figure 23). However, this hypothesis was shown to be false, as results from subsequent studies showed that the administration of antibiotics in the absence of anti-inflammatory treatment provided no benefit to virus-infected animals (Figure 25). Furthermore, the administration of FM in the absence of antibiotics provided nearly identical protection compared to those receiving FM in combination with antibiotics (Figure 26). These results lead to the conclusion that the beneficial effects observed were associated with anti-inflammatory treatment. Treatment with FM was also able significantly modulate the lymphocyte response to virus infection (Figure 45). FM can suppress production of TNF-alpha,<sup>33,152</sup> an inflammatory cytokine reported to reduce numbers of circulating lymphocytes. However, the observed effect of FM treatment improving circulating lymphocyte numbers in WEEV-inoculated animals may be more suggestive of the predictive value of lymphopenia as a marker for death than it is a description of a specific

mechanism for FM in virus-infected animals. These data strongly suggest that the anti-inflammatory capabilities of FM were the primary cause for its beneficial effects. The corollary being that virus-induced inflammation is a contributing factor to the morbidity and mortality observed in WEEV-infected hamsters. Additional support for an inflammatory component was gained from the observation that administration of dexamethasone to hamsters after virus inoculation was able to significantly improve survival while also suppressing fever (Figures 30 and 32).

Experimental results showing improvement in WEEV-inoculated hamsters treated with anti-inflammatory compounds suggested a role for the immune response and inflammation in the pathogenesis of WEEV in hamsters. Therefore, it was hypothesized that inflammation and the immune response were playing a significant role in the demise of WEEV-infected hamsters and that suppression of the immune response would provide improved outcomes for virus-inoculated hamsters. Therefore, an experiment was conducted in which hamsters received an immunosuppressive dose of dexamethasone or a placebo treatment for 5 d prior to inoculation with an approximate LD<sub>90</sub> dose of WEEV. The febrile response to WEEV was suppressed in animals receiving dexamethasone when compared to placebo-treated animals (Figure 17). Dexamethasone treatment also had significantly higher serum virus titers at 60 hpi compared to placebo-treated animals (Figure 18). Previous results indicate that there is little or no detectable virus in the serum at the relatively late time period of 60 hpi in immunocompetent hamsters, which was confirmed by the low average virus titer detected in placebo-treated animals. The suppression of fever and significant alterations to virus kinetics in WEEV-inoculated hamsters indicates that dexamethasone treatment is exerting effects on the immune

system of hamsters. However, dexamethasone treatment did not significantly alter disease outcome compared to placebo-treated animals (Figure 16).

While there appears to be clear evidence that inflammation plays a role in hamsters infected with WEEV, it should not be concluded that inflammation is the sole nor even the primary cause of disease and death associated with WEEV infection in hamsters. The inability of high doses of FM to provide additional benefit compared to the previously used standard dose suggest that maximum inhibition of inflammation had been achieved (Figure 28), and no further benefit would be observed through blocking inflammation. The concept that inflammation is a secondary contributing factor rather than the primary cause of WEEV-induced disease in hamsters is further supported by the inability of dexamethasone administered in an immunosuppressive-manner pre-virus inoculation to alter disease phenotype or outcome. This leads to the conclusions that animals are not dying from a septicemia, or a SIRS/MODS like syndrome, but that direct viral effects probably play the greatest role in WEEV-associated disease in Syrian golden hamsters. An additional conclusion is that the inflammatory response to virus infections enhances virus induced pathology.

### **The Effects of Virus Dose and Virus Strain**

As a result of previously described studies examining the effects of supportive care and dexamethasone immunosuppression on WEEV-inoculated animals it was hypothesized that death in WEEV infected hamsters was primarily due to virus destruction of target cells. A supporting hypothesis being that an increased virus inoculum would result in increased quantities of virus in hamsters and subsequently result

in a more severe disease process. A counter hypothesis was also considered.

Namely, that the pathological processes in WEEV-inoculated animals that succumb to virus infection are essentially identical, and that virus dose is only important in determining the rate of mortality within a group of hamsters. To test this hypothesis a comparison of pathophysiological effects of different virus doses was done by inoculating animals with either an LD<sub>50</sub> or a 10x LD<sub>90</sub> dose of WEEV, and then observing animals for morbidity and mortality. The degree of mortality for each group was approximately as expected, with animals receiving the higher viral dose showing 0% survival, while those receiving the lower dose had a significantly higher 20% survival rate (Figure 14). Virus titration experiments in hamsters showed that animals which succumb to the virus all die at approximately the same time regardless of virus dose.<sup>120</sup> Such results appear to support the second hypothesis that pathophysiological processes are similar in animals that die due to virus infection, regardless of virus dose. However, it is worth noting that even when comparing only nonsurvivors from each group the viral disease phenotype was significantly different depending upon the virus dose.

Nonsurviving hamsters receiving the higher viral dose had significantly more severe weight loss (Figure 15) and died significantly earlier in the disease than those receiving the lower viral dose (Table 9). These results support the hypothesis that disease severity is closely correlated with the amount of virus present, while contradicting the latter hypothesis that virus dose does not matter. These results, in conjunction with results from previously described experiments showing limitations on the ability of anti-inflammatory or immunosuppressive therapy to modulate disease outcome, also support

the hypothesis that death in WEEV-infected hamsters is due to direct virus killing of target cells, and not secondary immune or inflammatory events.

The WEEV disease phenotype of rapid death associated with a systemic virus infection is notably different than that observed in other animal models inoculated with encephalitic viruses. Therefore, it was hypothesized that the disease phenotype noted in hamsters inoculated with the California strain of WEEV is unique to this virus strain and animal model. The acquisition of a different strain of WEEV provided an excellent opportunity to test this hypothesis and compare the effects of two different strains in the same animal model. Such a comparison would allow for the identification of disease characteristics unique to the animal and virus model being used. Hamsters were inoculated with an LD<sub>50</sub> dose of the CA strain and a CCID<sub>50</sub> equivalent dose of the Kern strain of WEEV and monitored for outcome. Different characteristics of virus disease were observed in animals inoculated with the two different strains. As expected, hamsters inoculated with the CA strain appeared outwardly normal until approximately 60 hpi, at which time they exhibited fever and began showing signs of lethargy and apparent malaise, followed rapidly by death between 84 and 96 hpi. In contrast Kern-inoculated animals displayed no outward signs of disease until approximately 192-216 hpi (9-10 dpi), at which time animals underwent a wasting disease process with progressive weight loss leading to death between 288 and 312 hpi (11-13 dpi). In addition to these observed clinical differences statistically significant differences between animals inoculated with the CA strain and the Kern strain were noted in circulating lymphocytes (Figure 36), serum interferon concentration (Figure 38), and serum virus

titers at 36 hpi (Figure 37), body temperature at 60 hpi (Figure 35), and overall survival (Figures 34).

Conclusions from experiments comparing disease phenotype in hamsters inoculated with two different strains of WEEV are that the rapid death previously described in hamsters inoculated with the CA strain is a disease phenotype unique to this virus strain and animal model. Each of the statistically significant differences noted between CA- and Kern-inoculated hamsters, such as mortality, weight loss, lymphocyte count, and body temperature, highlight the unique characteristics of disease associated with the California strain of WEEV. Although spleen histopathology was not assayed, the lack of lymphopenia in Kern inoculated animals may suggest that lymphonecrosis does not occur in association with Kern strain infection; further enhancing the hypothesis that the CA strain infection in hamsters causes a unique disease phenotype.

#### **Identification of Potential Markers of Outcome in Hamsters Inoculated with WEEV**

Identification of markers for disease outcomes in virus infected animals is an important tool for developing animal models and designing experiments to test therapeutic efficacy of new treatment strategies or compounds. Identification of markers may also provide additional information about disease pathogenesis. In hamsters inoculated with WEEV an apparent correlation between low lymphocyte counts and poor clinical outcome was observed in animals at late stages in the systemic disease phase. Due to this observation it was hypothesized that severe lymphopenia in hamsters infected with WEEV is a marker for death. This hypothesis was proven to be correct. To test this

hypothesis a series of experiments was conducted in which circulating lymphocyte numbers were assayed and correlated with disease outcome. Repeated studies found that animals that eventually succumbed to virus infection in the systemic phase had significantly lower circulating lymphocyte counts than either sham-inoculated animals, or animals that subsequently survived WEEV infection (Figures 40, 42, 45). Additional confirmation of the correlation between decreased lymphocyte counts and death seen in hamsters inoculated WEEV was noted in experiments comparing differences between different strains of WEEV, wherein it was observed that the two CA strain survivors had noticeably higher numbers of lymphocytes in circulating blood than did the nonsurvivors (Figure 36).

In general, lymphopenia occurring in such a short time frame as that seen in WEEV-inoculated hamsters can occur either due to lymphocyte destruction or redistribution and sequestration of lymphocytes out of blood circulation. The current study shows that WEEV infection in hamsters can stimulate production of both TNF-alpha and interferons, both of which can induce sequestration of lymphocytes.<sup>123,238</sup> This study also shows that WEEV can directly induce lymphocyte cell death *in vitro*, which can be enhanced by inflammatory cytokines. Therefore, while the exact mechanism of lymphopenia in WEEV-inoculated hamsters is unknown it is likely due to a combination of factors including lymphocyte sequestration and viral induced lymphocyte destruction. The physiological or immunological significance of lymphopenia in WEEV-infected hamsters is also unclear. In the current study it is proposed that severe lymphopenia is a consistent and reliable marker of death in virus-infected hamsters. However, there is a potential for decreased lymphocyte numbers to be an inherent part of the viral

pathophysiology in hamsters. It could be argued that a lack of immune cells limits an animal's ability to mount both a humoral and cell-mediated immune response. This, in turn, would inhibit an animal's ability to effectively clear a virus infection and ultimately contribute to virus associated death.

It was observed that hamsters inoculated with the Kern strain of virus had an earlier expression of serum interferon than did hamsters inoculated with the CA strain (Figure 38), and that Kern-inoculated animals had a noticeably different disease phenotype with a significantly delayed onset of mortality when compared to CA-inoculated animals. Therefore, it was hypothesized that the timing of the endogenous interferon response in CA-inoculated animals may be an indicator of disease outcome in that an early interferon response may be more effective at limiting virus spread within an animal. To test this hypothesis a study was conducted wherein animals were inoculated with an LD<sub>50</sub> dose of WEEV and then assayed at various times post-virus inoculation for serum interferon concentrations. There were no significant differences between survivors and nonsurvivors in the serum interferon concentrations at either 20 or 44 (Figure 47). However, it was observed that nonsurvivors had significantly elevated rectal body temperature at 72 hpi when compared to either survivors or sham-inoculated animals (Figure 50). Additionally, serum virus titers (Figure 49) and serum TNF-alpha concentrations (Figure 48) were significantly higher in nonsurvivors than in survivors at 44 hpi. These results lead to the conclusion that serum interferon is not a reliable indicator of disease outcome in hamsters infected with WEEV. However, as previously described severe lymphopenia is a consistent indicator of poor disease outcome. Other potential markers of disease outcome include elevated body temperature, high serum



virus titers, and elevated serum TNF-alpha concentrations, all of which appear to indicate that death during the systemic phase of disease is likely. In addition to standing as indicators of disease outcome each of the parameters also likely indicates the presence of a robust systemic virus infection and associated increases in disease severity among animals that subsequently die. This is in contrast to what is likely a substantially limited virus infection in animals that survive. The presence of either a robust or limited systemic infection is also consistent with differences in serum virus titers between survivors and nonsurvivors as well as with the observation that survivors from groups of hamsters inoculated with LD<sub>50</sub> doses of WEEV rarely have any negative sequelae.

#### ***In vitro* Activity of WEEV in Hamster Splenocytes and Macrophages**

Experiments involving WEEV-infected hamsters provided evidence that WEEV stimulates production of TNF-alpha during virus infection. Other experiments showed that treatment of animals with anti-inflammatory agents provided improvements in disease outcomes. These results suggest a probable role for inflammatory cytokines in the pathogenesis of WEEV infection in hamsters *in vivo*. It was decided to examine the ability of WEEV to induce TNF-alpha production in cells *in vitro*, and to evaluate the ability of anti-inflammatory compounds to modulate the virus-induced production of TNF-alpha. From that, it was hypothesized that WEEV could stimulate TNF-alpha production from hamster macrophages *in vitro*, and that both flunixin meglumine and dexamethasone could inhibit WEEV-stimulated production of TNF-alpha from hamster macrophages. The data show that the WEEV can stimulate macrophages to produce the inflammatory cytokine TNF-alpha. The observations that TNF-alpha production appears

to occur in a dose-responsive manner (Figure 51), that increased TNF-alpha production can be measured as early as 6 h after virus inoculation of macrophage cultures (Figure 52), and that there is no detectable increase in WEEV titers after incubation with macrophages would all suggest that the virus particles are inducing TNF-alpha production in macrophages in a manner more consistent with a ligand rather than an actively infectious organism. The production of TNF-alpha can be significantly inhibited by both flunixin meglumine and dexamethasone in a dose dependant manner (Figure 53). Dexamethasone and flunixin meglumine are two anti-inflammatory compounds with divergent mechanisms of action that have both been shown to be able to reduce inflammatory cytokine production *in vitro*.<sup>24,47,142</sup> Neither dexamethasone nor flunixin meglumine has been reported to exhibited antiviral properties, a result that was confirmed by testing in a standard antiviral cytopathic assay (data not shown). The current report does not attempt to describe the means by which WEEV can stimulate macrophages to produce TNF-alpha. However, the ability of these two compounds to inhibit virus induced inflammatory cytokine production suggests that WEEV stimulates TNF-alpha production via common inflammatory pathways. Toll-like receptors (TLR) are potential mediators of the inflammatory response in macrophages because many are recognized for their ability to sense markers of pathogen infection, such as activation of TLR-3 by double-stranded RNA associated with viral infection.<sup>180</sup> Both TLR-3 and TLR-9 have been shown to interact with virus and participate in the production of TNF-alpha.<sup>141,154</sup> The common ability of flunixin meglumine and dexamethasone to inhibit TNF-alpha production would suggest their ability to modulate downstream regulators rather than the toll-like receptors themselves. Potential targets for the effects of dexamethasone and

flunixin meglumine seen here are NF-kappa-B and COX enzymes. Both NF-kappa-B and COX-2 are activated during TNF-alpha stimulation. TLR-3 can activate nuclear factor kappa-B<sup>3</sup> and the COX-2 enzyme.<sup>229</sup> However, cyclooxygenase enzymes may also stimulate the production of TNF-alpha via the production of various prostaglandin molecules<sup>41</sup> Both dexamethasone and flunixin meglumine can inhibit activation of NF-kappa-B and cyclooxygenase enzymes.<sup>1,24,33,82</sup>

Inoculation of macrophages with WEEV was able to reduce cell viability by approximately ½ within 18 h, a relatively short period of time compared to the 48-72 h necessary to see reductions in cell viability in the highly susceptible Vero 76 cell line. Both flunixin meglumine and dexamethasone were able to significantly ameliorate, and in some cases almost eliminate reductions in macrophage viability associated with exposure to WEEV, and did so in a dose-dependant manner. The degree of protection from FM or DEX appeared to correlate with their respective abilities to reduce macrophage production of TNF-alpha. The current study does not attempt to describe the exact mechanisms of decreased macrophage viability. However, the ability of anti-inflammatory agents to protect macrophages from virus-induced cytotoxicity in the absence of any recognized antiviral effect leads to the conclusion that cell death was most likely induced by inflammatory mediators rather than direct viral effects. One possible mechanism is inhibition of TNF-alpha production, which in turns blocks the cell death signals initiated by TNF-alpha.<sup>98,230</sup> Another potential target is the previously mentioned NF-kappa-B. As noted above, both FM and DEX can inhibit NF-kappa-B. Among its many recognized functions NF-kappa-B participates in the induction of apoptosis and can be induced by the presence of virus.<sup>156</sup> If NF-kappa B plays a significant role in WEEV-

induced macrophage death blocking it would certainly provide protection. Further studies will be necessary to determine if TNF-alpha is the primary mediator of decreased macrophage viability, or if some other effector or cell death mechanism is involved.

Due to the splenic necrosis observed following infections of hamster with WEEV it was hypothesized that WEEV could directly induce cytotoxicity in splenic cells, and that the cytotoxicity could be observed *in vitro*. Furthermore, following the stimulation of TNF-alpha production in hamster macrophages *in vitro*, the observed increase in TNF-alpha in WEEV infected animals, and the beneficial effects associated with the use of anti-inflammatory compounds *in vivo* it was hypothesized that macrophage-produced inflammatory cytokines could enhance virus-induced destruction of splenocytes. It was deemed important to use conspecific cells to study the effects of virus-stimulated cytokines on splenocyte-virus interactions rather than commonly available cell lines or recombinant cytokines. This was because of the uncertainty of the full range of cytokines that may be produced by macrophages under virus stimulation and because of the uncertainty of cross-species cytokine reactivity. Both the hypothesis regarding WEEV cytotoxicity of splenocytes and the hypothesis regarding the ability of macrophage produced cytokines to enhance WEEV cytotoxicity of splenocytes were shown to be correct. WEEV can induce reductions in splenocyte viability in a dose-dependent manner, although it requires 72 h after exposure to virus to detect substantive reductions in cell viability, compared to the less than 24 h needed in macrophages. No TNF-alpha could be detected in the supernatant from virus inoculated splenocytes, suggesting that reductions in splenocyte viability were due to direct virus actions rather than TNF-alpha as seen in macrophages. Additionally, the use of the same anti-inflammatory compounds

used successfully to protect macrophages did not provide any benefit when used on splenocytes. However, interpretation of the effects of anti-inflammatory agents on splenocytes must be somewhat tempered by the substantial compound-induced toxicity to splenocytes that was not observed in macrophages treated with similar concentrations of the drugs (Figure 57). The anti-inflammatory compound-associated toxicity may be due to the longer incubation period associated with splenocyte culture.

The results from experiments evaluating the effect of WEEV on splenocytes indicate that splenocyte destruction appears to be more related to direct virus effects rather than inflammatory mediators, in contrast to peritoneal macrophages. This is in concert with the proposed *in vivo* effects of virus on lymphoid cells wherein WEEV is the primary mediator of cell destruction. This is not to say that inflammatory mediators do not play a role in splenocyte destruction. Exposure of splenocytes to supernatant from WEEV-stimulated macrophages resulted in moderate but statistically significant enhancements to the virus cytotoxic effects (Figure 58). This also is in agreement with the proposed ability of inflammatory cytokines to enhance WEEV-mediated cytotoxicity *in vivo*. Although attempts were made to evaluate the ability of flunixin meglumine and dexamethasone to inhibit the ability of macrophages to produce pro-cytotoxic mediators, the apparent toxicity of splenocytes due to residual drugs found in the macrophage supernatant makes accurate interpretation of such data impossible (Figure 59).

This model of WEEV infection in the Syrian golden hamster was selected because of its unique disease phenotype. However, the use of a hamster-based animal model severely limits the ability to test for most cytokines due to a lack of species specific assays and reagents that are widely available in more commonly studies species such as

mice and humans. However, it is highly likely that WEEV induces macrophages to produce multiple inflammatory cytokines in addition to TNF-alpha. Identification of the specific role of TNF-alpha in causing or enhancing virus-associated decreases in cell viability in either splenocytes or macrophages was also limited by the inability to identify an agent or blocking antibody able to inhibit the activity of hamster TNF-alpha in spite of attempt to do so (data not shown). But due to the widely reported and investigated ability of TNF-alpha to induce either apoptosis or necrosis in a broad range of cells and tissues under widely varying conditions it seems likely that TNF-alpha is at least partially, if not wholly, responsible for the cytotoxic effects noted in WEEV-inoculated macrophages, and the cytotoxic enhancing effects observed in splenocytes.

### **Proposed Model of WEEV Infection in the Syrian Golden Hamster**

Interpretation of the results of the studies presented here in context of one another leads to the proposal of the following model for WEEV infection in the Syrian golden hamster (Figure 60). Following intraperitoneal inoculation of WEEV, 1 of 3 disease pathways is possible. First, a mild virus infection will be established, an adequate immune response will occur and the hamster will rapidly eliminate the virus with no negative sequelae. Second, a robust virus infection will be established leading to the clinical and pathological signs observed in WEEV-infected animals. These signs include increases in serum TNF-alpha, lymphopenia, fever, and virus-induced lymphocytotoxicity that may be enhanced by inflammatory cytokines. Animals following this infectious path will rapidly succumb to virus infection with death occurring by approximately 96 hpi. Although severe lymphocytic necrosis may be

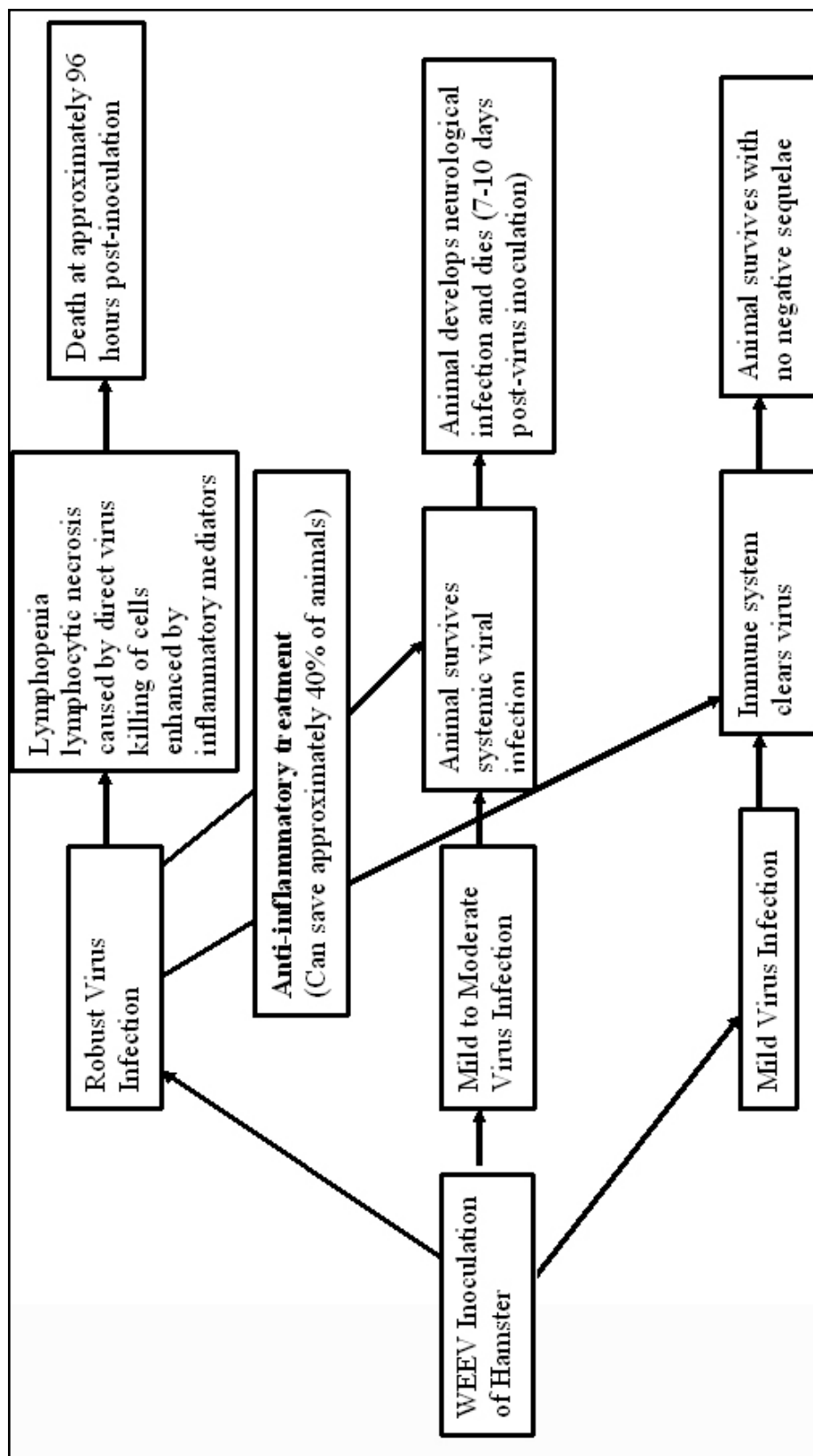


Figure 60: Proposed disease model of WEEV infection in the Syrian golden hamster. It is proposed that animals can follow one of three distinct disease paths. The path an individual animal inoculated with WEEV will follow is dependent upon viral dose, virus-host interactions, host immune status, and any subsequent anti-inflammatory or anti-viral therapy an animal

seen in these animals no histopathological evidence of neurological disease will be present. The third infectious pathway that may be taken occurs in animals in which a moderate virus infection is established. These animals will survive beyond the time period of animals suffering a robust virus infection, and display no signs of viral disease until 6-9 dpi. At this late time in the infectious process animals may develop overt signs of neurological damage, but the most common outward sign of disease noted is sudden death. Following death animals will display histopathological lesions in the central nervous system, and may show signs of resolving lymphocytic lesions in nonneuronal tissues. This encephalitic disease path was the least commonly observed of the 3 disease phenotypes. The reason for the low prevalence of the encephalitic disease path may be because the virus must maintain a delicate balance of having sufficient replication to maintain a persistent infection, but not so robust replication as to cause severe lymphocytic necrosis resulting in early death. Under such a hypothesis of the virus infection and the difficulty of maintaining the appropriate balance the encephalitic disease phenotype would be expected to have a low rate of occurrence. Administration of anti-inflammatory agents to WEEV-infected hamsters may protect some animals from death associated with the robust phenotype of WEEV infection and allow them to follow either the mild or encephalitic phenotypic pathways because anti-inflammatory drugs limit the cytotoxic enhancing effect of inflammatory cytokines. Interestingly, the 3 forms of WEEV-induced virus disease following establishment of mild, robust, or moderate virus infections described herein for hamsters mimic very closely the influenzal, fulminant and encephalitic forms of VEEV infection described in human cases.<sup>72</sup>



The ability of anti-inflammatory agents to protect some animals from the initial stages of disease highlights a probable role for inflammatory cytokines in causing morbidity and mortality. This becomes especially apparent when reviewing the composite survival results for WEEV-infected hamsters receiving anti-inflammatory treatment (Figure 33). Although the beneficial effect of anti-inflammatory therapy on survival was moderate, the repeatable nature of the results and the improved statistical power associated with the increased numbers of animals indicate a true and significant biological response. Support for the role of inflammatory cytokines in inducing or enhancing viral destruction of cells was also gained from the *in vitro* assays involving macrophages and splenocytes.

The factors that direct the infectious path that an individual hamster will follow are not known, but, at the very least, virus dose is a vital determining factor. Under the currently proposed model, benefit from anti-inflammatory treatment will only be observed when animals are inoculated with virus within a very narrow viral dosing range. In the current report the ability of anti-inflammatory agents to protect some animals from early death was observed in animals inoculated with a 10x LD<sub>90</sub>. The identification of the appropriate virus dose for recognizing the benefits of anti-inflammatory treatment and subsequently determining the potential role for inflammatory cytokines in the progression of WEEV-induced disease in hamsters was arrived at somewhat serendipitously. In retrospect it can be observed that almost any other viral dose would not have led to the current conclusions regarding the role of inflammation in the pathophysiology of WEEV in hamsters. Animals inoculated with high viral doses will almost always develop a robust virus infection and die by approximately 96 hpi. Use of such a dose would result

in an overwhelming infection and massive virus-induced destruction of cells regardless of the presence or absence of inflammatory cytokines. In contrast, animals inoculated with low doses of virus will rarely die or even show signs of disease. Because the beneficial effects of anti-inflammatory agents are somewhat moderate the use of LD<sub>50</sub> or otherwise low virus doses would require impractically large numbers of animals to detect statistically significant changes in outcome. The ability to detect effects from anti-inflammatory agents is further complicated by the observation that individual animals appeared most likely to follow either the robust or mild forms of disease, with only a very small percentage exhibiting the third encephalitic form of WEEV infection, even when hamsters are inoculated with viral doses intended to cause death in approximately half of the animals. Immune status may also play a role in determining disease phenotype as observed by the rapid death and uncommonly high serum virus titers seen in animals immunosuppressed with dexamethasone prior to virus inoculation.

### **Future Experiments**

The results of this work have led to several questions to be answered by future experiments. Several of these questions are discussed below.

What are the mechanisms of death in virus-inoculated splenocytes? The results of this report strongly support the hypothesis that splenocytes die directly from virus-mediated actions, and only secondarily due to inflammatory responses. However, this report does not describe whether cells die primarily to apoptotic or necrotic signaling pathways, nor what intracellular death pathways may be involved. Elucidation of such information may provide for novel therapeutic approaches to virus infections. This

hamster model of WEEV infection may present a unique opportunity for testing new therapeutic strategies. The blood-brain barrier has posed a significant hurdle to introducing experimental therapeutic agents into the target organ associated with infection by viral encephalitides. If virus-infected neurons follow similar intracellular pathways leading to cell death as do splenocytes the peripheral nature and apparent high susceptibility of splenocytes to WEEV may provide an adequate surrogate cell model to study basic mechanisms of virus-induced cell death as well as means to prevent cell death.

By what means does WEEV trigger cytokine production in macrophages, and what cytokines, in addition to TNF-alpha are produced in response to virus exposure? These results suggest that WEEV acts more as a ligand than as a replicating infectious agent in stimulating production and release of TNF-alpha from macrophages. Identification of receptor or cellular pathways by which this occurs would better define the disease process as well as provide additional targets for therapeutic investigations. Toll-like receptors are known to recognize characteristics of various pathogens and participate in the immune and inflammatory response,<sup>141,180</sup> and would provide an ideal starting place in attempts to answer this question. Use of cells from animals lacking specific toll-like receptors or other target receptors, the use of transfection technologies, and receptor blocking strategies may be used in such endeavors.

What are the mediators that enhance virus associated cytotoxicity in splenocytes? An obvious first step would be to identify which WEEV-induced macrophage-produced factors are able to increase the virus-mediated destruction of splenocytes. TNF-alpha is certainly a candidate for further consideration in this role as it has been shown to enhance

cell death in other virus models.<sup>251</sup> Identification of agents that specifically block TNF-alpha activity would help to delineate its role both in cell culture and animal-based models of WEEV infection. However, a multitude of other inflammatory cytokines has been shown to influence survival of virus-infected cells. The use of a hamster model severely limits the availability of commercial reagents and assays, such as antibodies and cytokine specific immunoassays, which would help answer this question. However, the relatively recent and ongoing identification of the mRNA sequences of hamster cytokines in combination with newer technologies, such as small-inhibitory RNA molecules able to inhibit mRNA transcription, may provide powerful research tools to better elucidate what macrophage-produced mediators are involved in enhancing cell destruction.

Three questions specific to the current animal model have been proposed for future research. An additional step would involve attempts to apply results gained in further elucidating the virus-cell or virus-host interaction to additional disease models or eventually to applicable human disease conditions.

### **Conclusion and Summary**

The findings from each of the specific aims of this project are summarized below:

Inoculation of mice with either Banzai or Semliki Forest viruses will cause increased permeability of the BBB to the small molecular weight marker NaFl. Virus-induced BBB permeability increases in a manner that is progressive with the viral infection *in vivo*. Similar increases in permeability demonstrated by two disparate virus species indicates that increased permeability of the BBB may be a pathophysiological event common to many forms of viral encephalitis. In agreement with published data

these results have also shown that administration of the immunomodulatory agent Ampligen™ prior to, but not after, virus exposure can significantly improve the survival, weight change, and tissue viral titers in mice inoculated with viral encephalitides. Ampligen™ treatment prior to virus exposure also results in virus-infected animals showing improved BBB function as indicated by a concomitant decrease in BBB permeability. This improved function appears to be positively correlated with improvements in disease outcome such as weight change, tissue viral titers, and survival. The improvement in BBB function was lost if Ampligen™ treatment was delayed until after virus inoculation. Hamsters inoculated with western equine encephalitis virus exhibited only mild increases in BBB permeability as measured via cerebrospinal fluid. However, there was no apparent correlation between degree of changes to BBB permeability and disease outcome in WEEV-inoculated hamsters.

Hamsters inoculated with the California strain of WEEV can potentially follow a mild form of disease with no negative sequelae, a robust virus infection with death occurring at approximately 96 hpi, or an encephalitic form of infection with overt neurological disease, and death occurring between 6-9 dpi. Virus dose was at least partially responsible for the disease phenotype expressed. Among hamsters that died, the robust form of infection was the most common disease phenotype. In the robust infection animals appeared to be dying primarily from a lymphonecrotic rather than encephalitic disease. At the time of death at approximately 96 hpi virus-infected hamsters had severe lymphocytic necrosis, primarily in the spleen, and no detectable histopathological lesions in the brain in spite of high brain viral titers. Bacterial isolates from WEEV-infected hamsters were similar to those isolated from sham-inoculated animals and antibiotic

treatment alone did not provide any benefit to animal survival. This indicates that in spite of similarities to lymphocytic necrosis seen in VEEV-infected hamsters, WEEV-infected hamsters are not dying from a secondary bacterial infection. Results of serum biochemistry analysis of WEEV-infected hamsters were essentially unremarkable. This suggests hamsters did not die from an overwhelming inflammatory disease and subsequent organ dysregulation as such changes would have been detected via standard serum biochemical analysis. However, inflammatory cytokines may play a role enhancing disease severity. Hematological analysis found WEEV-inoculated animals exhibited lymphopenia. Lymphopenia was found to be a consistent marker of poor disease outcome, although the exact mechanism and pathophysiological significance of lymphopenia is uncertain.

WEEV retained its ability to cause encephalitis in hamsters. Some hamsters inoculated with WEEV survived the initial systemic disease period or were protected from death by the use of anti-inflammatory agents. Among these animals, some displayed overt signs of neurological disease before death, while other animals died without displaying observed clinical signs. These events occurred at approximately 6-9 dpi. These animals had histopathological lesions in the brain consistent with published reports of neuropathology caused by alphavirus induced encephalitis. Hamsters inoculated with WEEV intracranially also exhibited overt signs of neurological disease. Animals receiving virus inoculation directly into the brain had neuropathology consistent with published reports of alphavirus encephalitis. The lesions were also very similar, albeit more severe, to that seen in animals that died 6-9 d after peripheral virus infection.

The cytokine TNF-alpha was increased in the serum of WEEV-infected hamsters, indicating a possible role for inflammatory cytokines in virus-induced disease. Treatment of WEEV-inoculated hamsters with the anti-inflammatory agents flunixin meglumine or dexamethasone resulted in moderate but statistically significant increases in animal survival, and in the case of FM treatment resulted in significantly improved lymphocyte counts. These results strongly suggest a potential role for inflammation to enhance virus disease *in vivo*. Peritoneal macrophages exposed to WEEV *in vitro* expressed TNF-alpha which could be measured in culture supernatant, and appeared to do so in a virus dose-responsive manner. The addition of high concentrations of virus could induce decreased macrophage viability within the relatively short time period of 18 h. The addition of known anti-inflammatory compounds to macrophage cultures exposed to WEEV significantly reduced TNF-alpha expression in a dose-responsive manner. Although the same anti-inflammatory compounds exhibited no detectable antiviral activity their use could also significantly protect macrophage viability in virus-exposed cultures. This result suggests that macrophage cell death was being induced by inflammatory mediators rather than virus effects. Hamster splenocytes exposed to WEEV displayed decreased cell viability in a virus dose-responsive manner although no TNF-alpha could be detected in splenocyte culture supernatant, indicating a primary viral mechanism for splenocyte death. Cell culture supernatant from WEEV-exposed macrophages could significantly enhance virus-induced killing of splenocytes. Anti-inflammatory agents provided no benefit to virus-inoculated splenocytes, and anti-inflammatory treatment of macrophage cell cultures also could not block cytotoxic

enhancement. In both cases of anti-inflammatory compound use in splenocytes, drug-associated toxicity limited effective interpretation.

In conclusion, these data support a disease model in WEEV-infected Syrian golden hamsters in which morbidity and mortality are associated with a non-neurological peripheral lymphonecrotic disease. Inflammation may enhance viral disease, but virus mediated cell killing is the primary cause of pathology and disease manifestations. In spite of the primarily peripheral disease phenotype, WEEV retains its ability to cause viral encephalitis in hamsters.



## REFERENCES

1. **Abraham SM, Lawrence T, Kleiman A, Warden P, Medghalchi M, Tuckermann J, Saklatvala J, Clark AR.** 2006. Antiinflammatory effects of dexamethasone are partly dependent on induction of dual specificity phosphatase 1. *J Exp Med* 203:1883-1889.
2. **Al-Hazmi M, Ayoola EA, Abdurahman M, Banzal S, Ashraf J, El-Bushra A, Hazmi A, Abdullah M, Abbo H, Elamin A, Al-Sammani el T, Gadour M, Menon C, Hamza M, Rahim I, Hafez M, Jambavalikar M, Arishi H, Aqeel A.** 2003. Epidemic Rift Valley fever in Saudi Arabia: a clinical study of severe illness in humans. *Clin Infect Dis* 36:245-252.
3. **Alexopoulou L, Holt AC, Medzhitov R, Flavell RA.** 2001. Recognition of double-stranded RNA and activation of NF-kappaB by Toll-like receptor 3. *Nature* 413:732-738.
4. **Alrajhi AA, Al-Semari A, Al-Watban J.** 2004. Rift Valley fever encephalitis. *Emerg Infect Dis* 10:554-555.
5. **Andersen IH, Marker O, Thomsen AR.** 1991. Breakdown of blood-brain barrier function in the murine lymphocytic choriomeningitis virus infection mediated by virus-specific CD8+ T cells. *J Neuroimmunol* 31:155-163.
6. **Anderson BA.** 1984. Focal neurologic signs in western equine encephalitis. *Can Med Assoc J* 130:1019-1021.
7. **Arakawa T, Hsu YR, Toth E, Stebbing N.** 1987. The antiviral activity of recombinant human tumor necrosis factor-alpha. *J Interferon Res* 7:103-105.
8. **Asnis DS, Conetta R, Waldman G, Teixeira AA.** 2001. The West Nile virus encephalitis outbreak in the United States (1999-2000): from Flushing, New York, to beyond its borders. *Ann N Y Acad Sci* 951:161-171.
9. **Atkins GJ, Sheahan BJ, Dimmock NJ.** 1985. Semliki Forest virus infection of mice: a model for genetic and molecular analysis of viral pathogenicity. *J Gen Virol* 66 ( Pt 3):395-408.
10. **Atkins GJ, Sheahan BJ, Mooney DA.** 1990. Pathogenicity of Semliki Forest virus for the rat central nervous system and primary rat neural cell cultures: possible implications for the pathogenesis of multiple sclerosis. *Neuropathol Appl Neurobiol* 16:57-68.

11. **Austin FJ, Scherer WF.** 1971. Studies of viral virulence. I. Growth and histopathology of virulent and attenuated strains of Venezuelan encephalitis virus in hamsters. *Am J Pathol* 62:195-210.
12. **Baeuerle PA, Baltimore D.** 1996. NF-kappa B: ten years after. *Cell* 87:13-20.
13. **Bahl K, Kim SK, Calcagno C, Ghersi D, Puzone R, Celada F, Selin LK, Welsh RM.** 2006. IFN-induced attrition of CD8 T cells in the presence or absence of cognate antigen during the early stages of viral infections. *J Immunol* 176:4284-4295.
14. **Balachandran S, Kim CN, Yeh WC, Mak TW, Bhalla K, Barber GN.** 1998. Activation of the dsRNA-dependent protein kinase, PKR, induces apoptosis through FADD-mediated death signaling. *Embo J* 17:6888-6902.
15. **Balachandran S, Roberts PC, Kipperman T, Bhalla KN, Compans RW, Archer DR, Barber GN.** 2000. Alpha/beta interferons potentiate virus-induced apoptosis through activation of the FADD/Caspase-8 death signaling pathway. *J Virol* 74:1513-1523.
16. **Balluz IM, Glasgow GM, Killen HM, Mabruk MJ, Sheahan BJ, Atkins GJ.** 1993. Virulent and avirulent strains of Semliki Forest virus show similar cell tropism for the murine central nervous system but differ in the severity and rate of induction of cytolytic damage. *Neuropathol Appl Neurobiol* 19:233-239.
17. **Barnard BJ, Voges SF.** 1986. Flaviviruses in South Africa: pathogenicity for sheep. *Onderstepoort J Vet Res* 53:235-238.
18. **Baskin CR, Garcia-Sastre A, Tumpey TM, Bielefeldt-Ohmann H, Carter VS, Nistal-Villan E, Katze MG.** 2004. Integration of clinical data, pathology, and cDNA microarrays in influenza virus-infected pigtailed macaques (*Macaca nemestrina*). *J Virol* 78:10420-10432.
19. **Baue AE.** 2006. MOF, MODS, and SIRS: what is in a name or an acronym? *Shock* 26:438-449.
20. **Baue AE, Durham R, Faist E.** 1998. Systemic inflammatory response syndrome (SIRS), multiple organ dysfunction syndrome (MODS), multiple organ failure (MOF): are we winning the battle? *Shock* 10:79-89.
21. **Bauer RW, Gill MS, Poston RP, Kim DY.** 2005. Naturally occurring eastern equine encephalitis in a Hampshire wether. *J Vet Diagn Invest* 17:281-285.

22. **Belle EA, Grant LS, Thorburn MJ.** 1964. An Outbreak of Eastern Equine Encephalomyelitis in Jamaica. II. Laboratory Diagnosis and Pathology of Eastern Equine Encephalomyelitis in Jamaica. *Am J Trop Med Hyg* 13:335-341.
23. **Ben-Nathan D, Kobiler D, Rzotkiewicz S, Lustig S, Katz Y.** 2000. CNS penetration by noninvasive viruses following inhalational anesthetics. *Ann N Y Acad Sci* 917:944-950.
24. **Beretta C, Garavaglia G, Cavalli M.** 2005. COX-1 and COX-2 inhibition in horse blood by phenylbutazone, flunixin, carprofen and meloxicam: an in vitro analysis. *Pharmacol Res* 52:302-306.
25. **Bhatt PN, Jacoby RO.** 1976. Genetic resistance to lethal flavivirus encephalitis. II. Effect of immunosuppression. *J Infect Dis* 134:166-173.
26. **Bhatt PN, Johnson EA, Smith AL, Jacoby RO.** 1981. Genetic resistance to lethal flaviviral encephalitis. III. Replication of Banzi virus in vitro and in vivo in tissues of congenic susceptible and resistant mice. *Arch Virol* 69:273-286.
27. **Bianchi TI, Aviles G, Monath TP, Sabattini MS.** 1993. Western equine encephalomyelitis: virulence markers and their epidemiologic significance. *Am J Trop Med Hyg* 49:322-328.
28. **Bidanset DJ, Placidi L, Rybak R, Palmer J, Sommadossi JP, Kern ER.** 2001. Intravenous infusion of cereport increases uptake and efficacy of acyclovir in herpes simplex virus-infected rat brains. *Antimicrob Agents Chemother* 45:2316-2323.
29. **Bradish CJ, Allner K, Maber HB.** 1971. The virulence of original and derived strains of Semliki forest virus for mice, guinea-pigs and rabbits. *J Gen Virol* 12:141-160.
30. **Brandriss MW, Schlesinger JJ, Walsh EE, Briselli M.** 1986. Lethal 17D yellow fever encephalitis in mice. I. Passive protection by monoclonal antibodies to the envelope proteins of 17D yellow fever and dengue 2 viruses. *J Gen Virol* 67 ( Pt 2):229-234.
31. **Brown TP, Roberts W, Page RK.** 1993. Acute hemorrhagic enterocolitis in ratites: isolation of eastern equine encephalomyelitis virus and reproduction of the disease in ostriches and turkey poults. *Avian Dis* 37:602-605.
32. **Bruyn HB, Lennette EH.** 1953. Western equine encephalitis in infants; a report on three cases with sequelae. *Calif Med* 79:362-366.

33. **Bryant CE, Farnfield BA, Janicke HJ.** 2003. Evaluation of the ability of carprofen and flunixin meglumine to inhibit activation of nuclear factor kappa B. *Am J Vet Res* 64:211-215.
34. **Bunning ML, Bowen RA, Cropp CB, Sullivan KG, Davis BS, Komar N, Godsey MS, Baker D, Hettler DL, Holmes DA, Biggerstaff BJ, Mitchell CJ.** 2002. Experimental infection of horses with West Nile virus. *Emerg Infect Dis* 8:380-386.
35. **Calisher CH.** 1994. Medically important arboviruses of the United States and Canada. *Clin Microbiol Rev* 7:89-116.
36. **Calisher CH, Karabatsos N, Dalrymple JM, Shope RE, Porterfield JS, Westaway EG, Brandt WE.** 1989. Antigenic relationships between flaviviruses as determined by cross-neutralization tests with polyclonal antisera. *J Gen Virol* 70 ( Pt 1):37-43.
37. **Calisher CH, Karabatsos N, Lazuick JS, Monath TP, Wolff KL.** 1988. Reevaluation of the western equine encephalitis antigenic complex of alphaviruses (family Togaviridae) as determined by neutralization tests. *Am J Trop Med Hyg* 38:447-452.
38. **Canonico PG, Kende M, Luseri BJ, Huggins JW.** 1984. In-vivo activity of antivirals against exotic RNA viral infections. *J Antimicrob Chemother* 14 Suppl A:27-41.
39. **Cantile C, Del Piero F, Di Guardo G, Arispici M.** 2001. Pathologic and immunohistochemical findings in naturally occurring West Nile virus infection in horses. *Vet Pathol* 38:414-421.
40. **Castelli JC, Hassel BA, Wood KA, Li XL, Amemiya K, Dalakas MC, Torrence PF, Youle RJ.** 1997. A study of the interferon antiviral mechanism: apoptosis activation by the 2-5A system. *J Exp Med* 186:967-972.
41. **Caughey GE, Pouliot M, Cleland LG, James MJ.** 1997. Regulation of tumor necrosis factor-alpha and IL-1 beta synthesis by thromboxane A2 in nonadherent human monocytes. *J Immunol* 158:351-358.
42. **CDC.** Fact Sheet: Western Equine Encephalitis. In: Centers for Disease Control and Prevention DoVBID editor.
43. **Chambers TJ, Nickells M.** 2001. Neuroadapted yellow fever virus 17D: genetic and biological characterization of a highly mouse-neurovirulent virus and its infectious molecular clone. *J Virol* 75:10912-10922.

44. **Chang KH, Kim JM, Kim HY, Song YG, Choi YH, Park YS, Cho JH, Hong SK.** 2000. Spontaneous programmed cell death of peripheral blood mononuclear cells from HIV-infected persons is decreased with interleukin-15. *Yonsei Med J* 41:112-118.
45. **Charles PC, Trgovcich J, Davis NL, Johnston RE.** 2001. Immunopathogenesis and immune modulation of Venezuelan equine encephalitis virus-induced disease in the mouse. *Virology* 284:190-202.
46. **Chaturvedi UC, Mathur A, Tandon P, Natu SM, Rajvanshi S, Tandon HO.** 1979. Variable effect on peripheral blood leucocytes during JE virus infection of man. *Clin Exp Immunol* 38:492-498.
47. **Chaudhri G.** 1997. Differential regulation of biosynthesis of cell surface and secreted TNF-alpha in LPS-stimulated murine macrophages. *J Leukoc Biol* 62:249-257.
48. **Choi KW, Chau TN, Tsang O, Tso E, Chiu MC, Tong WL, Lee PO, Ng TK, Ng WF, Lee KC, Lam W, Yu WC, Lai JY, Lai ST.** 2003. Outcomes and prognostic factors in 267 patients with severe acute respiratory syndrome in Hong Kong. *Ann Intern Med* 139:715-723.
49. **Chotpitayasunondh T, Ungchusak K, Hanshaoworakul W, Chunsuthiwat S, Sawanpanyalert P, Kijphati R, Lochindarat S, Srisan P, Suwan P, Osotthanakorn Y, Anantasetagoon T, Kanjanawasri S, Tanupattarachai S, Weerakul J, Chaiwirattana R, Maneerattanaporn M, Poolsavathitikool R, Chokephaibulkit K, Apisarnthanarak A, Dowell SF.** 2005. Human disease from influenza A (H5N1), Thailand, 2004. *Emerg Infect Dis* 11:201-209.
50. **Chowers MY, Lang R, Nassar F, Ben-David D, Giladi M, Rubinshtein E, Itzhaki A, Mishal J, Siegman-Igra Y, Kitzes R, Pick N, Landau Z, Wolf D, Bin H, Mendelson E, Pitlik SD, Weinberger M.** 2001. Clinical characteristics of the West Nile fever outbreak, Israel, 2000. *Emerg Infect Dis* 7:675-678.
51. **Clarke P, Meintzer SM, Gibson S, Widmann C, Garrington TP, Johnson GL, Tyler KL.** 2000. Reovirus-induced apoptosis is mediated by TRAIL. *J Virol* 74:8135-8139.
52. **Cole FE, Jr., McKinney RW.** 1971. Cross-protection in hamsters immunized with group A arbovirus vaccines. *Infect Immun* 4:37-43.
53. **Cole FE, Jr., Pedersen CE, Jr., Robinson DM.** 1972. Early protection in hamsters immunized with attenuated Venezuelan equine encephalomyelitis vaccine. *Appl Microbiol* 24:604-608.

54. **Conant K, McArthur JC, Griffin DE, Sjulson L, Wahl LM, Irani DN.** 1999. Cerebrospinal fluid levels of MMP-2, 7, and 9 are elevated in association with human immunodeficiency virus dementia. *Ann Neurol* 46:391-398.
55. **Cooper GL, Medina HA, Woolcock PR, McFarland MD, Reynolds B.** 1997. Experimental infection of turkey poultts with western equine encephalitis virus. *Avian Dis* 41:578-582.
56. **Cooper JA, Morser J, Colby MS, Burke DC.** 1979. The toxic effect of double-stranded RNA for interferon-treated cells: evidence for a heterogeneous cellular response and the role of the cell nucleus. *J Gen Virol* 43:553-561.
57. **Copeland S, Warren HS, Lowry SF, Calvano SE, Remick D.** 2005. Acute inflammatory response to endotoxin in mice and humans. *Clin Diagn Lab Immunol* 12:60-67.
58. **Coppenhaver DH, Singh IP, Sarzotti M, Levy HB, Baron S.** 1995. Treatment of intracranial alphavirus infections in mice by a combination of specific antibodies and an interferon inducer. *Am J Trop Med Hyg* 52:34-40.
59. **Cunha BA, McDermott BP, Mohan SS.** 2004. Prognostic importance of lymphopenia in West Nile encephalitis. *Am J Med* 117:710-711.
60. **Cunha BA, Minnaganti V, Johnson DH, Klein NC.** 2000. Profound and prolonged lymphocytopenia with West Nile encephalitis. *Clin Infect Dis* 31:1116-1117.
61. **Dallasta LM, Pisarov LA, Esplen JE, Werley JV, Moses AV, Nelson JA, Achim CL.** 1999. Blood-brain barrier tight junction disruption in human immunodeficiency virus-1 encephalitis. *Am J Pathol* 155:1915-1927.
62. **De Clercq E.** 2006. Interferon and its inducers--a never-ending story: "old" and "new" data in a new perspective. *J Infect Dis* 194 Suppl 1:S19-26.
63. **de la Monte S, Castro F, Bonilla NJ, Gaskin de Urdaneta A, Hutchins GM.** 1985. The systemic pathology of Venezuelan equine encephalitis virus infection in humans. *Am J Trop Med Hyg* 34:194-202.
64. **Del Piero F, Wilkins PA, Dubovi EJ, Biolatti B, Cantile C.** 2001. Clinical, pathologic, immunohistochemical, and virologic findings of eastern equine encephalomyelitis in two horses. *Vet Pathol* 38:451-456.
65. **Deli MA, Nemeth L, Falus A, Abraham CS.** 2000. Effects of N,N-diethyl-2-[4-(phenylmethyl)phenoxy]ethanamine on the blood-brain barrier permeability in the rat. *Eur J Pharmacol* 387:63-72.

66. **Der SD, Yang YL, Weissmann C, Williams BR.** 1997. A double-stranded RNA-activated protein kinase-dependent pathway mediating stress-induced apoptosis. *Proc Natl Acad Sci U S A* 94:3279-3283.
67. **Dietz WH, Jr., Peralta PH, Johnson KM.** 1979. Ten clinical cases of human infection with venezuelan equine encephalomyelitis virus, subtype I-D. *Am J Trop Med Hyg* 28:329-334.
68. **Doby PB, Schnurrenberger PR, Martin RJ, Hanson LE, Sherrick GW, Schoenholz WK.** 1966. Western encephalitis in Illinois horses and ponies. *J Am Vet Med Assoc* 148:422-427.
69. **Dolin R, Reichman RC, Fauci AS.** 1976. Lymphocyte populations in acute viral gastroenteritis. *Infect Immun* 14:422-428.
70. **Donnelly SM, Sheahan BJ, Atkins GJ.** 1997. Long-term effects of Semliki Forest virus infection in the mouse central nervous system. *Neuropathol Appl Neurobiol* 23:235-241.
71. **Dremov DP, Solyanik RG, Miryutova TL, Laptakova LM.** 1978. Attenuated variants of eastern equine encephalomyelitis virus: pathomorphological, immunofluorescence and virological studies of infection in Syrian hamsters. *Acta Virol* 22:139-145.
72. **Ehrenkranz NJ, Ventura AK.** 1974. Venezuelan equine encephalitis virus infection in man. *Annu Rev Med* 25:9-14.
73. **Einsele H, Ehninger G, Steidle M, Fischer I, Bihler S, Gerneth F, Vallbracht A, Schmidt H, Waller HD, Muller CA.** 1993. Lymphocytopenia as an unfavorable prognostic factor in patients with cytomegalovirus infection after bone marrow transplantation. *Blood* 82:1672-1678.
74. **Eralinna JP, Soilu-Hanninen M, Roytta M, Hukkanen V, Salmi AA, Salonen R.** 1996. Blood-brain barrier breakdown and increased intercellular adhesion molecule (ICAM-1/CD54) expression after Semliki Forest (A7) virus infection facilitates the development of experimental allergic encephalomyelitis. *J Neuroimmunol* 66:103-114.
75. **Erdlenbruch B, Alipour M, Fricker G, Miller DS, Kugler W, Eibl H, Lakomek M.** 2003. Alkylglycerol opening of the blood-brain barrier to small and large fluorescence markers in normal and C6 glioma-bearing rats and isolated rat brain capillaries. *Br J Pharmacol* 140:1201-1210.

76. **Fabry Z, Topham DJ, Fee D, Herlein J, Carlino JA, Hart MN, Sriram S.** 1995. TGF-beta 2 decreases migration of lymphocytes in vitro and homing of cells into the central nervous system in vivo. *J Immunol* 155:325-332.
77. **Fazakerley JK, Cotterill CL, Lee G, Graham A.** 2006. Virus tropism, distribution, persistence and pathology in the corpus callosum of the Semliki Forest virus-infected mouse brain: a novel system to study virus-oligodendrocyte interactions. *Neuropathol Appl Neurobiol* 32:397-409.
78. **Ficken MD, Wages DP, Guy JS, Quinn JA, Emory WH.** 1993. High mortality of domestic turkeys associated with Highlands J virus and eastern equine encephalitis virus infections. *Avian Dis* 37:585-590.
79. **Finley KH, Hollister AC.** 1951. Western equine and St. Louis encephalomyelitis. *Calif Med* 74:225-229.
80. **Finley KH, Kokernot RH, Lennette EH.** 1953. A preliminary nine months' follow up of over two hundred and fifty cases of Western Equine and St. Louis encephalomyelitis from a 1952 summer epidemic. *Trans Am Neurol Assoc* 3:22-25.
81. **Finley KH, Longshore WA, Jr., Palmer RJ, Cook RE, Riggs N.** 1955. Western equine and St. Louis encephalitis; preliminary report of a clinical follow-up study in California. *Neurology* 5:223-235.
82. **Fong CC, Zhang Y, Zhang Q, Tzang CH, Fong WF, Wu RS, Yang M.** 2007. Dexamethasone protects RAW264.7 macrophages from growth arrest and apoptosis induced by H<sub>2</sub>O<sub>2</sub> through alteration of gene expression patterns and inhibition of nuclear factor-kappa B (NF-kappaB) activity. *Toxicology* 236:16-28.
83. **Frankmann SP.** 1986. A technique for repeated sampling of CSF from the anesthetized rat. *Physiol Behav* 37:489-493.
84. **Fulop LD, Barrett AD, Titball RW.** 1995. Nucleotide sequence of the NS5 gene of Banzi virus: comparison with other flaviviruses. *J Gen Virol* 76 ( Pt 9):2317-2321.
85. **Gadina M, Bertini R, Mengozzi M, Zandalasini M, Mantovani A, Ghezzi P.** 1991. Protective effect of chlorpromazine on endotoxin toxicity and TNF production in glucocorticoid-sensitive and glucocorticoid-resistant models of endotoxic shock. *J Exp Med* 173:1305-1310.
86. **Gear JH.** 1982. The hemorrhagic fevers of Southern Africa with special reference to studies in the South African Institute for Medical Research. *Yale J Biol Med* 55:207-212.



87. **Gerdes GH.** 2002. Rift valley fever. *Vet Clin North Am Food Anim Pract* 18:549-555.
88. **Gibbs EP.** 1976. Equine viral encephalitis. *Equine Vet J* 8:66-71.
89. **Gilles PN, Fey G, Chisari FV.** 1992. Tumor necrosis factor alpha negatively regulates hepatitis B virus gene expression in transgenic mice. *J Virol* 66:3955-3960.
90. **Gorelkin L, Jahrling PB.** 1974. Pancreatic involvement by Venezuelan equine encephalomyelitis virus in the hamster. *Am J Pathol* 75:349-362.
91. **Gorelkin L, Jahrling PB.** 1975. Virus-initiated septic shock. Acute death of Venezuelan encephalitis virus-infected hamsters. *Lab Invest* 32:78-85.
92. **Gottdenker NL, Howerth EW, Mead DG.** 2003. Natural infection of a great egret (*Casmerodius albus*) with eastern equine encephalitis virus. *J Wildl Dis* 39:702-706.
93. **Greene IP, Paessler S, Anishchenko M, Smith DR, Brault AC, Frolov I, Weaver SC.** 2005. Venezuelan equine encephalitis virus in the guinea pig model: evidence for epizootic virulence determinants outside the E2 envelope glycoprotein gene. *Am J Trop Med Hyg* 72:330-338.
94. **Griffin DE, Byrnes AP, Cook SH.** 2004. Emergence and virulence of encephalitogenic arboviruses. *Arch Virol Suppl*:21-33.
95. **Grimley PM, Friedman RM.** 1970. Arboviral infection of voluntary striated muscles. *J Infect Dis* 122:45-52.
96. **Guidotti LG, Chisari FV.** 2001. Noncytolytic control of viral infections by the innate and adaptive immune response. *Annu Rev Immunol* 19:65-91.
97. **Gupta A, Agarwal R, Shukla GS.** 1999. Functional impairment of blood-brain barrier following pesticide exposure during early development in rats. *Hum Exp Toxicol* 18:174-179.
98. **Gupta S.** 2002. Tumor necrosis factor-alpha-induced apoptosis in T cells from aged humans: a role of TNFR-I and downstream signaling molecules. *Exp Gerontol* 37:293-299.
99. **Guy JS, Barnes HJ, Smith LG.** 1994. Experimental infection of young broiler chickens with eastern equine encephalitis virus and Highlands J virus. *Avian Dis* 38:572-582.

100. **Guy JS, Ficken MD, Barnes HJ, Wages DP, Smith LG.** 1993. Experimental infection of young turkeys with eastern equine encephalitis virus and highlands J virus. *Avian Dis* 37:389-395.
101. **Guy JS, Siopes TD, Barnes HJ, Smith LG, Emory WH.** 1995. Experimental transmission of eastern equine encephalitis virus and Highlands J virus via semen of infected tom turkeys. *Avian Dis* 39:337-342.
102. **Hammon WM, Reeves, W.C., Brookman, B.** 1942. Mosquitoes and encephalitis in the Yakima Valley, Washington. I. Arthropods tested and recovery of western equine and St. Louis viruses from *Culex tarsalis* Coquillett. *J Infect Dis* 70:263-266.
103. **Hardy JL, Presser SB, Chiles RE, Reeves WC.** 1997. Mouse and baby chicken virulence of enzootic strains of western equine encephalomyelitis virus from California. *Am J Trop Med Hyg* 57:240-244.
104. **Haseloff RF, Blasig IE, Bauer HC, Bauer H.** 2005. In search of the astrocytic factor(s) modulating blood-brain barrier functions in brain capillary endothelial cells in vitro. *Cell Mol Neurobiol* 25:25-39.
105. **Henderson DW, Peacock S, Randles WJ.** 1967. On the pathogenesis of Semliki forest virus (SFV) infection in the hamster. *Br J Exp Pathol* 48:228-234.
106. **Hinshaw LB, Emerson TE, Jr., Chang AC, Duerr M, Peer G, Fournel M.** 1994. Study of septic shock in the non-human primate: relationship of pathophysiological response to therapy with anti-TNF antibody. *Circ Shock* 44:221-229.
107. **Hogan MM, Vogel SN.** 1988. Production of tumor necrosis factor by rIFN-gamma-primed C3H/HeJ (Lpsd) macrophages requires the presence of lipid A-associated proteins. *J Immunol* 141:4196-4202.
108. **Hooper DC, Kean RB, Scott GS, Spitsin SV, Mikheeva T, Morimoto K, Bette M, Rohrenbeck AM, Dietzschold B, Weihe E.** 2001. The central nervous system inflammatory response to neurotropic virus infection is peroxynitrite dependent. *J Immunol* 167:3470-3477.
109. **Howitt B.** 1938. Recovery of the virus of equine encephalomyelitis from the brain of a child. *Science* 88:455-456.
110. **Iversson LB, Silva RA, da Rosa AP, Barros VL.** 1993. Circulation of eastern equine encephalitis, western equine encephalitis, Ilheus, Maguari and Tacaiuma viruses in equines of the Brazilian Pantanal, South America. *Rev Inst Med Trop Sao Paulo* 35:355-359.

111. **Jackson AC, SenGupta SK, Smith JF.** 1991. Pathogenesis of Venezuelan equine encephalitis virus infection in mice and hamsters. *Vet Pathol* 28:410-418.
112. **Jacoby RO, Bhatt PN.** 1976. Genetic resistance to lethal flavivirus encephalitis. I. Infection of congenic mice with Banzi virus. *J Infect Dis* 134:158-165.
113. **Jacoby RO, Bhatt PN, Schwartz A.** 1980. Protection of mice from lethal flaviviral encephalitis by adoptive transfer of splenic cells from donors infected with live virus. *J Infect Dis* 141:617-624.
114. **Jahrling PB, Dendy E, Eddy GA.** 1974. Correlates to increased lethality of attenuated Venezuelan encephalitis virus vaccine for immunosuppressed hamsters. *Infect Immun* 9:924-930.
115. **Jahrling PB, Hesse RA, Rhoderick JB, Elwell MA, Moe JB.** 1981. Pathogenesis of a pichinde virus strain adapted to produce lethal infections in guinea pigs. *Infect Immun* 32:872-880.
116. **Jahrling PB, Scherer F.** 1973. Histopathology and distribution of viral antigens in hamsters infected with virulent and benign Venezuelan encephalitis viruses. *Am J Pathol* 72:25-38.
117. **Janousek TE, Kramer WL.** 1998. Surveillance for arthropod-borne viral activity in Nebraska, 1994-1995. *J Med Entomol* 35:758-762.
118. **Jeha LE, Sila CA, Lederman RJ, Prayson RA, Isada CM, Gordon SM.** 2003. West Nile virus infection: A new acute paralytic illness. *Neurology* 61:55-59.
119. **Julander JG, Judge JW, Olsen AL, Rosenberg B, Schafer K, Sidwell RW.** 2007. Prophylactic treatment with recombinant Eimeria protein, alone or in combination with an agonist cocktail, protects mice from Banzi virus infection. *Antiviral Res* 75:14-19.
120. **Julander JG, Siddharthan V, Blatt LM, Schafer K, Sidwell RW, Morrey JD.** 2007. Effect of exogenous interferon and an interferon inducer on western equine encephalitis virus disease in a hamster model. *Virology* 360:454-460.
121. **Kaizu M, Ami Y, Nakasone T, Sasaki Y, Izumi Y, Sato H, Takahashi E, Sakai K, Shinohara K, Nakanishi K, Honda M.** 2003. Higher levels of IL-18 circulate during primary infection of monkeys with a pathogenic SHIV than with a nonpathogenic SHIV. *Virology* 313:8-12.

122. **Kalai M, Van Loo G, Vanden Berghe T, Meeus A, Burm W, Saelens X, Vandenabeele P.** 2002. Tipping the balance between necrosis and apoptosis in human and murine cells treated with interferon and dsRNA. *Cell Death Differ* 9:981-994.
123. **Kamphuis E, Junt T, Waibler Z, Forster R, Kalinke U.** 2006. Type I interferons directly regulate lymphocyte recirculation and cause transient blood lymphopenia. *Blood* 108:3253-3261.
124. **Karupiah G, Xie QW, Buller RM, Nathan C, Duarte C, MacMicking JD.** 1993. Inhibition of viral replication by interferon-gamma-induced nitric oxide synthase. *Science* 261:1445-1448.
125. **Katz JM, Lu X, Frace AM, Morken T, Zaki SR, Tumpey TM.** 2000. Pathogenesis of and immunity to avian influenza A H5 viruses. *Biomed Pharmacother* 54:178-187.
126. **Kawanishi M.** 2000. The Epstein-Barr virus latent membrane protein 1 (LMP1) enhances TNF alpha-induced apoptosis of intestine 407 epithelial cells: the role of LMP1 C-terminal activation regions 1 and 2. *Virology* 270:258-266.
127. **Kelser RA.** 1933. Mosquitoes as vectors of the virus of equine encephalomyelitis. *J Am Vet Med Assoc* 82:767-771.
128. **Kenyon RH, Rippey MK, McKee KT, Jr., Zack PM, Peters CJ.** 1992. Infection of *Macaca radiata* with viruses of the tick-borne encephalitis group. *Microb Pathog* 13:399-409.
129. **Keogh B, Atkins GJ, Mills KH, Sheahan BJ.** 2002. Avirulent Semliki Forest virus replication and pathology in the central nervous system is enhanced in IL-12-defective and reduced in IL-4-defective mice: a role for Th1 cells in the protective immunity. *J Neuroimmunol* 125:15-22.
130. **Keogh B, Atkins GJ, Mills KH, Sheahan BJ.** 2003. Role of interferon-gamma and nitric oxide in the neuropathogenesis of avirulent Semliki Forest virus infection. *Neuropathol Appl Neurobiol* 29:553-562.
131. **Keogh B, Sheahan BJ, Atkins GJ, Mills KH.** 2003. Inhibition of matrix metalloproteinases ameliorates blood-brain barrier disruption and neuropathological lesions caused by avirulent Semliki Forest virus infection. *Vet Immunol Immunopathol* 94:185-190.

132. **Khabar KS, Al-Zoghaibi F, Murayama T, Matsushima K, Mukaida N, Siddiqui Y, Dhalla M, Al-Ahdal MN.** 1997. Interleukin-8 selectively enhances cytopathic effect (CPE) induced by positive-strand RNA viruses in the human WISH cell line. *Biochem Biophys Res Commun* 235:774-778.
133. **Khalili-Shirazi A, Gregson N, Webb HE.** 1988. Immunocytochemical evidence for Semliki Forest virus antigen persistence in mouse brain. *J Neurol Sci* 85:17-26.
134. **Khatri M, Palmquist JM, Cha RM, Sharma JM.** 2005. Infection and activation of bursal macrophages by virulent infectious bursal disease virus. *Virus Res* 113:44-50.
135. **Kim WH, Hong F, Jaruga B, Zhang ZS, Fan SJ, Liang TJ, Gao B.** 2005. Hepatitis B virus X protein sensitizes primary mouse hepatocytes to ethanol- and TNF-alpha-induced apoptosis by a caspase-3-dependent mechanism. *Cell Mol Immunol* 2:40-48.
136. **Kishimoto C, Kawamata H, Sakai S, Shinohara H, Ochiai H.** 2000. Role of MIP-2 in coxsackievirus B3 myocarditis. *J Mol Cell Cardiol* 32:631-638.
137. **Kishimoto C, Kawamata H, Sakai S, Shinohara H, Ochiai H.** 2001. Enhanced production of macrophage inflammatory protein 2 (MIP-2) by in vitro and in vivo infections with encephalomyocarditis virus and modulation of myocarditis with an antibody against MIP-2. *J Virol* 75:1294-1300.
138. **Kokernot RH, Casaca, V.M.R., Weinbren, M.P., McIntosh, B. M.** 1965. Survey for antibodies against arthropod-borne viruses in the sera of indigenous residents of Angola. *Transactions of the Royal Society of Tropical Medicine and Hygiene* 59:563-570.
139. **Koyama AH, Arakawa T, Adachi A.** 1998. Acceleration of virus-induced apoptosis by tumor necrosis factor. *FEBS Lett* 426:179-182.
140. **Kozler P, Pokorny J.** 2003. Altered blood-brain barrier permeability and its effect on the distribution of Evans blue and sodium fluorescein in the rat brain applied by intracarotid injection. *Physiol Res* 52:607-614.
141. **Lafon M, Megret F, Lafage M, Prehaud C.** 2007. The Innate Facet of the Brain: Human Neurons Express TLR3 and Sense Viral dsRNA. *J Mol Neurosci* 33:224.
142. **Landoni MF, Foot R, Frean S, Lees P.** 1996. Effects of flunixin, tolfenamic acid, R(-) and S(+) ketoprofen on the response of equine synoviocytes to lipopolysaccharide stimulation. *Equine Vet J* 28:468-475.

143. **Leyssen P, Drosten C, Paning M, Charlier N, Paeshuyse J, De Clercq E, Neyts J.** 2003. Interferons, interferon inducers, and interferon-ribavirin in treatment of flavivirus-induced encephalitis in mice. *Antimicrob Agents Chemother* 47:777-782.
144. **Li AM, So HK, Chu W, Ng PC, Hon KL, Chiu WK, Leung CW, Yau YS, Mo WK, Fok TF.** 2004. Radiological and pulmonary function outcomes of children with SARS. *Pediatr Pulmonol* 38:427-433.
145. **Li XD, Kukkonen S, Vapalahti O, Plyusnin A, Lankinen H, Vaheri A.** 2004. Tula hantavirus infection of Vero E6 cells induces apoptosis involving caspase 8 activation. *J Gen Virol* 85:3261-3268.
146. **Lin C, Zimmer SG, Lu Z, Holland RE, Jr., Dong Q, Chambers TM.** 2001. The involvement of a stress-activated pathway in equine influenza virus-mediated apoptosis. *Virology* 287:202-213.
147. **Lin Y, Bright AC, Rothermel TA, He B.** 2003. Induction of apoptosis by paramyxovirus simian virus 5 lacking a small hydrophobic gene. *J Virol* 77:3371-3383.
148. **Luabeya MK, Dallasta LM, Achim CL, Pauza CD, Hamilton RL.** 2000. Blood-brain barrier disruption in simian immunodeficiency virus encephalitis. *Neuropathol Appl Neurobiol* 26:454-462.
149. **Lucas M, Mashimo T, Frenkiel MP, Simon-Chazottes D, Montagutelli X, Ceccaldi PE, Guenet JL, Despres P.** 2003. Infection of mouse neurones by West Nile virus is modulated by the interferon-inducible 2'-5' oligoadenylate synthetase 1b protein. *Immunol Cell Biol* 81:230-236.
150. **Lucin P, Jonjic S, Messerle M, Polic B, Hengel H, Koszinowski UH.** 1994. Late phase inhibition of murine cytomegalovirus replication by synergistic action of interferon-gamma and tumour necrosis factor. *J Gen Virol* 75 ( Pt 1):101-110.
151. **Lustig S, Danenberg HD, Kafri Y, Kobiler D, Ben-Nathan D.** 1992. Viral neuroinvasion and encephalitis induced by lipopolysaccharide and its mediators. *J Exp Med* 176:707-712.
152. **MacKay RJ, Merritt AM, Zertuche JM, Whittington M, Skelley LA.** 1991. Tumour necrosis factor activity in the circulation of horses given endotoxin. *Am J Vet Res* 52:533-538.
153. **Madani TA.** 2005. Alkhumra virus infection, a new viral hemorrhagic fever in Saudi Arabia. *J Infect* 51:91-97.

154. **Malmgaard L, Melchjorsen J, Bowie AG, Mogensen SC, Paludan SR.** 2004. Viral activation of macrophages through TLR-dependent and -independent pathways. *J Immunol* 173:6890-6898.
155. **Marchevsky RS, Freire MS, Coutinho ES, Galler R.** 2003. Neurovirulence of yellow fever 17DD vaccine virus to rhesus monkeys. *Virology* 316:55-63.
156. **Marianneau P, Cardona A, Edelman L, Deubel V, Despres P.** 1997. Dengue virus replication in human hepatoma cells activates NF-kappaB which in turn induces apoptotic cell death. *J Virol* 71:3244-3249.
157. **Martin M, Tsai TF, Cropp B, Chang GJ, Holmes DA, Tseng J, Shieh W, Zaki SR, Al-Sanouri I, Cutrona AF, Ray G, Weld LH, Cetron MS.** 2001. Fever and multisystem organ failure associated with 17D-204 yellow fever vaccination: a report of four cases. *Lancet* 358:98-104.
158. **Matsuda T, Almasan A, Tomita M, Tamaki K, Saito M, Tadano M, Yagita H, Ohta T, Mori N.** 2005. Dengue virus-induced apoptosis in hepatic cells is partly mediated by Apo2 ligand/tumour necrosis factor-related apoptosis-inducing ligand. *J Gen Virol* 86:1055-1065.
159. **McIntosh BM, Dos Santos IS, Meenehan GM.** 1976. *Culex* (Eumelanomyia) rubinotus Theobald as vector of Banzi, Germiston and Witwatersrand viruses. III. Transmission of virus to hamsters by wild-caught infected *C. rubinotus*. *J Med Entomol* 12:645-646.
160. **McIntosh BM, Jupp PG, Dos Santos IS, Meenehan GM.** 1976. *Culex* (Eumelanomyia) rubinotus Theobald as vector of Banzi, Germiston and Witwatersand viruses. I. Isolation of virus from wild populations of *C. rubinotus*. *J Med Entomol* 12:637-640.
161. **McNally JM, Zarozinski CC, Lin MY, Brehm MA, Chen HD, Welsh RM.** 2001. Attrition of bystander CD8 T cells during virus-induced T-cell and interferon responses. *J Virol* 75:5965-5976.
162. **Merrick AW, Durand DP, Kintner LD.** 1967. Semliki Forest virus effects on the rat central nervous system. *Electroencephalogr Clin Neurophysiol* 23:473-476.
163. **Metselaar D, Henderson BE, Kirya GB, Tukei PM, de Geus A.** 1974. Isolation of arboviruses in Kenya, 1966-1971. *Trans R Soc Trop Med Hyg* 68:114-123.
164. **Meyer KF, Haring, C.M., Howitt, B.** 1931. The etiology of epizootic encephalomyelitis of horses in the San Joaquin Valley, 1930. *Science* 74:227-228.

165. **Meyer KF, Haring, C.M., Howitt, B.** 1932. A summary of recent studies of equine encephalomyelitis. *Ann Intern Med* 6:645-654.
166. **Misra UK, Kalita J, Syam UK, Dhole TN.** 2006. Neurological manifestations of dengue virus infection. *J Neurol Sci* 244:117-122.
167. **Monlux WS, Luedke AJ.** 1973. Brain and spinal cord lesions in horses inoculated with Venezuelan equine encephalomyelitis virus (epidemic American and Trinidad strains). *Am J Vet Res* 34:465-473.
168. **Morahan PS, Pinto A, Stewart D, Murasko DM, Brinton MA.** 1991. Varying role of alpha/beta interferon in the antiviral efficacy of synthetic immunomodulators against Semliki Forest virus infection. *Antiviral Res* 15:241-254.
169. **Morrey JD, Day CW, Julander JG, Blatt LM, Smee DF, Sidwell RW.** 2004. Effect of interferon-alpha and interferon-inducers on West Nile virus in mouse and hamster animal models. *Antivir Chem Chemother* 15:101-109.
170. **Morrey JD, Day CW, Julander JG, Olsen AL, Sidwell RW, Cheney CD, Blatt LM.** 2004. Modeling hamsters for evaluating West Nile virus therapies. *Antiviral Res* 63:41-50.
171. **Morrey JD, Smee DF, Sidwell RW, Tseng C.** 2002. Identification of active antiviral compounds against a New York isolate of West Nile virus. *Antiviral Res* 55:107-116.
172. **Murphy FA, Harrison AK, Collin WK.** 1970. The role of extraneural arbovirus infection in the pathogenesis of encephalitis. An electron microscopic study of Semliki Forest virus infection in mice. *Lab Invest* 22:318-328.
173. **Nakamura Y, Murai T, Ogawa Y.** 1996. Effect of in vitro and in vivo administration of dexamethasone on rat macrophage functions: comparison between alveolar and peritoneal macrophages. *Eur Respir J* 9:301-306.
174. **Nalca A, Fellows PF, Whitehouse CA.** 2003. Vaccines and animal models for arboviral encephalitides. *Antiviral Res* 60:153-174.
175. **Narita M, Kawashima K, Kimura K, Mikami O, Shibahara T, Yamada S, Sakoda Y.** 2000. Comparative immunohistopathology in pigs infected with highly virulent or less virulent strains of hog cholera virus. *Vet Pathol* 37:402-408.



176. **Neuzil KM, Tang YW, Graham BS.** 1996. Protective Role of TNF-alpha in respiratory syncytial virus infection in vitro and in vivo. *Am J Med Sci* 311:201-204.
177. **O'Donnell DR, Carrington D.** 2002. Peripheral blood lymphopenia and neutrophilia in children with severe respiratory syncytial virus disease. *Pediatr Pulmonol* 34:128-130.
178. **Oishi K, Saito M, Mapua CA, Natividad FF.** 2007. Dengue illness: clinical features and pathogenesis. *J Infect Chemother* 13:125-133.
179. **Olsen AL, Morrey JD, Smee DF, Sidwell RW.** 2007. Correlation between breakdown of the blood-brain barrier and disease outcome of viral encephalitis in mice. *Antiviral Res* 75:104-112.
180. **Ozato K, Tsujimura H, Tamura T.** 2002. Toll-like receptor signaling and regulation of cytokine gene expression in the immune system. *Biotechniques Suppl*:66-68, 70, 72 passim.
181. **Paessler S, Aguilar P, Anishchenko M, Wang HQ, Aronson J, Campbell G, Cararra AS, Weaver SC.** 2004. The hamster as an animal model for eastern equine encephalitis--and its use in studies of virus entrance into the brain. *J Infect Dis* 189:2072-2076.
182. **Palmquist JM, Khatri M, Cha RM, Goddeeris BM, Walcheck B, Sharma JM.** 2006. In vivo activation of chicken macrophages by infectious bursal disease virus. *Viral Immunol* 19:305-315.
183. **Pepperell C, Rau N, Kraiden S, Kern R, Humar A, Mederski B, Simor A, Low DE, McGeer A, Mazzulli T, Burton J, Jaigobin C, Fearon M, Artsob H, Drebot MA, Halliday W, Brunton J.** 2003. West Nile virus infection in 2002: morbidity and mortality among patients admitted to hospital in southcentral Ontario. *Cmaj* 168:1399-1405.
184. **Pinto AJ, Morahan PS, Brinton M, Stewart D, Gavin E.** 1990. Comparative therapeutic efficacy of recombinant interferons-alpha, -beta, and -gamma against alphatogavirus, bunyavirus, flavivirus, and herpesvirus infections. *J Interferon Res* 10:293-298.
185. **Pinto AJ, Morahan PS, Brinton MA.** 1988. Comparative study of various immunomodulators for macrophage and natural killer cell activation and antiviral efficacy against exotic RNA viruses. *Int J Immunopharmacol* 10:197-209.

186. **Poonacha KB, Gregory CR, Vickers ML.** 1998. Intestinal lesions in a horse associated with eastern equine encephalomyelitis virus infection. *Vet Pathol* 35:535-538.
187. **Porter MB, Long MT, Getman LM, Giguere S, MacKay RJ, Lester GD, Alleman AR, Wamsley HL, Franklin RP, Jacks S, Buergelt CD, Detrisac CJ.** 2003. West Nile virus encephalomyelitis in horses: 46 cases (2001). *J Am Vet Med Assoc* 222:1241-1247.
188. **Pruslin FH, Rodman TC.** 1978. Venezuelan encephalitis virus: in vivo induction of a chromosomal abnormality in hamster bone marrow cells. *Infect Immun* 19:1104-1106.
189. **Pusztai R, Gould EA, Smith H.** 1971. Infection patterns in mice of an avirulent and virulent strain of Semliki Forest virus. *Br J Exp Pathol* 52:669-677.
190. **Quaresma JA, Barros VL, Pagliari C, Fernandes ER, Guedes F, Takakura CF, Andrade HF, Jr., Vasconcelos PF, Duarte MI.** 2006. Revisiting the liver in human yellow fever: virus-induced apoptosis in hepatocytes associated with TGF-beta, TNF-alpha and NK cells activity. *Virology* 345:22-30.
191. **Quaresma JA, Duarte MI, Vasconcelos PF.** 2006. Midzonal lesions in yellow fever: a specific pattern of liver injury caused by direct virus action and in situ inflammatory response. *Med Hypotheses* 67:618-621.
192. **Rayfield EJ, Gorelkin L, Curnow RT, Jahrling PB.** 1976. Virus-induced pancreatic disease by Venezuelan encephalitis virus. Alterations in glucose tolerance and insulin release. *Diabetes* 25:623-631.
193. **Reed DS, Lackemeyer MG, Garza NL, Norris S, Gamble S, Sullivan LJ, Lind CM, Raymond JL.** 2007. Severe encephalitis in cynomolgus macaques exposed to aerosolized Eastern equine encephalitis virus. *J Infect Dis* 196:441-450.
194. **Reed DS, Larsen T, Sullivan LJ, Lind CM, Lackemeyer MG, Pratt WD, Parker MD.** 2005. Aerosol exposure to western equine encephalitis virus causes fever and encephalitis in cynomolgus macaques. *J Infect Dis* 192:1173-1182.
195. **Reed DS, Lind CM, Lackemeyer MG, Sullivan LJ, Pratt WD, Parker MD.** 2005. Genetically engineered, live, attenuated vaccines protect nonhuman primates against aerosol challenge with a virulent IE strain of Venezuelan equine encephalitis virus. *Vaccine* 23:3139-3147.
196. **Reed DS, Lind CM, Sullivan LJ, Pratt WD, Parker MD.** 2004. Aerosol infection of cynomolgus macaques with enzootic strains of venezuelan equine encephalitis viruses. *J Infect Dis* 189:1013-1017.

197. **Rehle TM.** 1989. Classification, distribution and importance of arboviruses. *Trop Med Parasitol* 40:391-395.
198. **Richter S, Parolin C, Palumbo M, Palu G.** 2004. Antiviral properties of quinolone-based drugs. *Curr Drug Targets Infect Disord* 4:111-116.
199. **Roberts ED, Sanmartin C, Payan J, Mackenzie RB.** 1970. Neuropathologic changes in 15 horses with naturally occurring Venezuelan equine encephalomyelitis. *Am J Vet Res* 31:1223-1229.
200. **Roe MF, Bloxham DM, White DK, Ross-Russell RI, Tasker RT, O'Donnell DR.** 2004. Lymphocyte apoptosis in acute respiratory syncytial virus bronchiolitis. *Clin Exp Immunol* 137:139-145.
201. **Rosenberg YJ, Cafaro A, Brennan T, Greenhouse JG, Villinger F, Ansari AA, Brown C, McKinnon K, Bellah S, Yalley-Ogunro J, Elkins WR, Gartner S, Lewis MG.** 1997. Virus-induced cytokines regulate circulating lymphocyte levels during primary SIV infections. *Int Immunol* 9:703-712.
202. **Rothman AL.** 2003. Immunology and immunopathogenesis of dengue disease. *Adv Virus Res* 60:397-419.
203. **Sahu SP, Pedersen DD, Jenny AL, Schmitt BJ, Alstad AD.** 2003. Pathogenicity of a Venezuelan equine encephalomyelitis serotype IE virus isolate for ponies. *Am J Trop Med Hyg* 68:485-494.
204. **Sammin DJ, Butler D, Atkins GJ, Sheahan BJ.** 1999. Cell death mechanisms in the olfactory bulb of rats infected intranasally with Semliki forest virus. *Neuropathol Appl Neurobiol* 25:236-243.
205. **Sampson BA, Ambrosi C, Charlot A, Reiber K, Veress JF, Armbrustmacher V.** 2000. The pathology of human West Nile Virus infection. *Hum Pathol* 31:527-531.
206. **Sanchez-Cordon PJ, Nunez A, Salguero FJ, Pedrera M, Fernandez de Marco M, Gomez-Villamandos JC.** 2005. Lymphocyte apoptosis and thrombocytopenia in spleen during classical swine fever: role of macrophages and cytokines. *Vet Pathol* 42:477-488.
207. **Santoro MG, Rossi A, Amici C.** 2003. NF-kappaB and virus infection: who controls whom. *Embo J* 22:2552-2560.

208. **Sarzotti M, Coppenhaver DH, Singh IP, Poast J, Baron S.** 1989. The in vivo antiviral effect of CL246,738 is mediated by the independent induction of interferon-alpha and interferon-beta. *J Interferon Res* 9:265-274.
209. **Schobesberger M, Summerfield A, Doherr MG, Zurbriggen A, Griot C.** 2005. Canine distemper virus-induced depletion of uninfected lymphocytes is associated with apoptosis. *Vet Immunol Immunopathol* 104:33-44.
210. **Schultz-Cherry S, Hinshaw VS.** 1996. Influenza virus neuraminidase activates latent transforming growth factor beta. *J Virol* 70:8624-8629.
211. **Sejvar JJ, Leis AA, Stokic DS, Van Gerpen JA, Marfin AA, Webb R, Haddad MB, Tierney BC, Slavinski SA, Polk JL, Dostrow V, Winkelmann M, Petersen LR.** 2003. Acute flaccid paralysis and West Nile virus infection. *Emerg Infect Dis* 9:788-793.
212. **Sen GC.** 2001. Viruses and interferons. *Annu Rev Microbiol* 55:255-281.
213. **Senne DA, Pedersen JC, Hutto DL, Taylor WD, Schmitt BJ, Panigrahy B.** 2000. Pathogenicity of West Nile virus in chickens. *Avian Dis* 44:642-649.
214. **Sidwell RW, Huffman JH, Barnard DL, Smee DF, Warren RP, Chirigos MA, Kende M, Huggins J.** 1994. Antiviral and immunomodulating inhibitors of experimentally-induced Punta Toro virus infections. *Antiviral Res* 25:105-122.
215. **Sidwell RW, Smee DF.** 2003. Viruses of the Bunya- and Togaviridae families: potential as bioterrorism agents and means of control. *Antiviral Res* 57:101-111.
216. **Singh IP, Coppenhaver DH, Sarzotti M, Sriyuktasuth P, Poast J, Levy HB, Baron S.** 1989. Postinfection therapy of arbovirus infections in mice. *Antimicrob Agents Chemother* 33:2126-2131.
217. **Smee DF, Alaghamandan HA, Cottam HB, Sharma BS, Jolley WB, Robins RK.** 1989. Broad-spectrum in vivo antiviral activity of 7-thia-8-oxoguanosine, a novel immunopotentiating agent. *Antimicrob Agents Chemother* 33:1487-1492.
218. **Smee DF, McKernan PA, Nord LD, Willis RC, Petrie CR, Riley TM, Revankar GR, Robins RK, Smith RA.** 1987. Novel pyrazolo[3,4-d]pyrimidine nucleoside analog with broad-spectrum antiviral activity. *Antimicrob Agents Chemother* 31:1535-1541.
219. **Smithburn K.C. HAJ.** 1944. Semliki Forest virus. I. Isolation and pathogenic properties. *J Immunol* 49:141-173.

220. **Smithburn KC, Haddow, A.J.** 1944. Semliki Forest virus. I. Isolation and pathogenic properties. *J Immunol* 49:141-173.
221. **Smithburn KC, Paterson, H.E., Heymann, C.S., Winter, P.A.D.** 1959. An agent related to Uganda S. virus from man and mosquitoes in South Africa. *South African Medical Journal* 46:959-962.
222. **Snook CS, Hyman SS, Del Piero F, Palmer JE, Ostlund EN, Barr BS, Desrochers AM, Reilly LK.** 2001. West Nile virus encephalomyelitis in eight horses. *J Am Vet Med Assoc* 218:1576-1579.
223. **Soares CN, Faria LC, Peralta JM, de Freitas MR, Puccioni-Sohler M.** 2006. Dengue infection: neurological manifestations and cerebrospinal fluid (CSF) analysis. *J Neurol Sci* 249:19-24.
224. **Solomon T.** 2004. Flavivirus encephalitis. *N Engl J Med* 351:370-378.
225. **Solomon T, Dung NM, Vaughn DW, Kneen R, Thao LT, Raengsakulrach B, Loan HT, Day NP, Farrar J, Myint KS, Warrell MJ, James WS, Nisalak A, White NJ.** 2000. Neurological manifestations of dengue infection. *Lancet* 355:1053-1059.
226. **Solomon T, Mallewa M.** 2001. Dengue and other emerging flaviviruses. *J Infect* 42:104-115.
227. **Sponseller ML, Binn LN, Wooding WL, Yager RH.** 1966. Field strains of western encephalitis virus in ponies: virologic, clinical, and pathologic observations. *Am J Vet Res* 27:1591-1598.
228. **Steele KE, Linn MJ, Schoepp RJ, Komar N, Geisbert TW, Manduca RM, Calle PP, Raphael BL, Clippinger TL, Larsen T, Smith J, Lanciotti RS, Panella NA, McNamara TS.** 2000. Pathology of fatal West Nile virus infections in native and exotic birds during the 1999 outbreak in New York City, New York. *Vet Pathol* 37:208-224.
229. **Steer SA, Moran JM, Maggi LB, Jr., Buller RM, Perlman H, Corbett JA.** 2003. Regulation of cyclooxygenase-2 expression by macrophages in response to double-stranded RNA and viral infection. *J Immunol* 170:1070-1076.
230. **Streetz KL, Wustefeld T, Klein C, Manns MP, Trautwein C.** 2001. Mediators of inflammation and acute phase response in the liver. *Cell Mol Biol (Noisy-le-grand)* 47:661-673.

231. **Suckling AJ, Jagelman S, Illavia SJ, Webb HE.** 1980. The effect of mouse strain on the pathogenesis of the encephalitis and demyelination induced by avirulent Semliki Forest virus infections. *Br J Exp Pathol* 61:281-284.
232. **Summerfield A, Knotig SM, McCullough KC.** 1998. Lymphocyte apoptosis during classical swine fever: implication of activation-induced cell death. *J Virol* 72:1853-1861.
233. **Swayne DE, Beck JR, Smith CS, Shieh WJ, Zaki SR.** 2001. Fatal encephalitis and myocarditis in young domestic geese (*Anser anser domesticus*) caused by West Nile virus. *Emerg Infect Dis* 7:751-753.
234. **Takano T, Hohdatsu T, Hashida Y, Kaneko Y, Tanabe M, Koyama H.** 2007. A "possible" involvement of TNF-alpha in apoptosis induction in peripheral blood lymphocytes of cats with feline infectious peritonitis. *Vet Microbiol* 119:121-131.
235. **Tanaka N, Sato M, Lamphier MS, Nozawa H, Oda E, Noguchi S, Schreiber RD, Tsujimoto Y, Taniguchi T.** 1998. Type I interferons are essential mediators of apoptotic death in virally infected cells. *Genes Cells* 3:29-37.
236. **Tigertt WD, Downs WG.** 1962. Studies on the virus of Venezuelan equine encephalomyelitis in Trinidad, W.I. I. The 1943-1944 epizootic. *Am J Trop Med Hyg* 11:822-834.
237. **Tumpey TM, Lu X, Morken T, Zaki SR, Katz JM.** 2000. Depletion of lymphocytes and diminished cytokine production in mice infected with a highly virulent influenza A (H5N1) virus isolated from humans. *J Virol* 74:6105-6116.
238. **Ulich TR, del Castillo J, Ni RX, Bikhazi N, Calvin L.** 1989. Mechanisms of tumor necrosis factor alpha-induced lymphopenia, neutropenia, and biphasic neutrophilia: a study of lymphocyte recirculation and hematologic interactions of TNF alpha with endogenous mediators of leukocyte trafficking. *J Leukoc Biol* 45:155-167.
239. **Ulloa A, Langevin SA, Mendez-Sanchez JD, Arredondo-Jimenez JI, Raetz JL, Powers AM, Villarreal-Trevino C, Gubler DJ, Komar N.** 2003. Serologic survey of domestic animals for zoonotic arbovirus infections in the Lacandon Forest region of Chiapas, Mexico. *Vector Borne Zoonotic Dis* 3:3-9.
240. **Veazey RS, Vice CC, Cho DY, Tully TN, Jr., Shane SM.** 1994. Pathology of eastern equine encephalitis in emus (*Dromaius novaehollandiae*). *Vet Pathol* 31:109-111.
241. **Victor J, Smith DG, Pollack AD.** 1956. The comparative pathology of Venezuelan equine encephalomyelitis. *J Infect Dis* 98:55-66.

242. **Vogel P, Kell WM, Fritz DL, Parker MD, Schoepp RJ.** 2005. Early events in the pathogenesis of eastern equine encephalitis virus in mice. *Am J Pathol* 166:159-171.
243. **Walker DH, Harrison A, Murphy K, Flemister M, Murphy FA.** 1976. Lymphoreticular and myeloid pathogenesis of Venezuelan equine encephalitis in hamsters. *Am J Pathol* 84:351-370.
244. **Wan Y, Freeswick PD, Khemlani LS, Kispert PH, Wang SC, Su GL, Billiar TR.** 1995. Role of lipopolysaccharide (LPS), interleukin-1, interleukin-6, tumor necrosis factor, and dexamethasone in regulation of LPS-binding protein expression in normal hepatocytes and hepatocytes from LPS-treated rats. *Infect Immun* 63:2435-2442.
245. **Wang J, Guan E, Roderiquez G, Norcross MA.** 2001. Synergistic induction of apoptosis in primary CD4(+) T cells by macrophage-tropic HIV-1 and TGF-beta1. *J Immunol* 167:3360-3366.
246. **Wang JF, Meissner A, Malek S, Chen Y, Ke Q, Zhang J, Chu V, Hampton TG, Crumpacker CS, Abelmann WH, Amende I, Morgan JP.** 2005. Propranolol ameliorates and epinephrine exacerbates progression of acute and chronic viral myocarditis. *Am J Physiol Heart Circ Physiol* 289:H1577-1583.
247. **WHO.** Arthropod-borne and rodent-borne viral diseases. Geneva: World Health Organization.
248. **Williams MC, Woodall, J.P.** 1964. An epidemic of an illness resembling Denué in the Morogoro district of Tanganyika. *East African Medical Journal* 41:271-275.
249. **Wong GH, Goeddel DV.** 1986. Tumour necrosis factors alpha and beta inhibit virus replication and synergize with interferons. *Nature* 323:819-822.
250. **Xiao SY, Guzman H, Zhang H, Travassos da Rosa AP, Tesh RB.** 2001. West Nile virus infection in the golden hamster (*Mesocricetus auratus*): a model for West Nile encephalitis. *Emerg Infect Dis* 7:714-721.
251. **Yamane D, Nagai M, Ogawa Y, Tohya Y, Akashi H.** 2005. Enhancement of apoptosis via an extrinsic factor, TNF-alpha, in cells infected with cytopathic bovine viral diarrhoea virus. *Microbes Infect* 7:1482-1491.
252. **Zitzow LA, Rowe T, Morken T, Shieh WJ, Zaki S, Katz JM.** 2002. Pathogenesis of avian influenza A (H5N1) viruses in ferrets. *J Virol* 76:4420-4429.

253. **Zlotnik I.** 1968. The reaction of astrocytes to acute virus infections of the central nervous system. *Br J Exp Pathol* 49:555-564.
254. **Zlotnik I, Harris WJ.** 1970. The changes in cell organelles of neurons in the brains of adult mice and hamsters during Semliki Forest virus and louping ill encephalitis. *Br J Exp Pathol* 51:37-42.
255. **Zlotnik I, Peacock S, Grant DP, Batter-Hatton D.** 1972. The pathogenesis of western equine encephalitis virus (W.E.E.) in adult hamsters with special reference to the long and short term effects on the C.N.S. of the attenuated clone 15 variant. *Br J Exp Pathol* 53:59-77.



## CURRICULUM VITAE

Aaron Olsen  
December 2007

EDUCATION

August 2004 – April 2008 Utah State University Logan, Utah

**Doctor of Philosophy- Bioveterinary Sciences**

- Investigated pathobiology of viral encephalitides
- Evaluated efficacy of potential antiviral agents
- Dissertation available upon request

August 1998 – May 2002 Purdue University West Lafayette, Indiana

**Doctor of Veterinary Medicine**

- Graduated with honors in top 10% of class
- Areas of interest include: Laboratory Animal Medicine, Anesthesia, Hematology and Cytology

August 2000 - December 2002 Purdue University West Lafayette, Indiana

**MS- Molecular Biology**

- Dual-degree with DVM
- Studied role of growth factors in skeletal muscle atrophy
- Developed and implemented animal models to study gene expression patterns
- Techniques learned include:
  - PCR
  - Immunohistochemistry
  - In Situ Hybridization
- Thesis available upon request

March 1996 – June 1998 Utah State University Logan, Utah

**BS- Animal, Dairy, and Veterinary Medicine**

Graduated cum laude

EMPLOYMENT EXPERIENCE

July 2005-Present Utah State University Logan, Utah

**Director Laboratory Animal Research Center****Utah State University Attending Veterinarian****IACUC Administrator**

- Maintain AAALAC Accreditation status
- Direct animal care program for laboratory animals on USU campus
- Develop and direct animal health monitoring program
- Train individuals in the care and use of laboratory animals
- Operate program in accordance with all USDA and PHS regulations
- Oversee function of Institutional Animal Care and Use Committee
- Advise on construction and renovation projects
- Licensed to practice veterinary medicine in the State of Utah
- Federally Accredited veterinarian

November 2003-July 2005

Institute for Antiviral Research, Utah State University Logan, Utah

**Senior Research Associate**

- Work with Biohazard Level 2 and 3 viral agents in both cell culture and animal models.
- Design and implement experiments to evaluate the antiviral efficacy of test compounds
- Perform duties of Attending Veterinarian for research projects operated by the Institute

May 2002 - May 2003 Animal Health Clinic Blackfoot, Idaho

**Associate Veterinarian**

- Examine and diagnose and direct medical treatment animals presented to the clinic
- Perform and assist in a wide variety of surgical procedures

AFFILIATIONS

American Veterinary Medical Association (AVMA)

American Association of Laboratory Animal Science (AALAS)

American Society of Laboratory Animal Practitioners (ASLAP)

PUBLICATIONS

- Olsen, A. L.**, J. D. Morrey, D. F. Smee and R. W. Sidwell (2007). "Correlation between breakdown of the blood-brain barrier and disease outcome of viral encephalitis in mice." *Antiviral Res* 75(2): 104-12.
- Eash, J., **A. Olsen**, G. Breur, D. Gerrard and K. Hannon (2007). "FGFR1 inhibits skeletal muscle atrophy associated with hindlimb suspension." *BMC Musculoskeletal Disord* 8: 32.
- Julander, J. G., Q. A. Winger, **A. L. Olsen**, C. W. Day, R. W. Sidwell and J. D. Morrey (2005). "Treatment of West Nile virus-infected mice with reactive immunoglobulin reduces fetal titers and increases dam survival." *Antiviral Res* 65(2): 79-85.
- Morrey, J. D., V. Siddharthan, **A. L. Olsen**, G. Y. Roper, H. Wang, T. J. Baldwin, S. Koenig, S. Johnson, J. L. Nordstrom and M. S. Diamond (2006). "Humanized monoclonal antibody against West Nile virus envelope protein administered after neuronal infection protects against lethal encephalitis in hamsters." *J Infect Dis* 194(9): 1300-8.
- Morrey, J. D., C. W. Day, J. G. Julander, **A. L. Olsen**, R. W. Sidwell, C. D. Cheney and L. M. Blatt (2004). "Modeling hamsters for evaluating West Nile virus therapies." *Antiviral Res* 63(1): 41-50.
- Taylor, J., C. F. Babbs, M. B. Alzghoul, **A. Olsen**, M. Latour, A. L. Pond and K. Hannon (2004). "Optimization of ectopic gene expression in skeletal muscle through DNA transfer by electroporation." *BMC Biotechnol* 4(1): 11.